



University
of Glasgow

Mathers, Hannah (2014) *The impact of the Minch palaeo-ice stream in NW Scotland: Constraining glacial erosion and landscape evolution through geomorphology and cosmogenic nuclide analysis*. PhD thesis.

<http://theses.gla.ac.uk/5302/>

Copyright and moral rights for this thesis are retained by the author

A copy can be downloaded for personal non-commercial research or study, without prior permission or charge

This thesis cannot be reproduced or quoted extensively from without first obtaining permission in writing from the Author

The content must not be changed in any way or sold commercially in any format or medium without the formal permission of the Author

When referring to this work, full bibliographic details including the author, title, awarding institution and date of the thesis must be given

**The impact of the Minch palaeo-ice stream in NW
Scotland: Constraining glacial erosion and landscape
evolution through geomorphology and cosmogenic nuclide
analysis.**

Hannah Mathers

Thesis submitted to the University of Glasgow

For the degree of Doctor of Philosophy

School of Geographical and Earth Sciences

University of Glasgow

June 2014

I, Hannah Mathers, hereby certify that this thesis, which is approximately 48,000 words in length, has been written by me, that it is the record of work carried out by me and that it has not been submitted in any previous application for a higher degree.

Date 25.06.2014 Signature of candidate

I was admitted as a research student in October 2006 and as a candidate for the degree of PhD in October 2007; the higher study for which this is a record was carried out in the University of Glasgow between 2006 and 2013.

Date 25.06.2014 Signature of candidate

I hereby certify that the candidate has fulfilled the conditions of the Resolution and Regulations for the degree of PhD in the University of Glasgow and that the candidate is qualified to submit this thesis in application for that degree.

Date 25.06.2014 Signature of supervisor

Unrestricted

In submitting this thesis to the University of Glasgow I understand that I am giving permission for it to be made available for use in accordance with the regulations of the University Library for the time being in force, subject to any copyright vested in the work not being affected thereby. I also understand that the title and abstract will be published, and that a copy of the work may be made and supplied to any bona fide library or research worker.

Date 25.06.2014 Signature of candidate

ABSTRACT

The British-Irish Ice Sheet (BIIS) is predicted to have deglaciated rapidly from ~ 18 ka, in response to rising sea level and temperature, similar forcings experienced by modern polar ice sheets. As the main conduits of ice mass loss, the reaction of ice streams to these forcings is thought to have been central in determining the mode and timing of this deglaciation. However, lack of understanding of ice stream influence on the glaciology and deglaciation of ice sheets limits confidence in ice sheet model predictions.

NW Scotland is an area of the last BIIS predicted to have been dominated by ice stream onset conditions. This thesis presents results from a geomorphological and terrestrial cosmogenic nuclide (TCN) analysis study which resulted in the production of a composite ice-sheet thermal regime map and retreat chronology for the last BIIS in this region.

Mapping and surface exposure dating suggest that the regional glaciology and landscape evolution was dominated by the presence of ice-stream onset zones during Greenland Stadial-2 (GS-2). Mountain top erratics were uplifted and transported to high elevation during GS-2, before 16.5 ka BP. By inference, mountain summits were covered by ice during maximal ice sheet conditions.

The existence of sharp thermo-mechanical contrasts, developed in response to ice streaming, are proposed as the main controls on bedrock erosion and terrestrial sediment deposition. The interpretation of 'trimlines' in NW Scotland as englacial thermo-mechanical boundaries, is verified by the identification of 'rip-offs', a newly recognised geomorphic feature in the UK, and by quantitative demonstration of the increase in glacial erosion in the vicinity of these boundaries. Geomorphic and TCN data supports a conceptual model of thermal inversion following ice-stream cessation. The first description of 'till tails' in the UK provides insight into the glaciological organisation and thermal evolution of the BIIS.

A dated (17.6 ka BP) terrestrial glacial limit on the north Sutherland coast indicates early ice retreat from the shelf and provides a minimum

constraint on ice-stream cessation. This indicates rapid loss of ice extent and volume following shutdown of the Minch palaeo-ice stream. Major ice sheet reorganisation c. 15-16 ka BP is suggested by the correlation of some lateral margin ages with high elevation erratic deposition ages implying significant ice thinning and margin retreat prior to this time. Additionally, thinning of ~300 m is predicted for some areas prior to 14 ka BP.

TABLE OF CONTENTS

ABSTRACT	i
LIST OF FIGURES	vii
LIST OF TABLES	xi
LIST OF ACCOMPANYING MATERIAL	xii
ACKNOWLEDGEMENTS	xiii
PREFACE: A GOOD DAY BY NORMAN MACCAIG	xiv
CHAPTER 1: INTRODUCTION	1
1.1. Thesis Conceptual Framework and Research Objectives	6
1.2. Study Area	9
1.3. Geology of NW Scotland	10
1.4. Palaeo-ice streams and glaciological organisation	12
1.5. Constraining the basal thermal regime of the last British-Irish Ice Sheet	16
1.5.1. Spatial and chronological retreat of the last BIIS	18
1.6. Thesis scope	26
1.7. Wider Implications	28
CHAPTER 2: METHODOLOGY	29
2.1. Introduction	29
2.2. Geomorphic mapping	30
2.2.1. Mapping, observation and sampling	31
2.3. Terrestrial Cosmogenic Nuclide (TCN) Analysis	32
2.3.1. TCN theory	33
2.3.1.1. TCN Production	33
2.3.1.2. Utilisation of TCN data in glacial studies	35
2.3.2. Processing from rock to TCN concentration	37

2.3.2.1.	Sampling	37
2.3.2.2.	Extracting Be and Al from a whole rock sample	40
2.3.2.3.	Calculating a surface exposure age	43
2.3.2.4.	Use of a local production rate	44
CHAPTER 3: RESULTS		46
3.1.	Introduction	46
3.2.	N coast, Sutherland	48
3.2.1.	Regional geomorphology	48
3.2.1.1.	Kyle of Durness	51
3.2.1.2.	Rispond	52
3.2.1.3.	Eriboll Valley	56
3.2.1.4.	Eriboll: W flank	56
3.2.1.5.	Srath Beag	61
3.2.1.6.	Cranstackie	69
3.2.1.7.	Eriboll: Eastern flank	75
3.2.1.8.	Loch Hope	80
3.2.1.9.	Ben Loyal	82
3.2.1.10.	Cape Wrath Area	83
3.3.	W Sutherland: Oldshoremore & Sheigra	85
3.4.	Assynt Mountains: Glas Bheinn, Beinn Uidhe, Conival, Breabeg	92
3.5.	Coigach	100
3.5.1.	Cul Beag	100
3.5.2.	Beinn an Eòin	103
3.5.3.	Stac Pollaidh	105
3.5.4.	Ben More Coigach & Spidean Còinnich	106
3.5.5.	Tanera Mòr	108
3.6.	Wester Ross	112

3.6.1.	Glen Achall	112
3.6.2.	Sail Liath	116
3.6.3.	Little Loch Broom	119
3.6.4.	Gruinard Bay	120
3.7.	Newly identified geomorphic features	122
3.7.1.	'Rip-off zones'	122
3.7.2.	Till Tails	128

CHAPTER 4: DISCUSSION: HORIZONTAL & VERTICAL ICE MARGIN RETREAT CHRONOLOGY

4.1.	Introduction	133
4.2.	Lateral ice margins	133
4.2.1.	North Sutherland coast	133
4.2.2.	Sheigra - Oldshoremore	140
4.2.3.	Summer Isles - Glen Achall	147
4.2.4.	Glen Achall	150
4.2.5.	Little Loch Broom	150
4.2.6.	Gruinard Bay	150
4.3.	Ice sheet thinning	151
4.4.	Ice sheet stability	154
4.5	Ice sheet sector deglaciation: Major findings regarding chronology of retreat and glaciological organisation	158

CHAPTER 5: DISCUSSION: THERMAL STRUCTURE AND FLOW REGIME OF THE LAST BIIS IN NW SCOTLAND

5.1.	Introduction	159
5.2.	Relict surfaces & Glacial modification	159
5.2.1.	High and intermediate level surfaces: Tors, Blockfields & Rip- offs	163
5.2.2.	Low level surfaces	187

5.3.	Thermal transitions & Flow Organisation	192
5.3.1.	Vertical thermal zonation	192
5.3.2.	Flow Disruption & Organisation	197
5.3.3.	Vertical transportation of erratics	206
5.3.3.1.	Glaciological significance of erratic uplift	209
5.3.3.2.	Timing of erratic deposition	213
5.4.	Ice sheet thermal and land surface evolution	215
5.4.1.	Towards an understanding of thermo-mechanical organisation of the last BIIS in NW Scotland	215
5.4.2.	Glaciological evolution of the BIIS in NW during GS-2	219
5.4.3.	Evidence of active periglacial processes during the Holocene	221
5.5.	Key findings regarding the thermal and landscape evolution history of NW Scotland	223
	CHAPTER 6: CONCLUSIONS	224
	REFERENCES	227

LIST OF FIGURES

Figure 1.1: North west Scotland field area.	3
Figure 1.2: Schematic of the western calving margins of the last BLS	4
Figure 1.3: Relative sea-level (RSL) observations and model predictions.	5
Figure 1.4: Schematic of thesis knowledge structure	7
Figure 1.5: 'Typical' landscapes of the field study area in NW Scotland	11
Figure 1.6: Ice sheet models predicting ice streaming in The Minch.	14
Figure 1.7: The Minch palaeo-ice stream at maximum extent.	15
Figure 1.8: Schematic W-E transect across Scotland	17
Figure 1.9: A poorly mapped BGS Quaternary Geology sheet.	19
Figure 1.10: Charlesworth's (1955) ice limits map for Sutherland.	20
Figure 1.11: Max. altitude achieved by last ice sheet in NW Scotland.	22
Figure 1.12: The West Sutherland Younger Dryas ice field.	24
Figure 2.1: Neutron flux below the air-surface interface.	37
Figure 2.2: Conceptual model of moraine degradation.	39
Figure 2.3: The SUERC 5MV accelerator mass spectrometer.	43
Figure 3.1: Meltwater channels in the Eriboll-Hope area.	49
Figure 3.2: Creag na Griosach, Portnancon.	50
Figure 3.3: TCN sampling sites and geomorphic features, Rispond.	55
Figure 3.4: Glaciofluvial sediment, W flank of Loch Eriboll.	57
Figure 3.5: Glacially transported bedrock raft, W Eriboll.	58
Figure 3.6: Context PORT samples, Portnancon, Loch Eriboll.	59
Figure 3.7: ERW samples, Loch Eriboll.	60
Figure 3.8: Context of LAID TCN samples, west side of Loch Eriboll.	60
Figure 3.9: Glacial contact sediments, head of Loch Eriboll.	61
Figure 3.10: Terrace feature, head of Loch Eriboll.	63
Figure 3.11: Sediment limits, Strath Coille na Feàrna.	63

Figure 3.12: West side terrace feature, Srath Beag.	66
Figure 3.13: Srath Beag kame terrace suite.	68
Figure 3.14: Cranstackie slopes and plateau.	70
Figure 3.15: Inferred cirque glacier limits, Coire an Uinnseinn.	70
Figure 3.16: Plateau geomorphology, Cranstackie.	72
Figure 3.17: TCN sampling CRAN04, Cranstackie.	73
Figure 3.18: Cranstackie tor.	74
Figure 3.19: Glacial sediments, Rubh' Ard Bhaideanach, E. Eriboll.	76
Figure 3.20: Glacial deposits, Eriboll farm.	77
Figure 3.21: Glacial features at Roadstead, E Loch Eriboll.	78
Figure 3.22: TCN sampling, near Heilam between Lochs Eriboll & Hope.	80
Figure 3.23: Raised glaciomarine features of Loch Hope.	81
Figure 3.24: Ben Loyal summits.	82
Figure 3.25: Cape Wrath coast.	84
Figure 3.26: Scoured ground beneath Foinaven at Càrn Leacach.	84
Figure 3.27: Aerial image of W Sutherland showing lochan distribution.	85
Figure 3.28: Geomorphology & sediment cover around Oldshoremore.	86
Figure 3.29: Sampling the boulder spread at Oldshoremore.	87
Figure 3.30: Sheigra TCN samples.	91
Figure 3.31: Geomorphic features of the Beinn Uidhe plateau, Assynt.	97
Figure 3.32: Beinn Uidhe plateau.	98
Figure 3.33: Geomorphic features, Breabeg.	99
Figure 3.34: Geomorphology of Cul Beag, Coigach.	103
Figure 3.35: Beinn an Eòin.	104
Figure 3.36: Glacial modification on the summit ridge of Stac Pollaidh.	105
Figure 3.37: Weathering features, Stac Pollaidh.	105
Figure 3.38: Ben More Coigach and Specein Còinnich.	107
Figure 3.39: TCN sampling, Tanera Mòr.	109

Figure 3.40: Geomorphic features of Tanera Mòr.	110
Figure 3.41: Retreat moraines within WRR limits.	111
Figure 3.42: Geomorphic context of TCN sampling, Glen Achall.	115
Figure 3.43: Sail Liath, An Teallach, Wester Ross.	117
Figure 3.44: Close context Sail Liath.	118
Figure 3.45: Samples acquired from submerged moraine, L. L. Broom.	119
Figure 3.46: Setting of DD TCN samples, Gruinard Bay.	121
Figure 3.47: Beinn Uidhe rip-off, Assynt Mountains.	123
Figure 3.48: Conival rip-off, Assynt Mountains.	124
Figure 3.49: Relation of GTBs to rip-offs, Assynt Mountains.	125
Figure 3.50: Breabeg rip-off, Assynt Mountains.	126
Figure 3.51: Rip-off features, Cranstackie range, Sutherland.	127
Figure 3.52: Till tails of NW Scotland.	129
Figure 3.53: Stac Pollaidh - Ben Mor Coigach till tail.	130
Figure 3.54: Till tail geomorphology: B. Ghobhlach, Wester Ross.	131
Figure 3.55: Till tail sediments, Stac-Pollaidh.	132
Figure 4.1: Relation of MPIS operation to ice flow, Eriboll-Hope area.	134
Figure 4.2: Glacial landforms on the continental shelf, NW Scotland.	135
Figure 4.3: Mapped and inferred ice limits Eriboll-Hope area.	137
Figure 4.4: Proposed late stage ice margin configuration, Oldshoremore.	143
Figure 4.5: Proposed late stage ice margin configuration, Oldshoremore.	144
Figure 4.6: Laxford ice stream tributary palaeo-ice sheet dynamics.	145
Figure 4.7: Landforms of the frozen-bed patch environment.	146
Figure 4.8: Time slices from BIIS thermo-mechanical model.	149
Figure 4.9: Seabed landforms on the northern UK continental shelf.	154
Figure 4.10: ^{10}Be exposure ages against NGRIP ice core $\delta^{18}\text{O}$ record	156
Figure 5.1: Inversion key for glacial geomorphology.	161
Figure 5.2: The Minch palaeo-ice stream onset zone catchments.	162

Figure 5.3: Landscape development & Assynt panorama.	164
Figure 5.4: Distribution of main tor groups.	165
Figure 5.5: Glacial modification of Tor at An Cnoidh, Cairngorms.	166
Figure 5.6: Megagrooves in Assynt.	170
Figure 5.7: Subglacial hydrology relation to megagroove formation.	170
Figure 5.8: Erosional landscapes and glacial erosion.	171
Figure 5.9: Glacial modification of pre-glacial surfaces, Cranstackie.	173
Figure 5.10: Model of tor emergence and blockfield evolution.	174
Figure 5.11: Deep subaerial weathering of quartzite, Cranstackie.	176
Figure 5.12: Debris entrainment & subglacial basal thermal regime.	179
Figure 5.13: Rip-offs of the Assynt Mountains.	180
Figure 5.14: Rip-offs and deeper glacial erosion, W. Loch Eriboll.	185
Figure 5.15: Depth of glacial erosion, western flank of Loch Eriboll.	186
Figure 5.16: Gneiss bedrock morphology, Sheigra.	189
Figure 5.17: Comparison of lochan density across NW Scotland.	191
Figure 5.18: Regional thermal zones & supporting geomorphic evidence.	193
Figure 5.19: Frozen/thawed boundary types.	195
Figure 5.20: Thermal zonation in the vicinity of the E. Assynt Mountains.	196
Figure 5.21: Thermal zones within Laxford ice-stream tributary.	197
Figure 5.22: Geomorphic evidence for a shear margin on B.M. Coigach	201
Figure 5.23: Experimental model analogue for 'till tail' - scour forms.	202
Figure 5.24: A model of flute formation.	203
Figure 5.25: Torridon boulder trains, Assynt.	205
Figure 5.26: Erratic transport along four profiles.	208
Figure 5.27: Suggested explanation of erratic uplift.	210
Figure 5.28: Quartzite erratics and 'rip-offs', Assynt Mountains.	212
Figure 5.29: Large scale freeze on of basal ice, Antarctica.	214
Figure 5.30: Landform of a Boothia-type dispersal train.	219

LIST OF TABLES

Table 1.1: Thesis aims and research methodologies.	8
Table 1.2: Geomorphological criteria for identifying palaeo-ice streams.	13
Table 2.1: TCNs used in this study.	35
Table 3.1: Acronyms for TCN sample locations & physical characteristics.	2
Table 3.2: TCN sample locations & physical characteristics, W. Eriboll.	53
Table 3.3: TCN sampling data and surface exposure ages, W.Eriboll.	54
Table 3.4: TCN sample characteristics, S. Beag, Cranstackie & E. Eriboll	64
Table 3.5: TCN data & exposure ages, S. Beag, Cranstackie & E. Eriboll	65
Table 3.6: TCN sample locations & characteristics, OSM & Sheigra.	88
Table 3.7: TCN sampling data & surface exposure ages, OSM & Sheigra	89
Table 3.8: TCN sample locations & characteristics, B. Uidhe & Breabeg	94
Table 3.9: TCN sampling data & exposure ages, B. Uidhe & Breabeg.	95
Table 3.10: TCN sample locations & characteristics, Coigach & T. Mor.	101
Table 3.11: TCN sampling data, Coigach Mountains & Tanera Mor.	102
Table 3.12: TCN sample locations & characteristics, G. Achall & S. Liath.	113
Table 3.13: TCN sampling data & exposure ages, G. Achall & S. Liath.	114
Table 3.14: TCN sample characteristics, L.L. Broom & G. Bay.	120
Table 3.15: TCN sampling data & exposure ages L.L. Broom & G. Bay.	120
Table 4.1: Exposure ages from Achiltibuie - CRONUS and local p. rate.	148
Table 4.2: Minimum ice sheet thinning during the Lateglacial.	153
Table 5.1: Comparison of tor features, NW Scotland.	168
Table 5.2: Summary of blockfield features of selected mountains.	181
Table 5.2 (continued): Summary of blockfield features.	182
Table 5.3: Summary of vertical thermal zonation.	194
Table 5.4: Comparison of horned crag and tail features with till tails.	202

LIST OF ACCOMPANYING MATERIAL

- FOLIO 1: MAP OF NW SCOTLAND (SLEEVE)**
- FOLIO 2: GEOLOGICAL MAP OF NW SCOTLAND (SLEEVE)**
- FOLIO 3: GEOMORPHOLOGY AND SURFACE COVER OF LOCH ERIBOLL REGION (SLEEVE)**
- FOLIO 4: COMPOSITE ICE-SHEET THERMAL REGIME MAP FOR NW SCOTLAND (SLEEVE)**
- APPENDIX 1: University of Glasgow Geographical and Earth Sciences - Mineral Separation and Quartz Cleaning Procedures Manual.**
- APPENDIX 2: University of Glasgow - Cosmogenic isotope laboratory Terrestrial in situ cosmogenic ^{10}Be and ^{26}Al chemistry procedures manual.**

ACKNOWLEDGEMENTS

The completion of this thesis has been supported by many contributions. For sharing my excitement and engagement with the writing process, providing an inspiring scientific standard, and great field company I thank Dr Derek Fabel (DF in photo credits). I also thank Dr Tom Bradwell for providing field training and support, access to BGS data, provision of great field photos (TB in photo credits) and incisive writing direction.

Discussions with Dr Maarten Krabbendam (BGS) were extremely useful in probing the geological complexities of the northwest Highlands and Tim Atkinson provided advice regarding the quartzite karst of the Assynt region and illustrative images which he has kindly granted permission to be used in this thesis (TA in photo credits).

At the University of Glasgow practical help with labwork was provided by John Gillece and with visual materials by Les Hill, for which I thank them. At SUERC I thank the whole team, but particularly Maria Miguens-Rodriguez, Henriette Linge (University of Bergen) and David Small (University of Glasgow) for assistance in sample processing. Reka Fulop (RF in photo credits) and Tibi Codilean (AC in photo credits) are thanked for generous access to their photographs from the field area.

This research was carried out while I was in receipt of a NERC Blue Skies studentship (NER/S/A/2006/14322) served through a British Geological Survey Universities Funding Initiative (S106).

For support at a personal level the discussions and distractions of the following people have been most beneficial: Katie Whitbread, Helen Murray, Alessa Geiger, Delia Gheorghiu, Andy Singleton and Mae Boyd. For their tolerance and support over the last six years of study I am indebted to my extended family in Glasgow, particularly Sue Duff, whose un-minced words and compassion kept me going.

This thesis is the product of six years of work, academically mine, but literally the work of a team. To my dad John, sister Al and partner Ali I am extremely grateful for your understanding and patience with the years of physical and emotional absence.

Finally, a special mention, to two very strong women who have been there for me everyday in this endeavour. Without the support of my Mum Jenny's unshakeable resolve to facilitate, support and nurture, this thesis may not have been possible. And to Freya, my amazing daughter, born at the end of my first PhD year, supportive beyond your years and always inspirational, what would this be without you. This is for you both.

A GOOD DAY

Sun-stunned the water; trees hold their breath.
The bracken smell is six foot deep
And never stirs. I feel green crumbs of heather
Crawling on cheekbones . . . stillness but not sleep.

A heron, folded round himself,
Stands in the ebb, as I in mine.
I feel my world beneath me, like his, shelving
To darker depths of dark and bitter brine.

Suddenly round the cliff face bolt
Pigeon and falcon - they tear the air
And are gone in it. And the day stands, without motion,
As though nothing had drawn that savage blue stroke there.

What has been wounded? Only false
Images. Nothing can betray
Wise heron, shattering light or breathless alder
Or water slipping soundlessly away.

Norman MacCaig

Chapter 1: INTRODUCTION

It has been recognised for some time that ice streams have a significant influence on the surface morphology, basal thermal regime and mass flux of ice sheets. Along with increases in sea surface, and air, temperatures, and reduced sea ice extent, and persistence, in polar regions (IPCC, 2013); high magnitude changes have been observed in marine ice-streams of both the Antarctic and Greenland ice sheets (Pritchard *et al.*, 2009). To improve the accuracy and precision of ice sheet-response-forecasting, we must have an in-depth understanding of the role ice streams fulfil in the dynamic interplay between cryosphere, ocean and atmosphere.

The landform record left behind by palaeo-ice sheets can be analysed to understand how an ice sheet evolved over many thousands of years. By coupling these observations to the palaeo-climate record it is possible to quantitatively improve ice sheet models to characterise ice sheet response to environmental forcings, such as sea level rise or atmospheric warming.

The last British-Irish Ice Sheet (BIIS), which existed c. 38-10.4 ka BP, (Scourse *et al.*, 2009, Clark *et al.*, 2012) is one of the best studied palaeo-ice sheets in the world. Recent high resolution ice sheet models (Boulton and Hagdorn, 2006; Hubbard *et al.*, 2009) have provided detailed information regarding the predicted dynamic response of this ice-sheet to internal glaciological organisation and external forcings. The lateral extent at the last local glacial maximum has been physically well-constrained, and the limited extent of ice expansion during the Younger Dryas, the Loch Lomond Readvance in Scotland, has left a wealth of Lateglacial palaeo-environmental and ice sheet evidence in the landscape.

With its situation as a marine-influenced ice sheet moving over both crystalline basement rocks and exposed marine sediments, palaeo-glaciological observations from the BIIS provide useful analogies for aspects of the modern Greenland and West Antarctic ice sheets. It is estimated that 90% of mass loss from the modern West Antarctic Ice Sheet (WAIS) is evacuated through ice streams (Payne *et al.*, 2004). Dynamic thinning has been highlighted as an

important deglacial process currently operating at the coastal sectors of both polar ice sheets. However, the mechanisms by which this thinning is achieved remain 'poorly understood' (Pritchard *et al.*, 2009). The BIIS is predicted to have deglaciated rapidly in response to rising sea level and temperature (Clark *et al.*, 2012), similar to forcings experienced by modern polar ice sheets. Lack of understanding of ice stream dynamic response to sea level, currently limits confidence in ice sheet models (Clark *et al.*, 2012).

Specifically, around northwest Scotland, the interaction of the BIIS with the ocean is particularly pertinent, as the ice sheet is known to have had calving marine margins. It is known that water depth, salinity and temperature are important in the dynamics of ice streams and ice shelves because of influence as they influence the position of the grounding line and the calving rate (Benn and Evans, 2010). Identification of BIIS-sourced ice rafted debris (IRD) in sediment sequences at the Barra-Donegal Fan and other shelf edge fans (Figure 1.1) provides evidence for marine calving (Figure 1.2) along the western margin of the late Devensian BIIS (Scourse *et al.* 2008). It is predicted that most IRD was derived from icebergs calved from 'local' palaeo-ice streams (Scourse *et al.*, 2008).

Early work by Sutherland (1984) around St Kilda established the basis of a Devensian sea level at - 120 m OD. Evidence of higher marine surfaces at -80 to - 40 m was suggested to relate to post-Last Glacial Maximum (LGM) to Younger Dryas sea level stages. This indicates that sea level remained relatively low until the Lateglacial transition. On mainland NW Scotland, the main relative sea level record comes from Coigach (Figure 1.3), where there is no evidence of a Late Devensian relative sea level high stand (Shennan *et al.* (2000).

However, raised marine features associated with glacial sedimentation are seen both along the northern coast and further south around the Broom lochs and Gruinard Bay (King and Wheeler, 1963 and Kirk *et al.* 1966). Loch Broom and coasts to the south around Gruinard Bay etc. show evidence of a higher relative sea level (Kirk *et al.* 1966) in the form of erosional and depositional marine features. The exact timing of high sea level stands around NW Scotland remains unconstrained.

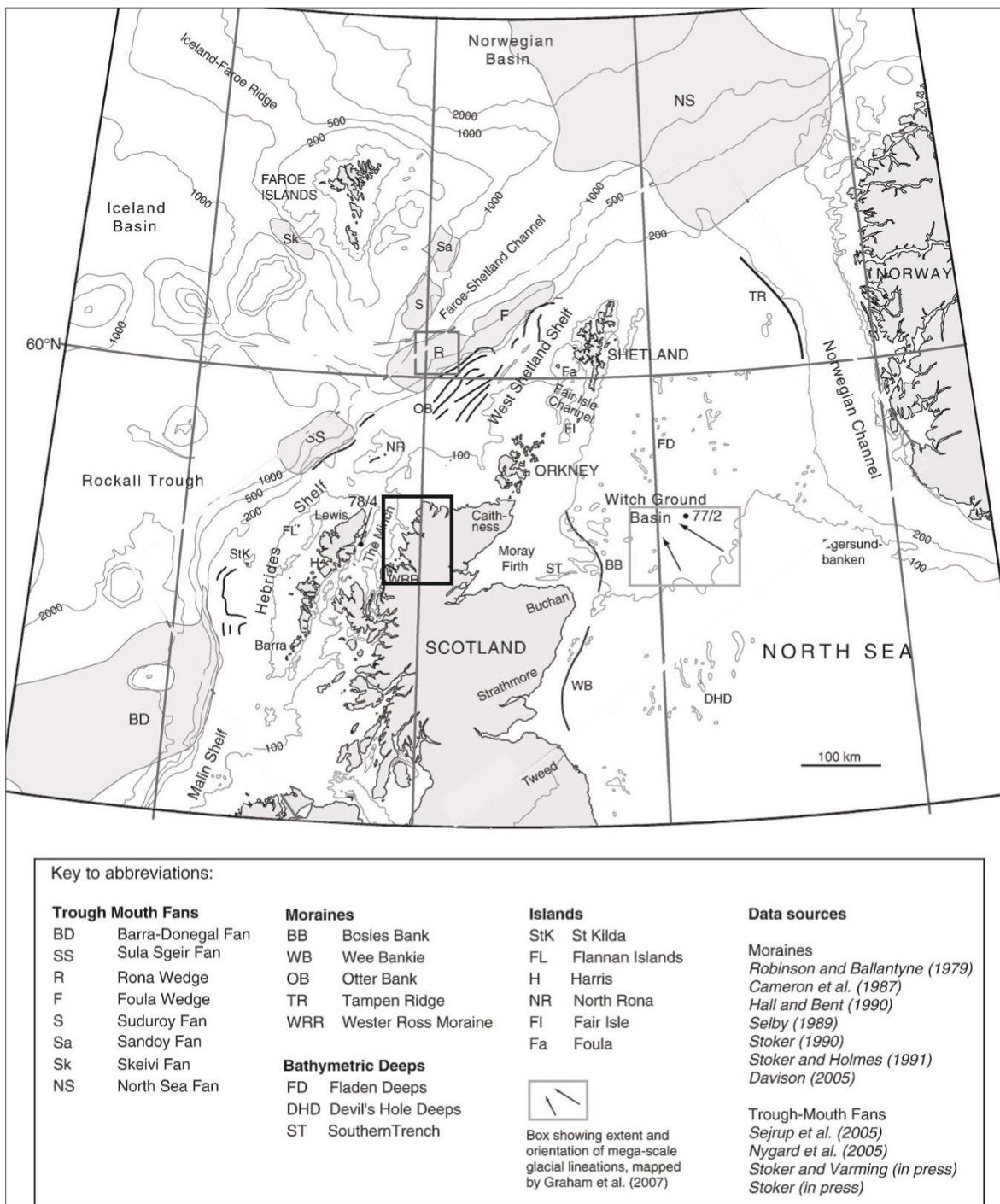


Figure 1.1: North west Scotland field area (Folio 1 extent indicated by black-edged box) contextualised with key glacial features of the northern extent of the BIIS. Modified from Bradwell et al. (2008).

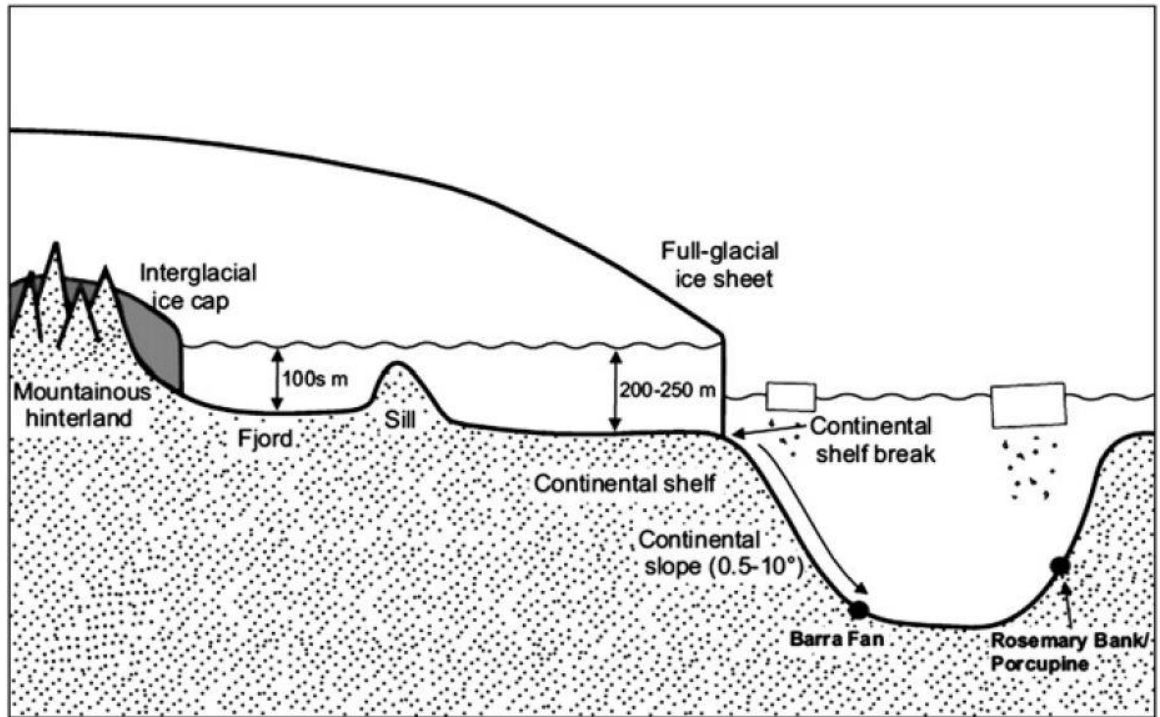


Figure 1.2: Schematic of the western calving margins of the last BIIS at full-glacial extent and interglacial ice cap configuration. Note the difference in relative sea level at these stages. The relative positions of cores taken at the Barra Fan and Rosemary Bank/ Porcupine Seabight are shown. Scourse et al. (2009) modified from Dowdeswell et al. (2002).

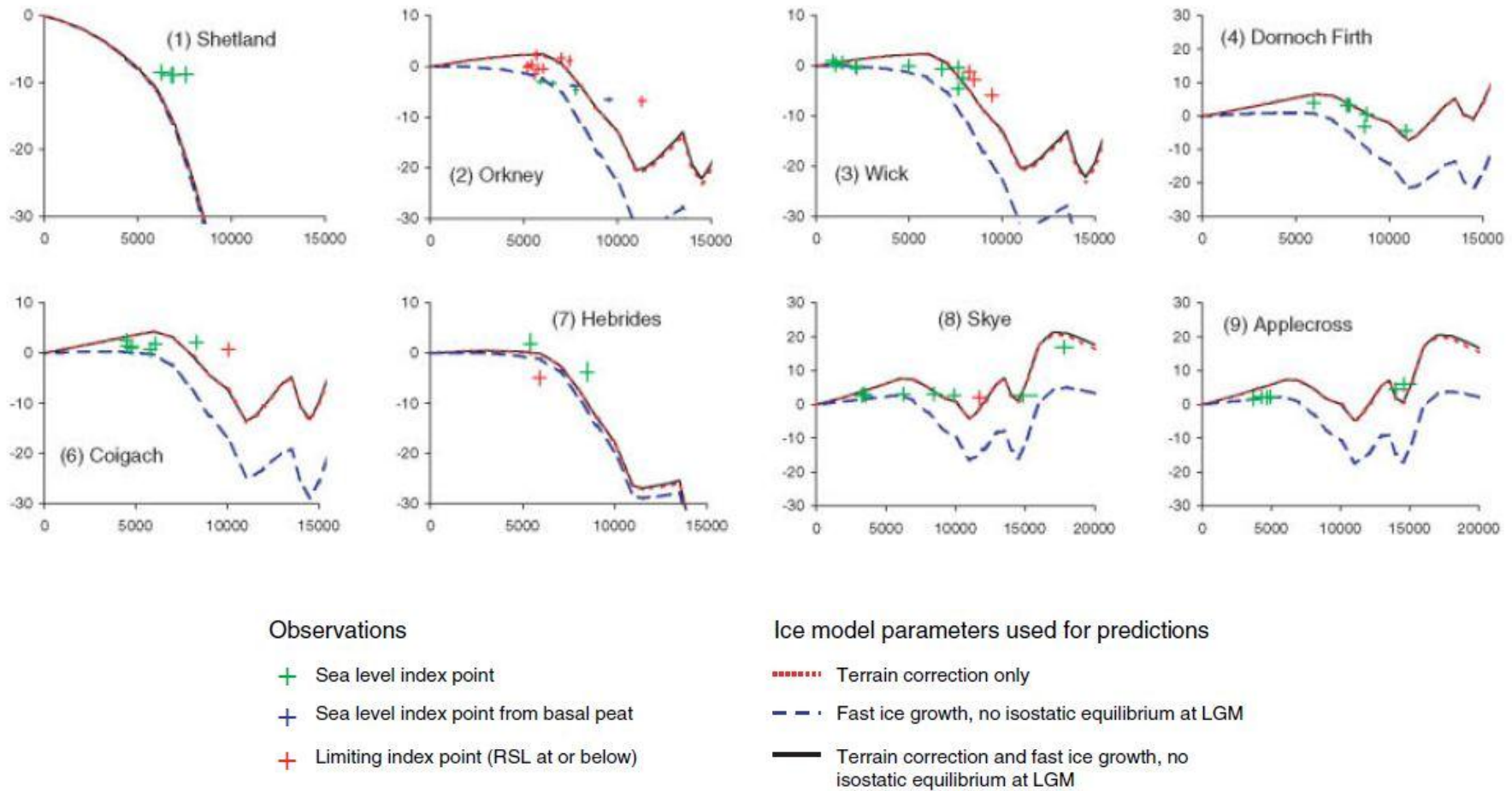


Figure 1.3 : Relative sea-level (RSL) observations and model predictions for 3 ice models for sites in Northern Scotland. Modified from Shennan et al. (2006).

1.1. Thesis Conceptual Framework and Research Objectives

The dramatic landscape of NW Scotland with its spectacular geological structures has inspired geological investigations for more than a century (insert refs). Previous studies in the region have worked at local scale or high elevation only and have not merged geomorphic observations into a regional theoretical model. This field and laboratory-based study investigates the palaeo-glaciology of NW Scotland through a landsystems approach. By understanding the process and temporal framework by which glacial features are developed, and spatially organised, it is possible to gain insight into the subglacial thermal organisation and ice stream configurations of the last BISS.

Major research questions limiting our understanding of this unique region can be grouped into two main topics: glaciological and landscape evolution, though there is significant overlap between these areas. Previous research is outlined in this chapter and discussed further, in context, within each chapter. Informed by a review of the existing literature; a methodological approach (Figure 1.4: Schematic of thesis knowledge structure) was developed to help strengthen the empirical constraints on ice sheet models (of the BISS and elsewhere) and tie together disparate multi-proxy datasets in order to synthesise the influence and behaviour of the NW sector of the BISS, together with its dynamic fast-flow systems such as the Minch Palaeo-Ice Stream (MPIS).

The conceptual framework guiding the thesis (Figure 1.4) is built around three main research aims which guide investigations into the functioning of the NW sector of the last BISS. These are to:

- Determine the influence of the Minch palaeo-ice stream on the glaciological organisation of the last BISS.
- Provide empirical boundary constraints for basal thermal regime of the NW sector of the last BISS over the last glacial cycle.
- Spatially and chronologically improve the retreat history of the NW sector of the last BISS.

These main research aims are addressed by investigation of specific research questions, which in turn guided the development of experimental hypotheses and ultimately determined the research methodologies used in this project. These are field mapping and remote survey at a variety of scales (Folio 1 and Methodology 2.2) and surface exposure dating using terrestrial cosmogenic nuclides (TCNs) (Methodology 2.3).

The data is synthesised and discussed in a wider, regional ice sheet context in Chapters 4 and 5. The summation and reduction of data into a single theoretical model allows discussion of evolving ice sheet dynamics, at an ice stream ‘drainage basin’ scale.

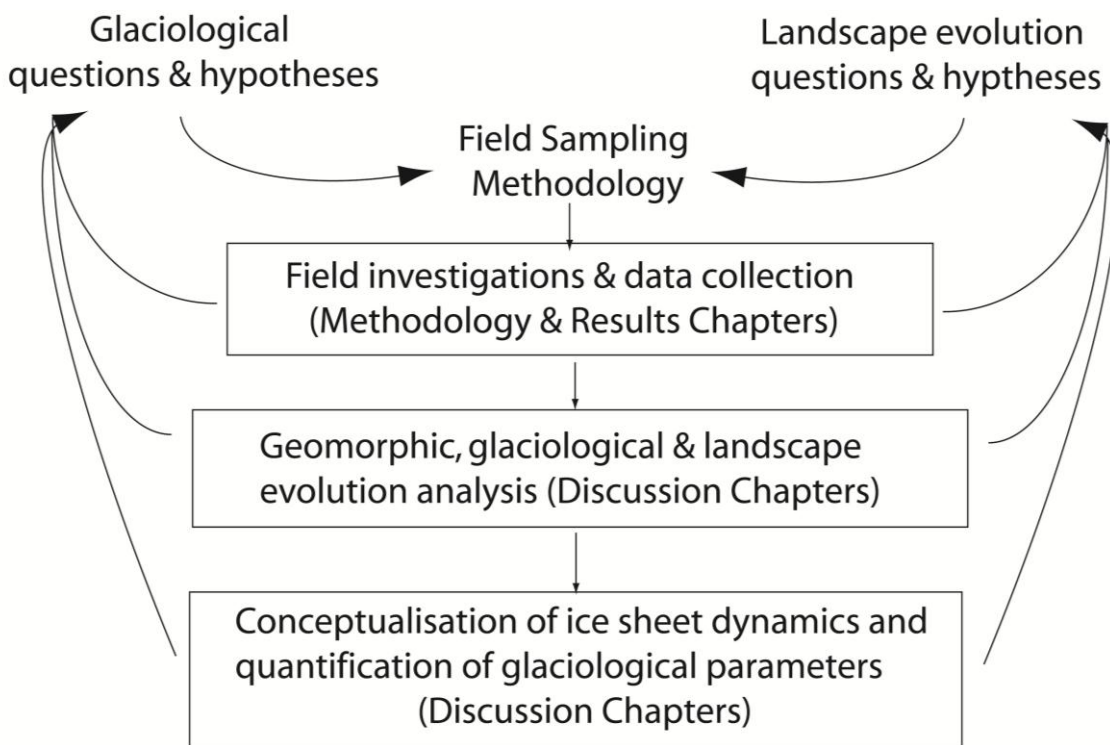


Figure 1.4: Schematic of thesis knowledge structure

Table 1.1: Thesis aims and research methodologies.

Research Aims	Research Methodology	Thesis section
<p>Determine the effect of operation of the Minch palaeo-ice stream on the glaciological organisation of the last BIIS.</p>	<p>Geomorphic mapping of glacial flow pattern.</p> <p>Map ice marginal features bordering Cape Wrath.</p> <p>Target ice marginal deposits for TCN analysis at Oldshoremore and around the Loch Eriboll area.</p> <p>Map ice marginal features outside Younger Dryas (YD) limits to trace retreat</p>	<p>DISCUSSION: THERMAL STRUCTURE AND FLOW REGIME OF THE LAST BIIS IN NW SCOTLAND</p>
<p>Provide empirical boundary constraints for basal thermal regime over the last glacial cycle.</p>	<p>Use bedrock-erratic paired TCN analysis (above the trimline) to investigate the severity of glacial erosion.</p> <p>Map glacial basal thermal regime from field data.</p>	<p>DISCUSSION: THERMAL STRUCTURE AND FLOW REGIME OF THE LAST BIIS IN NW SCOTLAND</p>
<p>Chronologically and spatially constrain the retreat history of the NW sector of the last BIIS.</p>	<p>Locate the highest erratic boulders in the study area and date their glacial deposition using TCN analysis.</p> <p>Establish the recessional ice limit pattern reflected in the geomorphic record and use TCN analysis to constrain the abandonment of significant ice limits.</p>	<p>DISCUSSION: HORIZONTAL AND VERTICAL ICE MARGIN RETREAT CHRONOLOGY</p>

1.2. Study Area

The field area comprises a ~35 km wide strip along a 100 km transect of the coast of NW Scotland, covering large portions of the counties of Sutherland and Ross & Cromarty (Figure 1.1 and Folio 1). Folio 1 serves two purposes; firstly, to familiarise the reader with locations referred to in the text, and secondly to contextualise these localities with respect to the proposed footprint of the onset zone of MPIS (Bradwell *et al.*, 2007). It should be noted that as the MPIS is anticipated to have existed during full glacial conditions, when sea level may have been up to 120m lower, the contemporary coastline would have been significantly further offshore at this time. Consequently, the blank space between the modern coastline and ice stream feeder limbs is only an artifice of the juxtaposition of mapped elements.

The western seaboard of northern Scotland is a low coastal plain c. 100-200 m a.s.l. At Cape Wrath higher ground forms a broad plateau at c. 200-350 m a.s.l. Mountains often occur as inselbergs (island mountains) up to 849 m a.s.l. (Cul Mor, Assynt) through Coigach, Western Assynt and Western Sutherland where high ground has been heavily dissected. Further east high ground occurs as slivers of remnant high level plateaux - the eastern Assynt Mountains (c. 700-800 m a.s.l.). Major breaches traverse the region interrupting the east-west watershed at the valley of Dirrie More-Loch Glascarnoch and the Borrolan Gap at the southern end of the Assynt Mountains. Local incomplete breaches of importance to this study are the Bealach Traligill, Assynt and the Glengolly pass, Sutherland. The regional watershed runs c. N-S in the southern part of the field study area, defined generally by the position of the Moine Thrust Zone until the vicinity of Foinaven from which point it trends east-west, with most major catchments draining northward to the Atlantic coast.

1.3. Geology of NW Scotland

The western margin of the field study area comprises exposed Archaean Lewisian basement rocks (> 2.5 Ga) and Neoproterozoic sandstones of the Torridon Group. These form the characteristic low-lying knock and lochan landscapes typical of western Assynt and west Sutherland (Figure 1.5 C & G). This ground is frequently scattered with perched, glacially transported, often erratic, boulders (Figure 1.5 B). Bounding the study area to the east is the NNW strike of the Moine Thrust Zone. Exposed in this narrow Moine Thrust Zone (Folio 2) and more extensively in the Assynt Culmination are the predominantly Cambro-Ordovician rocks comprising the hills of Assynt (Figure 1.5 A) and Western Sutherland. Here quartzites of the Eriboll Group overlie Torridon sandstones (Figure 1.5 E) creating resistant caps and forming blockfield over the plateaux and upper slopes of the high ground (Figure 1.5 D). Psammites and semi-pelites make up the Moine Supergroup an aerially extensive geological cover group stratigraphically above, and to the east of the Moine Thrust Zone. The region is punctuated by small alkaline intrusions including the Ben Loyal syenite and the Loch Borrolan Group intrusives.

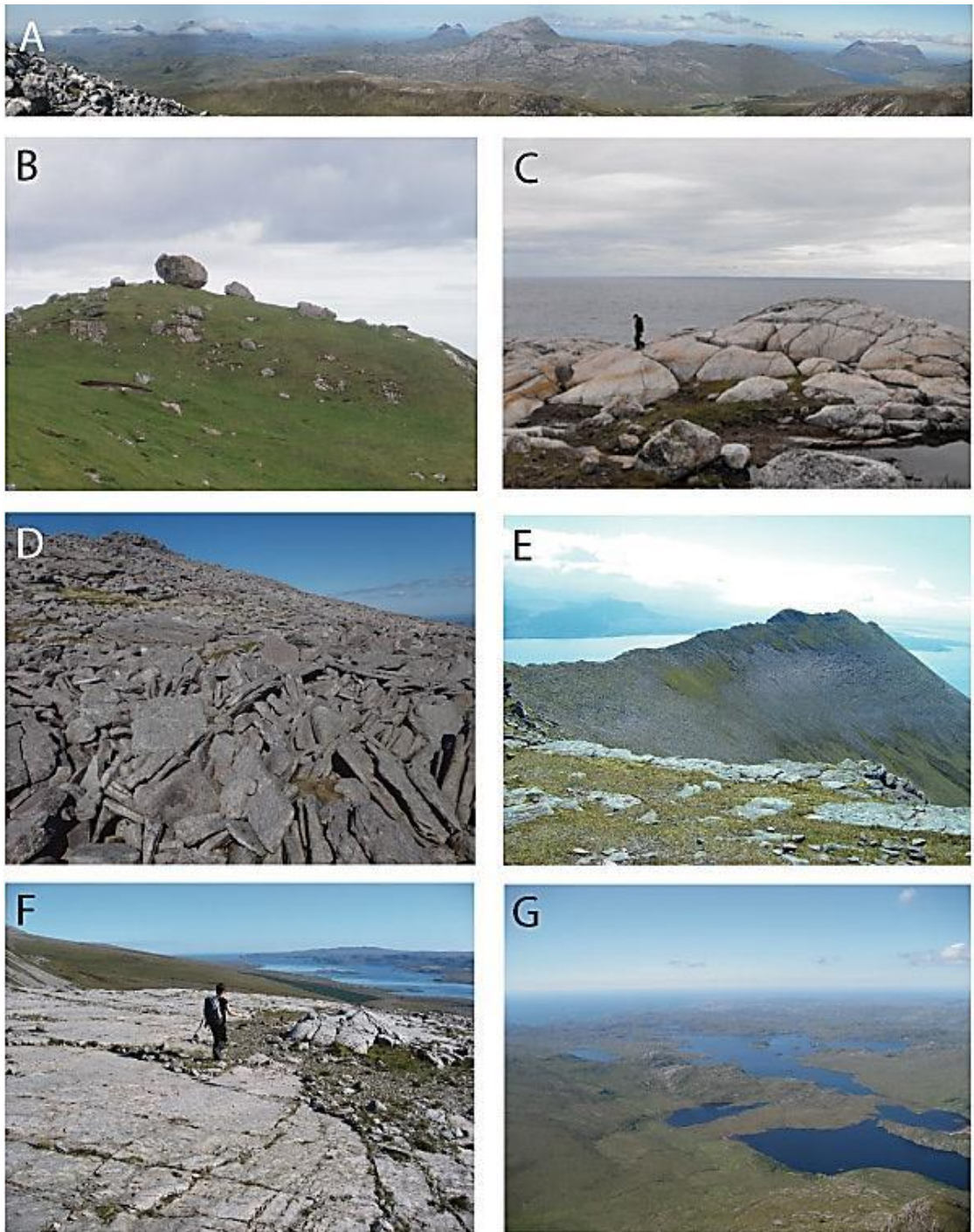


Figure 1.5: ‘Typical’ landscapes of the field study area in NW Scotland. A - Assynt inselbergs. B - Perched boulders below Ceannabeinne, N. Sutherland. C - Mammilated Lewisian bedrock, near Oldshoremore. Photo: RF/AC. D - Blockfield in Piperock (quartzite), Cranstackie. E - Exposed bedrock and regolith in Torridon sandstone, Ben Mor Coigach SW ridge. F - Selective glacial regolith clearance and moulding of Basal Quartzite, Cranstackie. Photo: DF. G - Low-lying ‘knock and lochan’ landscape prevalent in the Lewisian basement of the western seaboard, Assynt coast.

1.4. Palaeo-ice streams and glaciological organisation

Ice sheet modelling outputs for the last BISS have consistently predicted the existence of ice streams as large, dynamic components of the glaciological system (Figure 1.6). These palaeo-ice streams have influenced the maximum extent of the ice sheet, particularly in the Irish Sea and down the eastern coast of England, and increased the sensitivity of the ice sheet to sea level which may have governed its rapid collapse (Reference).

Several palaeo-ice streams have now been identified in Scotland in the following basins: the Moray Firth (Merritt *et al.*, 1995), the Tweed (Everest *et al.*, 2005), Strathmore (Golledge and Stoker, 2006), the Clyde (Finlayson *et al.*, 2014) and The Minch (Bradwell *et al.*, 2007). These features have been identified by their characteristic subglacial bedforms, often including the high elongation ratios associated with fast-flowing ice (Table 1.2).

The potential existence of a palaeo-ice stream in the Minch basin was proposed by Denton and Hughes (1981), though convincing empirical data supporting ice streaming in the Minch has only recently been identified (reference). The innovative merged on- and offshore survey administered through the BGS North West Highlands Project brought together side-scan sonar, multibeam, borehole, DEM and field data to allow high definition mapping and stratigraphic interpretation of a large ice stream draining ~15,000 km² of NW Scotland (Stoker and Bradwell, 2005, Bradwell *et al.*, 2007). Strongly influenced by the North Atlantic climate, the response of the Minch palaeo-ice stream to environmental forcings provides an analogous model for modern processes at marine margins of polar ice masses.

It is widely proposed that the LGM ice sheet margin reached the shelf edge around 25 - 30 ka BP along the whole boundary of the British Isles from SW Ireland to Shetland (Bradwell *et al.*, 2008c; Scourse *et al.*, 2009; Peck *et al.*, 2006, King *et al.*, 1998). A review of data relating to the deglaciation of the continental shelf off NW Scotland (Bradwell *et al.*, 2008c), indicates that The Minch experienced open marine conditions from c. 15 ka BP. TCN exposure ages from eastern Harris (Stone and Ballantyne, 2006) and Gairloch support the case for a Scottish ice-sheet margin at or close to the modern coastline before or at this time (c. 15-17 ka BP from CRONUS standard global production rate).

Encompassed by the field area are four, of the proposed six, ice stream onset zone catchments in mainland Scotland (Figure 1.7 and Folio 1): Loch Broom, Central Assynt (Oykel), Northern Assynt (Glencoul) and Loch Laxford) and as such, observations should allow discussion of former palaeo-flow lines.

Table 1.2: Geomorphological criteria for identifying palaeo-ice streams (Stokes and Clark, 1999).

Contemporary ice-stream characteristic	Proposed geomorphological signature
Characteristic shape and dimension	Highly convergent flow patterns
Rapid velocity	Highly attenuated bedforms (length-to-width >10:1) Boothia type erratic dispersal trains
Sharply defined shear margin	Abrupt lateral margin Lateral shear moraine
Deformable bed conditions	Glaciotectonic and geotechnical evidence of pervasively deformed till Submarine till delta or sediment fan

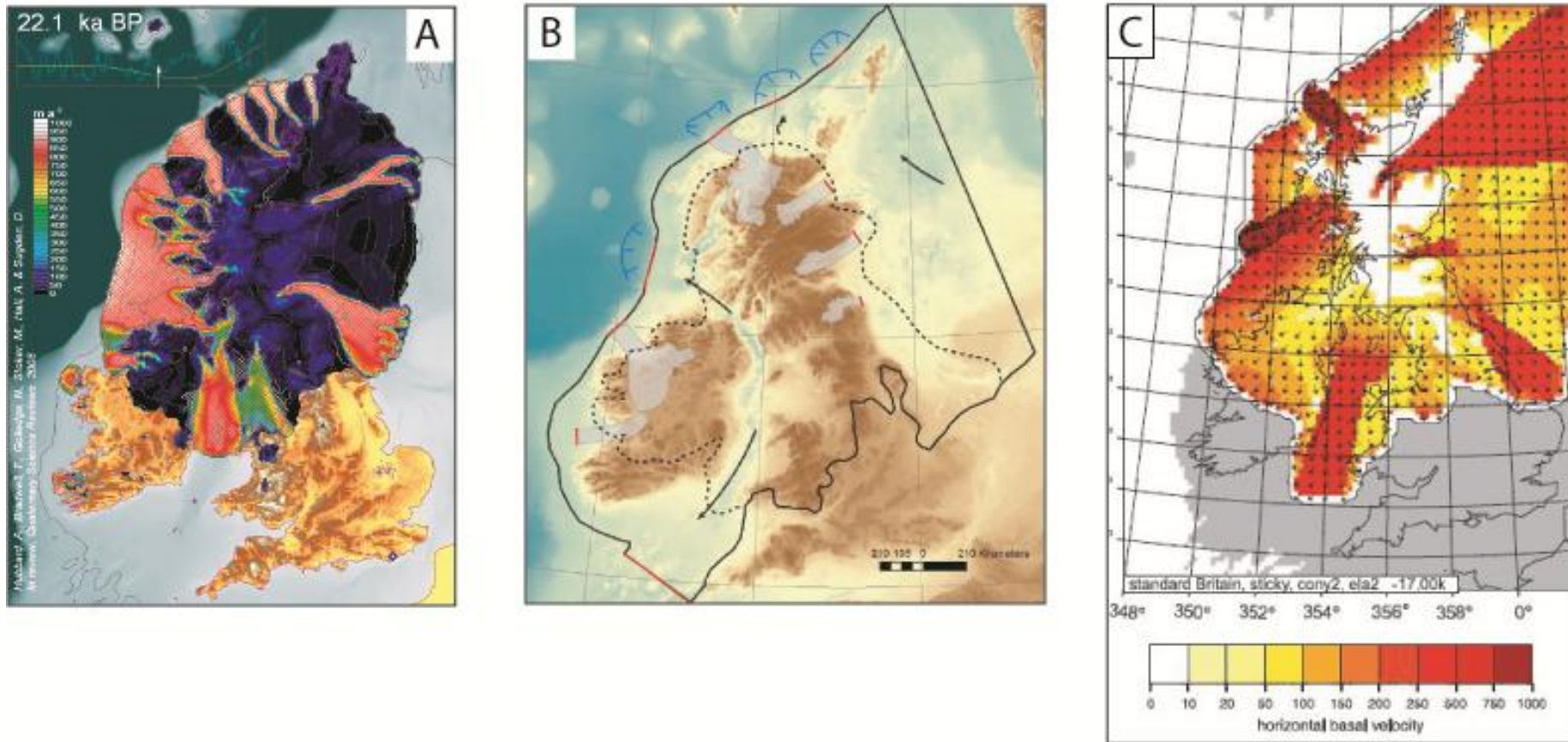


Figure 1.6: Selected ice sheet models predicting ice streaming in the vicinity of The Minch. A - (Hubbard et al., 2009), B - (Boulton and Hagdorn, 2006), C - (Clark et al., 2012).

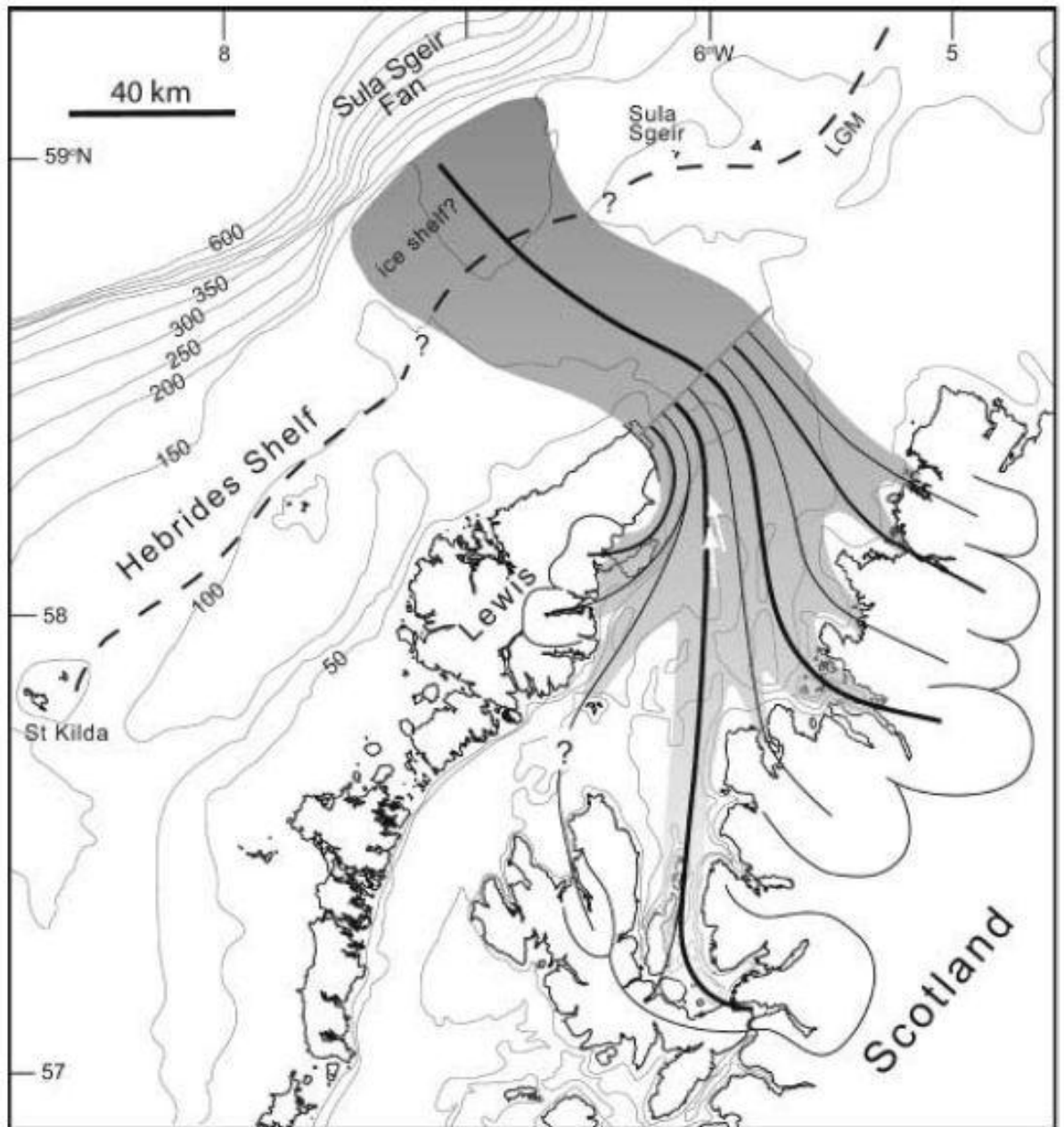


Figure 1.7: Reconstruction of The Minch palaeo-ice stream at maximum extent in the Pleistocene. Grey shaded area shows main trunk of ice stream and tributaries. Black lines are hypothesised palaeo-flow paths; line thickness gives impression of flow strength. Generalised ice-stream onset zone catchments are also shown. After Bradwell et al.(2007). The proposed ice stream catchments and onset zones are replicated on Folio 1.

1.5. Constraining the basal thermal regime of the last British-Irish Ice Sheet (BIIS)

The distinctive landscape of the far north west of mainland Scotland, with its characteristic inselberg hills, juxtaposed plateau remnants against knock and lochan lowlands and unusual occurrence of tors in multiple lithologies, is unique within the UK. These unusual geomorphological relationships typify the 'special geological problems' which have aroused the interest of scientists working in this region but have, so far, not been adequately explained in terms of landscape evolution. For example, the significance of sub-aerially weathered bedrock and extensive blockfield at high level sites remains largely unaccounted for in relation to survival through one or more glacial cycle.

Godard (1965) suggested that the broken plateaux of NW Scotland represented relict Tertiary surfaces preserved with minimal glacial modification. Investigation of these plateaux has been continued through Ballantyne and co-workers' extensive research on summit areas throughout the region (Ballantyne, 1997, McCarroll *et al.*, 1995b, Ballantyne *et al.*, 1997, Ballantyne and McCarroll, 1995). The presence of weathering limits separating glacially scoured surfaces from unmodified summits was initially explained by the exclusion of these areas from main stage glacial ice cover - the trimline theory (Ballantyne and co-workers). Glaciological impossibilities associated with the reconstruction of these weathering limits as trimlines relating to maximum ice surface elevations and increasing scientific support for the prior existence of cold-based ice at high elevation, has led to reassessment of these features (Ballantyne, 2003, Boulton and Hagdorn, 2006, Bradwell and Krabbendam, 2003). The significance of trimlines in Scotland has recently been reinterpreted as likely to represent minimum ice limits and probable englacial thermal boundaries (Ballantyne, 2010a). However, sufficient quantitative evidence for this theory has not been provided to reconstruct the regional pattern of subglacial thermal regime.

The subglacial thermal regime of the West Scottish Highlands has generally been presented as one of wet-based erosive ice (Figure 1.8), despite the aforementioned unanswered questions relating to preservation of probable pre-glacial land surfaces. Recent landform-focussed investigations have read important basal thermal regime signatures in the landscape of NW Scotland. Brook *et al.* (2004) contrasted the valley forms of NW Scotland with those of the Cairngorms suggesting greater glacial modification in the former, distinct from the selective linear erosion which characterises the latter. Bradwell (2005) linked the existence of bedrock megagrooves to the erosional activity beneath a fast flow ice sheet corridor in the south of the region while recognising that the sharp boundaries of landform suites, even on hard beds, probably related to a transition in basal thermal regime (Bradwell *et al.*, 2008b).

Research and resurvey in the area since 2004, has been led by the British Geological Survey (BGS) Northwest Highlands project, a combined bedrock and Quaternary mapping venture. Research focus has consequently shifted to examination of subglacial bedforms and particularly the role played by geological structural control. Underlying geological structures can have a dominating effect on the style and degree of bedrock erosion and weathering. Unless well-constrained and understood, the underlying geological structures can cloud interpretation of glacial landforms and hence glacial dynamics.

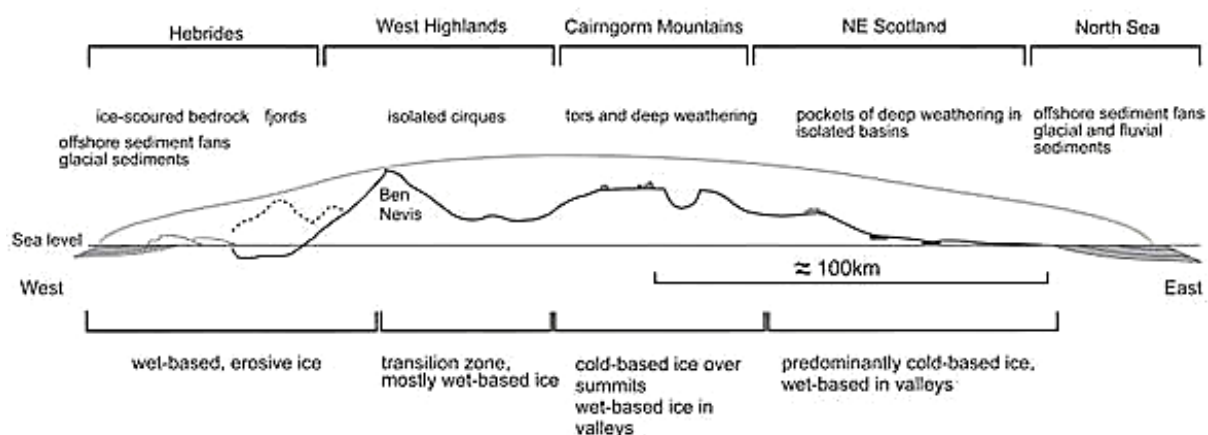


Figure 1.8: Schematic west-east transect across Scotland, showing the basal thermal regime inferred from diagnostic landforms, landform assemblages and deposits (Kleman and Glasser, 2007).

This complication is particularly prevalent in NW Scotland where a high geodiversity (recognised by the allocation of European Geopark status in 2004)

can prove both instructive in and obstructive to, landform-process determination. Recently, research interest (Bradwell, 2013, Krabbendam and Bradwell, 2011, Krabbendam and Glasser, 2011) has turned to quantitative geomorphology to characterise the influence of bedrock structure on the style and efficacy of subglacial erosion, and highlights the importance of observation-based landscape evolution theory in regions where bedrock land surfaces dominate. Ice sheet models of the last BISS lack constraints, particularly quantitative ones, of several fundamental parameters: influence of major ice streams, spatial distribution of cold-based ice, existence of nunataks and evolution of the basal thermal regime through the last glacial cycle.

1.5.1. Spatial and chronological retreat of the last BISS

Most mapping of Quaternary Geology in NW Scotland was undertaken by the original Geological Survey in the 19th century and has only recently been updated from the original survey (Peach and Horne, 1892) and 50k BGS sheets (92, 101E, 107E). Therefore, in places such as the surrounds of Loch Eriboll, this thesis maps and describes the Quaternary geology of previously unmapped ground (Figure 1.9).

Early geomorphic mapping by Charlesworth (1955) detailed multiple nested terrestrial ice limits and hinted at an offshore continuation to some of these. Charlesworth included a large piedmont lobe straddling the Summer Isles; later verified by onshore-offshore mapping and dated as a Lateglacial ice sheet limit by Bradwell *et al.*(2008a). Charlesworth's detailed ice limit map of Northern Sutherland (Figure 1.10) delimits confluent ice in the Eriboll- Hope catchments, and recognised the importance of a south eastern ice source for glaciers in this area.

In the last thirty years, field research into the Quaternary geology of far NW mainland Scotland has been facilitated by improved access to Western Sutherland offered by the Kylesku Bridge (1984) and has been driven primarily by members of the Quaternary Research Association (QRA). Enhanced interest during this time led to the publication of The Quaternary of Wester Ross Field Guide (Ballantyne and Sutherland, 1987) and Quaternary of Assynt & Coigach (Lawson, 1995). Lawson's work on erratic transport, boulder trains and the

orientation of striae in Assynt (Lawson, 1996, Lawson, 1990) has remained central to our knowledge of regional ice flow directions.

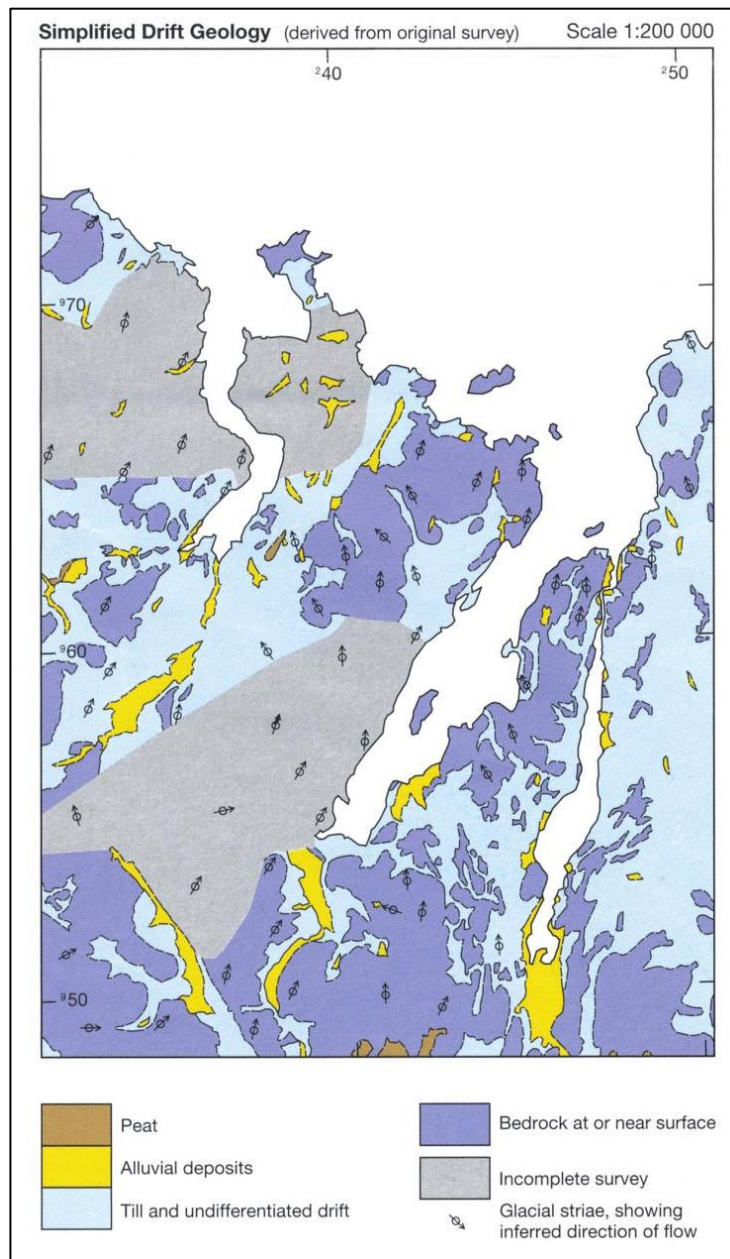


Figure 1.9: Example of a poorly mapped BGS Quaternary Geology sheet. Note the grey areas denoting “no data”. Simplified Drift Geology of the Eriboll area (BGS, 2002).

The aforementioned regional summit surveys undertaken by Ballantyne and co-workers resulted in the first empirically-based high resolution ice sheet reconstruction for NW Scotland (Figure 1.11). During the Last Glacial Maximum (LGM) the BIIS ice margin lay offshore of the current NW coast (Stoker *et al.*, 1993, Hall *et al.*, 2003). The search for ice sheet moraines, scarce on land, moved offshore with access to extensive and high resolution new bathymetric data (Bradwell *et al.*, 2008c). These near-shore echo-sounder bathymetry surveys have revealed a clear moraine sequence with evidence of oscillations and minor readvances relating to Lateglacial ice margin recession. Remote sensing survey and field mapping the last BIIS has built on these offshore observations towards a suite of retreat configurations for the entire ice sheet (Clark *et al.*, 2012). However, and somewhat fundamentally, ice sheet models of the BIIS currently lack quantitative constraints on the chronology of ice margin retreat and the lifespan of major ice streams.

Until application of TCN analysis in the 1990s, the main constraints on timing of ice-free conditions were derived from low elevation lake sediment studies, particularly the work of Pennington and co-workers who surveyed and sampled a number of freshwater bodies (lochs and lochans) throughout Assynt and Wester Ross. A general absence of glaciers in Assynt during the Lateglacial was proposed from the sedimentary and palynological record at Loch Sionascaig (Folio 1) with cold but open water conditions active snow beds indicated (Pennington *et al.*, 1972). This regional picture concurred with previous evidence of ice-free conditions at Loch Droma to the south c. 14.0-12.9 cal. ka BP during the Lateglacial Interstadial (Kirk and Godwin, 1963, Lowe *et al.*, 2008). At Cam Loch in central Assynt ice-free conditions are recorded prior to 13 ka BP (Pennington, 1977a, Pennington, 1977b, Pennington, 1975, Pennington *et al.*, 1972) with regional deglaciation of the area c. 15.5 ka BP implied (Lawson, 2010). In Assynt ice-free conditions at low elevation, prior to 13 ka BP, is also supported by radiocarbon dating of faunal remains from Antler Cave in the Allt nan Uamh cave system (Lawson, 2010).

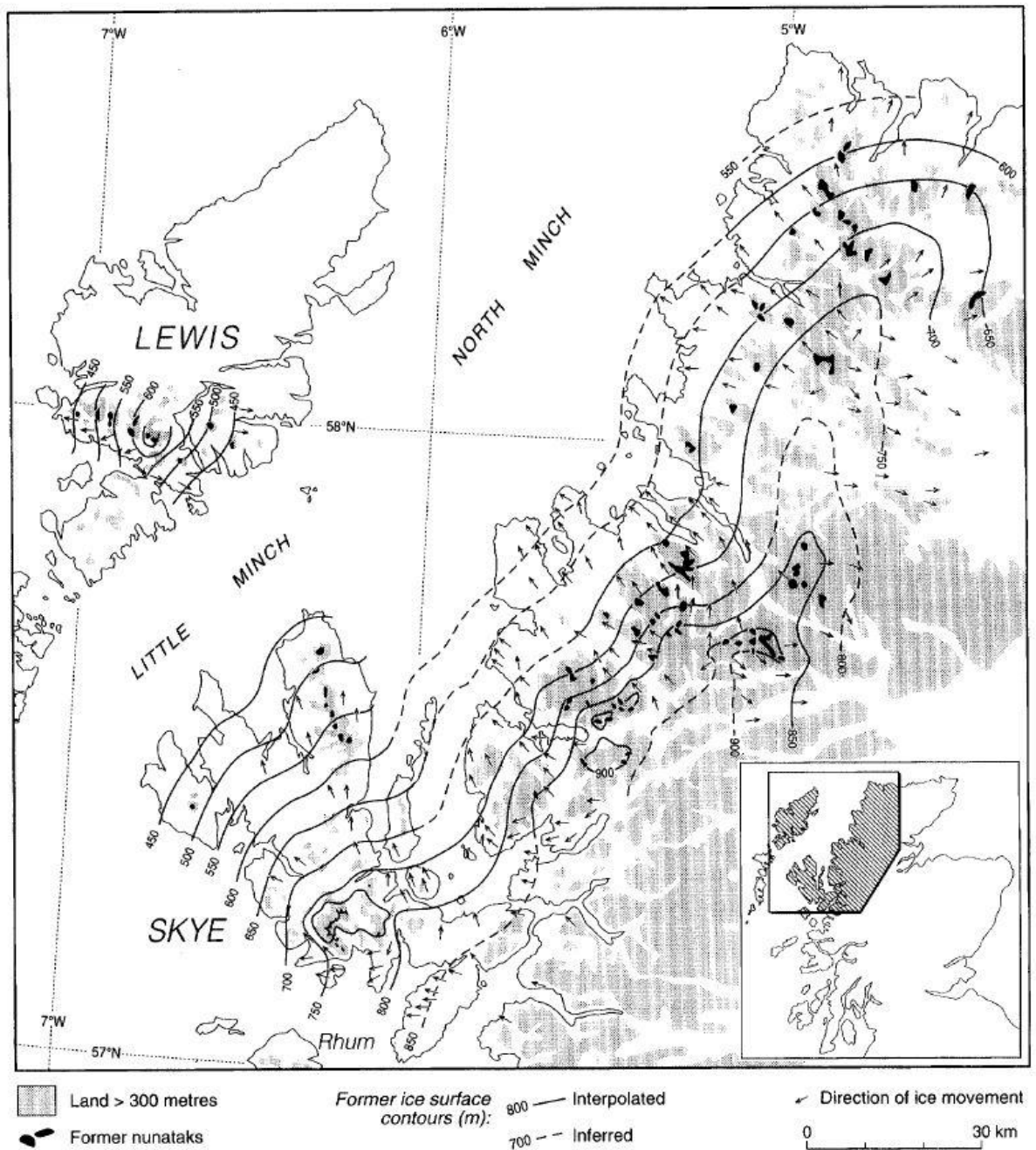


Figure 1.11: Maximum altitude achieved by last ice sheet in NW Scotland, based on periglacial, over-ridden summits and ice flow indicators at low level (Ballantyne et al., 1998).

On the north coast of Sutherland, deglaciation is minimally constrained by a radiocarbon date from lacustrine sediments in the kettle hole of Lochan an Druim adjacent to Loch Eriboll (Folio 1; Folio 3) of >12.5 ka BP (Birks, 1984). But, as this data may be subject to hard-water error, and has never been set in context of regional ice retreat it has been hard to constrain the extent of ice-free conditions at this time.

With the regional scarcity of Lateglacial sediments, most 'recent' mapping campaigns have concentrated on the clearer morainic limits associated with Lateglacial margin oscillations including the Wester Ross Readvance and the Younger Dryas glaciation (Robinson and Ballantyne, 1979, Bradwell, 2006, Bradwell *et al.*, 2008a, Ballantyne and Stone, 2012, Everest *et al.*, 2006). Much of this work was collated in a QRA field guide (Lukas and Bradwell, 2010a).

Reconstruction of the Younger Dryas equilibrium line altitude for the Western Sutherland ice field is 334 m a.s.l. (Lukas and Bradwell, 2010b). With much of the ground below 200 m a.s.l., major valley and coastal plain features sit outside these limits (Figure 1.12). Consequently the majority of glacial features and deposits in the study area relate to post-LGM recession of the ice sheet retreat (or Lateglacial) land system.

Detailed mapping (this study) around Loch Eriboll and Oldshoremore and on Beinn Uidhe addresses key issues of glacial landscape evolution, ice sheet recession and ice sheet thermal organisation. This mapping also contextualises the large exposure age dataset which provides a chronological framework for lateral and vertical retreat histories throughout the northwest of mainland Scotland. The exposure ages provide absolute rather than relative ages for the occupation of glacial limits and also provide age brackets for longer term landscape evolution processes such as tor and blockfield formation and modification. Furthermore this allows glacio-geomorphic process theories, such as the trimline theory, to be tested quantitatively rather than by unsatisfactory qualitative approaches. The precision gained by utilising a local TCN production rate (Methods: 2.2.1.4) yields high confidence in resolving closely spaced (geo)-chronological events.

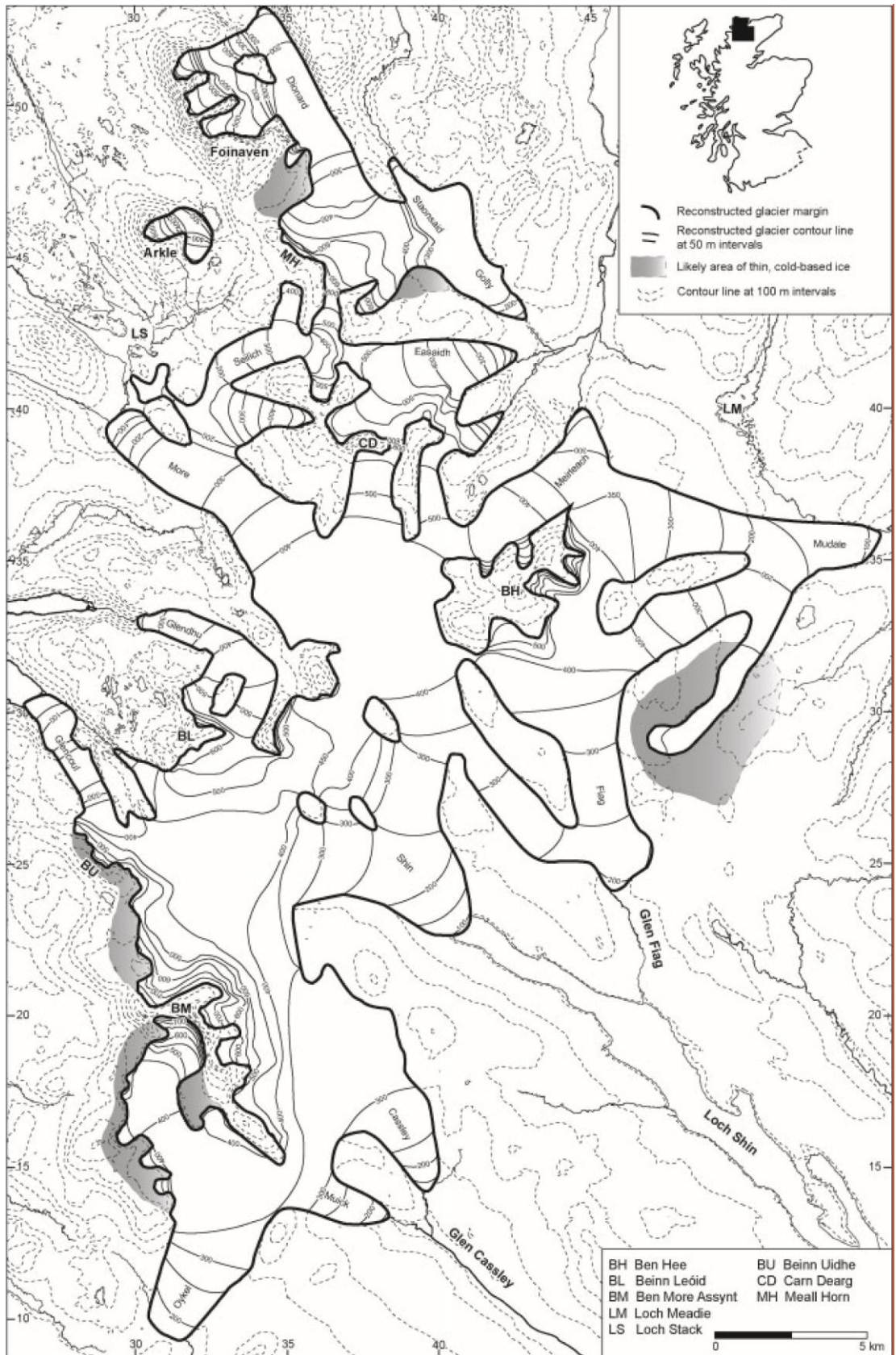


Figure 1.12: The West Sutherland Younger Dryas ice field, Lukas & Bradwell (2010). Field area of this study borders on the ice field at Assynt Mountains (bottom left) and Srath Coille nan Feàrna at toe of the Staonsaid Glacier (top centre).

Ice sheet thinning, and deglaciation of higher ground, which is harder to constrain, due to the absence of organic material, has received less attention in the literature. Cave deposits of the Allt nan Uamh and Traligill systems located in central Assynt (Folio 1) shed some light on local ice extent. The dating of a polar bear skull found in the Allt nan Uamh caves at 22.2-22.7 cal. ka BP (Kitchener and Bonsall, 1997) could suggest significant ice-thinning at or before this time in order that the animal remains could be brought to their sampled location below 340 m a.s.l. Speleothem growth activity, chronologically constrained with U-Th dating, requires ice-free or significantly thinned ice cover prior to ~18 ka BP in the Traligill valley (Kitchener and Bonsall, 1997).

The distribution of high level erratics has also been used by several authors to delimit conservative estimates of maximum vertical glacial extent (Lawson, 1990, McCarroll *et al.*, 1995a), though confident assignment of these erratics to a particular glacial stage has proved difficult. Ballantyne, McCarroll and co-workers' models of ice sheet thickness and operation are based on surveys of selected mountains in NW Scotland with interpolations made between these data points. These studies also use the elevation distributions of a single lithology of erratics (Lewisian) to support their model suppositions. In this thesis, observations of erratic transport, of multiple lithologies, provide increased detail on glaciological mechanisms. The associated exposure ages, constrain the timeframe in which specific glaciological regimes operated, as well the location-specific timing of ice-free conditions. Ballantyne *et al.*'s survey is augmented with data from selected hills: Beinn Uidhe, Sail Liath, and Speceinn Còinnich whose location, high level erratic distribution and elevation have been strategically chosen to help reconstruct previously unconstrained ice sheet parameters.

TCN analysis has so far (prior to this study) only been attempted in the south of the field study area (Stone *et al.*, 1998). The methodology for sampling at this site is questioned in relation to pressure shadow effects. More recently TCN dating, from nearby Torridon (Fabel *et al.*, 2012), has used the bedrock-erratic pair method to undertake glacial history analysis, but only in below-weathering limit situations. Hence the existing studies all have limited value for evaluating glacial erosion at high level (i.e. above weathering limits). Consequently the methodology employed in this study supplements and advances

the regional dataset by examining subglacial erosion at high elevation in addition to deglaciation of these sites. At all elevations, the limited sediment cover aids application of surface exposure dating by providing ‘clean’ sampling surfaces (Figure 1.5 C & F). In addition, the predominance of ‘zero-erosion’ post-glacial quartzite surfaces at high level sites (Figure 1.5 F) is particularly conducive to high confidence bedrock dating.

1.6. Thesis scope

This thesis is centred around a substantial new TCN dataset (63 samples in total) providing information on the erosional regime and retreat history of the last ice sheet, as well as answering longer term landscape evolution questions. This new data is put firmly in context by new geomorphic mapping and field observations with the aim of improving our understanding of the form and behaviour of a large ice-stream-dominated sector of the last BIIS. Utilising ^{10}Be as the predominant terrestrial cosmogenic nuclide restricts studies to investigation of surfaces less than 2.2 Ma (Gosse and Phillips, 2001).

Surface exposure dating in this thesis utilises a local production rate (Chapter 2) that significantly improves age uncertainties and interpretation (Fabel, 2012). Exposure dating was focussed on bedrock and erratic boulders to derive, not just surface exposure ages, but also, information on ice sheet basal thermal regime. The benefit of using these methodologies was the ability to understand a range of different geomorphic processes resulting in distinctive landforms e.g. knock and lochan topography, and subtle plateaux blockfields. The dataset, and its interpretation, is discussed at two scales. Firstly, to foster holistic understanding of *local* glaciological processes, field observations and surface exposure ages are reported by local geographic area (Results Chapter). This brackets datasets into glaciologically related groups which are used in later discussions of margin retreat (Chapter 4) and basal thermal regime (Chapter 5). Secondly, patterns in TCN and geomorphic data are analysed at a regional scale to characterise ice sheet catchment scale processes and glaciological events. The thesis is structured to facilitate discussion of the scope of this large new dataset and its implications for our understanding of the dynamics of the last British-Irish ice sheet in the following way:

- **Chapter 1 (Introduction):** The reader is familiarised with the remit of the project, the research context and conceptual framework. The field study area is also introduced.
- **Chapter 2 (Methodology):** This chapter briefly introduces the principles and considerations necessary to understand the application of terrestrial cosmogenic nuclide (TCN) analysis in this study. The chapter also details why, where and when the field campaigns were undertaken and how field observations were made.
- **Chapter 3 (Results):** Here the site-specific rationale for gathering data is presented and field data and observations are described by region. A final section introduces ‘newly identified geomorphic features’ previously undescribed in the British Isles.
- **Chapter 4 (Discussion: Horizontal and Vertical Ice Margin Retreat Chronology):** The post-LGM deglacial history of the ice sheet is discussed here through interpretation of TCN results from former ice margin positions. Data is discussed by region to investigate local ice organisation. The horizontal and vertical evolution of the ice sheet is discussed in terms of thinning, organisation and geometry of this sector of the last BIIS.
- **Chapter 5 (Discussion: Thermal structure and flow regime of the last BIIS in NW Scotland):** The significance of glacial and pre-glacial land surfaces are discussed here in relation to the evolution of the thermal regime of the NW sector of the last BIIS.
- **Chapter 6 (Conclusions):** Findings are summarised and current wider scientific debates of landscape evolution are discussed. The role of ice streams in the collapse of ice sheets and the response of ice sheets to external forcings is also discussed.

1.7. Wider Implications

Importantly, this work pre-empts, and dovetails with, the collaborative 5-year BRITICE-CHRONO (NERC consortium) project whose remit it is to “collect and date material to constrain the timing and rates of change of the collapsing British Irish Ice Sheet”. By numerically constraining ice-sheet retreat rates, investigating basal thermal regime and quantitatively constraining the severity of subglacial erosion over at least one full glacial cycle, the research within this thesis will hopefully provide valuable numerical boundary conditions for ice-sheet and landscape evolution models.

2. METHODOLOGY

2.1. Introduction

This research is the first geo-chronological study of a palaeo-ice stream initiation zone on predominantly hard bed terrain in the British Isles. Field campaigns in NW Scotland were directed towards gathering data to improve understanding of ice stream operation on the glacial dynamics of the last BISS; and answering questions relating to the long term landscape evolution. To this end, geomorphic mapping and terrestrial cosmogenic nuclide (TCN) analysis have been undertaken to:

- Characterise ice sheet flow organisation and thermal evolution;
- Constrain retreat of the NW sector of the last BISS spatially and temporally;
- Specifically this was achieved via three main strands of enquiry which aimed to constrain:
 - the retreat chronology of the ice margin following demise of the MPIS;
 - the cumulative ice sheet basal thermal regime (BTR) through time;
 - the minimum surface elevation of the ice sheet during the glacial maximum.

The geomorphic mapping methods are described first, followed by description of TCN methods and data analysis. The production mechanics of TCNs are introduced and the application of the technique to glacial studies is detailed. The implications of TCN data analysis, when working in a geologically complex area which includes the Moine Thrust Zone, is discussed; as are processing concerns and implications of sampling 'old' rocks such as Torridon Sandstone. Use of a new local production rate - the

Loch Lomond Stadial local production rate (Fabel, 2012) is explained and justified.

2.2. Geomorphic mapping

This study involved investigations over a large geographic area, ~2,300 km². Parts of the study area have been mapped by the BGS as part of the NW Highlands project (BGS, 2008, BGS, 2012, BGS, 2007, BGS, 2011). However in some areas mapping of the Quaternary geology is still incomplete - particularly around Loch Eriboll, Cape Wrath, parts of western Assynt and on the Wester Ross Headlands. Understanding the Quaternary history of this region through mapping, is particularly important as the landscape displays a juxtaposition of textures and contrasting geomorphic processes, with potential to inform on important glaciological boundary conditions. With the suggestion that the area was dominated by the activity of a palaeo-ice stream during much of the Devensian glaciation, mapping this area allows the signature of this ice stream to be recorded and investigated with limited interference of overprinting by Loch Lomond Stadial glacial activity.

Choice of mapping areas was informed by the omissions highlighted above and by the ice limit retreat pattern observed in the offshore record (Bradwell *et al.*, 2008a and c). Early stage ice limits, apparent on the continental shelf, were interpolated to have intersected the north coast near Eriboll and the west coast at Oldshoremore. Bracketing Cape Wrath, it was anticipated that mapping either side of a palaeo-ice sheet bed high would help to capture the geometries of the landward retreat of the ice sheet margin.

Field observation and mapping, supplemented by mapping from remote survey sources (NEXTMap DEM/DTM and Aerial Photos, Google Earth and MS Bing Maps (online aerial photograph resource) was used to investigate the geomorphology and Quaternary sediment cover across the region. Field mapping was carried out using 1: 10,000 scale field slips upon which geomorphic features, TCN samples and sediment sections were noted. Data from the field slips was then digitised in Adobe Illustrator.

2.2.1. Mapping, observation and sampling

Following an initial reconnaissance in October 2006, fieldwork was carried out during six fieldwork stints spread over four years:

- May 2007: TCN sampling on Beinn Uidhe, first mapping and TCN sampling survey around Eriboll, Glen Achall sampling.
- June 2007: Breabeg TCN sampling, Cul Beag TCN sampling, second Eriboll mapping and TCN sampling campaign, Sail Liath TCN sampling, Tanera More TCN sampling.
- May 2009: First Oldshoremore & Sheigra sampling and mapping campaign, first Ben Mor Coigach TCN sampling campaign.
- August 2009: Second Oldshoremore & Sheigra TCN sampling and mapping campaign.
- August 2010: Third Eriboll mapping campaign.
- September 2010: Targeted TCN sampling trip: Cranstackie, Portnancon, Oldshoremore, Ben Mor Coigach, Beinn an Eòin.

Field mapping was concentrated around Loch Eriboll where a complex and extensive suite of glacial landforms is identified and where BGS mapping is currently incomplete. The most detailed mapping of the Eriboll area, prior to this study, had been that of Charlesworth with the BGS mapping of the Loch Eriboll area omitting the whole eastern slope of Cranstackie and much of the western flank of Loch Eriboll. This BGS map (derived from the original survey by Peach *et al.* 1889 revised 1893) distinguishes only between peat, alluvium, till/drift, bedrock and striae. This basic mapping has been augmented (this study) with discrimination of blockfield, slope regolith, fluvioglacial and marine deposits. The occurrence of larger glacially abraded forms with flow direction is also noted.

Glacial landforms and sediments were mapped in the field in selected areas (Loch Eriboll and Oldshoremore) where previous mapping was incomplete and additional interpretation was required. Boulder and bedrock surfaces were selected for TCN analysis and details of their location recorded (See Results chapter). Field observations and mapping were supplemented with remote survey using NEXTMap supplied through studentship eligibility by the Natural Environmental Research Council Earth Observation Data Centre (NEODC). NEXTMap tiles were mosaicked and hill shaded to aid identification of geomorphic features and overlain by aerial photography held by the British Geological Survey. Interpretations were further aided by observation of features using the aerial imagery of 'Bing' maps and 3-D visualisations created using Google Earth.

2.3. Terrestrial Cosmogenic Nuclide (TCN) Analysis

TCN analysis was used in this study for three reasons:

- The technique allows assessment of 'event surfaces' therefore providing information on both erosion and exposure duration-key questions in glacial landsystems;
- It utilises quartz-rich rocks, which are common, rather than sediments, which are scarce, throughout the majority of the field study area;
- The half-life of the nuclides used, ^{10}Be and ^{26}Al , easily spans the entire Pleistocene, with applicability at both the Holocene and early Devensian (c. 110 ka BP) ends of the period.

This section of the methodology chapter introduces the main principles of TCN analysis and application. An outline description of the laboratory and analytical procedures used to convert a whole rock sample into an AMS target is then provided. Finally, the calculations required to derive an exposure age from the AMS data are discussed. Full details of laboratory procedure are in Appendix 1 & 2.

2.3.1. TCN theory

2.3.1.1. TCN Production

Terrestrial cosmogenic nuclides are rare atomic species, differing from those found inherently in rocks of the surface in their nucleic constitution. TCN are the products of primary and secondary cosmic ray particles produced from super novae. At the Earth's surface, secondary cosmic-ray particles, produced following interaction of primary cosmic rays with the Earth's atmosphere account for >98% of nuclide production. TCN nuclei may be produced by collision of high energy neutrons with atomic nuclei resulting in detachment of neutrons and protons in lighter atomic nuclei. This is spallation, accounting for >98% of TCN production at the ground surface.

Negative muon capture reactions only account for c. 2% of TCN production of ^{10}Be and ^{26}Al at sea level high latitude (SLHL) (Heisinger et al., 2002) (Table 2.1), with recent research and debate suggesting that the contribution of muons has been overestimated (Stone, 2000). SLHL ($\geq 60^\circ$) is used as a baseline from which site specific nuclide production rates can be scaled. Between latitudes of 60° to 90° geomagnetic variation does not affect the cosmic ray flux, and, due to high atmospheric shielding, production rates are low at sea level (Phillips, 2001). However, muogenic TCN production increases with depth such that they become important contributors to exposure histories in burial studies and areas with high levels of erosion over the time span of interest. Site specific production rate calculations in this study do not include a muonic contribution. Production of ^{10}Be in surface rocks is largely by spallation reactions from O, with heavier elements like Mg, Al, Si and Ca contributing nuclides from a small number of reactions. Consequently the target minerals for ^{10}Be extraction are usually silicates, specifically quartz.

Meteoric ^{10}Be is produced in the atmosphere and can be adsorbed to sample material. As meteoric ^{10}Be is produced at a rate 10^3 faster than the average rate in surface rocks, removal of this surficial component is required to avoid contamination of the sample with nuclides which do not

relate to the exposure of the surface. As meteoric contamination of the ^{10}Be concentration is of significant concern, quartz has been used as the target mineral in this study as selective etching to clean grain surfaces is easier than in other mineral systems.

In silicate minerals ^{26}Al is produced from ^{27}Al and Si. ^{27}Al is native in many mineral structures and can present a major issue in accurate calculation of the nuclide concentration by swamping the ^{26}Al signal. The selective etching employed to clean quartz grains also works to reduce the background concentration of ^{27}Al by preferentially removing feldspars which are a common accompanying mineral to quartz in many rock types and the main source of ^{27}Al in a sample. Samples must have <300 ppm Al so that the $^{26}\text{Al}/^{27}\text{Al}$ ratio can be measured.

As ^{26}Al and ^{10}Be are both radionuclides, their concentration in a surface is dependent upon the balance of decay rate, exposure duration and erosion rate:

$$N = \frac{P e^{-\frac{\rho z}{\Lambda}}}{\lambda + \frac{\epsilon \rho}{\Lambda}} \left(1 - e^{-(\lambda + \frac{\epsilon \rho}{\Lambda})t} \right) + N_{inh} e^{-\lambda t}$$

(1)

Where N is the total nuclide concentration in the sample (atoms g^{-1}), N_{inh} is any inherited nuclide concentration from previous exposure (atoms g^{-1}), P is the nuclide production rate at the surface ($\text{atoms g}^{-1} \text{ yr}^{-1}$), ρ is density (g cm^3), z is sample thickness (cm), Λ is attenuation length (g cm^{-2}), λ is the decay constant ($^{10}\text{Be} = 5.09667 \times 10^7 \text{ yr}$, $^{26}\text{Al} = 9.83187 \times 10^7 \text{ yr}$), ϵ is the surface erosion rate ($\text{g cm}^{-2} \text{ yr}^{-1}$) and t is time (yr).

The production rate ratio of ^{26}Al to ^{10}Be is 6.75 (Balco et al., 2008). For a buried surface, i.e. no longer accumulating nuclides, the $^{26}\text{Al}/^{10}\text{Be}$ ratio in the surface changes over time as ^{26}Al decays quicker than ^{10}Be . Present analytical uncertainty means that the minimum burial time that can be detected is about 100 kyr. Consequently, in surfaces where a long (>100 kyrs) burial history, whether by ice, sediments or water is suspected,

dual-isotope analysis of surface samples with a constrained erosion history may clarify complex exposure in the past. Detecting exposure histories complicated by burial is particularly important for the high level sampling sites in this study as their glacial history remains unclear due to the scarcity of geomorphic evidence and historic difficulties of interpretation.

Table 2.1: TCNs used in this study (after Dunai, 2010).

<i>Isotope (half-life)</i>	<i>Main target minerals</i>	<i>Predominant target elements</i>	<i>Reaction pathways (SLHL)</i>
¹⁰ Be (1.36 ± 0.07 Ma)	Quartz	O, Si (Mg)	Spallation: >98%
²⁶ Al (708 ± 17 ka)	Quartz	Si	Spallation: >98%

2.3.1.2. Utilisation of TCN data in glacial studies

TCN analysis is well suited to glacial studies in that samples may be derived from bedrock surfaces as well as, and often in preference to, sediments. This is an extremely useful feature of the technique as glacial, or glacially-affected, landscapes, especially in hard rock terrains, may be sediment-poor, with sediment depocentres lying offshore, or with fine sediments removed by aeolian or fluvial erosion. Consequently, bedrock or boulder-dominated terrains provide ideal sampling grounds for cosmogenic studies given one major caveat - the exposure age will only be as accurate as the understanding of the geomorphic history of that site. A statistically significant sample set may be used to argue between conflicting hypotheses, and a single exposure age can provide an absolute age for a feature or surface, but *only* where the geomorphic history of the surface is well-constrained such that the origin of, and processes which have potentially affected, an event surface are defined. Ergo, accurate mapping, and an understanding of the possible equifinality of feature formation is essential in understanding the data produced by TCN analysis.

In particular, understanding how the environment of a sampled surface has changed through time and the effects this has on TCN production and decay in this surface is essential. The exposure age of a sample is dependent upon the production rate of the nuclide of interest, and this in turn scales with the depth of the sample below the surface. Therefore the small scale landscape evolution history of the sample site must be constrained to understand the exposure history. This history can be divided into erosional and landform stability components. As nuclide production decreases with depth into the substrate (**Figure 2.1**), coverage of a site by sediment, snow, rock, water, ice, and vegetation thick enough to obstruct or attenuate the cosmic ray flux will lead to a reduction or cessation in nuclide production. Consequently this shielding will lead to a reduction in TCN concentration, and therefore surface exposure age, in the measured sample surface. This can produce unexpectedly ‘young’ ages for sites where the shielding history is under-estimated.

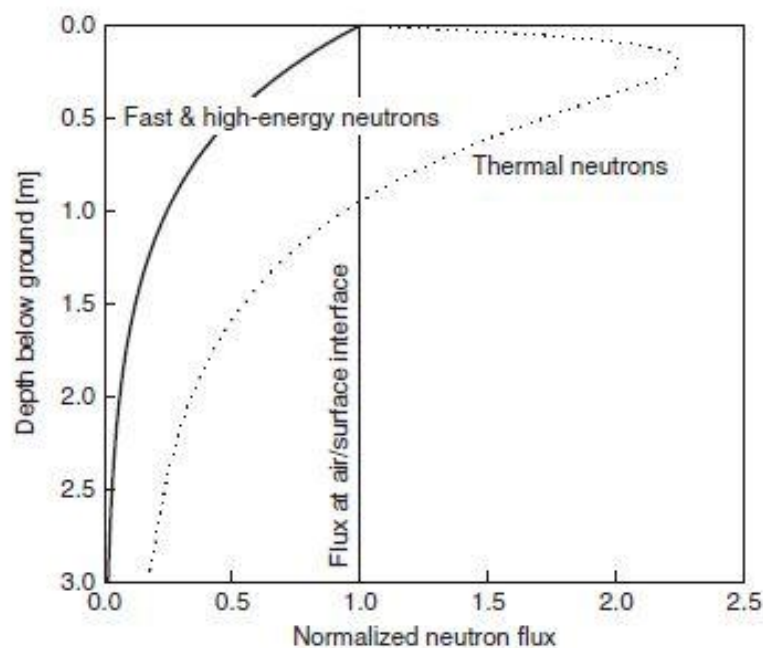


Figure 2.1: Neutron flux below the air-surface interface. The fast- and high- energy neutron flux decreases exponentially with depth. After (Dunai, 2010).

The stability of landforms has a strong influence on the interpretation of TCN concentrations. Boulders in unstable situations, such as embedded

in moraines or on sloping blockfields, may experience overturning, downslope ploughing and emergence from sediment cover. Applegate (2009) outlines the main processes boulders are subjected to in the construction and degradation of moraines and the resulting effect on TCN concentration (Figure 2.2). Consequently, sampled surfaces may contain a concentration reflective of a complex exposure history which includes variation in depth beneath the ground, or rock, if overturned. Overturning, periods of burial and (if involving a significant reduction in elevation) boulder ploughing, will all result in a reduction in production rate and therefore in resulting exposure age. Unless these factors can be quantified, ages from samples which have potentially experienced these situations must be stated as *minimum ages*.

2.3.2. Processing from rock to TCN concentration

2.3.2.1. Sampling

As mentioned above, recording the geomorphic context of a sample is integral to deriving an accurate and meaningful exposure age. When collecting samples, the following protocol (after Dunai, 2010) was used to ensure that sufficient contextual information required for calculating and interpreting TCN data was obtained from each site. The shielding (past or present) of the site by sediment, snow, water or ice cover was assessed. Topographic shielding was estimated through measurement of the 360° skyline geometry to provide a shielding factor, this included local ‘self-shielding’ by dipping sample surfaces and nearby boulders. The ‘originality’ of the surface i.e. whether a surface was freshly (post-glacially) exposed or had experienced previous exposure was investigated.

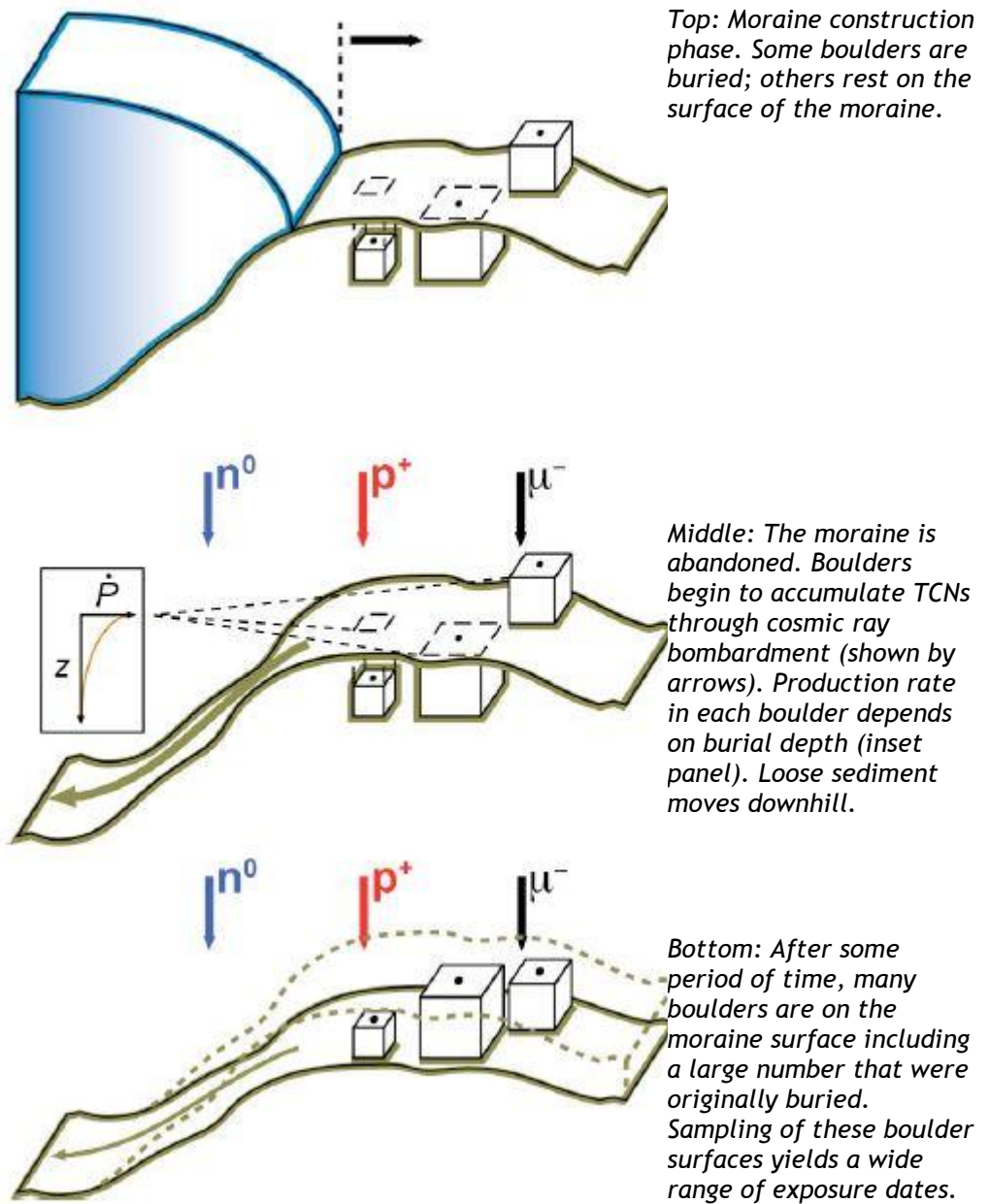


Figure 2.2: Conceptual model of moraine degradation, after Applegate (2009).

When sampling boulders, the stability of their current location was of particular concern especially where underlain by mobile sediments such as on a moraine. Therefore potential overturning of boulders was assessed by examining the relative 'freshness' of boulder surfaces, the local mobility of slope sediments and evidence for post-depositional mass movement processes such as boulder ploughing or moraine degradation. Evidence of weathering was noted and assessed during sample selection and features associated with the sampled surface such as solution pits, weathering rinds, edge rounding and granular disaggregation were recorded and quantified. Where possible, multiple samples were collected at each site to increase statistical confidence. Where lithologies allowed Basal Quartzites were sampled by preference because of their acknowledged resistance to post-glacial weathering and therefore potential retention of the event surface of interest. Where erratics on quartzite bedrock were to be sampled, quartz-rich lithologies were targeted with sample size adjusted according to quartz content. Hardness and susceptibility to chemical and physical weathering were taken into account when collecting boulders. Where boulders were quartzite, a hard chemically resistant lithology, rounder forms were chosen to ensure they had experienced subglacial conditions. Conversely where Torridon sandstone was been sampled blockier specimens were preferred under the hypothesis that they had preserved less pre-glacial subaerial weathering or had lost less surface material to post-glacial weathering.

Where exposure ages were to be compared between lithologies, quartzite ages were prioritised as having a more-well-constrained zero postglacial erosion history. Constraint on the post-glacial exposure history of Torridon sandstone, Lewisian Gneiss and Moinian lithologies could not be well-constrained due to lack of erosion datasets and controls for the specific region and lithologies of interest.

A mallet and chisels were used in the field to remove quartz-rich material from bedrock or larger boulders. Rounded and/or smaller boulders were marked up with top surface and any portion of boulder which was buried was indicated. The desired portion (usually 2-5 cm thickness of the

top surface) of these larger samples was separated from the mass using a rock saw.

2.3.2.2. Extracting Be and Al from a whole rock sample

This section summarises the main steps of sample preparation. Full details are given in Appendix 1. Sample preparation for TCN analysis is aimed at:

- Concentrating and purifying the selected target mineral by physical and chemical procedures;
- Extracting the Al and Be from the quartz;
- Measuring the ratio of the radionuclide to the stable nuclide.

The samples underwent physical and chemical preparation at the Gregory Building mineral separation laboratories of the School Geographical and Earth Sciences at the University of Glasgow. To initiate the extraction process, the samples were crushed and ground into component grains and the desired sample material grain size (250-500 μm) was separated by sieving. The grains were then cleaned in aqua regia (HCl and HNO_3) to remove surficial contaminants such as carbonates, metal from crusher and grinder, and organic compounds. Depending on the mineralogical composition of the rock, a number of different purification processes were used to remove heavy minerals and aluminosilicates from the sample.

Only a few of the samples ($n = 14$) were put through heavy liquid separation. Heavy liquid separation was found to be largely ineffective on quartzite lithologies (where the main contaminant was feldspar) and Torridon Sandstone where grains are often lithic composites and not responsive to this type of separation. Froth floatation was found to be more effective and efficient at mineral separation for these lithologies. This procedure separates feldspar and mica from quartz using electrostatic differences of the mineral surfaces. Phosphoric acid treatment, which

selectively dissolves aluminosilicates but not quartz, was necessary for two samples (TANM02 and BGSD1) with very high feldspar content.

Following mineral separation, selective etching of the mineral grains was carried out in a dilute solution of hydrofluoric (HF) and nitric (HNO₃) acid. This removes soluble impurities and meteoric ¹⁰Be by removing the outside surface of the grains. The inherent ²⁷Al is also reduced by this process through preferential removal of aluminosilicates over quartz. A minimum of three etches was used for all samples. Most vein quartz samples were 'clean' following three etches, though high feldspar contributions in quartzite samples, and contamination by iron and other fine-grained lithic residues in the Torridon Sandstone samples required an extended leaching process of up to 23 etches in some cases (CULB01 and SAIL02). To establish the purity of the quartz, small aliquots of the samples were dissolved in HF and Al concentrations were determined using flame atomic absorption spectrometry (AAS). A high Al content (>120 ppm) was taken to indicate that the sample still contained a large proportion of feldspar contaminants and, potentially, that the surface of the quartz would also not be free of meteoric ¹⁰Be contamination. Consequently samples were either re-entered into the etching process or deemed 'clean' and ready for chemical preparation.

The chemical processing required to extract ¹⁰Be from prepared clean quartz was completed in the GU-SUERC clean laboratories at the Scottish Universities Environmental Research Centre (SUERC). A mass of the purified quartz (c. 20-30 g in most sample cases) was dissolved in HF to liberate the elemental components. The solutions were 'spiked' with ⁹Be carrier, and also Al carrier if the initial Al assay revealed a low Al content (<1000 µg Al in the total sample) in order to create a sufficient amount of target material for analysis by accelerator mass spectrometry (AMS). The fluorosilicate was fumed off and the residue (containing Be, Al, Ti and alkali earth elements) was taken up in HCl. Resin columns were used to separate Be and Al from undesirable elements. Iron was removed by anion-exchange and exchange removed Ti and allowed separation of Al and Be. Beryllium was precipitated out of solution as Be(OH)₂ with B(OH)₃ removed by rinsing. In a furnace the Be(OH)₂ was decomposed, or calcinated, to

BeO. Niobium was mixed with the crushed BeO to add bulk to the target material and improve thermal conductivity before the mixture was pressed into Accelerator Mass Spectrometer (AMS) cathodes. An equivalent process was used to convert the Al fraction to AMS targets. For ^{26}Al a separate determination of the ^{27}Al content of the sample was acquired utilising an Inductively Coupled Plasma Mass Spectrometer (ICPMS).

In order to derive the ratio of ^9Be and ^{10}Be atoms in each sample from which an exposure age can be calculated, the prepared target (cathode) is inserted into the AMS (Figure 2.3). Caesium (Cs) ions focused onto the cathode and used to ‘sputter’ the sample material in the target cathode to initiate a beam of negatively charged ions, which accelerate towards the positive terminal charge at the centre of the 5 MV Pelletron. The beam is bent by the first 90° analysing magnet which filters out the majority of undesirable elements and molecules. The beam then enters the tank of the accelerator where it passes through an argon gas stripper at the centre of the tank that strips electrons from the negatively charged ions and changes them to positive ions. The beam is bent by the second 90° analysing magnet which filters out the majority of undesirable elements and molecules. The beam then enters the tank of the accelerator where it passes through an argon gas stripper at the centre of the tank that strips electrons from the negatively charged ions and changes them to positive ions.

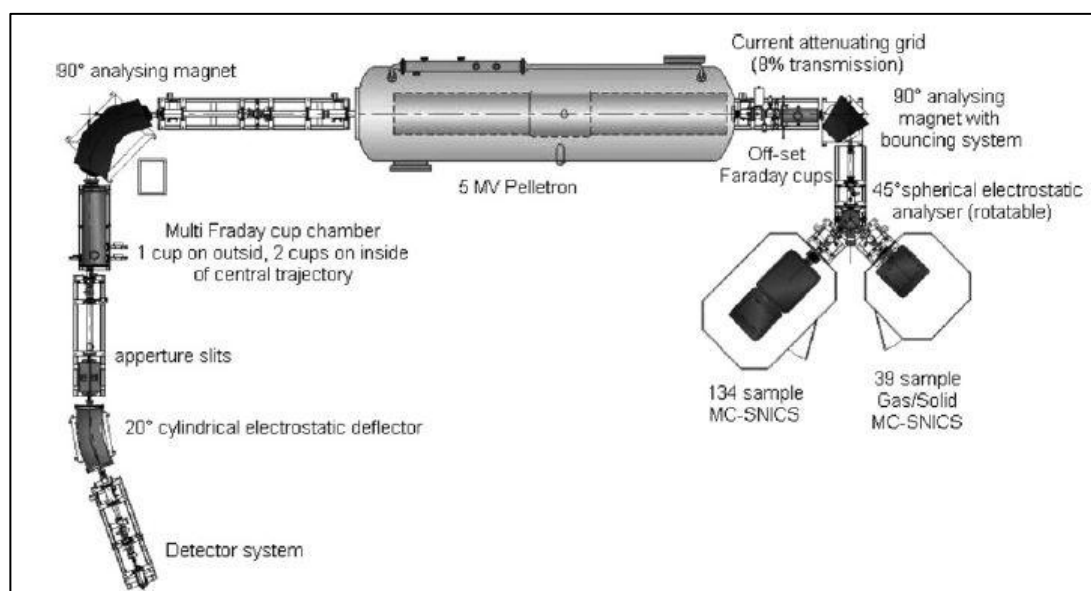


Figure 2.3: Schematic layout of the SUERC 5MV accelerator mass spectrometer. After Maden et al. (2007).

Following acceleration away from the 5 MV terminal at the centre of the Pelletron, the ion beam is separated by the second 90° analysing magnet into stable- and radioisotopes. Faraday cups collect the stable isotopes and measure the current through current amplifiers. The radioisotope beam is further cleaned by a 20° electrostatic analyser before passing through a membrane that removes B, and into a gas ionisation detector where individual radionuclides are counted.

2.3.2.3. Calculating a surface exposure age

The AMS measures the ratio of ^9Be and ^{10}Be atoms in a target (Figure 2.3). From the known quantity of ^9Be atoms added with the Be carrier the concentration of ^{10}Be atoms may be calculated. From this concentration an exposure age may be calculated by solving Equation (1) for time t (exposure duration). The final uncertainty in the calculated exposure duration includes the analytical and systematic uncertainties. The latter is dominated by production rate uncertainties - 9% for the global reference production rate (Balco et al., 2008). Accurate measurement of a surface's exposure age is dependent upon three things:

- Minimisation of uncertainties and error in the lab processing;
- Full accounting of site specific production-rate affecting variables/site characteristics (Tables 3.2, 3.4, 3.6, 3.8, 3.10, 3.12, and 3.14 in Results Chapter);
- Use of a local production rate to reduce the production rate uncertainty and increase the accuracy of assignment of exposure ages to event surfaces.

The first two variables have been outlined in the preceding sections with site variables discussed in more depth in the Results chapter. The following section discusses the implementation of a local production rate in calculation of surface exposure ages for samples in this study. All exposure ages quoted in this thesis are 'apparent exposure ages'. This is because, in

the absence of independent control on erosion rate, they represent the minimum exposure time required for the sample to accumulate their measured ^{10}Be concentration. With additional information on erosion history for the sample and site, ages may increase.

2.3.2.4. Use of a local production rate

In order to interpret a nuclide concentration, a production rate that reflects *local* changes in TCN production over time must be used. These changes, which occur over timescales of 10^3 - 10^6 years (which has repercussions for the exposure history of the sampled surfaces in this study) are caused by solar modulation of the galactic cosmic ray flux, changes in atmospheric shielding variations, and changes in the intensity and configuration of the Earth's magnetic field (Schaefer and Lifton, 2007). The CRONUS global reference production rate is based on a calibration dataset of samples from seven studies, some of which self-assign feature ages without independent age control. Recently, several authors from the TCN community have challenged the global CRONUS production rate (4.39 ± 0.37 atoms/g/yr Lm scaling) as being too high to accurately evaluate surface exposure ages in western Europe (Goehring *et al.*, 2012; Fenton *et al.*, 2011). Consequently, in order to derive the most accurate exposure age for a surface and to avoid the ~9% uncertainty associated with the reference production rate, it is important to use a local production rate.

A local production rate uses an independent chronometer to calibrate a measured nuclide concentration. In this study a Scottish local production rate, known hereafter as the Loch Lomond Stadial Local Production Rate or LLS LPR is used. This production rate of 3.92 ± 0.18 atoms $\text{g}^{-1} \text{yr}^{-1}$ is 11% lower than the CRONUS global production rate, consequently yielding *11% older* ages for a given nuclide concentration (Fabel, 2012). This LPR was developed by utilising the positioning of TCN materials in an independently constrained morpho-stratigraphic assemblage. The TCN concentrations are derived from boulders on a moraine complex thought to represent a single chronological limit - the Loch Lomond Stadial readvance limit. The age of the moraine limit is

tightly constrained by varve sequencing and plant macrofossil radiocarbon dating in a palaeo-ice-dammed lake formed by the blocking presence of ice at the moraine from which the boulders are sampled (MacLeod et al., 2011).

Importantly, not only is the production rate lower for the LLS LPR, but the uncertainties, dependent *only* upon uncertainties in the age constraint of the chronostratigraphy at Loch Lomond, are c. 3.8% lower than those associated with the multi-study calibration-dataset-controlled CRONUS global production rate. Consequently use of the LPR allows greater confidence in discrimination between geomorphic events with close chronological spacing.

In the following Results chapter, use of a higher precision (than the CRONUS global reference production rate) local production rate is seen to highlight sampling and landform process issues that would otherwise be masked by systematic uncertainty. Geomorphic and surface exposure data are described in parallel to facilitate the best appreciation of the formation processes of event surfaces, the significance of features in the deglacial chronology and to provide the necessary full geomorphic explanatory context for TCN data.

3. RESULTS

3.1. Introduction

This chapter describes the geomorphic features mapped from fieldwork and remote sensing data across the field area. In areas of high density sampling for terrestrial cosmogenic nuclide (TCN) analysis, detailed ground survey and geomorphic field mapping have been completed specifically: around Loch Eriboll (Folio 3); on Beinn Uidhe (Figure 3.31) and at Sheigra and Oldshoremore (Figure 3.28). Intervening areas have been investigated through general field observations and mapping using remotely sensed datasets.

TCN samples have been collected under two main rationales: firstly, tracing the retreat, at low level, of lateral ice margins and secondly; constraining the geometry and thermal regime of the British-Irish ice sheet in the vertical plane. Forty one TCN ages were obtained from samples collected at well-defined low elevation former ice limits. Sampling was focused along three former ice sheet flow lines in an attempt to track ice front retreat during deglaciation:

- Transect 1: Eriboll (Rispond to Srath Beag; ~18 km from N-S);
- Transect 2: Oldshoremore (5 km from NW-SE);
- Transect 3: Summer Isles (Tanera Mor to Glen Achall; ~25 km from NW-SE).

Samples from transects 1 and 2 bracket disintegration of the Minch palaeo-ice stream by dating retreat of separate, topographically constrained outlet glaciers on either side of Cape Wrath during ice sheet wastage.

The Summer Isles transect dates two significant ice margin positions occupied during offshore to onshore retreat of the ice sheet. These samples lie on a 25 km long flow line between an equivalent of the Wester Ross Readvance Moraine (consistent with ice *sheet* geometry) and the well-defined outlet glaciers of the independent Beinn Dearg ice cap (which existed during the Younger Dryas and some or all of the Lateglacial Interstadial) (Finlayson *et al.*, 2011). Consequently, and importantly, Transect 3 charts the chronology of retreat from a major marine-influenced ice sheet outlet through terrestrial ice-cap retreat back to an independent Lateglacial mountain ice-field. Additional samples presented here for the first time, from the Gruinard Bay area (DD01/2) and Little Loch Broom (BGSD1/2) advance earlier work by Bradwell *et al.* (2008) and constrain the marine-influenced margin following ice-stream decay.

The second sampling rationale investigates former ice sheet thickness and basal thermal regime in the NW sector of the BIIS. Sampling of high elevation bedrock-erratic pairs constrains the minimum elevation of the Late Devensian (Weichselian) ice sheet and also provides information on the former distribution of cold-based vs warm-based ice. Erratic boulders, deposited on mountain summits and flanks by the ice sheet margin during ice sheet retreat, track deglaciation and also constrain minimum ice sheet altitude; while paired bedrock samples indicate relative subglacial erosion efficacy and consequently shed light on the ice sheet's basal thermal regime. Seven mountains were sampled, generating twenty two exposure ages.

3.2. N coast, Sutherland

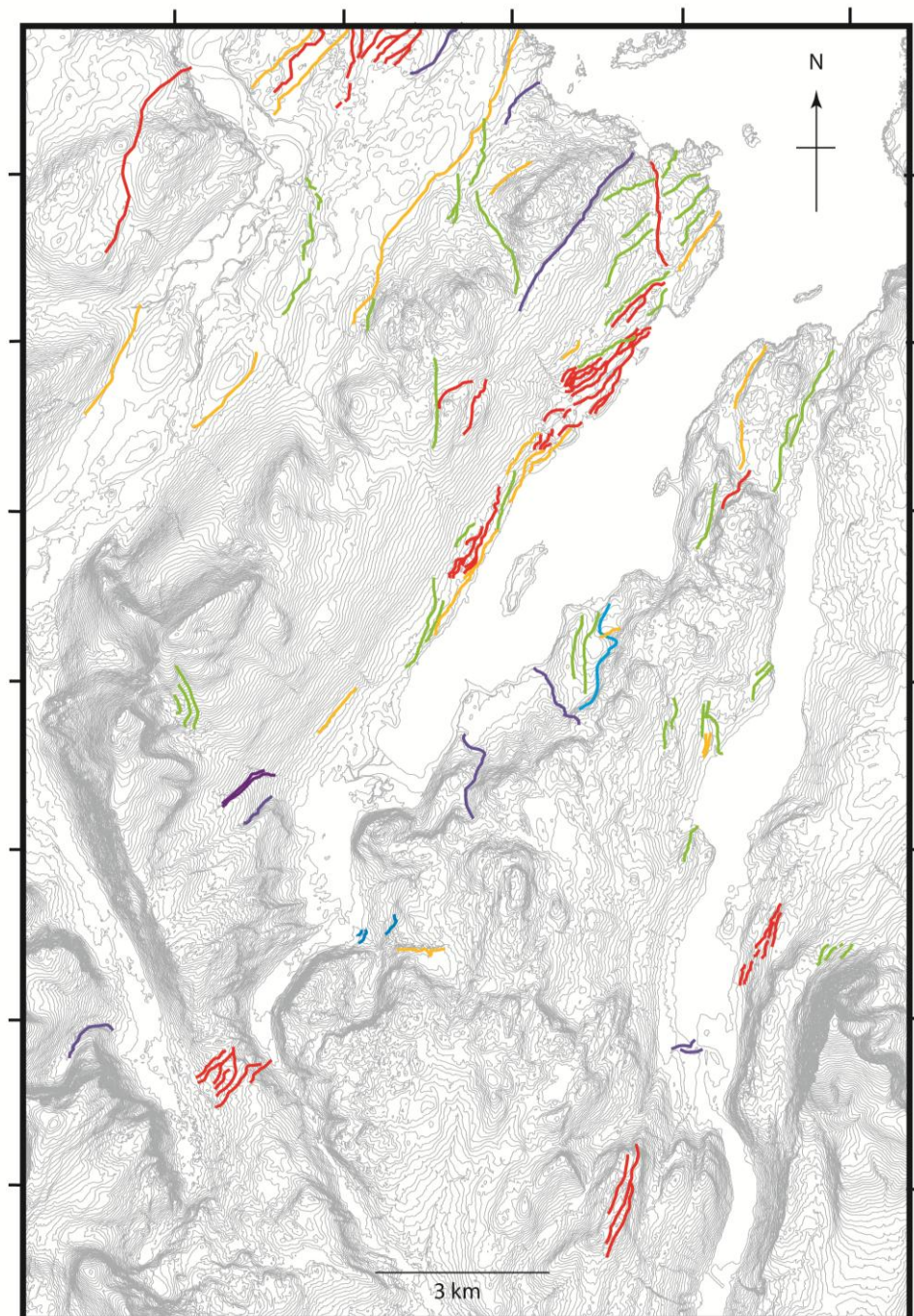
3.2.1. Regional geomorphology

Kyles and lochs indent the NW Sutherland coast (Folio 1). The Kyle of Durness and Loch Eriboll are sea lochs; the former is shallow (<50 m), the latter is deeper (>100 m) in places due to regional structural geological control (discussed later in this chapter). Loch Hope, ~2 km east of Loch Eriboll, is currently a freshwater loch (lake) c. 10 m above present sea level. Evidence of a previously higher relative sea level (RSL) is preserved around the margins of the two lochs (detail in these sections 3.2.1.5, 0, 3.2.1.8).

Widespread evidence of glaciation is clearly discernible in the Loch Eriboll area (Folio 3). Geomorphological mapping of regional ice flow sets, meltwater channels, raised glaciomarine features and glacially transported boulders was undertaken in this area. Meltwater channels have been classified according to criteria compiled by Greenwood *et al.* (2007) (Figure 3.1) which allows the environment of channel formation to be established. Five types of channels are recognised by their three dimensional forms and orientations: subglacial, sub-marginal, englacial channels which have been 'let down' on to the land surface, as ice deflates, lateral and pro-glacial. The latter two classes are particularly useful in the interpretation and placement of ice margins (Discussion: Thermal structure).

The region displays the glacial signature of three major flow sets. These are largely manifest as erosional bedrock grooves and strongly streamlined bedrock, though some streamlined sediment forms are also seen towards the coast. The most extensive flow set (collection of surface markings imparted by the flow of ice over the ground) trends NE, sub-parallel to Loch Eriboll. The majority of flow-related features can be classified as glacial bedforms and occur below 150 m a.s.l., around the Kyle of Durness and the mouth of Loch Eriboll, though similar vectors are seen to the SE, with some bedforms initiating at ~400 m a.s.l., beneath Ben Hope. Small scale abrasional features also exhibit similar flow orientations - striae and roches moutonnées on the E slopes below Cranstackie, and

striae and whalebacks on the valley floor near Portnancon and at the head of Loch Eriboll (Folio 3).



Channel classifications (based on Greenwood et al., 2007)

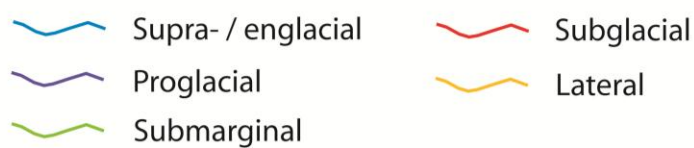


Figure 3.1: Meltwater channels in the Eriboll-Hope area. Channel classifications after Greenwood et al. (2007).

Development of lee side NW cliff faces is seen across the area (Folio 3). These features form part of a flow set with large-scale expression on the An Lèan Chàrn interfluvial plateau and the Meall Meadhonach interfluvial above Strath Dionard; limited to surfaces at ~160-270 m a.s.l. A number of lochans on Beallach na Sgeulachd lie at the centre of this flow set. Many exhibit lenticular or teardrop-shape outlines with elongation parallel to the main flow set, forming a knock and lochan topography.

A final, tightly grouped flow set with a northerly trend occurs mainly above 110 m a.s.l. (up to 310 m a.s.l.) on the An Lèan Chàrn interfluvial between the two lochs. Erosional forms at Portnancon such as Creag na Griosaich (Figure 3.2) preserve this flow trace at lower level.



Figure 3.2: Creag na Griosaich, Portnancon. N-facing plucked face in Cambrian quartzite echoing form of Cranstackie seen in background skyline. Figure for scale. Photo: DF.

The pervasive nature of flow indicators across the region owes much to the predominantly bedrock landscape where superficial sediment occurs in isolated patches around the margins of water bodies and as a discontinuous layer on low relief ground. Quaternary sediment cover is variable but generally thin with bedrock-derived colluvium and blockfield being common. Protrusion of bedrock knolls through sediment suggests a varied and irregular bedrock relief across much of the study area. Glacially transported boulders are particularly prevalent on the western side of Loch Eriboll where durable quartzite lithologies outcrop. Boulder cover includes occasional erratics which give information on ice flow direction and erosional regimes.

3.2.1.1. Kyle of Durness

The Kyle of Durness is a shallow sandy N-S orientated embayment, at the marine mouth of Strath Dionard. Towards the head of the estuary, remnants of deltaic sediments are seen; the extension of the outwash sandur valley fill seen in Strath Dionard. Much of the Kyle, however, is bounded by exposed bedrock with knolls of Eilean Dubh formation dolostones and Cambrian quartzites seen to protrude through sediment cover at the head of the Kyle. Quaternary sediment cover is thickest over the E flank of Strath Dionard and towards the North coast where till overlies dolostones of the Durness Group.

Many meltwater channels are broadly parallel with the previously described glacial lineaments in this region; trending consistently NNE, indicating flow towards the present coastline. The majority of the channels are cut in bedrock and have undulating profiles suggesting a subglacial origin with increasing complexity and density towards the coast. Long, linear channels, along the margins of Strath Dionard, and on the low ground north of the Kyle, may represent lateral ice margin positions.

3.2.1.2. Rispond

The headland of Rispond is notable for its exceptional preservation of large scale glacially moulded bedrock features (Figure 3.3). The wide joint spacing of the bedrock (Lewisian gneiss with granite sheets) granite in this location has facilitated formation of large whalebacks, rock drumlins and roches moutonnées under an erosional NW-NNW ice flow regime (striae $\sim 340^\circ$). In combination with scalloped p-forms, the features are indicative of high pressure subglacial conditions or rheologically soft ice and basal meltwater (Benn and Evans, 2010). This indication of warm-based conditions, the presence of glacially transported boulders and the geographical location at the mouth of Loch Eriboll, allows TCN samples (Table 3. 2 and Table 3.3) to constrain the deglacial transition from thick ice sheet covering the entire headland, to the topographically confined outlet glacier in Loch Eriboll. TCN samples RISP1 (bedrock) and RISP2 (erratic), were collected from a group of scattered glacially transported boulders perched on moulded bedrock on the Rispond headland. The pair yield statistically inseparable ages (RISP01 17.5 ± 1.1 ka BP and RISP02 17.7 ± 1.1 ka BP) with a mean of 17.6 ka BP.

Table 3.1: Acronyms for following TCN sample locations and physical characteristics of samples data tables.

AE	Acid etching from peat cover	MT	Metatonalite
Bedrock	Sample from sound in-situ bedrock	Mtop	Microtopography of surface
BQ	Basal Quartzite (false cross-bedded member of the Eriboll Form.)	N/A	Not applicable
ER	Edge rounding	NW	Nodular weathering
Erratic	Allocthonous glacially transported material	OT	Overturning possible
G (VQ)	Gneiss (undefined) sample derived from vein quartz	P	Possible
Gr	Granite	PR	Piperock (fossiliferous quartzite member of the Eriboll Form.)
GTB	Glacially transported boulder	Q	Quartzite (undifferentiated)
JD	Joint deepening	QVP	Quartz vein protrusion
LG	Lewisian Gneiss	SL	Surface loss
LM	Lateral movement	TS	Torridon Sandstone
MO	Marine organisms	U	Unlikely
Moraine	Boulder from a moraine	VM	Vertical movement
MS	Moine Supergroup (psammities with pelitic layers)	WP	Weathering pits
MS(QV)	Sample from quartz vein in Moine	WR	Weathering rind

Table 3. 2: TCN sample locations and physical characteristics of samples from the west bank of Loch Eriboll, Northern Sutherland. See Table 3.1 for acronyms.

Location	Sample ID	Lat.	Long.	OS grid ref.	Elev. (m)	Sample type	Sample dimensions a,b,c axes (m)	Litho.	Previous sediment cover	Post-depo. move.	Weathering indicators
Rispond	RISP01	58.55058	-4.66278	NC: 245149, 965574	31	Bedrock	N/A	Gr	U	N/A	SL ≤20cm
	RISP02	58.5509	-4.66239	NC: 245173, 965609	20	Erratic	0.6,0.5,0.3	BQ	U	U	None
Portnancon	PORT1	58.50502	-4.70092	NC: 242727, 960582	31	Moraine	3,1.5,1.5	Q	U	U	None
	PORT2	58.50502	-4.70092	NC: 242727, 960583	31	Moraine	1.25,1.25,1	Q	U	U	None
	PORT3	58.50502	-4.70092	NC: 242727, 960584	31	Moraine	1.5,1.25,1.25	Q	U	U	None
Loch Eriboll, West bank	ERW01	58.4907	-4.71909	NC: 241603, 959042	13	Moraine	0.15,0.10,0.10	BQ	Partial peat shielding <0.5m	None	None
	ERW02	58.49052	-4.71935	NC: 241587, 959022	12	Moraine	0.12,0.12,0.10	BQ	Partial peat shielding <1m	None	None
Laid	LAI01	58.47394	-4.73512	NC: 240593, 957214	21	Moraine	0.5,0.4,0.3	BQ	U	U	None
	LAI02	58.47406	-4.73361	NC: 240682, 957224	13	Moraine	0.3,0.3,0.2	BQ	U	U	None

Table 3.3: TCN sampling data and surface exposure ages of samples from the west bank of Loch Eriboll, Northern Sutherland.

Location	Sample ID	Lat.	Long.	Elev. (m)	Sample thickness (cm)	Topo shielding factor	[¹⁰ Be] (×10 ⁶ atom g ⁻¹)	Apparent exposure age (¹⁰ Be) kyr*
Rispond	RISP01	58.55058	-4.66278	31	3	0.9992	8.12 ± 0.38	17.5 ± 1.1 (0.8)
	RISP02	58.5509	-4.66239	20	3	0.9992	8.12 ± 0.36	17.7 ± 1.1 (0.8)
Portnancon	PORT1	58.50502	-4.70092	31	1	0.9997	7.98 ± 0.34	16.9 ± 1.1 (0.7)
	PORT2	58.50502	-4.70092	31	1	0.9996	8.13 ± 0.33	17.3 ± 1.0 (0.7)
	PORT3	58.50502	-4.70092	31	1	0.9998	7.73 ± 0.31	16.4 ± 1.0 (0.7)
Loch Eriboll, West bank	ERW01	58.4907	-4.71909	13	4.5	0.9881	6.62 ± 0.40	14.9 ± 1.1 (0.9)
	ERW02	58.49052	-4.71935	12	3	0.9905	7.43 ± 0.36	17.1 ± 1.1 (0.8)
Laid	LAID01	58.47394	-4.73512	21	3	0.9993	7.88 ± 0.32	17.2 ± 1.0 (0.7)
	LAID02	58.47406	-4.73361	13	3	0.9994	6.88 ± 0.32	15.1 ± 1.0 (0.7)

*Minimum ¹⁰Be ages calculated assuming rock density of 2.7 g cm⁻³ and zero erosion. Calculated with the CRONUS-Earth online calculator (Balco et al., 2008) version 2.2 (<http://hess.ess.washington.edu/>), using the time dependent Lal/Stone scaling scheme and a local spallation production rate of 3.92 ± 0.18 ¹⁰Be atoms g⁻¹ yr⁻¹ and 26.45 ± 1.2 ²⁶Al atoms g⁻¹ yr⁻¹ (Fabel, 2012). The uncertainties are 1 sigma systematic uncertainties with the analytical uncertainties shown in brackets. ¹⁰Be and ²⁶Al procedural blanks were all lower than 8% of the total atoms counted in the samples, except for sample HUTC01 where the blank was 28% of the sample because the clean quartz mass processed was less than 5 grams, resulting in a low total atom count.



Figure 3.3: TCN sampling sites and geomorphic features, Rispond. A - Glacial scallop sampled for RISP01 (31m a.s.l). Photo: DF. B - RISP01 pegmatitic texture. Rucksack and chisel for scale. C - RISP02 quartzite erratic. Rock drumlin (background) indicates NW ice flow. Photo: DF. D - Whaleback displaying plucking. E - Glacial grooves and crescentic cracks on the flank of a whaleback. BGS notebook for scale. Photo: TB.

3.2.1.3. Eriboll Valley

The Eriboll valley is orientated NE-SW with an asymmetric cross section comprising a rectilinear W slope and irregular E flank. This asymmetric valley form is defined by the regular (c. 10°/130) dip slope surface of the Cambrian quartzites on the W flank and the craggier expression of the Moine Thrust complex on the east. The highest land in the area comprises the peaks cresting the W edge of the quartzite outcrop - Cranstackie (800 m a.s.l.) and Ben Spionnaidh (772 m a.s.l.). The short, broad valley of Srath Beag leads south from the head of Loch Eriboll narrowing abruptly where the thrust controlled valley turns west beneath the steep crags of Creag Shomhairle to become Srath Coille na Feàrna. To the SE the ground rises to a low undulating plateau c. 300-400 m a.s.l., underlain by Moine lithologies, which separates the valleys of Loch Eriboll and Loch Hope.

3.2.1.4. Eriboll: West bank

The W flank of the Eriboll valley is characterised by a SE sloping sheet of fluvio-glacial sediment (Figure 3. 4) interrupted by bedrock highs and rock basins and dissected by meltwater channels. Significant local bedrock relief is indicated by the juxtaposition of glacially abraded knolls (including the island of Eilean Choraigh) with rock basins (Folio 3). Consequently, glacial sediment thickness varies over the undulating bedrock surface. A small quarry between Portnancon and Laid (NC: 42184, 60266) reveals glacially moulded bedrock beneath 5 m of sands and gravels. The polished quartzite surface of the quarry floor glacial abrasion marks. Crescentic gouges of ~30-100 mm in length are seen to vary from open and shallow forms, through arcuate to tightly closed with straight limbed shapes. Impact grooves up to 600 mm long by 200 mm wide, and 2-20 mm deep indicate NNE flow.

The glacial sediments of W Eriboll comprise sands, gravels and boulders, almost exclusively of quartzite lithology. The sugary character of the Piperock member comprises the majority of the finer grade sediment - sands and gravels. Fifteen small quarry exposures (Figure 3. 4) suggest

glacial sediment cover is commonly 3-5 m thick, often with an upper unit composed of a boulder pavement.

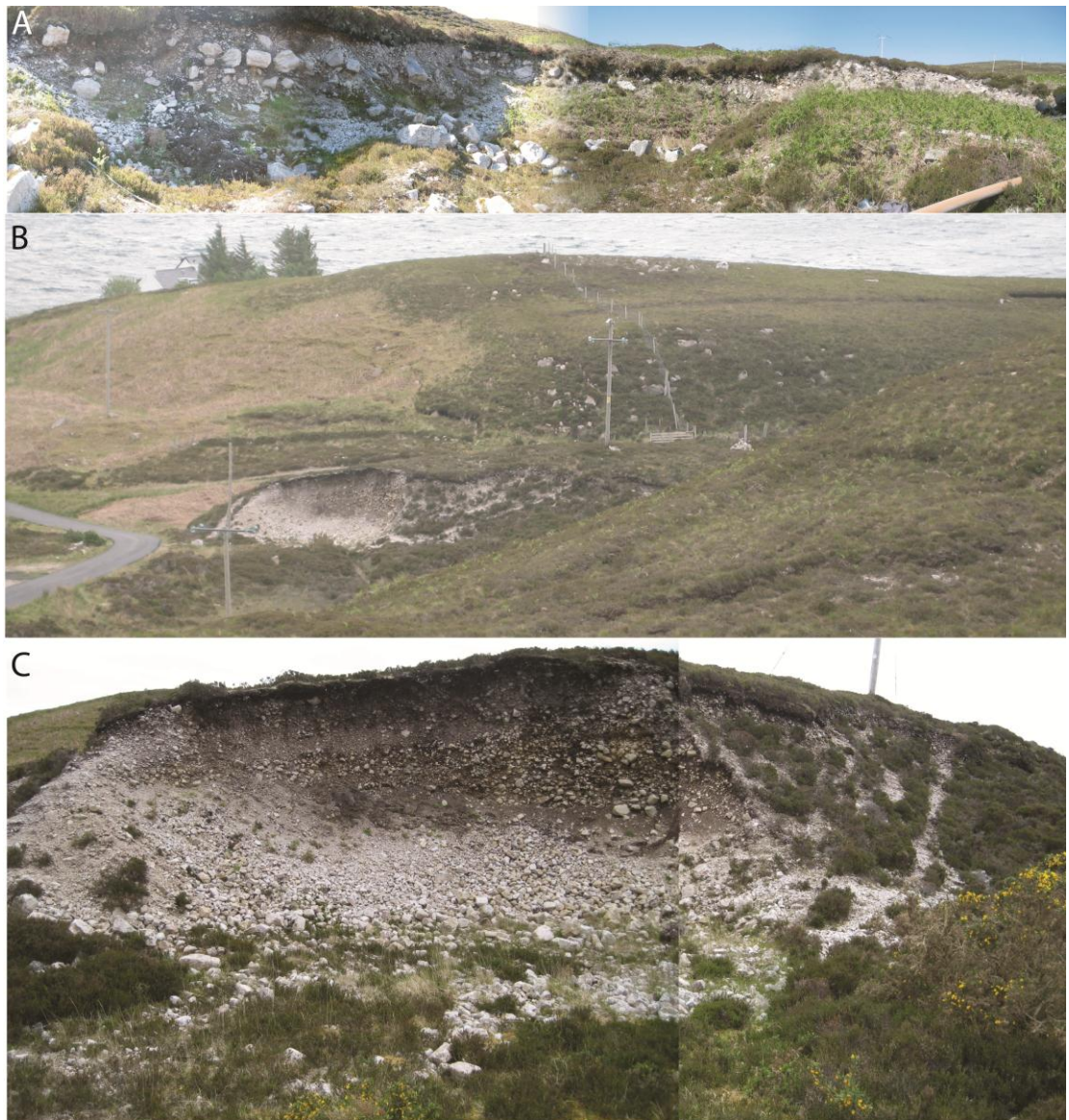


Figure 3. 4: Glaciofluvial sediment, W flank of Loch Eriboll. A - Sediment with boulder stringer, Port Chamuill access road. B - Quarried flank of sediment mound, Portnancon access road. C - Stratified sediments exposed in disused quarry on main road, west of Portnancon.

These larger blocky boulders are typically Basal Quartzite, as are the bedrock rafts, large glacially-transported bedrock blocks, occasionally found across the surface (Figure 3.5). Occasional low level erratics are found amongst the quartzite boulder lag around the W flank of the loch. Erratic transport oblique or transverse to loch strike (in a NW direction) is indicated by dolostone erratics near Portnancon, as limestones only outcrop on the E side and islands of the loch.



Figure 3.5: Glacially transported bedrock raft, W Eriboll. Large (c. 7.5 m a.s.l.) glacially moulded quartzite bedrock raft (circled) perched on Basal Quartzite bedrock following northerly transport along west side of loch Eriboll. Source scar indicated by dashed line.

Near Portnancon, the incised and ridged sediment cover is marked by a string of glacially transported boulders (Figure 3.6) perched on a ridge of high ground. This feature is interpreted as a boulder moraine (c. 355 x 90 m). Three TCN (Table 3. 2 and Table 3.3) samples constrain the abandonment of a former ice margin position. The ages cluster around a mean of 16.9 ka BP (PORT01 16.9 ± 1.0 ka BP, PORT02 17.3 ± 1.0 ka BP, PORT03 16.4 ± 1.0 ka BP).

The surficial sediments on the slope of Loch Eriboll's W margin are dissected into a series of ridges and mounds by multiple meltwater channels (Figure 3.7) which occur in greatest density between Portnancon and Loch Sian, towards the mouth of Loch Eriboll. Subglacial channels predominate, often forming dendritic networks of sub-parallel channels. The majority of channels trend c. 35° N, sub-parallel to the strike of Loch Eriboll. Between Rispond and Portnancon, sub-marginal channels, draining

NE, bracket two suites of subglacial channels in turn bounded by a short lateral channel c.20m higher.

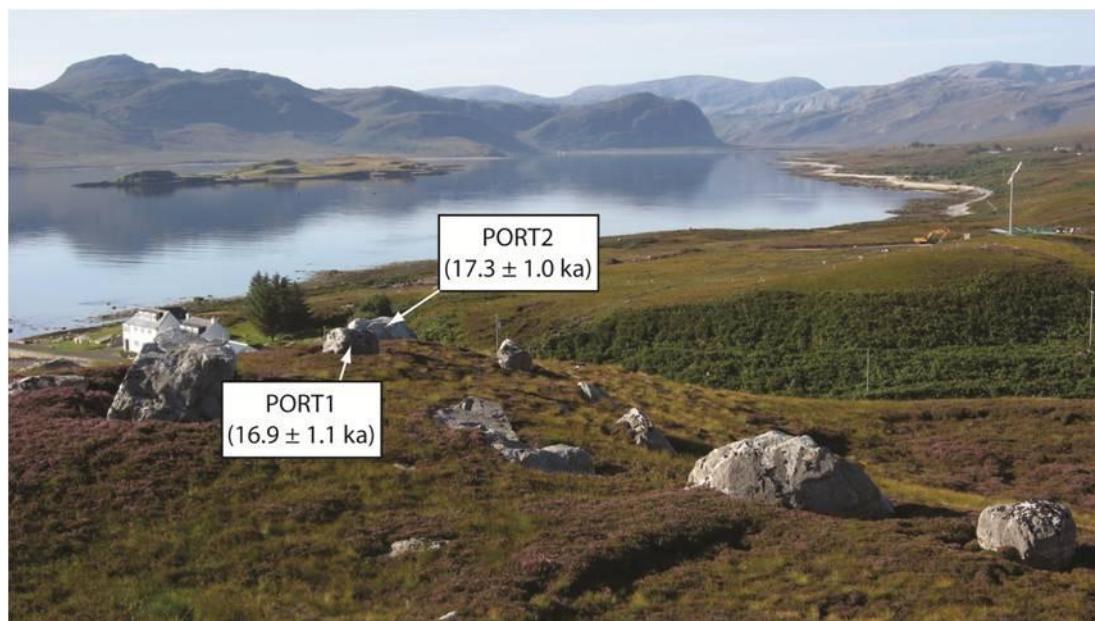


Figure 3.6: Context PORT samples, Portnancon, Loch Eriboll. A - Cluster of boulders sampled for PORT 1-3, Portnancon. Meltwater channel (dark green bracken) cuts down slope right to left. Photo: DF. B - Sediment morphology, Portnancon.

Moving up valley a sequence of three lateral channels is seen north of Laid. Around Laid itself, the channels show sinuous forms and a narrow dendritic network bounded by sub-marginal forms to the NE and SW. Here a south-south-west-trending channel aligns with higher sub-marginal channels cut in bedrock on the Meall Meadhonach interfluvium. Two Basal Quartzite cobbles sampled for TCN analysis (ERW02 17.1 ± 1.1 ka BP and ERW01 14.9 ± 1.1 ka BP) from the upper surface of the dissected sediment sheet near Laid (Figure 3.7), constrain abandonment of the sandur by retreating valley ice. Further (~2 km) south west along the loch shore, at the southern end of Laid, a boulder limit of quartzite blocks is observed (Figure 3.8B). Boulders sampled here yield apparent exposure ages, comparable to those at the ERW site, of 17.2 ± 1.0 ka (LAID01) and 15.1 ± 1.0 ka (LAID02). All details in Table 3. 2 and Table 3.3.

At Rubh' Armlì, a small cusped foreland towards the head of Loch Eriboll, a small mound of till occurs in isolation Figure 3.9). The mound (c. 6 m a.s.l.) exhibits a bouldery crest, steeper eastern slope which is also bouldery and a gentler western flank. It is very likely that the steeper E flank of the mound represents an ice contact slope and that this feature therefore represents a portion of an ice limit.

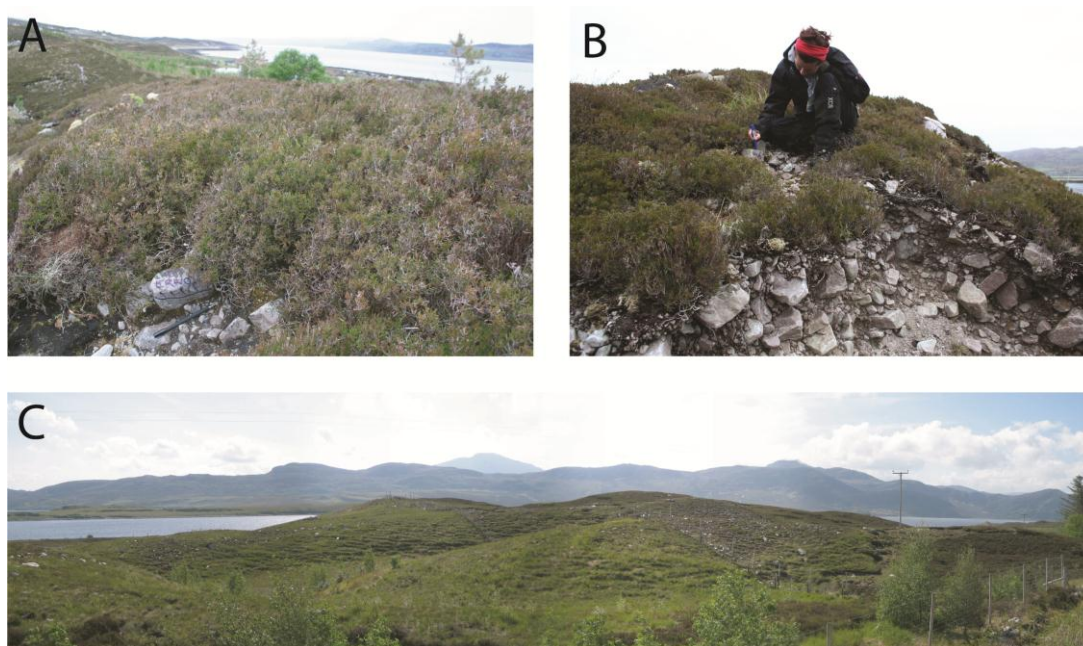


Figure 3.7: ERW samples, Loch Eriboll. A - Sampling ERW02, surface of glacial sediment near Laid. River cliff exposes underlying diamict sediment of sub-rounded basal quartzite boulders in sandy matrix. Photo: TB. B - ERW01. Photo: TB. C - Morphology of sediment along W margin of Loch Eriboll, looking east.

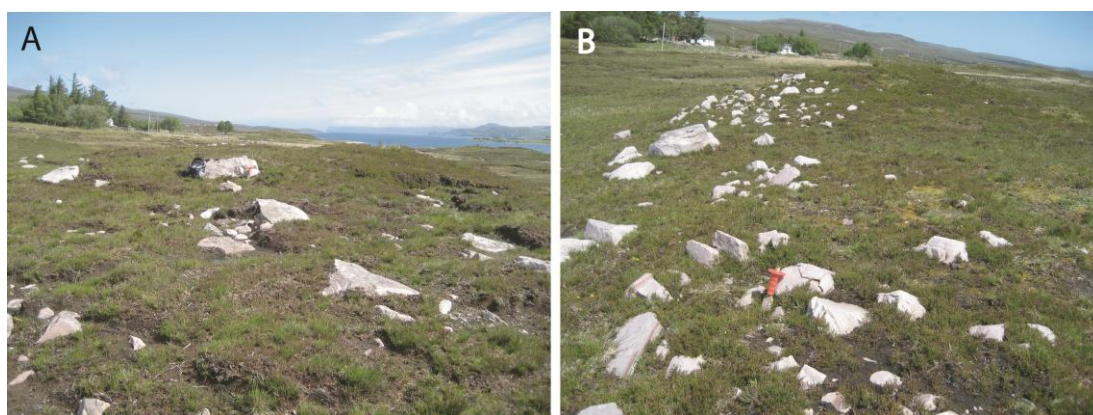


Figure 3.8: Context of LAID TCN samples, west side of Loch Eriboll. A - Large sub-angular glacially transported basal quartzite boulder (LAID01) in middle distance with red handled chisel. B - Context of TCN sample LAID02 in shallow ridge crest near Laid.



Figure 3.9: Glacial contact sediments, head of Loch Eriboll. Glacial contact mound (middle ground with light green vegetation) at Rubh' Armlì and beyond terrace (c. 10 m above present sea level) of fluvioglacial sediments.

3.2.1.5. Srath Beag

Srath Beag, and its up-valley continuation Strath na Coille na Feàrna, are structurally controlled valleys where outcrops of the Moine and Sole thrusts along their E walls produces crags, and the quartzite on the W margin manifests as a gentle dip slope. The valley is characterised by glacial sediments along the E and W margins of the strath where they have not been obliterated by the wandering courses of the rivers Allt Srath Coille na Feàrna and Amhainn an t-Sratha Bhig.

The geomorphology can be described as three main assemblages. Firstly, at the head of Loch Eriboll a flat topped terrace-like feature stands c. 10-15 m above of modern high water mark (Figure 3.10 A). The surface of the feature is pitted by lochans, including the large tidally-eroded Lochan Havurn, and bedrock protrudes through the sediment in places as polished whalebacks suggesting undulating bedrock relief beneath the sediment cover. To the SW, the modern river; responding to a lowered base level, has trimmed the feature as a terrace. The feature is likely to be

contemporaneous with similar sediment bodies around the rim of the loch - at Rubh' Ard Bhaideanach and near Eriboll farm. Sediment sections around Lochan Havurn reveal a stratified sequence of coarsely sorted matrix-supported poorly consolidated sands and gravels (Figure 3.10B & C).

Terrace sediments (interpreted from exposures NC: 39889, 54282 and NC: 43155, 57482) vary laterally in structure and texture from N to S. A levelled bedrock platform in some areas suggests sediment thickness of ≥ 2 m. At the N end of the section, the sediment consists of rounded to sub-angular gravels and boulders in a coarse granular matrix with occasional normally graded sand lenses. At the southern end of the section four units are discernible. The lowest exposed unit is a heavily compacted matrix-supported sandy diamict ~ 30 cm thick with varying proportion of clast content. Clasts are a poorly sorted mix of sub-angular to rounded gravels and cobbles. In some areas this unit comprises compacted well-sorted fine-medium grade sand. Above this, a laterally discontinuous unit comprises poorly sorted sands, gravels and boulders. These low angle cross-bedded sandy gravels consist of sub-rounded clasts alternating between sand and gravel beds with increasing matrix component upwards. Throughout all but the top 40 cm of the exposed sediments tabular clasts appear to display sub-horizontal a-axis alignment. Small platy rip-up clasts of slightly hardened sand are also seen. A final unit (40-50 cm thick) of bedded sandy gravels comprises 3-4 fining up sequences grading from clast-supported to granule. Disruption of beds by normal faulting (Figure 3.10 B) is noted towards the S end of the section.

Against the W margin of the valley there is a second terrace comprised of sands and gravels (Figure 3.11; Figure 3.12 A), again pitted on its top surface - notably with the large lochan of Loch Badna h-Achlaise, now partially in-filled by a relict alluvial fan. The sediments within this feature are finer (Figure 3.12) suggesting a lower energy environment. This is interpreted as an ice-contact assemblage, in a terrestrial setting, c. 20 m above the raised sea level indicated by the terrace at the head of Loch Eriboll. As the final ice-contact assemblage outside of proposed Younger Dryas ice limits (Lukas and Bradwell, 2010b), samples from this feature were taken to inform on late stage deglaciation. Boulders sampled on this

limit give surface exposure ages of 12.9 ± 0.9 ka BP (SRAB02) and 16.7 ± 1.2 ka BP (SRAB01). This age disparity is discussed in Chapter 4.



Figure 3.10: Terrace feature, head of Loch Eriboll. A - Eriboll head complex (looking east). B - Normal faulted stratified sands. Yellow field notebook for scale. C - Coarse massive gravels in sand matrix. Camera case at centre of image for scale.



Figure 3.11: Sediment limits, Strath Coille na Feàrna. Channel topped (dashed line) sediment limit seen at right in dark green. 30 m terrace level in foreground. Looking west SW up Strath Coille na Feàrna with Creag Shomhairle at left and Foinaven in background.

Table 3.4: TCN sample locations and physical characteristics of samples from Srath Beag, Cranstackie and the east bank of Loch Eriboll, Sutherland. See Table 3.1 for acronyms.

Location	Sample ID	Lat.	Long.	OS grid reference	Elev. (m)	Sample type	Sample dimensions a,b,c axes (m)	Litho.	Previous sediment cover	Post-depo. move.	Weathering indicators
Srath Beag	SRAB01	58.42312	-4.76449	NC: 238648, 951629	34.5	Moraine	2,2,1.5	Q	U	U	JD
	SRAB02	58.42312	-4.76437	NC: 238655, 951629	33	Moraine	1,0.8,?	Q	P	OT	None
	SBLM01	58.42801	-4.74771	NC: 239650, 952133	93	Moraine	3,3,3	MT	U	P	QVP 3cm
	SBLM02	58.42573	-4.74942	NC: 239540, 951883	71	Moraine	2,2,1.5	BQ	U	U	Not apparent
	SBLM03	58.42947	-4.75302	NC: 239347, 952308	31	Moraine	2.5,2.5,2.5	MT	U	U	QVP 1cm
Cranstackie	CRAN01	58.745268	-4.82748	NC: 236403, 987589	733	Tor surface	N/A	PR	U	U	MT ~3cm JD 4cm.
	CRAN04	58.4349	-4.82375	NC: 235246, 953071	528	Erratic	0.3,0.25,0.2	G(VQ)	U	OT	Not apparent
Loch Eriboll, East bank	HUTC01	58.45558	-4.72524	NC: 241086, 955148	39	Moraine	0.7,0.6,?	Moine	U	U	JD >15cm
	ERE01	58.50096	-4.63790	NC: 246379, 959995	60	Erratic	0.23,17,15	BQ	P	P	None
	ERE02	58.50073	-4.63797	NC: 246374, 959969	60	Erratic	0.18,0.15,0.12	LG	P peat <50cm	OT	None
	ERE03b	50.74317	-4.17868	NC: 246380, 959994	60	Bedrock	N/A	PR	P	N/A	None
	ERE3c	51.74317	-4.17868	NC: 246380, 959994	60	Bedrock	N/A	PR	P	N/A	None

Table 3.5: TCN sampling data and surface exposure ages of samples from Srath Beag, Cranstackie and the east bank of Loch Eriboll, Northern Sutherland. For calculation details see footnote to Table 3.3.

Location	Sample ID	Lat.	Long.	Elev. (m)	Sample thickness (cm)	Topo shielding factor	[¹⁰ Be] (x10 ⁶ atom g ⁻¹)	Apparent exposure age (¹⁰ Be) kyr*
Srath Beag	SRAB01	58.42312	-4.76449	34.5	3	0.9483	7.38 ± 0.39	16.7 ± 1.2 (0.9)
	SRAB02	58.42312	-4.76437	33	3	0.9812	5.89 ± 0.32	12.9 ± 0.9 (0.7)
	SBLM01	58.42801	-4.74771	93	3	0.9757	7.40 ± 0.34	15.3 ± 1.0 (0.7)
	SBLM02	58.42573	-4.74942	71	3	0.9946	7.64 ± 0.29	15.9 ± 0.9 (0.6)
	SBLM03	58.42947	-4.75302	31	3	0.9976	7.55 ± 0.31	16.3 ± 1.0 (0.7)
	Cranstackie	CRAN01	58.74527	-4.82748	733	2	0.9997	114.79 ± 3.96
	CRAN04	58.4349	-4.82375	528	3	0.9994	11.44 ± 0.88	15.2 ± 1.4 (1.2)
Loch Eriboll, East bank	HUTC01	58.4556	-4.7252	39	3	0.9985	8.47 ± 0.86	18.1 ± 2.0 (1.9)
	ERE01	58.50096	-4.63790	60	3	0.9992	6.81 ± 0.61	14.2 ± 1.4 (1.3)
	ERE02	58.50073	-4.63797	60	3	0.9923	6.88 ± 0.54	14.5 ± 1.3 (1.1)
	ERE03b	50.74317	-4.17868	60	3	0.9992	7.59 ± 0.28	16.4 ± 1.0 (0.6)
	ERE3c	51.74317	-4.17868	60	3	0.9992	8.00 ± 0.29	16.7 ± 1.0 (0.6)



Figure 3.12: West side terrace feature, Srath Beag. A - Panorama of hummocky lochan-pitted terrace top. B - Terrace sediments exposed in river cliff near Strabeg farm. C - Context of SRAB02 TCN sample. Sample. D - Large quartzite block on S limit of terrace top surface sampled for SRAB01.

Traces of esker ridges emerge as curvilinear forms on the SE margin of Loch Badna h-Achlaise showing some continuity across the valley floor where the ridges switch to form an anastomosing braided pattern. This in turn becomes a broken series of hummocks, channels and depressions to the north of the terrace feature. Up valley, where the glen turns south as Srath Coille na Feàrna, three nested channel-topped glacial sediment limits descend from c. 60 m a.s.l. to the valley floor.

On the east side of Srath Beag a flight of terraces (Figure 3.13) represent the third main sediment mass. The upper surfaces of each terrace are sub-horizontal (Figure 3.13 D) with these planar surfaces separated by rectilinear slopes. The terrace flight extends above 90 m a.s.l., c. 60 m above the valley floor. A deep channel incises the sediment, descending from the An Lèan Chàrn plateau at the kames' S end. At least three levels are clearly discernible in the field, the lowest sharing the level of the W terrace. TCN samples (SRABLM01-3) taken from these levels constrain valley deglaciation (15.3 ± 1.0 , 15.9 ± 0.9 , 16.3 ± 1.0) and overlap with a mean age of 15.9 ka BP (Table 3.4 and Table 3.5). The lowest of the ridges is conspicuously bouldery with large metatonalite blocks suggesting a greater component of supra-glacial material in comparison to higher benches.

In a feeder valley to the south of Srath Beag, sitting atop Creag Shomhairle, and beneath the crags of Creag a Chaoruinn, a distinct sediment limit, bordered by glacially transported boulders up to 6 m in diameter, abuts exposed bedrock. The setting and landform assemblage suggests the margin of a small, low level cirque glacier.

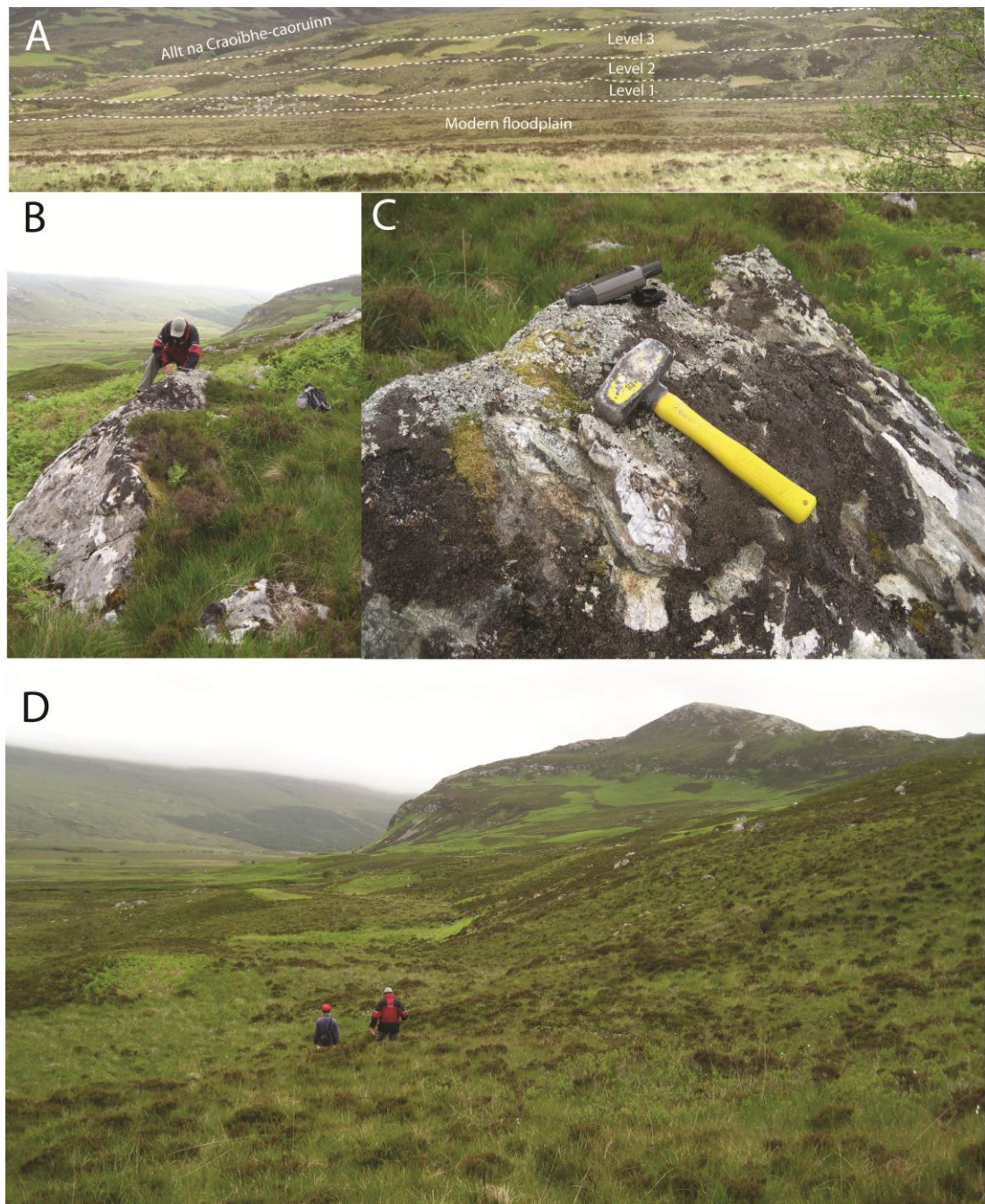


Figure 3.13: Strath Beag kame terrace suite. A - Lateral benches on the east side of Strath Beag (looking NW). Lowest ridge is marked by boulder cover. B - SBLM01 a large metatonalite boulder on uppermost bench (93 m a.s.l.). C - Large metatonalite boulder sampled for SBLM03. Protrusion of quartz by ~1 cm. D - Kames, looking north towards Creag na Faolinn.

3.2.1.6. Cranstackie

The summit ridge of Cranstackie (801 m a.s.l.) is the highest point in the Eriboll catchment and forms the watershed with Strath Dionard. The mountain represents the peak of the quartzite dipslope which defines the W wall of the valley (Figure 3.14). Cranstackie's E flank is delineated by the dipslope of the Basal Quartzite. Glacially abraded surfaces are common here, with P-forms, plucked faces and dilated joints covered by frequent well-rounded Piperock boulders. Above Creag nan Gobhar (NC: 36361, 53495) bedrock is marked by crescentic cracks and gouges aligned in an ENE flow direction. The glacially abraded surface is also interrupted by deep (~30 cm) open joints.

Deep, bedrock cut meltwater channels form the middle courses of two burns, Creag nan Gobhar and Allt Coire na Cùile. The highest local meltwater features are c. 600 m a.s.l. as three nested sub-marginal channels between Cranstackie and Ben Spionnaidh. The channels are sub-parallel; with an initially linear descent followed by a sharp double bend in their lower third where the slope shallows into Coire an Uinnseinn c. 460 m a.s.l.. The channels incise colluvium and underlying bedrock and terminate in open chutes c. 400 m a.s.l. Evidence for a small low level cirque-style glacier is seen in a series of arcuate depression-backed ramps beneath Coire an Uinnseinn (Figure 3.15).

Two erosional features, one at the north eastern flank of Meall nan Crà and the other at Coire na Cùile, here termed 'rip-offs'. These are identified by the exposure of bedrock in contrast to surrounding regolith cover, and additionally, in the case of Coire na Cùile, by a rectilinear scarp on the eastern slopes of Cranstackie. The material cleared from the scarp is absent from the local surrounding area suggesting a significant transport distance (see Chapter 5 for details of proposed rip-off formation). The Coire na Cùile rip-off, has a stepped profile consisting of three steps with surfaces at 300 m, 420 m and 460 m a.s.l. the highest terminating in the main (70m high) scarp. Below Meall nan Crà steps are shallower at 370 m, 380 m and 400 m. In both cases, the step treads are conspicuously cleared of

regolith in comparison to surrounding slopes and, below Coire na Cùile, are glacially abraded and dotted with GTBs.

The upper slopes of Cranstackie consist of an inclined plateau mainly of Piperock Quartzite. The plateau possesses a variable thickness of blockfield, on a partially exposed quartzite pavement, with a discontinuous spread of erratic boulders. As is typical, but not documented, of the quartzite plateaux summits of the NW Highlands, bedrock surfaces display evidence of long term subaerial weathering immediately adjacent to evidence of mobile ice. Cranstackie is a remarkably good example of this.

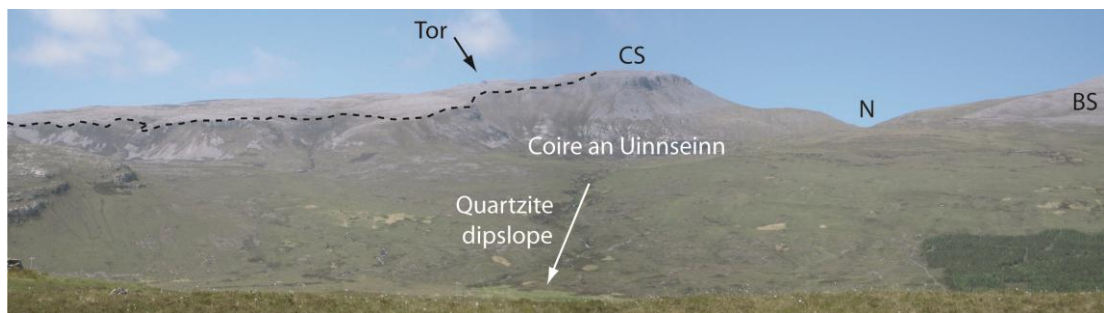


Figure 3.14: Cranstackie slopes and plateau. Looking west up into Coire an Uinnseinn on the E slopes of Cranstackie. Erosional nick (N) in watershed seen at right of image separating Cranstackie (CS) and Beinn Spionnaidh (BS). Quartzite blockfield on Cranstackie (delimited by dashed line). Active talus fans in middle distance.



Figure 3.15: Inferred cirque glacier limits, Coire an Uinnseinn. Boulder spread and moraine detail. Loch Eriboll beyond.

The thickness and character of the openwork quartzite blockfield (Figure 3.16) is seen to vary from a deep cover (up to ~10 m) of soliflucted and rotated slabs (Figure 3.16 A & B) to a stripped pavement displaying evidence of long-term chemical weathering (Figure 3.16 C & D) alongside glacially transported boulders and glacially plucked bedrock (Figure 3.16 E & F).

The highest erratics (Salterella Grit) in the Eriboll area were observed at 618 m a.s.l. on Cranstackie, but were not suitable for TCN analysis owing to their mineralogy. As Salterella Grit is extremely friable, the occurrence of this cobble-sized clast suggests that it was locally derived with only a limited transport path. A source outcrop (c. 5 km) to the SE in Strath Coille nan Feàrna would indicate NW flow up the quartzite dipslope of the mountain, oblique to the main valley.

Similarly, the frequent metatonalite erratics at lower elevation on Cranstackie, c. 540 m a.s.l. (Figure 3.16 F) have isolated local sources in the faces of Creag Shomhairle and Crag na Faolinn strongly suggesting NW transport c. 3.8 km (shortest straight line distance) from Creag Shomhairle the more tenable source. Sampled at 528 m a.s.l., vein quartz from a Lewisian erratic (Figure 3.17) returned an apparent exposure age of 15.2 ± 1.4 ka BP indicating deglaciation at this elevation during the early Lateglacial period (Table 3.4 and Table 3.5).

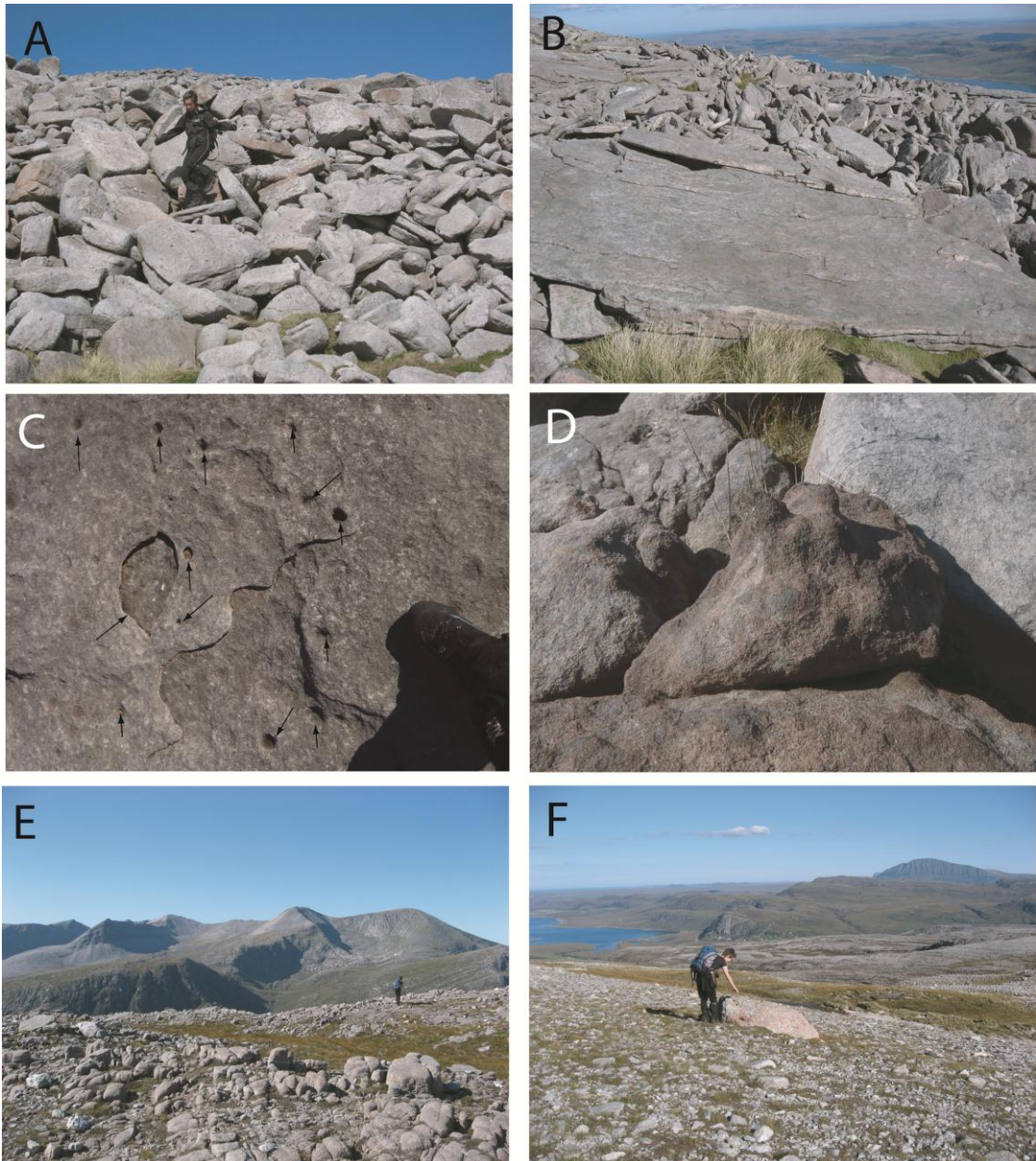


Figure 3.16: Plateau geomorphology, Cranstackie. A - Solifluction lobe riser; Piperock clasts. Figure for scale. Photo: DF. B - Periglacial slab rotation. Photo: DF. C - Solution pits in quartzite. D - Nodular pitted surface on Piperock in blockfield. E - Glacially stripped Piperock pavement with corestones upstanding and scattered erratics. Beyond Foinaven to the SW. Photo: DF. F - Large metatonalite erratic in boulder lag, SE slope of Cranstackie. Photo: DF

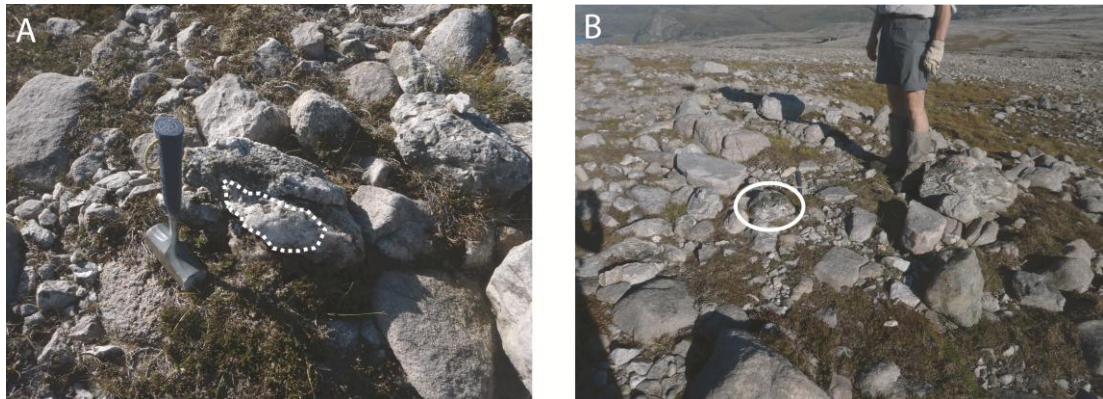


Figure 3.17: TCN sampling CRAN04, Cranstackie. A - Vein quartz (dashed area) of CRAN04 Lewisian sample. B - CRAN04 (circled) context - boulder lag amid blockfield, Cranstackie plateau ridge.

A well-preserved Piperock quartzite tor, unique in NW Scotland, (Figure 3.18) is seen on the summit plateau of Cranstackie. The tor maintains a significant superstructure and preserves long-term weathering features on its upper surface in the form of 3 mm of micro-relief (Figure 3.18 B). However, significant evidence of glacial modification is seen in the form of rotation and toppling of blocks particularly on the tor's SW flank (Figure 3.18 C & D). A sample for TCN extraction was retrieved from the upper tor surface at 733 m a.s.l. (Figure 3.18 B). This bedrock sample yielded a high concentration of cosmogenic ^{10}Be , indicating an apparent exposure age of 129.3 ± 7.6 ka BP (Table 3.4 and Table 3.5).

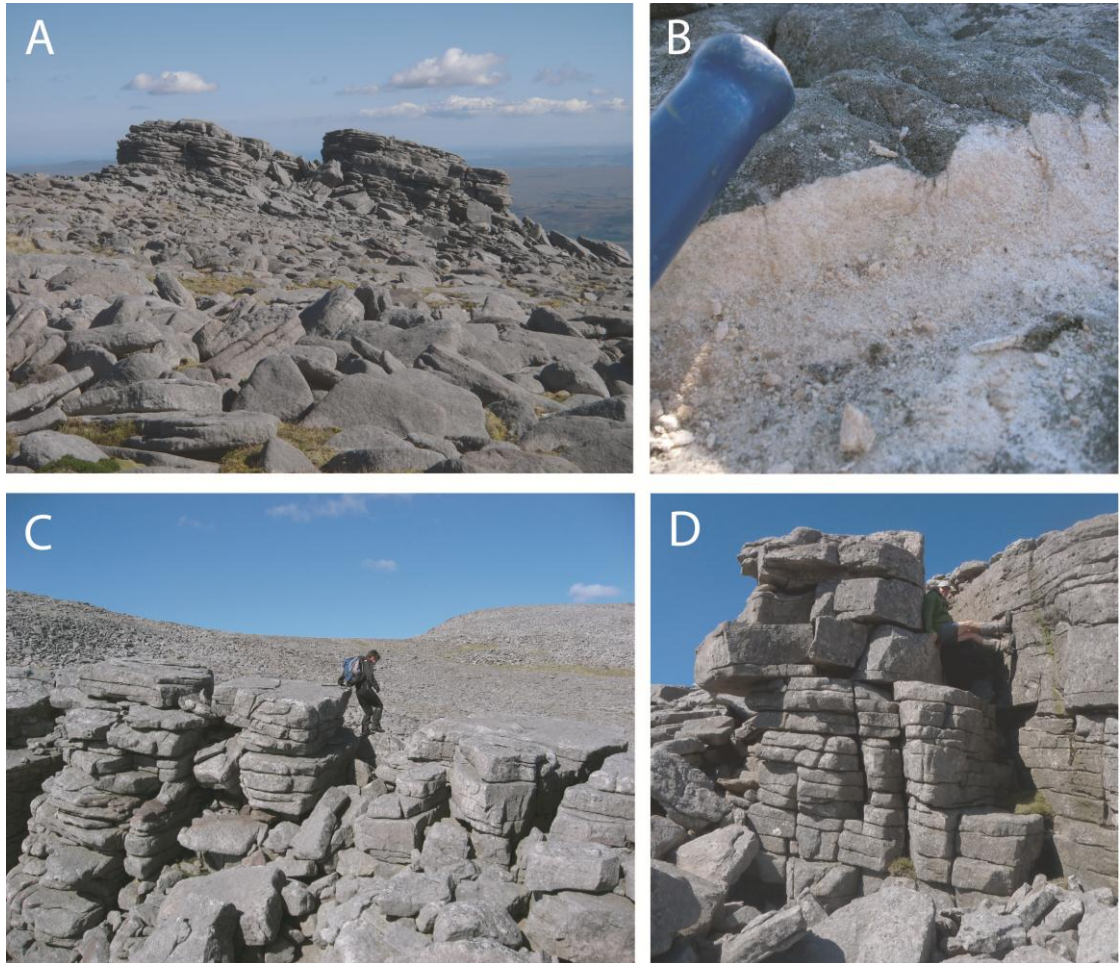


Figure 3.18: Cranstackie tor. A - Quartzite tor c.720m. Thin blockfield cover in foreground. B - Micro-relief of tor surface, CRAN01 sample. Chisel handle for scale. Photo: DF. C - Block toppling and face plucking tangential to ice flow direction. Photo: DF. D - Rotation of upper blocks (right to left).

3.2.1.7. Eriboll: Eastern flank

The character of the eastern flank of Loch Eriboll is in strong contrast to that of the W flank. In the east, the outcrop of Moine metasediments and Eilean Dubh dolostones increases the abundance, and changes the texture, of sediment deposits around the loch shore. A duplex stack of thrust Cambro-Ordovician rocks crops forms the craggy eastern margin of Loch Eriboll. A shallow unconsolidated sediment drape overlies the dolostone outcrop between Rubh' Árd Bhaideanach and Roadstead. Till-cored wedge-shaped mounds occur at Rubh' Árd Bhaideanach (Figure 3.19 A) and north of Eriboll farm (Figure 3.19 C).

In both situations, a steep loch side slope contrasts with a gently sloping landside limb which gently grades into a terrace surface. The steep loch-side slope and high angle beds exposed at Rubh' Árd Bhaideanach suggest glaciotectionic deformation or thrusting by the ice margin (Figure 3.19 A, C & D). The sandy till is exposed at Eriboll Farm (Figure 3.20 A) displaying a transition to a silty and fissile texture in the upper 30 cm. Strong horizontal a-axis alignment, in predominantly gneiss clasts, suggests a subglacial origin.

The two aforementioned ice contact features bracket a basin fill of glacial sediment which marks the major sediment depocentre on this side of the loch. Here, fluvio-glacial sediments (Figure 3.20B) form shallow fans filling the basin between Rubh' Árd Bhaideanach and Eriboll Farm. Plateau-sourced meltwater channels cut down-slope at the margins of this sediment body. On the E slopes of Loch Eriboll, pro-glacial meltwater channels are northward flowing (10-20° N) and cut steeply downslope, in contrast to the gentler fall, and predominantly subglacial origin, of channels on the west bank. Lateral margin constraints are suggested by channels skirting Lochan an Druim and the headland around Ben Heilam.

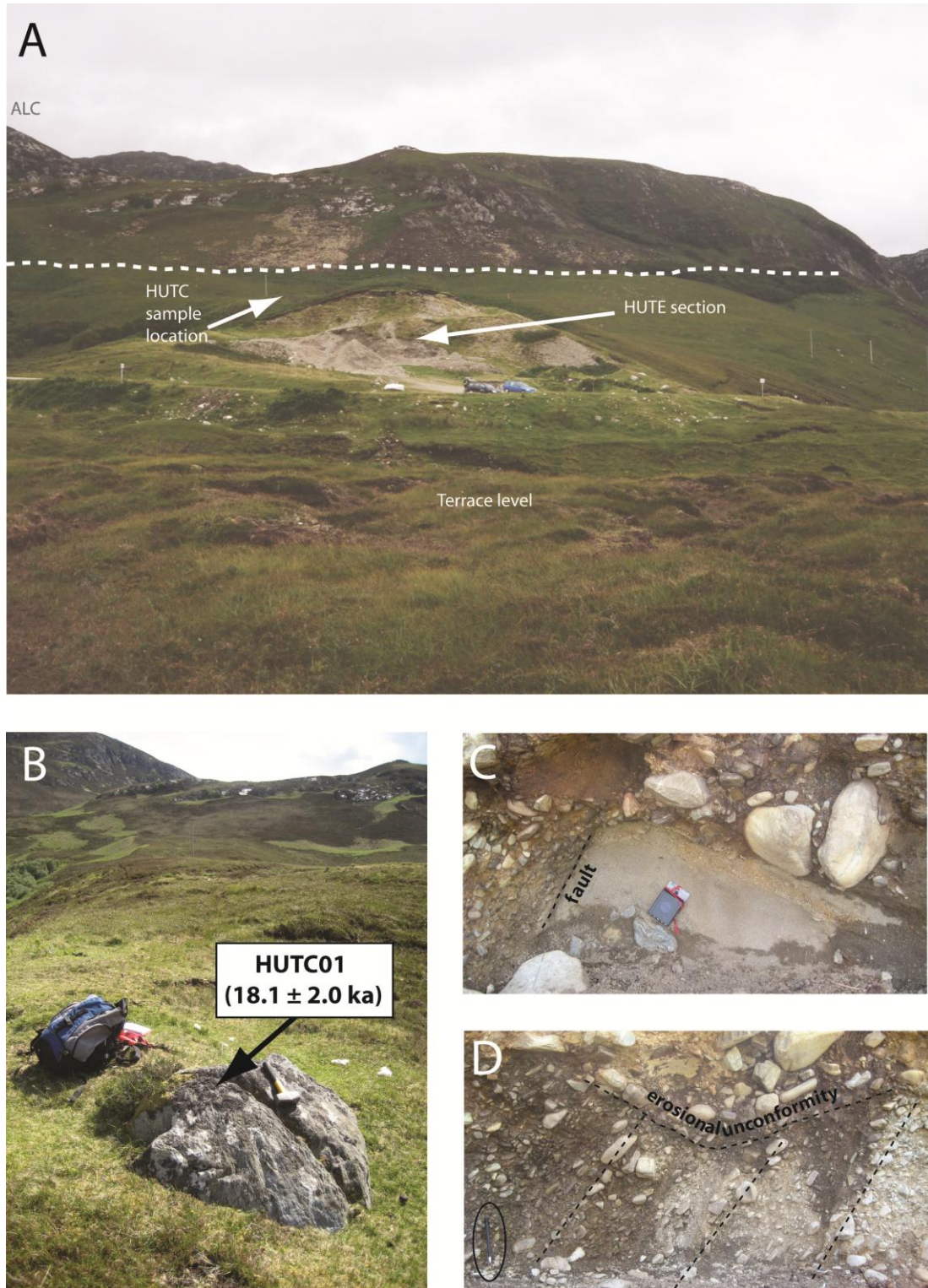


Figure 3.19: Glacial sediments, Rubh' Ard Bhaideanach, E Eriboll. A - Sediments exposed in quarried face of deposit. HUTC01 boulder sampled in mound surface at apex of feature. Dashed line indicates upper limit of sediment body. B - HUTC01 Moine boulder sample in crest of ridge. Looking SSE towards An Lèan Chàrn. C - High angle bedded gravels. Black pencil at bottom left for scale. D - Fault bound sands beneath unsorted bouldery diamict. Compass at centre of image for scale.

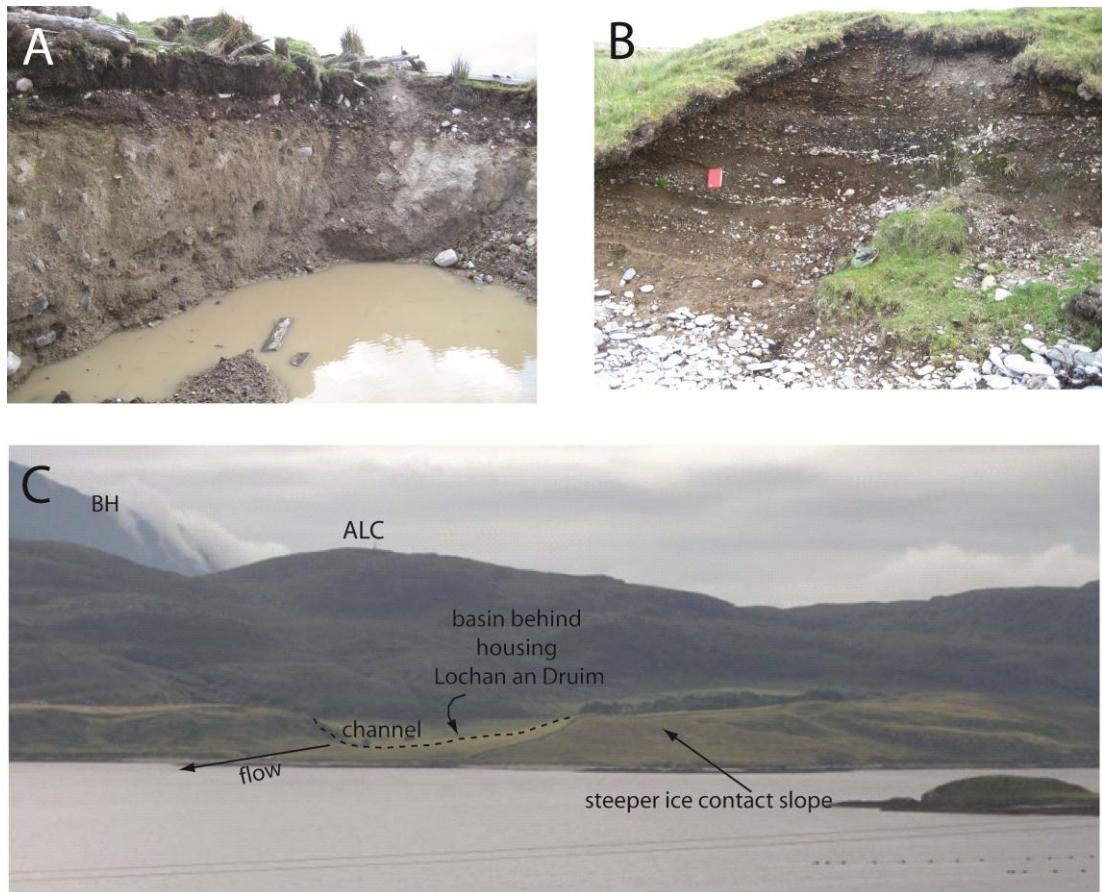


Figure 3.20: Glacial deposits, Eriboll farm. A - 1.5 m of matrix-supported Moinian till exposed in waste pit, Eriboll farm. The only 'true' till seen around Loch Eriboll. B - Sub-horizontally bedded fluvio-glacial sands and gravels exposed at back of modern beach, north of Eriboll farm. Red field notebook for scale. C - Ice contact slope (centre right) and fan at Eriboll farm. Glacial sediments with limestone content shown by bright green improved land.

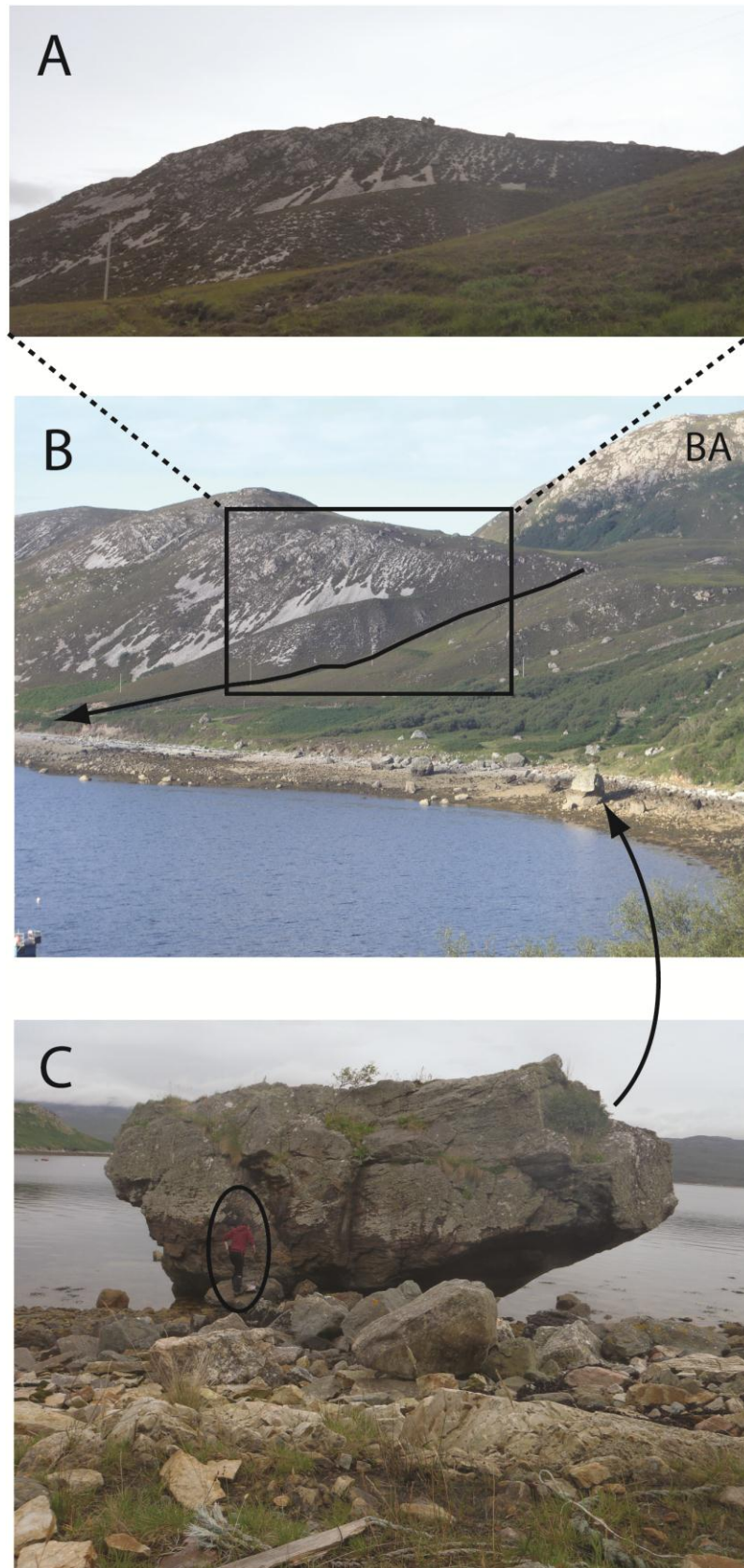


Figure 3.21: Glacial features at Roadstead, E Loch Eriboll. A - Perched Lewisian erratics. B - Giant erratic with faceted form. Figure for scale. C - Roadstead overview. Outcrop of gneiss on high ground. Boulder spread on beach in foreground, over channel dissected glaciofluvial sediments behind and perched on quartzite ridge.

Moine erratics on the surface of these features indicate a NW ice flow direction from the Moine nappe outcropping at An Lean Chàrn, probably with a short transport path c. 2 km. A TCN sample was taken from a Moine erratic (HUTC01) embedded in the crest of sediments at Rubh' Árd Bhaideanach (Figure 3.19 B), and yielded an exposure age of 18.1 ± 2.0 ka BP (Table 3.4 and Table 3.5). Further north, at Roadstead, glacial deposits become clast-supported or matrix-poor, typically forming a spread of glacially transported Lewisian boulders (Figure 3.21), notable both for their size (up to 13 m long axis) and density of concentration. The outcrop of Lewisian lithologies to the east on the slopes of the interfluvium suggests that erratic transport has been westward with ice flow oblique to the long axis of Loch Eriboll.

A thin lag of glacially transported cobbles is observed on the intermediary ground between Loch Eriboll and Loch Hope, just east of Heilam. Local sources to the south suggest short transport paths with delivery of basal quartzite from the E slopes of Loch Eriboll above Roadstead and Lewisian clasts from Ben Arnaboll. Bedrock-erratic pairs were sampled here for TCN analysis, yielding Lateglacial ages for both components. The erratics (ERE01 14.2 ± 1.4 ka BP Basal quartzite) and (ERE02 14.4 ± 1.3 ka BP Lewisian) show slightly younger apparent ages than those returned from the quartzite bedrock - ERE03b 16.4 ± 1 ka BP from top surface and ERE03c 16.7 ± 1 ka BP from plucked stoss face (Table 3.4 and Table 3.5). Ages differences are discussed in Chapter 4.

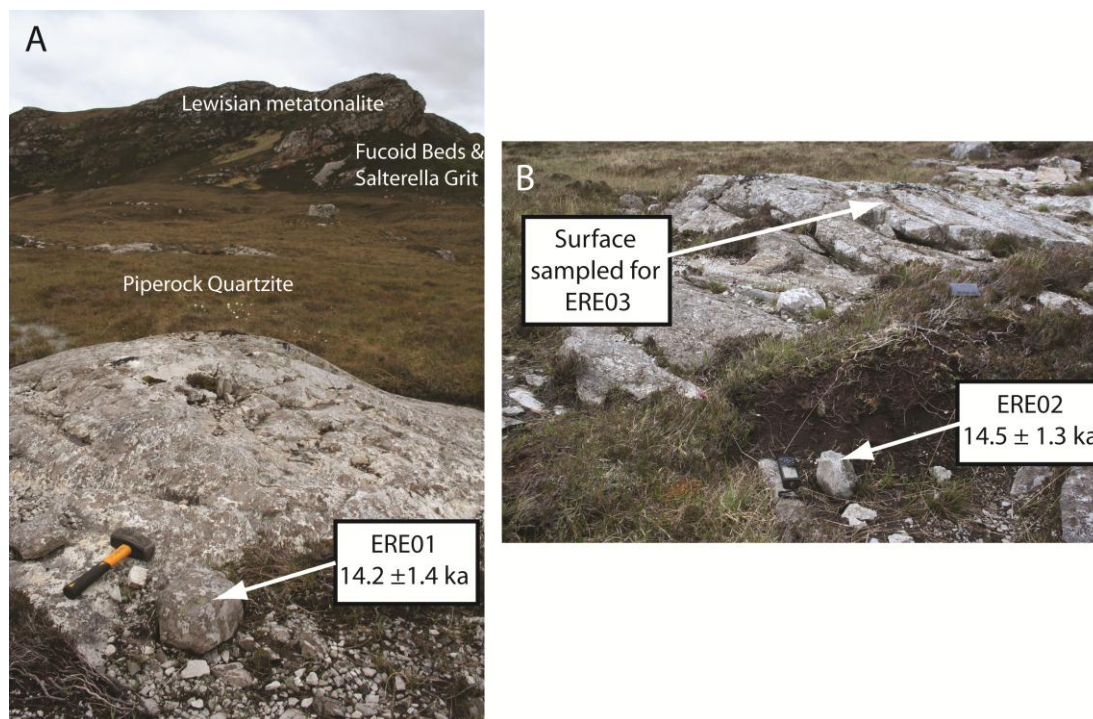


Figure 3.22: TCN sampling, near Heilam between Lochs Eriboll and Hope. A - ERE01 Rounded basal quartzite erratic on Piperock bedrock. B - ERE02 Lewisian erratic sample seen in foreground next to GPS. Bedrock samples (ERE03b, ERE03c) were taken from the glacially abraded surface of the Piperock outcrop to pair the erratic boulder samples.

3.2.1.8. Loch Hope

Loch Hope (Folio 3) is a deep (> 56 m) but narrow freshwater body with its outlet c. 10 m above present sea level. The steep slopes of Ben Hope define its SE margin while the W side of the loch rises to the An Lean Chàrn interfluvium separating the Hope valley from neighbouring Loch Eriboll. The Moine Thrust cuts obliquely across the N third of the loch separating Moine cover rocks to the south from a complex package of Cambrian and pre-Cambrian meta-sediments to the north.

Patchy flat-topped terraces seen around the head of Loch Hope consist of well-sorted and rounded gravels. A relict beach berm level 1.5-2.0 m above present sea level (Figure 3.23) associated with the shallow terrace deposits indicates a marine origin for these features and requires a higher relative sea level in Lateglacial times when local glaciers would have supplied sediments into the loch or temperate processes under a mid-Holocene raised sea level.



Figure 3.23: Raised glaciomarine features of Loch Hope. A - Raised beach berms, E Loch Hope. B - Ice contact deposits, mouth of Loch Hope (looking west). Photos: DF.

A thick drape (>15 m) of glacial sediment is evident below An Lean-Chàrn on the W slopes above Loch Hope. Three sediment limits are notable here; (Folio 3) discernible by break in slope and surface texture. Where the loch narrows glacial sediment on the valley sides form conspicuous lozenge-shaped mounds appearing loch-side aligned down valley.

The E flank of the loch displays glacial moulded bedrock and sediment mounds in line with a northerly ice flow regime. Valley-oblique ridges overprint this grain including, above Braesgill, a lozenge-shaped mound trending SE-NW towards the loch shore. The ridge morphology and valley traverse orientation suggest it is the terminal moraine of a small palaeo-valley glacier. At the head of the loch, a series of sub-parallel curvilinear meltwater channels occur beneath Ben Hope aligned roughly north-south.

3.2.1.9. Ben Loyal

The syenite tors of Ben Loyal (Folio 1) are large monoliths, morphologically and lithologically unusual in the region (Figure 3.24). The apparent absence of weathered debris around the summit tors of Ben Loyal (Figure Figure 3.24), relative paucity of boulders on slopes and occurrence of large boulders at the foot of the mountain suggests glacial transport of tor blocks from An Caisteal for greater than 1.5 km in a north westerly direction. Summit surfaces show juxtaposed evidence of slab loss by glacial transport and solutional features associated with long-term subaerial weathering (Figure Figure 3.24 A).

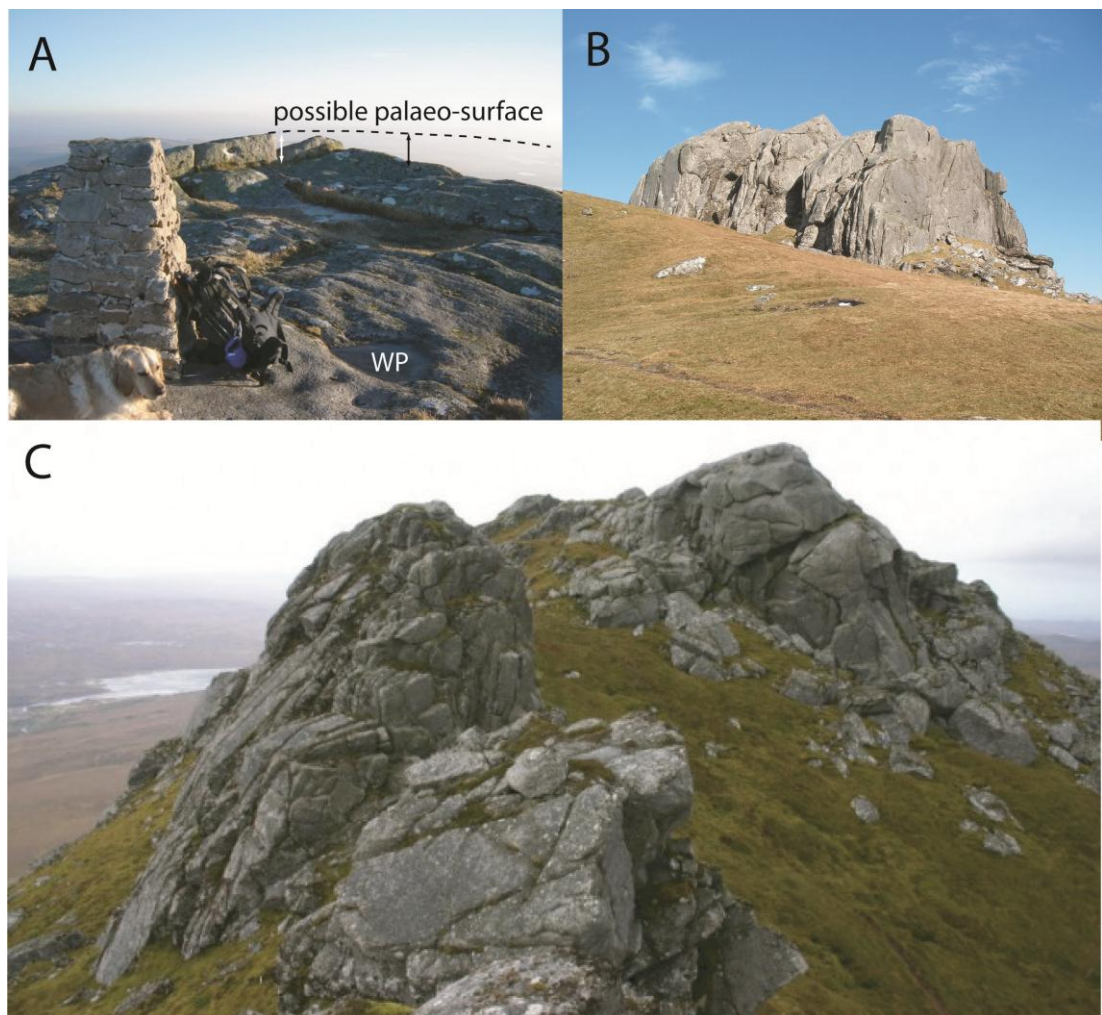


Figure 3.24: Ben Loyal summits. A - An Caisteal summit. WP - Weathering pits. Image: <http://mountainsofscotland.co.uk>. B - Tor context. Image: activespiritblog.blogspot.co.uk. C - Tor detail. Image: Jason Bonniface.

3.2.1.10. Cape Wrath Area

All high points ground on Cape Wrath (Folio 1) show strong evidence of glacial streamlining (Figure 3.25). Fashven is orientated as a large-scale roches moutonnées developed under a northerly flow regime; Sgribhis-bheinn is similarly moulded in a NNE direction just above the coast. Creag Riabhach also displays cliffed faces on its NW and NE sides.

A large humpbacked subglacial meltwater channel traverses the headland from SW to NE. Clais Leobairnich and Clais Chàrnach are steep-sided gorges with Allt na Clais Leobairnich to the North (N of Sandwood Bay) wrapping around the tip of Cape Wrath. This channel initiates abruptly, and deepens quickly down-course 40 m depth. Clais Chàrnach to the east of Cape Wrath is similarly deeply cut. Another wide, this time shallow, channel terminates near Kearvaig.

Bordering Cape Wrath, low scoured bedrock (Torridon Sandstone and Lewisian Gneiss) terrain typical of the W maritime margin is seen throughout W Sutherland (Figure 3.26). In contrast to adjacent terrain around Loch Eriboll and Oldshoremore, Cape Wrath appears to be covered in a reasonably thick and consistent cover of glacial sediment, probably till. The intervening land between Cape Wrath and Oldshoremore is pocked by many lochans, the locations of which coincide with distinct changes in thickness of till cover. The lochans often encircle large shallow sediment-lined depressions while beyond, towards the coast, bedrock is exposed (Figure 3.27).



Figure 3.25: Cape Wrath coast. Looking WSW to the glacially streamlined headland above Stack Clò Kearvaig W of the Kyle of Durness.



Figure 3.26: Scoured ground beneath Foinaven at Càrn Leacach. Looking SE to roche moutonnées and knock and lochan landscape formed in Lewisian basement. Photo: DF.

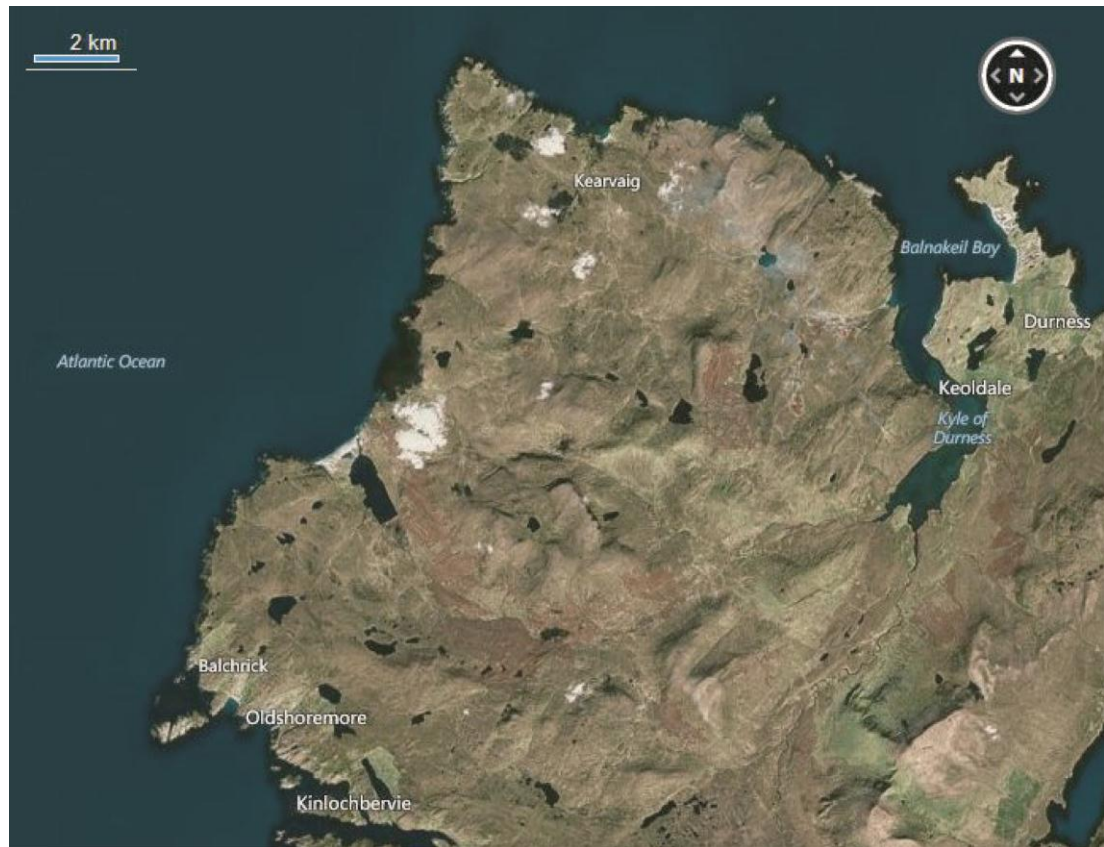


Figure 3.27: Aerial image of W Sutherland showing lochan distribution. Image: Bing maps.

3.3. Western Sutherland: Oldshoremore & Sheigra

The area around Oldshoremore and Sheigra (Folio 1, Figure 3.28, Figure 3.29) on the NW coast of Sutherland was investigated to determine the significance of a regionally unusual concentration of glacially transported boulders. With the general scarcity of depositional glacial landforms, the occurrence, of a notable coverage of boulders around this W headland area, is significant. As a feature of significant size (lateral continuity of ~3km), this coastal boulder spread may be important in understanding the retreat history of the ice sheet margin following collapse of the Minch palaeo-ice stream.

Much of the northwest is peppered by a conspicuous cover of glacially transported boulders, often dramatically perched on exposed bedrock whalebacks of the knock and lochan landscape which typifies the

appearance of the Lewisian complex of the NW coast. Around Oldshoremore the boulder cover is distinct from this ‘dropped crumb’ boulder sprinkling, as discernible boulder belt deposits of grouped clasts. As such, the distribution attracted attention because it represents an uncharacteristic concentration of glacially transported material suggestive of ice margin stabilisation around Oldshoremore.

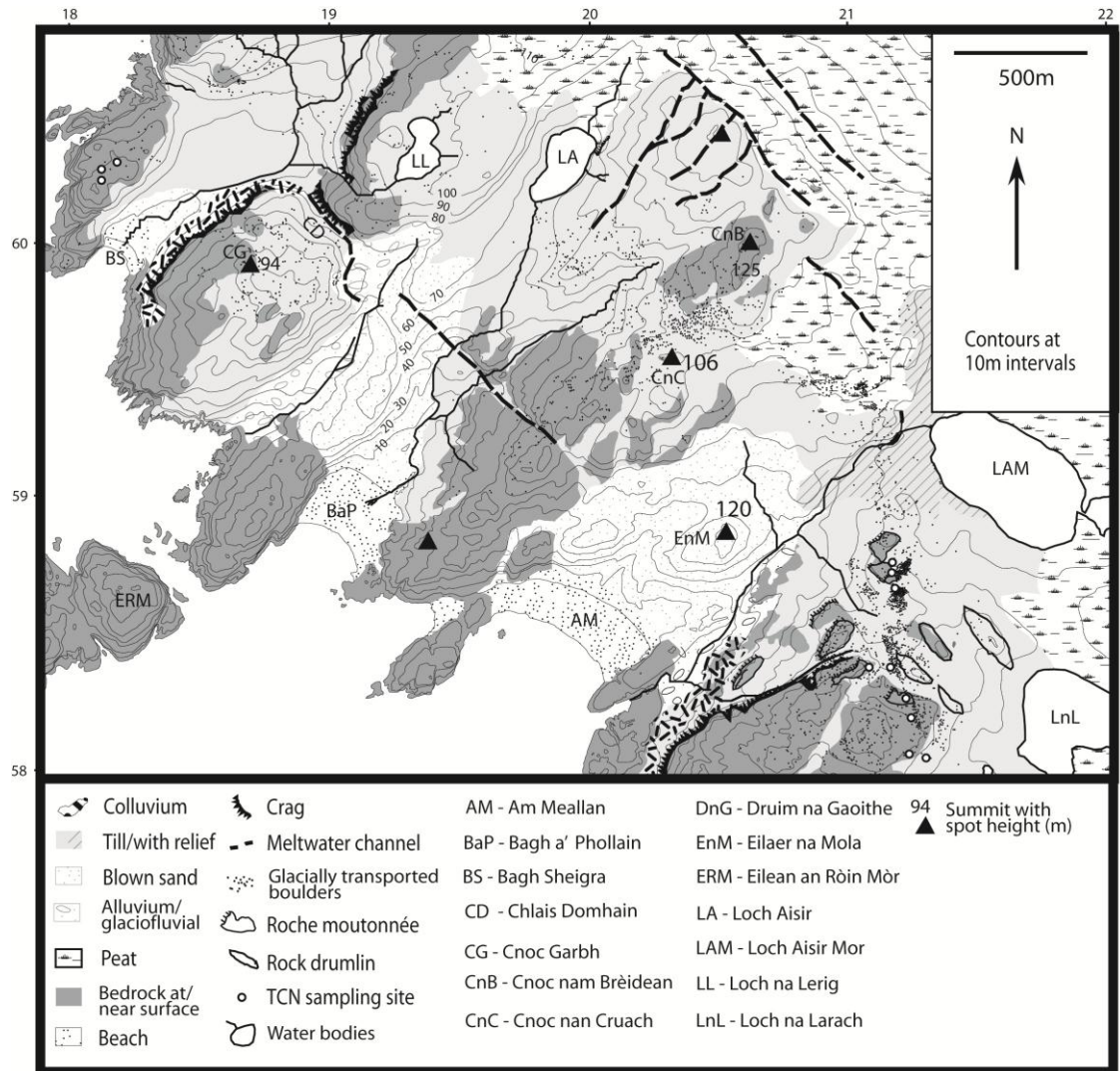


Figure 3.28: Geomorphology and sediment cover of the Oldshoremore area, Western Sutherland. For location see Folio 1.

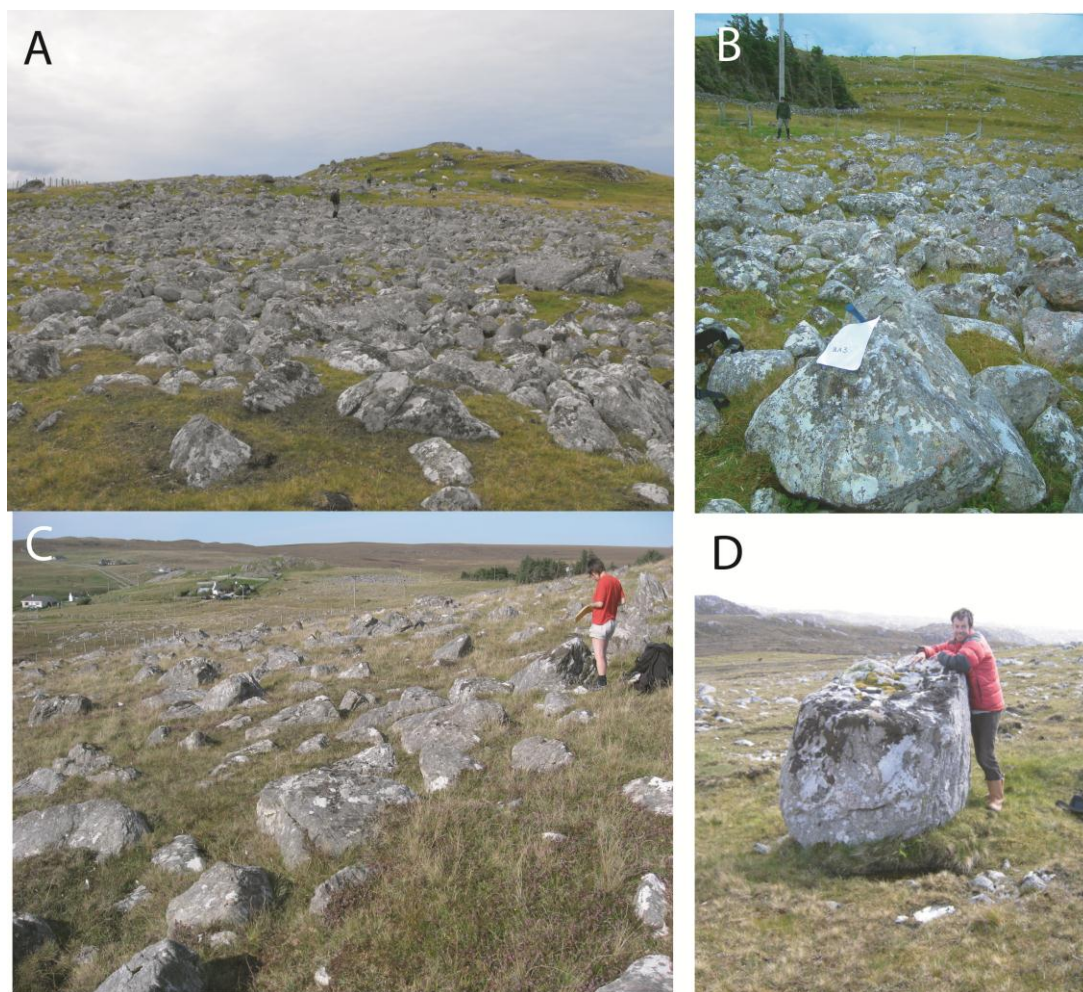


Figure 3.29: Sampling the boulder spread at Oldshoremore. A - Oldshoremore boulder spread. Perched boulders on skyline. Photo: AC. B - BLA3 Lewisian erratic amid boulder spread. C - Oldshoremore boulder spread. Photo: DF. D - OSM3 a large orthogneiss boulder at the southeast end of the boulder belt.

The Oldshoremore boulder spread manifests as a discontinuous band of boulders (Figure 3.29), commonly one to two boulders thick, mainly (>90%) of locally sourced orthogneiss. Erratics of quartzite and Torridon sandstone occur as minor constituents of the boulder deposit. On Figure 3.28 the relative densities of dots representing glacially transported boulders give an impression of the density and distribution of the deposit. Overall the boulder band has a sinuous shape, wrapping around the bedrock knolls from SE to NW. The deposit does however show some topographic independence with boulders spreading upslope to 110 m a.s.l. Many of the larger boulders lie stranded on moulded whaleback highs with swathes, two boulders deep, of smaller boulders around the sides and base of hills.

Table 3.6: TCN sample locations and physical characteristics of samples from Oldshoremore and Sheigra, Western Sutherland. See Table 3.1 for acronyms.

Location	Sample ID	Lat.	Long.	OS grid reference	Elev. (m)	Sample type	Sample dimensions a,b,c axes (m)	Litho.	Previous sediment cover	Post-depo. move.	Weathering indicators
Oldshoremore	BLA1	58.48007	-5.07041	NC: 221079, 958741	82	GTB	2,1.5,1	G (VQ)	U	U	QVP ≤4cm
	BLA2	58.48033	-5.07033	NC: 221085, 958770	77	GTB	1.5,1.5,1	G (VQ)	U	U	QVP ≤4cm
	BLA3	58.4738	-5.06964	NC: 221092, 958670	77	GTB	1.5,1.5,1	G (VQ)	U	U	QVP ≤4cm
	OSM1	58.47421	-5.06749	NC: 221143, 958042	93	Erratic	1,1,?	BQ	P ≤2m sediments or peat	VM ≤2m	None
	OSM3	58.47547	-5.06739	NC: 221155, 958181	93	GTB	1.2,1.2,1.2	G (VQ)	U	U	QVP ≤1.5cm
	OSM5	58.47583	-5.06906	NC: 221138, 958254	97	GTB	2,1.25,0.3	G (VQ)	U	U	Not apparent
Sheigra	SHE3	58.49292	-5.12236	NC: 218120, 960298	56	Erratic	0.4,0.25,0.2	Q	P	U	None
	SHE4	58.49292	-5.12236	NC: 218120, 960298	62	Bedrock	N/A	G (VQ)	U	U	QVP ~1cm Pseudo-polish preserved

Table 3.7: TCN sampling data and surface exposure ages of samples from Oldshoremore and Sheigra, Western Sutherland. For calculation details see footnote to Table 3.3

Location	Sample ID	Lat.	Long.	Elev. (m)	Sample thickness (cm)	Topo shielding factor	[¹⁰ Be] (x10 ⁶ atom g ⁻¹)	Apparent exposure age (¹⁰ Be) kyr*
Oldshoremore	BLA1	58.48007	-5.07041	82	2	0.9994	7.13 ± 0.6	14.4 ± 1.4 (1.2)
	BLA2	58.48033	-5.07033	77	1.5	0.9994	6.99 ± 0.54	14.2 ± 1.3 (1.1)
	BLA3	58.4738	-5.06964	77	4	0.9999	8.23 ± 0.58	17.0 ± 1.4 (1.2)
	OSM1	58.47421	-5.06749	93	3	0.9996	7.97 ± 0.34	16.1 ± 1.0 (0.7)
	OSM3	58.47547	-5.06739	93	3	0.9995	8.10 ± 0.50	16.4 ± 1.2 (1.0)
	OSM5	58.47583	-5.06906	97	3	0.9990	6.89 ± 0.26	13.7 ± 0.8 (0.5)
Sheigra	SHE3	58.49292	-5.12236	56	3	0.9998	7.70 ± 0.29	16.2 ± 1.0 (0.6)
	SHE4	58.49292	-5.12236	62	3	0.9976	13.21 ± 0.41	27.7 ± 1.5 (0.9)

Boulders appear most concentrated in the SE of the area towards Loch na Larach. Boulders vary in size from c. 30 cm to > 3 m a-axis with more than ninety five percent of clasts of Lewisian lithology. Six boulders were sampled between 77 and 97 m a.s.l. Samples were collected from the SE end of the boulder spread where it crosses through the village of Oldshoremore. The boulder population is at its most concentrated, and the geomorphic expression of the feature most pronounced, here (Figure 3.29). All exposure ages derived from the boulders are post-LGM: BLA1 - 14.4 ± 1.4 ka BP, BLA2 - 14.2 ± 1.3 ka BP, BLA3 - 17 ± 1.4 ka BP, OSM1 - 16.1 ± 1.0 ka BP, OSM3 - 16.4 ± 1.2 ka BP, OSM5 - 13.7 ± 0.8 ka BP (Full details in Table 3.6 and Table 3.7). Age spread of boulders will be discussed in Chapter 4.

The headland of Sheigra (northwest of Oldshoremore) also hosts a low density scatter of glacially transported boulders in some places directly perched on glacially abraded orthogneiss bedrock (Figure 3.30B). The continuity of this boulder spread with the aforementioned spread through Oldshoremore cannot be confirmed as extensive deposits of blown sand reaching inward from the coast may obscure the full extent of the boulder belt. Sampling in this locality allows assessment of the age of the recessional stage which deposited the regional boulder lag and also the severity of the subglacial erosion by the last ice sheet. Bedrock on the headland (Figure 3.30 D) returned an age of 27.7 ± 1.5 ka BP (SHE4) with paired erratics giving statistically indistinguishable deglaciation ages of 16.2 ± 1.0 ka BP (SHE3) and 15.2 ± 1.1 ka BP (SHE2) (Figure 3.30 A&C).

Bedrock appears in ribs of the more resistant orthogneiss, often distinctively glacially moulded, while Torridon bedrock outcrops are often eroded and obscured by a cover of blown sand towards the coast, and till inland. In the SE of the area, towards Loch na Larach, bedrock has been eroded into rock drumlin spindles (up to 250 m in length) orientated NW where rock structure is conducive, or roches moutonnées with plucked faces on their northwest flank. Preservation of long striations at Sheigra support strong NW ice flow across the area.

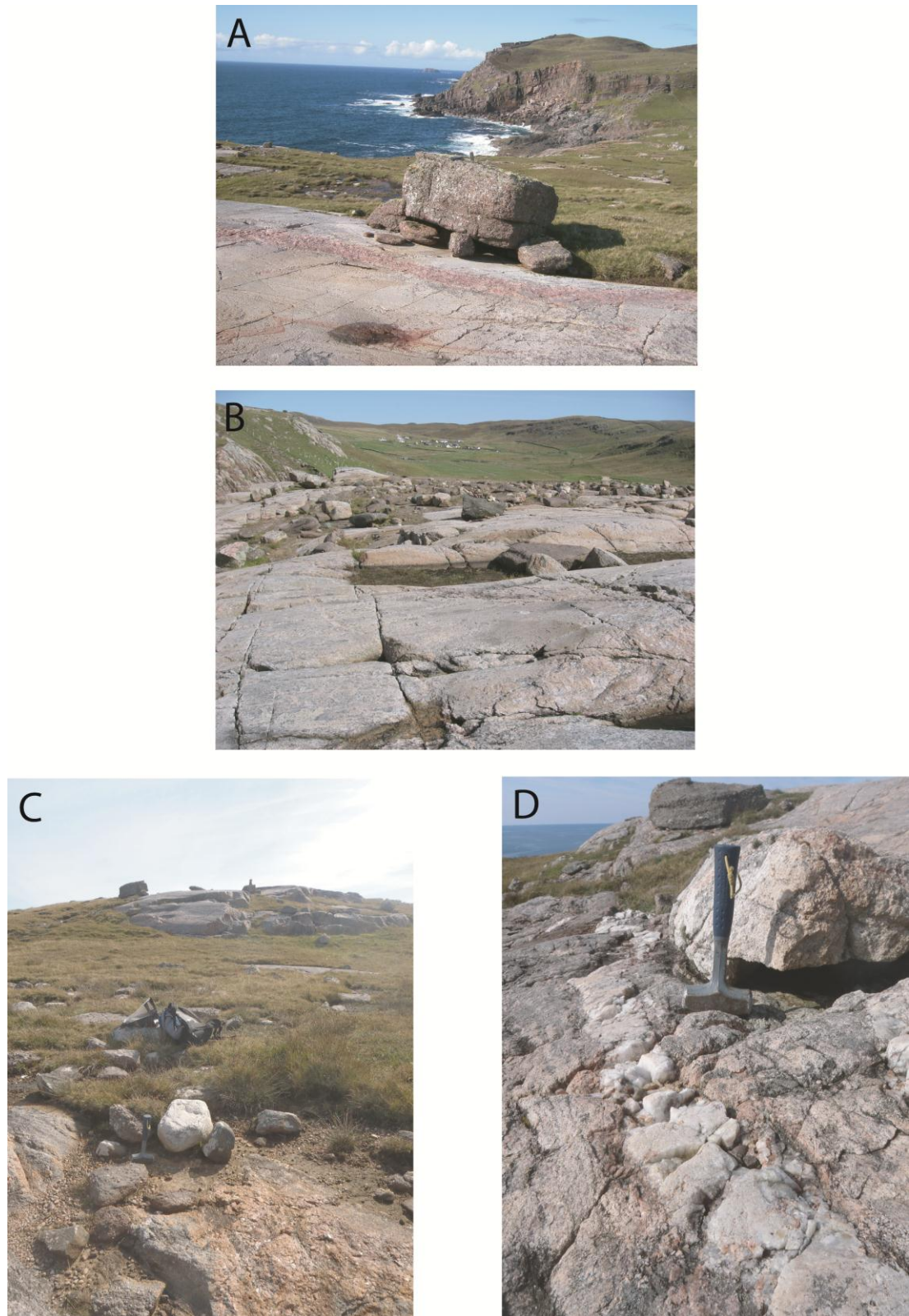


Figure 3.30: Sheigra TCN samples. A - SHE2 Torridon erratic, 50 m a.s.l. on orthogneiss bedrock with striations orientated 320°N. B - Erratic boulder lag over Lewisian bedrock. Photo: DF. C - SHE3 quartzite erratic above Na Stacain, Sheigra D.- Wide quartz vein surface (SHE4) in moulded orthogneiss bedrock. Vein protrusion of 1cm above groundmass.

The area is also traversed by meltwater channels cut in bedrock and up to 1 km in length. Three trends of meltwater channel exist. A first parallel to the coast (striking NW - SE) in a flight of straight sub-parallel forms independent from topographic control. Once such channel trenches the hill of Cnoc Bearaich and continues as a narrow gorge through the sandstone at Chlais Domain. The second trend is normal to the first (trending NE - SW), is more sinuous and appears to feed into the channel system NE of Loch Aisir. A third class of shorter more sinuous channels, one at the outlet of Loch Aisir Mor and one which flows through Chlais Domhain, adhere to topographic control and feed into modern fluvial valleys. These appear to drain from the peatland to the north of the area; a shallow sediment filled depression marked by a sprinkling of lochans (Figure 3.27).

A blanket of till is found across the inland area exposed where the surface has not been inundated by blown sand. Where exposures exist the till is seen as a massive red sandy diamict with reworked quartz pebbles sourced from the Torridon Sandstone. Frequent quartzite cobbles and boulders embedded in a Torridon grös at the ground surface near Loch Aisir may represent a winnowed till. This suggests that some quartzite boulders found amid the boulder train may belong to an underlying eroded till sheet.

3.4. Assynt Mountains: Glas Bheinn, Beinn Uidhe, Conival, Breabeg

The Assynt plateaux exhibit a subtle suite of glacial geomorphic features, owing in part to the governing physical structure and chemical resistance of the underlying Cambrian quartzite bedrock. The peaks investigated in this study - Glas Bheinn, Beinn Uidhe, Conival and Breabeg rise gently from the regional plateau (~600-700 m a.s.l.) as whaleback summits. The continuity of the plateau surface is broken in several places by glacial back wearing, towards and sometimes through, the spine of the mountains. At the northwest end of the chain Bealach na h-Uidhe separates Glas Bheinn from the long ridge of Beinn Uidhe (Folio 1), and to the south,

the Beallach Traligill isolates Breabeg from the higher peaks of Conival and Ben More Assynt.

Rough altitudinal banding of geomorphic characteristics is seen across the plateau with two distinctive thresholds, the upper relating to increased expression of glacial erosion, manifest in incidence of exposed bedrock and meltwater channels, and the lower to the onset of glacial deposition. The elevation of these thresholds varies across the mountains but occurs roughly at 750-650 m for the upper threshold and below 500 m a.s.l. for the lower. The summit area of Glas Bheinn (650-776 m a.s.l.) is armoured by blockfield formed in both quartzite members. Erratics appear to be absent at this level but orthogneiss erratics, common as sub-rounded cobbles, pebbles and small boulders are distributed on the Bealach na h-Uidhe from 620 m a.s.l., SE of the summit.

Periglacial features including sorted nets are seen on the higher ground towards the summit of Beinn Uidhe, and solifluction lobes descend the slopes on the plateau's NE margin. On the summit ridge, blockfield cover thins towards the SE (Figure 3.31) and isolated ribs of quartzite bedrock, undulating in tight antiforms, protrude through the regolith cover. The exposed bedrock often bears evidence of glacial abrasion in erosional p-forms or surface markings (Figure 3.32 F). Striae and crescentic gouges indicate westerly ice flow over the plateau. BU04 was sampled from this glacially modified bedrock (Figure 3.32 C) and yielded an exposure age equivalent to 86.4 ± 4.7 ka BP. Below 700 m a.s.l. the incidence of bedrock free of regolith increases as does cover by till sheets. Meltwater channels, associated with plateau drainage, appear from 650 m a.s.l., incise sediment from ~550 m a.s.l., below Bealach a' Mhadaidh, and translate to a system of ridges and subglacial bedforms from 480 m a.s.l.

Table 3.8: TCN sample locations and physical characteristics of samples from Beinn Uidhe and Breabeg, Assynt. See Table 3.1 for acronyms.

Location	Sample ID	Lat.	Long.	OS grid reference	Elev. (m)	Sample type	Sample dimensions a,b,c axes (m)	Litho.	Previous sediment cover	Post-depo. move.	Weathering indicators
Beinn Uidhe	BU01	58.1753	-4.90586	NC: 229204, 924400	712	Erratic	0.2,0.2,0.2	BQ	U	N/A	None
	BU02	58.1753	-4.90586	NC: 229204, 924400	712	Erratic	0.2,0.15,0.15	LG	U	N/A	None
	BU03	58.1753	-4.90586	NC: 229204, 924400	712	Bedrock (in blockfield)	N/A	PR	U	N/A	None
	BU04	58.17674	-4.90331	NC: 229361, 924554	714	Bedrock (glacially abraded)	N/A	PR	U	N/A	WR 1cm
	BU05	58.17675	-4.90341	NC: 229355, 924555	714	Erratic	0.15,0.15,0.10	LG	U	N/A	None
	BREA01	58.09702	-4.90846	NC: 228675, 915696	812	Bedrock	N/A	PR	N/A	U	None
	BREA03	58.09793	-4.90778	NC: 228720, 915796	810	Bedrock	N/A	PR	U	U	None
	BREA04	59.09793	-4.90778	NC: 228720, 915796	810	Bedrock	N/A	PR	U	U	None

Table 3.9: TCN sampling data and surface exposure ages of samples from Beinn Uidhe and Breabeg, Assynt. For calculation details see Table 3.3 footnote.

Location	Sample ID	Lat.	Long.	Elev. (m)	Sample thickness (cm)	Topo shielding factor	[¹⁰ Be] (x10 ⁶ atom g ⁻¹)	[²⁶ Al] (x 10 ⁶ atom g ⁻¹)	Apparent exposure age (¹⁰ Be) kyr*	²⁶ Al/ ¹⁰ Be ratio
Beinn Uidhe	BU01	58.1753	-4.90586	712	3	1.0000	14.62 ± 0.52		16.5 ± 1.0 (0.6)	
	BU02	58.1753	-4.90586	712	3	1.0000	11.59 ± 0.50		13.1 ± 0.8 (0.6)	
	BU03	58.1753	-4.90586	712	3	1.0000	48.02 ± 1.76	295.26 ± 7.14	54.7 ± 3.2 (2.0)	6.73 ± 0.3
	BU04	58.17674	-4.90331	714	3	0.9874	74.43 ± 2.04	462.92 ± 11.22	86.4 ± 4.7 (2.4)	6.81 ± 0.25
	BU05	58.17675	-4.90341	714	4	0.9958	12.71 ± 0.75		14.5 ± 1.1 (0.9)	
Breabeg	BREA01	58.09702	-4.90846	812	3	1.0000	97.99 ± 3.12	591.43 ± 14.41	103.6 ± 5.9 (3.4)	6.61 ± 0.28
	BREA03	58.09793	-4.90778	810	3	1.0000	99.03 ± 3.19	581.18 ± 14.22	104.9 ± 6.0 (3.5)	6.43 ± 0.26
	BREA04	59.09793	-4.90778	810	3	1.0000	94.95 ± 2.66	560.29 ± 13.76	99.9 ± 5.5 (2.9)	6.46 ± 0.24

Lewisian erratics are large and common across the Beinn Uidhe plateau and at lower elevation. Their distribution is particularly dense in the concave slope of Corrag Ghorm (Figure 3.32 E) on the E plateau margin (see also 3.7.1). Lewisian erratics occur, along with glacially transported “pseudo-erratics” of Basal Quartzite (short transport distance only on the plateau from a local but not adjacent outcrop), across both the regolith cover and exposed bedrock surfaces. On Beinn Uidhe, all erratics yield post-LGM ages. An orthogneiss erratic (BU05) perched on the quartzite surface of BU04 returned a deglaciation age of 14.5 ± 1.1 ka BP. Two metres lower on the plateau surface, and closer to the E plateau edge, two erratics (BU01 - quartzite and BU02 - orthogneiss), amid blockfield, yielded GI-1 ages (16.5 ± 1 ka BP and 13.1 ± 0.8 ka BP respectively). The age variation between the erratics is not anticipated to represent different deglaciation ages or inheritance, but rather, unresolved variation in surface erosion governed by lithological control (TCN details in Table 3.8 and Table 3.9).

Regional observations of gneiss outcrops (30-90 m a.s.l.) suggest ca. 3 cm of postglacial surface loss based on protruding quartz veins. Erosion limited calculations are employed to generate exposure ages for BU02 and BU05 (Table 3.9). A bedrock surface amid the blockfield provides a pair for the erratics with an exposure age of 54.7 ± 3.2 ka BP. $^{26}\text{Al}/^{10}\text{Be}$ ratios calculated for BU03 (6.73 ± 0.30 atm/g/yr) and BU04 (6.81 ± 0.25 atm/g/yr) show no significant reduction from the production ratio excluding the possibility of long-term (>100 kyr) burial beneath thick (>50 m) ice.

Blockfield on Breabeg’s summit is thin and patchy, and in some areas partially vegetated where Salterella Grit and Furoid Beds outcrop amid the predominant quartzite cover. Regolith generally extends down to 650 m (Figure 3.33C) a.s.l. on the W slope of the ridge though a lineament at c. 600 m a.s.l., near the head of the Allt nam Uamh, separates the blockfield regolith above, from glacially cleared slopes below (see also 3.7.1). However, on the S slopes below Creag Liath, blockfield extends further, down to 550 m a.s.l. Towards Creag Liath at the S end of Breabeg, a large

rock slope failure, sourced at ~700 m a.s.l. scars the W flank of the mountain (Figure 3.33).

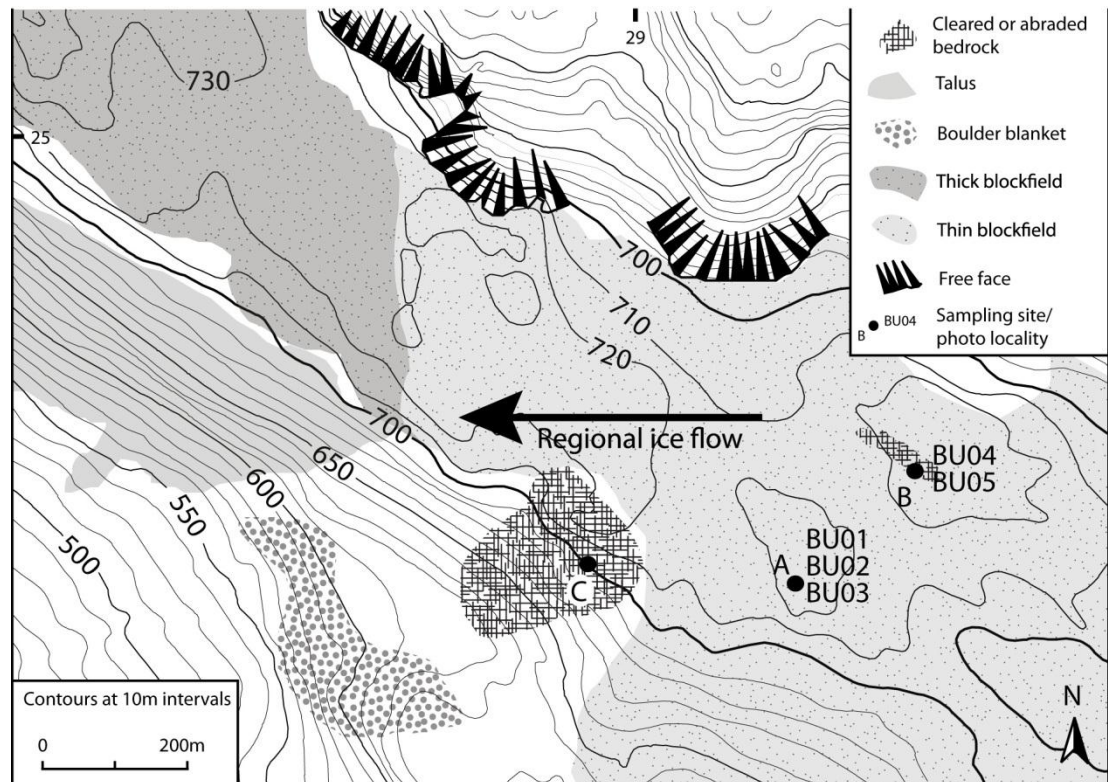


Figure 3.31: Geomorphic features of the lower Beinn Uidhe plateau, Assynt.

Evidence of glacial overriding of the Breabeg summit is subtle but tangible in the occurrence of microdiorite local pseudo-erratics which provide a bouldery lag of cobbly lichen-covered clasts 20-40 cm in diameter from ~810 m a.s.l. downwards. These erratics were unsuitable for TCN analysis due to their mafic composition, so all exposure ages have been derived from bedrock amongst regolith cover. Though high level striae (807 m a.s.l. (Lawson, 1990)) have been previously noted on Breabeg (summit - 815 m a.s.l.), evidence of long term solutional weathering of the quartzite is also apparent (Figure 3.33 D). All Breabeg bedrock samples (Figure 3.33 A&B) yield statistically inseparable TCN concentrations equivalent to exposure periods of: BREAO1 - 104.0 ± 5.9 ka BP, BREAO3 - 105.0 ± 6.0 ka BP, BREAO4 - 100.0 ± 5.5 ka BP. The $^{26}\text{Al}/^{10}\text{Be}$ data for these samples, as on Beinn Uidhe, show no significant reduction from the

production ratio with a mean of 6.5 ± 0.26 atm/g/yr therefore excluding the possibility of long-term burial.

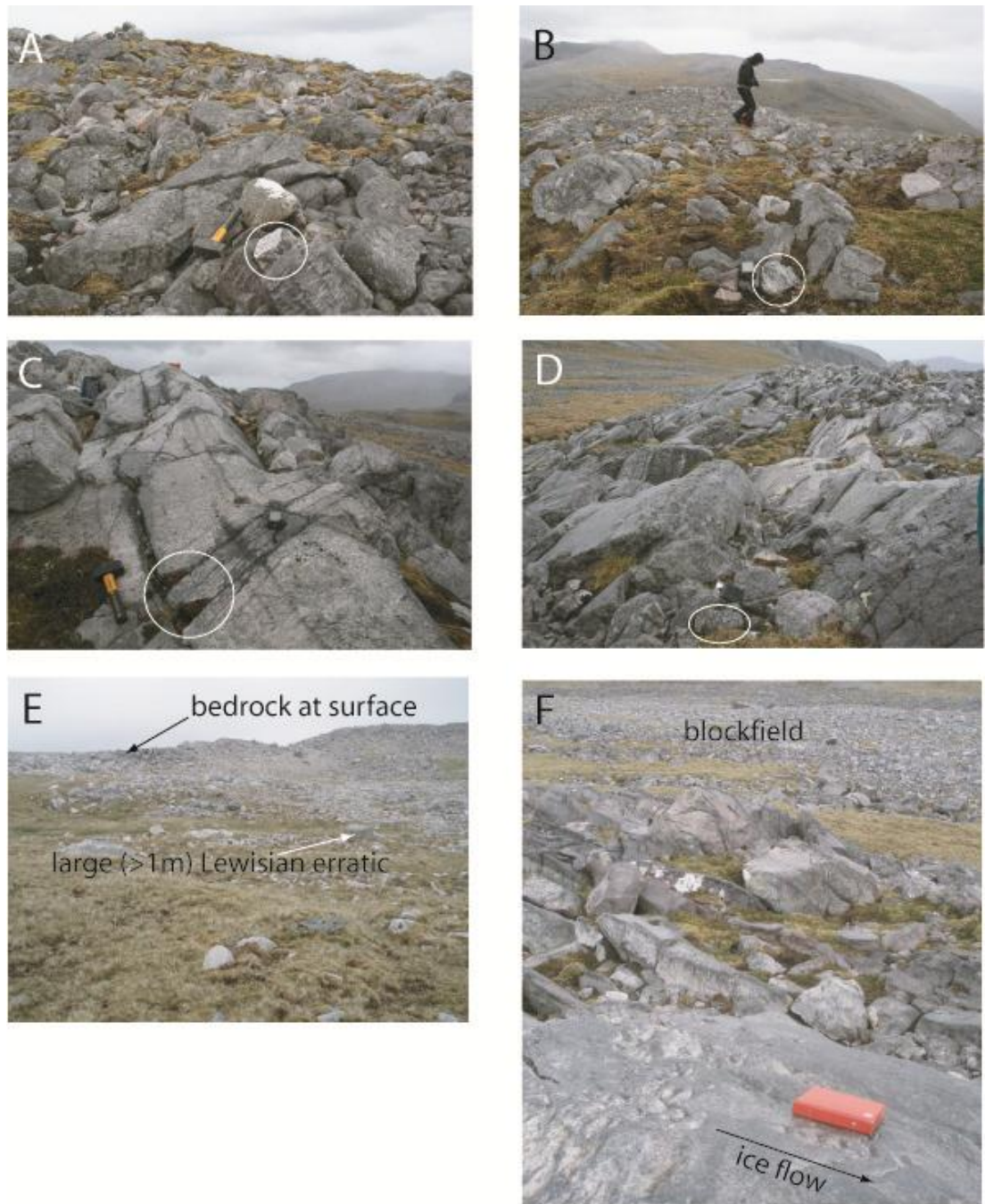


Figure 3.32: Beinn Uidhe plateau. A - Basal quartzite pseudo-erratic (BU01) on Piperock regolith. Hammer for scale. Photo: TB. B - BU02 Lewisian erratic sample on blockfield near plateau edge. Photo: TB. C - Quartzite bedrock rib (714m). Surface between GPS and hammer sampled for TCN analysis (BU04). Photo: TB. D - BU05 Lewisian erratic on quartzite bedrock with p-forms. Photo: TB. E - Dense bouldery cover including erratics, Corrag Ghorm, below E lip of Beinn Uidhe plateau. F - Cresecentic gouges.

Descending SE from the summit plateau, streamlined bedforms appear abruptly from c. 650 m a.s.l. in Garbh Choire indicating initiation of basal sliding. Elongate directional bedforms on the E slopes of Sgonnan Mòr terminate abruptly upslope at 480 m a.s.l.

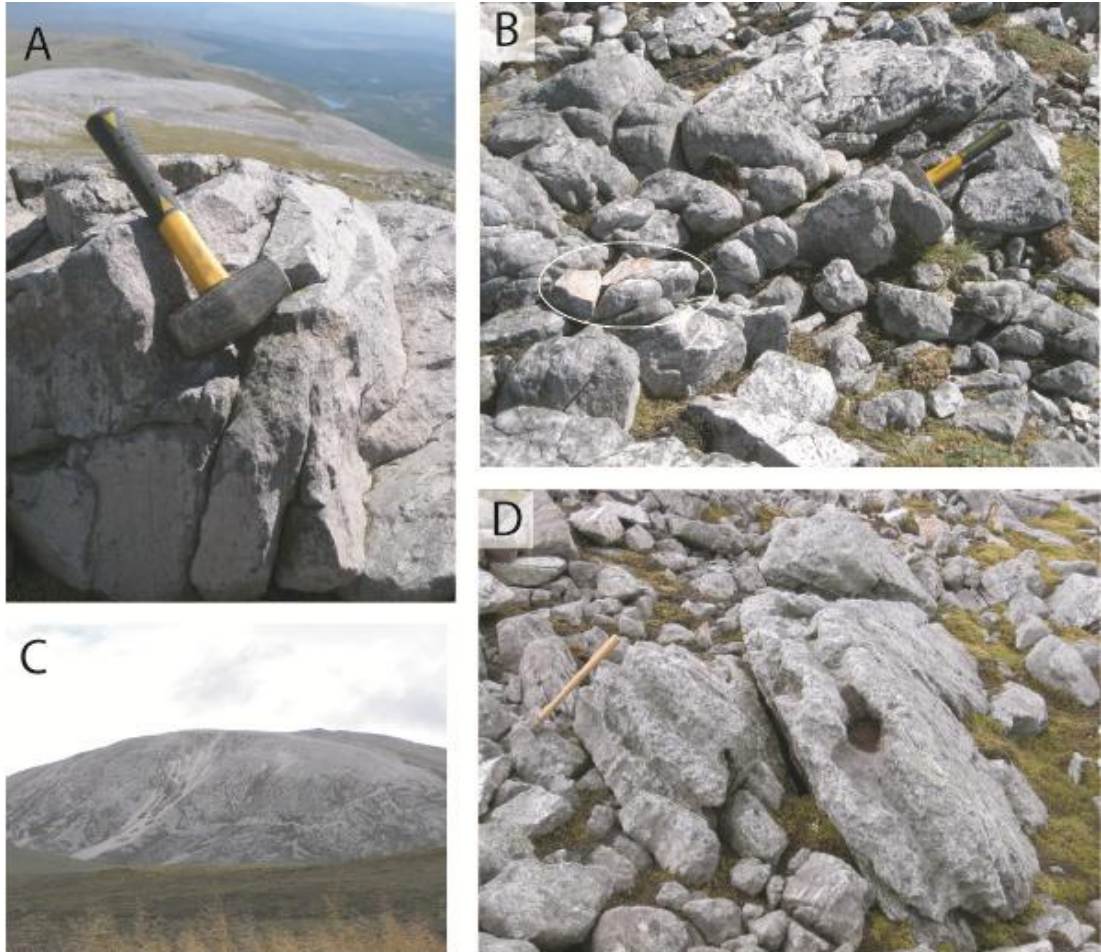


Figure 3.33: Geomorphic features, Breabeg. A - BREA01 bedrock sample. B - BREA04 bedrock sample. C - Breabeg seen from the SW. Quartzite regolith seen across SW slopes with failure. Photo: TA/RF. D - Solutional weathering of quartzite near summit of Creag Liath. Photo: TA.

3.5. Coigach

Lying west of the Moine thrust, the Coigach region is dominated by the outcrop of the Applecross Formation, part of the Torridon Sandstone group typified by a coarse, gritty or occasionally pebbly texture. The landscape is characterised by inselbergs separated by wide u-shaped valleys and, towards the coast, a low knock and lochan topography of islets and rock basins.

3.5.1. *Cul Beag*

With a SE ramp and steeply cliffed NW face, Cul Beag (769 m a.s.l.) echoes the form of its larger, wedge-shaped, neighbour Cul Mor (849 m a.s.l.). Though glacially abraded surfaces are identifiable at lower elevations, significant postglacial erosion of summit bedrock surfaces is evident from strong edge-rounding of outcrops (Figure 3.34) and protrusion of pebbles from boulder surfaces (Figure 3.34 D). TCN exposure ages from bedrock on Meall Dearg (13.3 ± 0.9 ka BP) and Cul Beag (15.7 ± 1.1 ka BP) suggest different exposure histories (discussed in Chapter 4).

Glacial transport of material to at least 657 m a.s.l. is apparent from the occurrence of perched Torridon boulders on the subsidiary summit of Meall Dearg (Figure 3.34 A). Erratic material is sparse, small in size and a component of a sediment lag, largely comprising weathered Torridon materials, lying on the upper slopes of the mountain. A sample combined from quartzite pebbles in the surface lag yielded an exposure age of 12.8 ± 0.9 ka BP while a larger erratic quartzite pebble in the same lag returned 23.6 ± 1.4 ka BP (Table 3.10 and Table 3.11). This age discrepancy will be discussed in Chapter 4.

Table 3.10: TCN sample locations and physical characteristics of samples from Cul Beag, Beinn an Eòin, Ben Mor Coigach and Tanera Mor, Coigach. See Table 3.1 for acronyms.

Location	Sample ID	Lat.	Long.	OS grid reference	Elev. (m)	Sample type	Sample dimensions a,b,c axes (m)	Litho.	Previous sediment cover	Post-depo. move.	Weathering indicators
Cul Beag	CULB01	58.02782	-5.13813	NC: 214786, 908603	650	Bedrock	N/A	TS	U	N/A	ER
	CULB02	58.02945	-5.15042	NC: 214069, 908819	760	Bedrock	N/A	TS	U	U	SL ≤20cm
	CULB03C	58.02929	-5.14871	NC: 214169, 908796	733	Erratic (composite sample)	cobbles	Q	P	VM <2m	None
	CULB04	58.02902	-5.14791	NC: 214215, 908764	710	Erratic	0.2,0.15,0.2	BQ?	P ≥10cm sediments	VM ≥2m	None
Beinn an Eòin	BAE1	58.00673	-5.20873	NC: 210511, 906443	617	Erratic	0.4,0.4,0.3	BQ	None	None	None
	BAE2	58.00632	-5.20912	NC: 210485, 906397	618	Erratic	0.4,0.35,0.3	BQ	None	None	None
Ben Mor Coigach	BMC2	57.98728	-5.21008	NC: 210249, 904259	711	Bedrock	N/A	TS	P 1m sediments	U	SL 5-10cm
	BMC3	57.98811	-5.20745	NC: 210486, 904367	716	Erratic	0.3,0.25,0.25	MS	P	U	WR
	BMC4	57.98673	-5.19555	NC: 211182, 904180	566	Erratic	0.4,0.3,??	Q	U	U	Not apparent
Tanera Mor	TANM01	58.01966	-5.40886	NB: 98761, 908471	32	Erratic		BQ?	P	U	WR 1cm
	TANM02	58.01823	-5.41087	NB: 198634, 908318	30	GTB	1,0.8,0.5	TS	U	U	WP 10cm
	TANM03	58.00632	-5.40889	NB: 198684, 906987	35	Erratic	0.5,0.4	PR	P ≥1m peat	None	None

Table 3.11: TCN sampling data and surface exposure ages of samples from Cul Beag, Beinn an Eòin, Ben Mor Coigach and Tanera Mor, Coigach. For calculation details see footnote of Table 3.3.

Location	Sample ID	Lat.	Long.	Elev. (m)	Sample thickness (cm)	Topo shielding factor	[¹⁰ Be] (x10 ⁶ atom g ⁻¹)	Apparent exposure age (¹⁰ Be) kyr*
Cul Beag	CULB01	58.02782	-5.13813	650	3	0.9996	11.17 ± 0.56	13.3 ± 0.9 (0.7)
	CULB02	58.02945	-5.15042	760	5	0.9980	14.23 ± 0.74	15.7 ± 1.1 (0.8)
	CULB03C	58.02929	-5.14871	733	3	0.9932	11.44 ± 0.63	12.8 ± 0.9 (0.7)
	CULB04	58.02902	-5.14791	710	3	0.9871	20.56 ± 0.81	23.6 ± 1.4 (0.9)
Beinn an Eòin	BAE1	58.00673	-5.20873	617	3	1.0000	12.77 ± 0.43	15.7 ± 0.9 (0.5)
	BAE2	58.00632	-5.20912	618	2	0.9998	12.59 ± 0.74	15.3 ± 1.1 (0.9)
Ben Mor Coigach	BMC2	57.98728	-5.21008	711	3	0.9992	9.41 ± 0.48	10.6 ± 0.7 (0.5)
	BMC3	57.98811	-5.20745	716	4.75	0.9992	10.50 ± 0.41	12.0 ± 0.7 (0.5)
	BMC4	57.98673	-5.19555	566	3	0.9974	10.32 ± 0.52	13.3 ± 0.9 (0.7)
Tanera Mor	TANM01	58.01966	-5.40886	32	3	0.9960	6.17 ± 0.30	13.3 ± 0.9 (0.7)
	TANM02	58.01823	-5.41087	30	3	0.9999	7.49 ± 0.68	16.2 ± 1.6 (1.5)
	TANM03	58.00632	-5.40889	35	3	0.9922	8.00 ± 0.35	17.3 ± 1.1 (0.8)

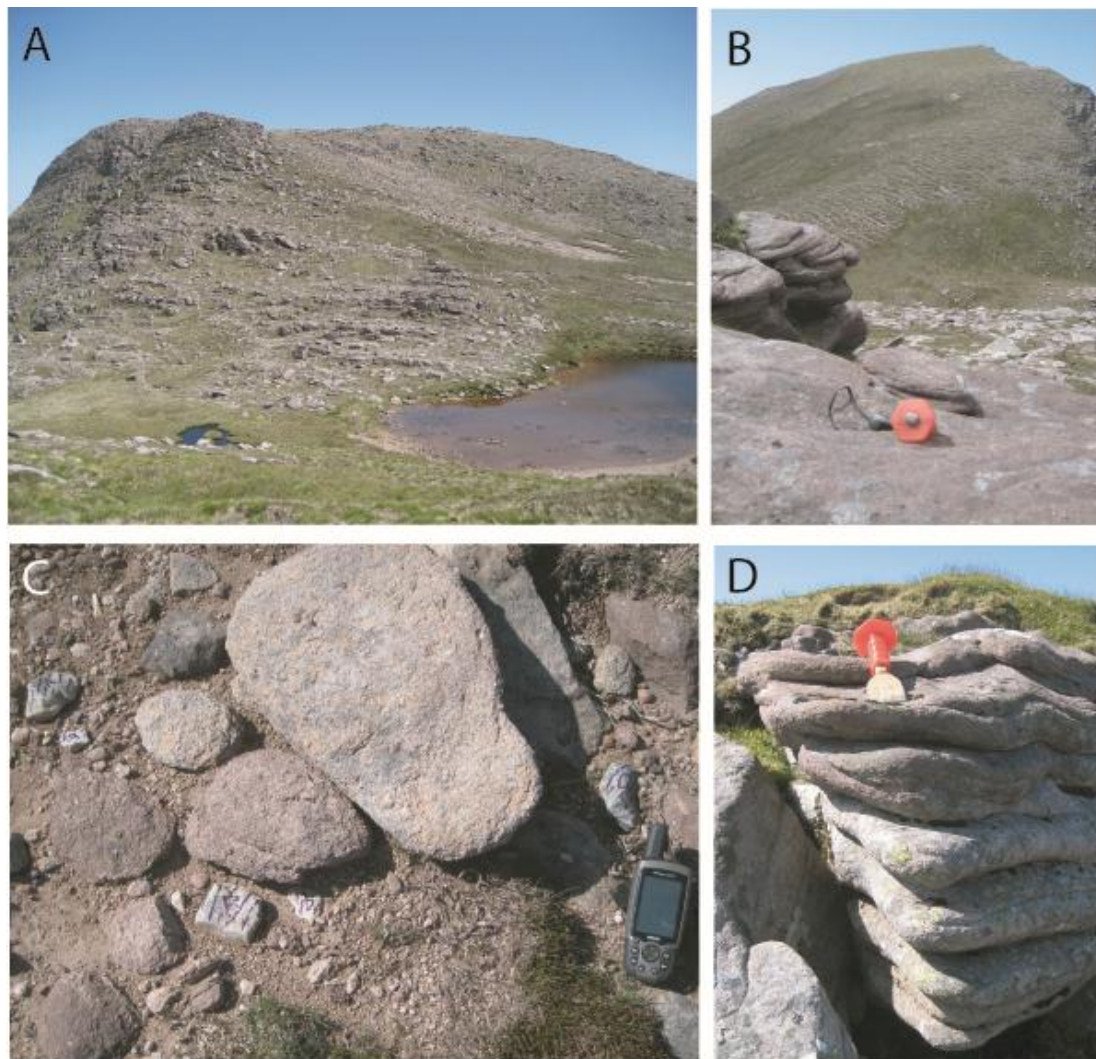


Figure 3.34: Geomorphology of Cul Beag, Coigach. A - Meall Dearg, subsidiary peak of Cul Beag. Sediment lag on surface and well-rounded summit. B - Looking towards the rounded summit of Cul Beag from Meall Dearg. Strongly edge-rounded Torridon bedrock (CULB01) in foreground. C - Labelled quartz pebbles sampled for CULB03c. D - Woolpack form edge-rounded weathering of Torridon bedrock, Cul Beag summit. Chisel indicates location of surface sampled for CULB02.

3.5.2. Beinn an Eòin

Beinn an Eòin (619 m a.s.l.) and neighbouring Stac Pollaidh (612 m a.s.l.) are similar in situation, elevation and lithology, but polar in character (Figure 3.35 D). The former, is smooth and glacially abraded to summit level (Figure 3.35 C), the latter delicately ornamented with towers and pinnacles (Figure 3.35 D). Perched Basal Quartzite erratics were sampled

on the summit of Beinn an Eòin (Figure 3.35 A, B & D) produce statistically identical deglaciation ages of 15.7 ± 0.9 ka BP (BAE1) and 15.3 ± 1.1 ka BP (BAE2) (Full details in Table 3.10 and Table 3.11).

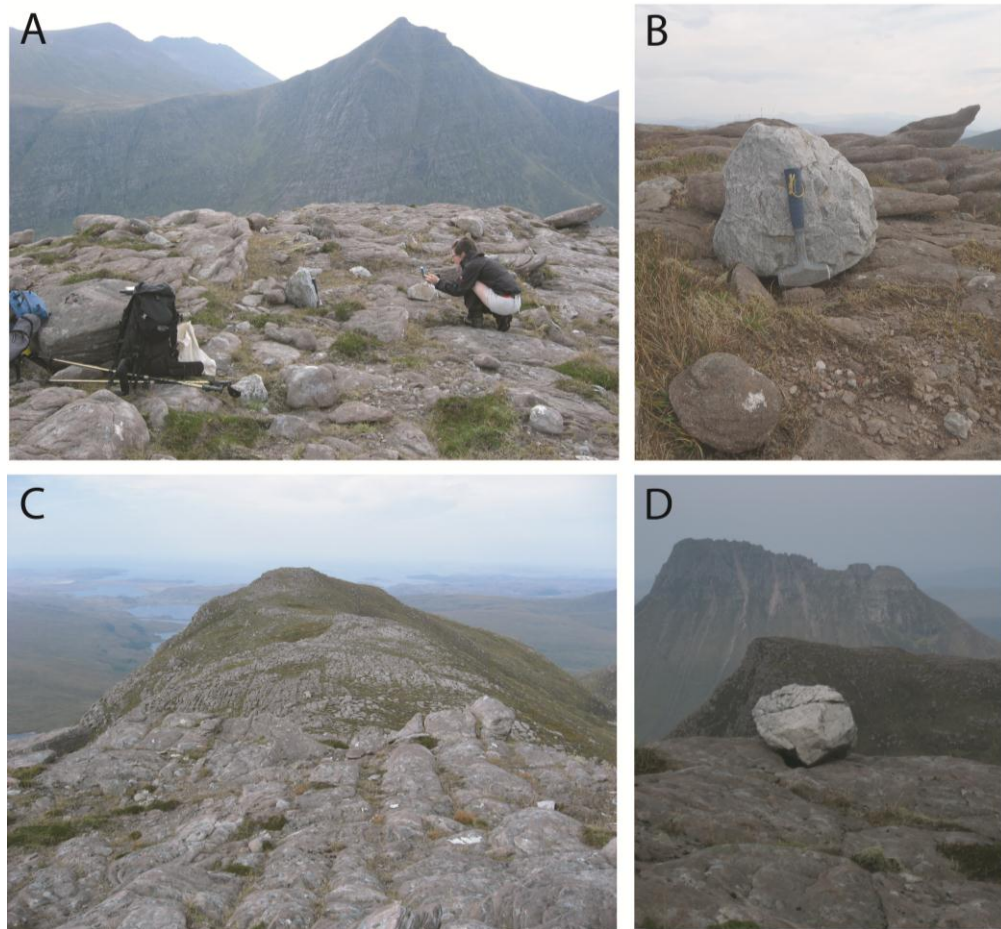


Figure 3.35: Beinn an Eòin. A - Context of BAE1 Beinn an Eòin plateau with Sgurr an Fhidhleir, Ben More Coigach massif behind. Photo: DF. B - BAE1 quartzite erratic. Wind sculpted Torridon bedrock behind. C - Character of the Beinn an Eòin plateau looking north-NW. Photo: DF. D - BAE2 quartzite erratic perched on Torridon bedrock, summit of Beinn an Eòin. Narrow ridge of Stac Pollaidh behind (north). Photo: DF.

3.5.3. Stac Pollaidh

Field evidence and remote sensing observations from Stac Pollaidh indicate the close spatial juxtaposition of glacial overriding evidence with landforms indicative of deep subaerial weathering (Figure 3.36 D).

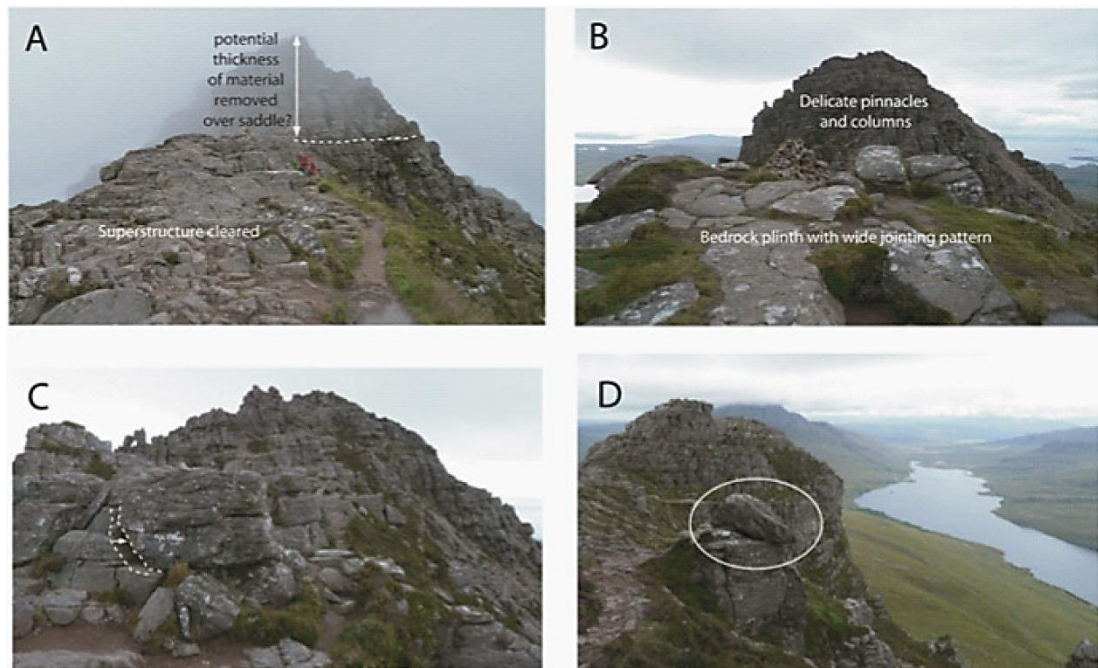


Figure 3.36: Evidence of glacial modification on the summit ridge of Stac Pollaidh. A & B: Evidence of differential erosion over saddle vs summit. C: Evidence of block shunting indicated by void opening. D: Perched block. Photos: Turriff Mountaineering and Hillwalking Club.

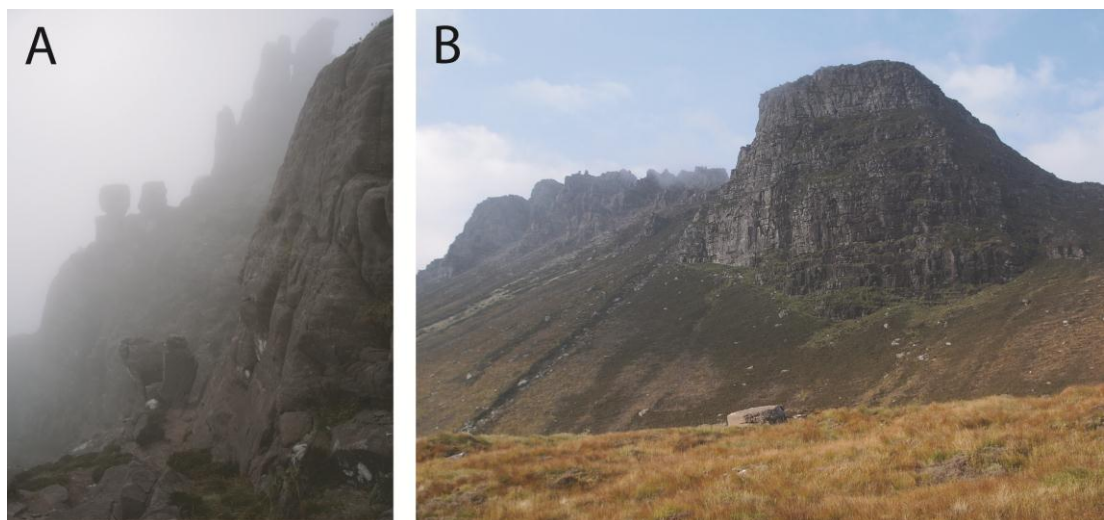


Figure 3.37: Weathering features, Stac Pollaidh. A - Pinnacles on summit ridge. B - Active scree chutes and large relict talus cones, southern flank of Stac Pollaidh.

3.5.4. *Ben More Coigach & Spidean Còinnich*

The Ben More Coigach massif (Figure 3.38 D) rises directly from the sea on the edge of the Coigach peninsula. The mountain is dissected by valleys in the west and flanked by sheer cliffs on the north, south and E sides. A large plateau c. 1km², above 550 m a.s.l., connects the main summit with those of Sgurr an Fhìdhleir to the north and Speceinn Còinnich to the east. The plateau is characterised by blown sands (Figure 3.38 C) and periglacial features as described by Ballantyne (1995).

The highest erratic on Ben More Coigach, a Moine psammite boulder (BMC3 - 12.0 ± 0.7), was found at 716 m a.s.l (Table 3.10 and Table 3.11). The likelihood of finding erratics higher than this elevation is severely diminished by the cover of aeolian and soliflucted sediment. A Torridon bedrock sample (BMC2), from the plateau edge at 711 m a.s.l. yields a young exposure age of 10.6 ± 0.7 ka BP. Below the plateau, increasing slope angle and exposure reduces aeolian sediment cover. The abundance of erratics increases and boulder size quartzite erratics appear with BMC4 (13.3 ± 0.9 ka BP) was sampled at 566 m a.s.l (Figure 3.38 B). Below ~450 m a.s.l. the E ridge of Speceinn Còinnich (subsidiary peak of Ben More Coigach) is a stripped bedrock pavement scattered with glacially transported boulders (Figure 3.38 A).

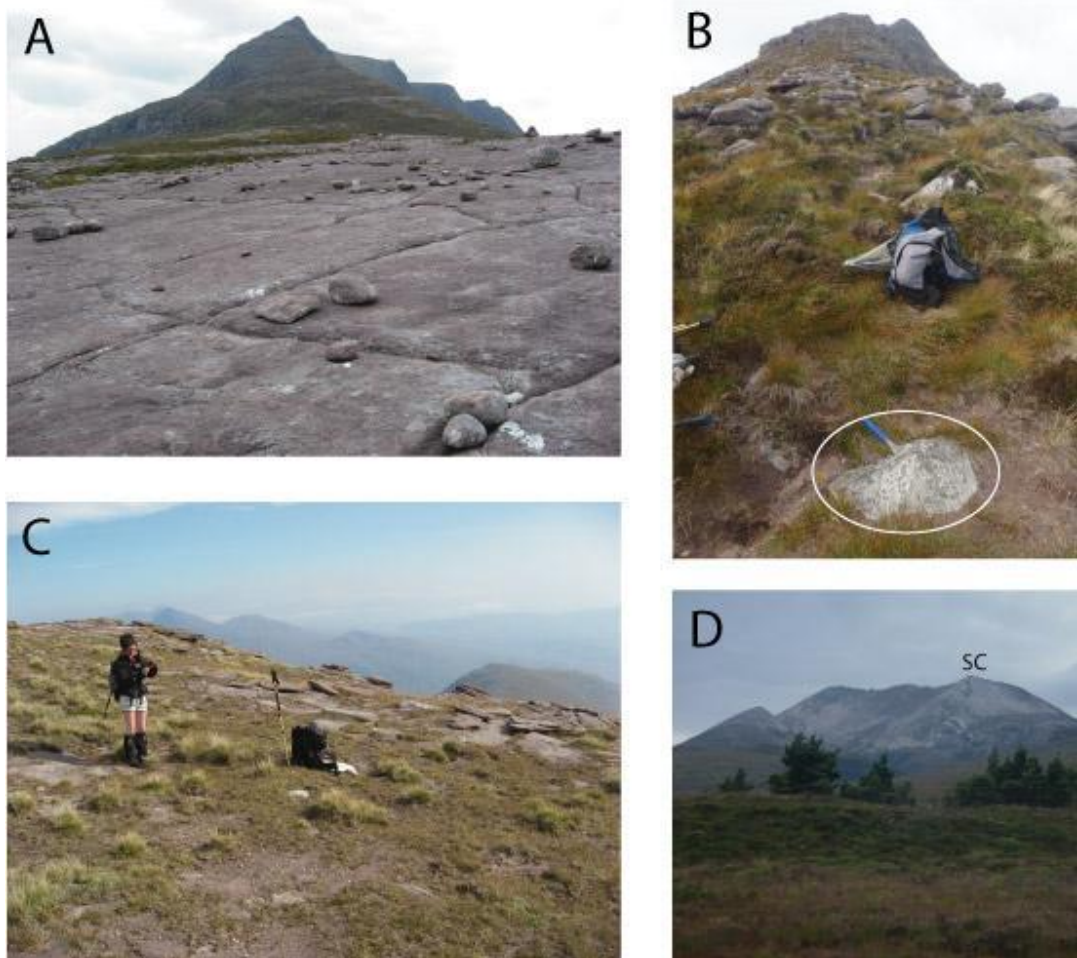


Figure 3.38: Ben More Coigach and Speceinn Còinnich. A - GTBs on glacially scoured Torridon pavement, Speceinn Còinnich (c. 350m). Photo: DF. B - BMC4 Basal quartzite erratic (circled) embedded in flank of Speceinn Còinnich. C - BMC3 Moine psammite erratic (chisel and rucksack for scale) embedded in blown Torridon sand at 716m on shoulder of Ben More Coigach. Photo: DF. D - Ben More Coigach massif, Speceinn Còinnich (SC) at right. Photo: DF.

3.5.5. Tanera Mòr

Tanera Mòr is the largest of the Summer Isles, lying south of the Coigach Peninsula, in the eastern Minch just 1.5 km offshore. The island rises to 124 m a.s.l. at Meall Mòr, though most of the land is below 80 m a.s.l. as glacially abraded bedrock knolls and basins (Figure 3.39 A). Previous mapping by Bradwell *et al.* (2008a) identified a series of recessional moraines crossing the eastern Minch in the vicinity of the Summer Isles (Figure 3.41). These moraines have been correlated with onshore limits in Coigach and further south in Wester Ross. Correlation of offshore features with onshore moraines at Achiltibuie on the Coigach peninsula suggest that an ice limit may have stabilised in the vicinity of Tanera Mor, with the Summer Isles acting as pinning points for the retreating ice sheet.

Evidence of N, and later NW, ice flow is seen in the preservation of surface markings on bedrock surfaces emerging from sediment cover (Figure 3.40 B). The island's butterfly shape is bisected by a humpbacked meltwater channel crossing the island between the harbours of Mol Mòr and The Anchorage with a NE course. In this central saddle of the island, wedged in a sediment lag overlying the bedrock, TANM03 a Piperock quartzite erratic returned an exposure age of 17.3 ± 1.1 ka BP (Full sampling details Table 3.10 and Table 3.11). TANM01 (Figure 3.39 D) an erratic Basal quartzite boulder sampled from amongst cobbly lag on bedrock in the north of the island yielded an exposure age of 13.3 ± 0.9 ka BP. TANM02 (Figure 3.39B), also from the north of the island, a large perched Torridon boulder with surface weathering, yielded 16.2 ± 1.6 ka BP.

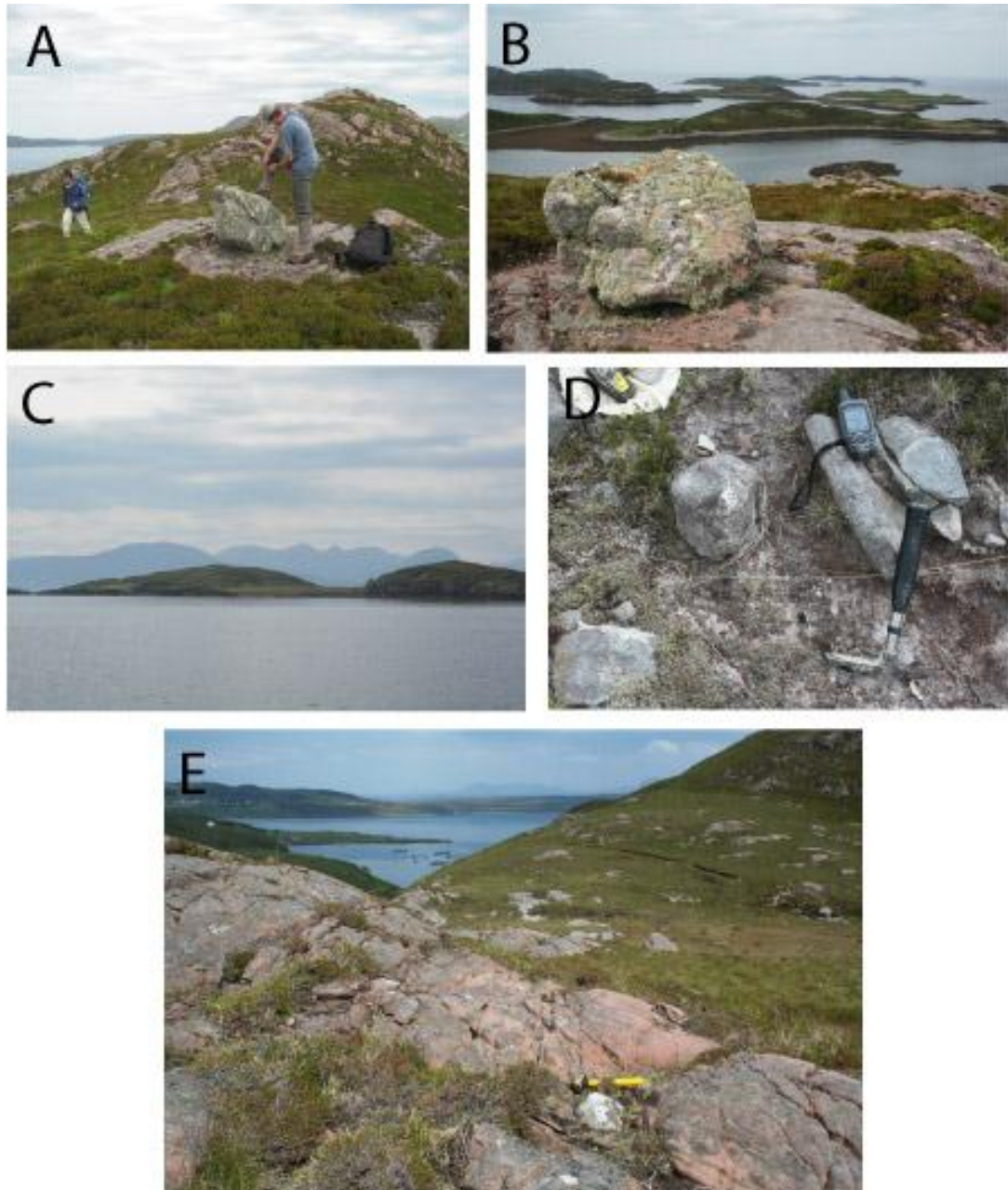


Figure 3.39: TCN sampling, Tanera Mòr. A - TANM02 perched glacially transported boulder. Looking SE. B - TANM02 with view NW over Summer Isles. Photo: TB. C - Profile of Tanera Mòr showing trench of meltwater channel which dissects the island. Looking SE towards An Teallach massif in background. Photo: TB. D - Basal quartzite erratic TANM01 in boulder lag. Photo: TB. E - TAN03 Piperock erratic (white-grey by hammer) on Torridon Sandstone. Looking SW. Photo: TB.



Figure 3.40: Geomorphic features of Tanera Mòr. A - Island topography. B - Crescentic fractures in Torrison bedrock overprinted by glacial striae and grooves (320 °N).

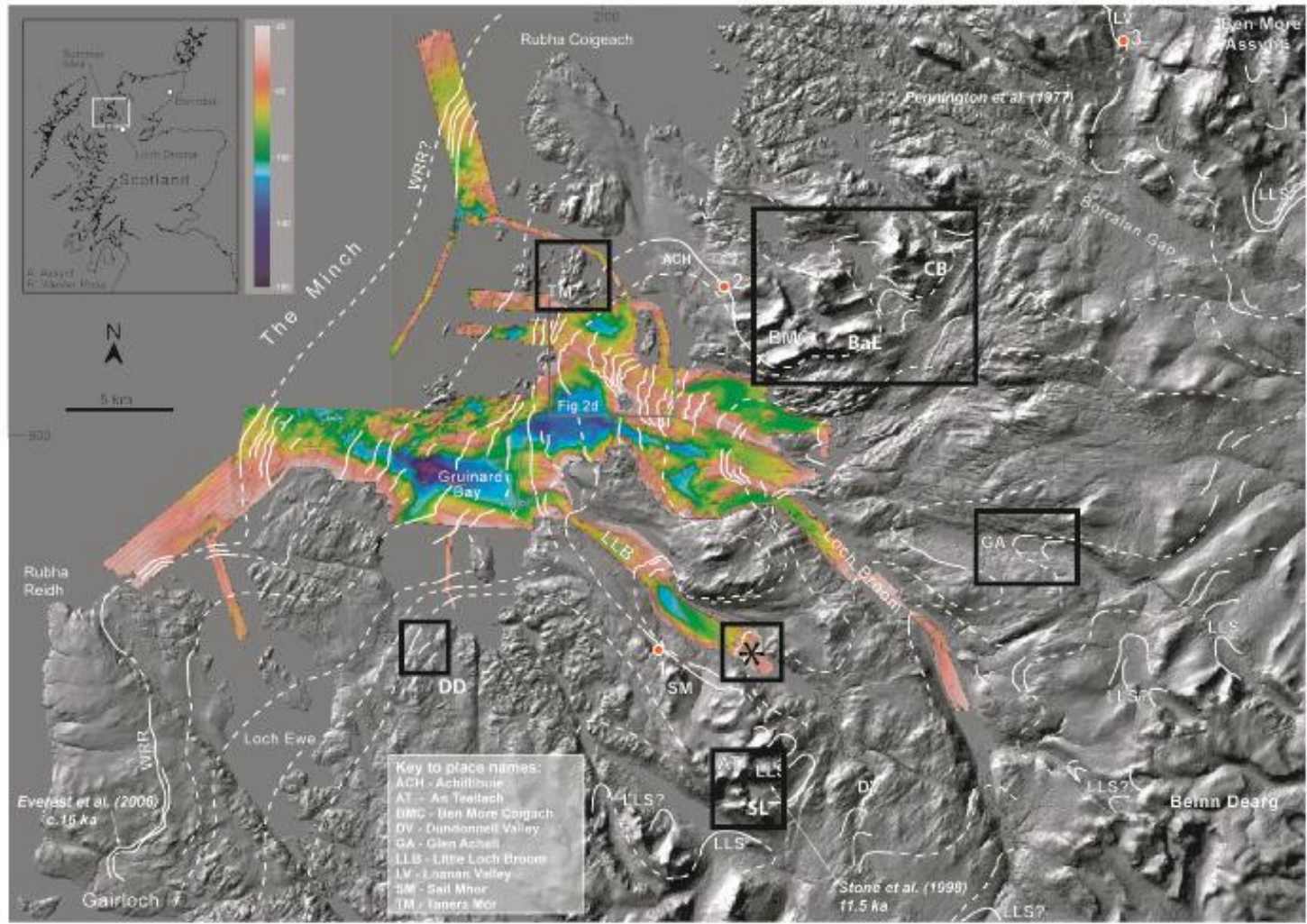


Figure 3.41: Retreat moraines within WRR limits. Adapted from (Bradwell et al., 2008a). Study regions (this study) in heavy black boxes. Dived samples (BGSD1/2) from the moraine separating inner and outer basins of LLB marked with an asterisk. DD = Dundonnell (DD) samples on the edge of Gruinard Bay. SL = Sail Liath (SAIL samples, An Teallach). BaE = Beinn an Eoinn. CB = Cul Beag.

3.6. Wester Ross

3.6.1. Glen Achall

In Glen Achall a moraine complex has been mapped to the east of Loch Achall (Bradwell *et al.*, 2008a). These moraines are thought to represent part of a recessional series stepping back from the Wester Ross Readvance near the coast towards the maximum extent of the Younger Dryas ice cap centred on the Beinn Dearg massif to the SE (Finlayson *et al.*, 2011). The moraine suite manifests as a series of arcuate cross-valley trending ridges orientated roughly NE to SW. The surfaces of the ridges are smooth and maintain a relatively low angle of repose suggesting a high component of fine grained material or possibly ice over-riding.

Sparse blocky boulders, predominantly schists and psammites of Morar Group (Moine Supergroup) are found on sides near the crests of ridges. A meltwater channel runs along the north wall of the valley behind the moraines and probably post-dates them, suggesting a later presence of plateau ice on the Rhidorroch uplands. All TCN samples are derived from large Moine schistose boulders sitting on ridge crests or moraine mound peaks. GAC01 and GAC02 are statistically indistinguishable with a mean of 10.1 ± 1.2 ka BP. GAC02 returns an older surface exposure age of 14.8 ± 1 ka BP (Table 3.12 and Table 3.13).

Table 3.12: TCN sample locations and physical characteristics of samples from Glen Achall and Sail Liath, Wester Ross. See Table 3.1 for acronyms.

Location	Sample ID	Lat.	Long.	OS grid reference	Elev. (m)	Sample type	Sample dimensions a,b,c axes (m)	Litho.	Previous sediment cover	Post-depo. movement	Weathering indicators
Glen Achall	GAC01	57.90822	-5.03808	NH: 220093, 895026	100	Moraine		MS	U	U	None
	GAC02	57.90649	-5.02789	NH: 220688, 894806	95	Moraine	2,1.5,??	MS	U	U	Pyrites weathered out
	GAC03	57.90715	-5.02301	NH: 220980, 894867	109	Moraine		MS	U	VM <1m	None
Sail Liath	SAIL01	57.79032	-5.24589	NH: 207156, 882481	949	Erratic	0.2,0.2,0.2	TS	P	LM ≤5m lateral	None
	SAIL02	57.78704	-5.23847	NH: 207579, 882095	840	Erratic	3,3,2	TS	P	VM ≤ 2m	NW JD 10cm
	SAIL03	57.78708	-5.23839	NH: 207584, 882099	837	GTB		PR	P	U	None
	SAIL04	57.78722	-5.23839	NH: 207585, 882115	830	Erratic	2,1.25	TS	U	U	None
	SAIL05	57.78718	-5.23815	NH: 207599, 882110	831	GTB		Q	P	U	WR 1cm

Table 3.13: TCN sampling data and surface exposure ages of samples from Glen Achall and Sail Liath, Wester Ross. For calculation details see footnote of Table 3.3.

Location	Sample ID	Lat.	Long.	Elev. (m)	Sample thickness (cm)	Topo shielding factor	[¹⁰ Be] (x10 ⁶ atom g ⁻¹)	Apparent exposure age (¹⁰ Be) kyr*
Glen Achall	GAC01	57.90822	-5.03808	100	3	0.9984	5.02 ± 0.55	10.1 ± 1.2 (1.1)
	GAC02	57.90649	-5.02789	95	4	0.9978	7.25 ± 0.34	14.8 ± 1.0 (0.7)
	GAC03	57.90715	-5.02301	109	3	0.9975	5.02 ± 0.55	10.0 ± 1.2 (1.1)
Sail Liath	SAIL01	57.79032	-5.24589	949	3	0.9999	9.11 ± 0.54	8.4 ± 0.6 (0.5)
	SAIL02	57.78704	-5.23847	840	3	0.9996	15.55 ± 0.73	15.8 ± 1.0 (0.7)
	SAIL03	57.78708	-5.23839	837	3	0.9996	14.19 ± 0.71	14.4 ± 1.0 (0.7)
	SAIL04	57.78722	-5.23839	830	3	0.9996	14.23 ± 0.73	14.5 ± 1.0 (0.8)
	SAIL05	57.78718	-5.23815	831	3	0.9996	15.25 ± 0.69	15.6 ± 1.0 (0.7)

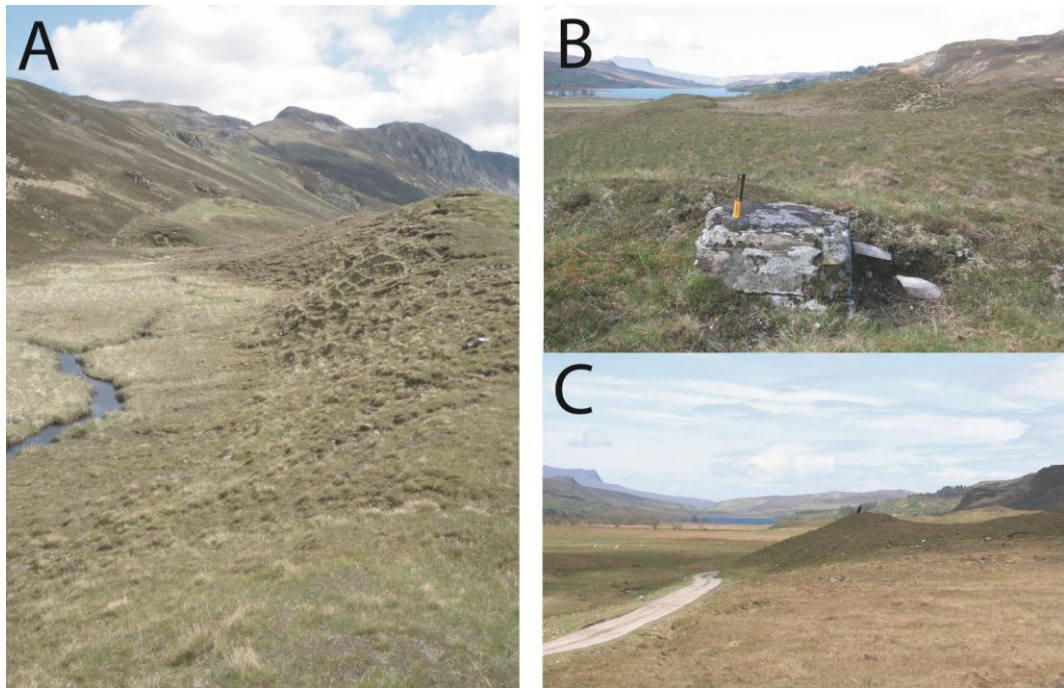


Figure 3.42: Geomorphic context of TCN sampling, Glen Achall. See also mapped recessional moraine series (Figure 3.41). A - Channel-backed moraine, Glen Achall. B - GAC01 on moraine peak, valley context, Loch Achall in background (looking west). Photo: TB. C - Sampling GAC02 on top of morainic mound. Looking west to Loch Achall in background. Photo: TB.

3.6.2. *Sail Liath*

Sail Liath (954 m a.s.l.) comprises the SE flank of the An Teallach mountain massif (Figure 3.43A). It is predominantly composed of Torridon Sandstone (pebbly Applecross Member) with a summit cap of Cambrian Quartzite (Basal Quartzite Member) (Figure 3.43 D). This lithological configuration is common to Glas Mheall Mòr and Glas Mheall Liath, other easterly An Teallach peaks. The mountain rises above the surrounding ground from ~450 m a.s.l. as a wedge-shaped buttress whose slopes are largely obscured by a thick pebbly regolith cover (Figure 3.44 A). The character of the surficial cover betrays elements of the glacial and periglacial history experienced as well as the nature of the underlying lithology.

At summit level, mountain top sediments comprise angular fragments with some evidence of size segregation in nets (Figure 3.43 C and Figure 3.44 B). A very short exposure history is indicated here by a Torridon erratic embedded in the quartzite blockfield (SAIL01 - 8.4 ± 0.6 ka BP). All TCN sampling details can be found in Table 3.12 and Table 3.13.

Between 940-915 m conspicuous solifluction lobes with low amplitude are studded with smaller, rounder clasts suggestive of remobilised glacial lag deposits. Surface sediment cover is thinner between 915-855 m a.s.l. exposing the underlying undulations of the quartzite bedrock beneath more angular material. Descending from the narrow summit plateau, below 855 m a.s.l., large Torridon erratics begin to appear (Figure 3.44 C & D) along with other erratic lithologies including Fucoid, Piperock quartzite and Orthogneiss (Figure 3.44 A). SAIL-02, -03, -04 and -05 were sampled between 831-840 m a.s.l. and all four yield overlapping ages with a mean of c. 15.1 ka BP (Table 3.13). Very large glacially transported boulders occur at lower elevation.

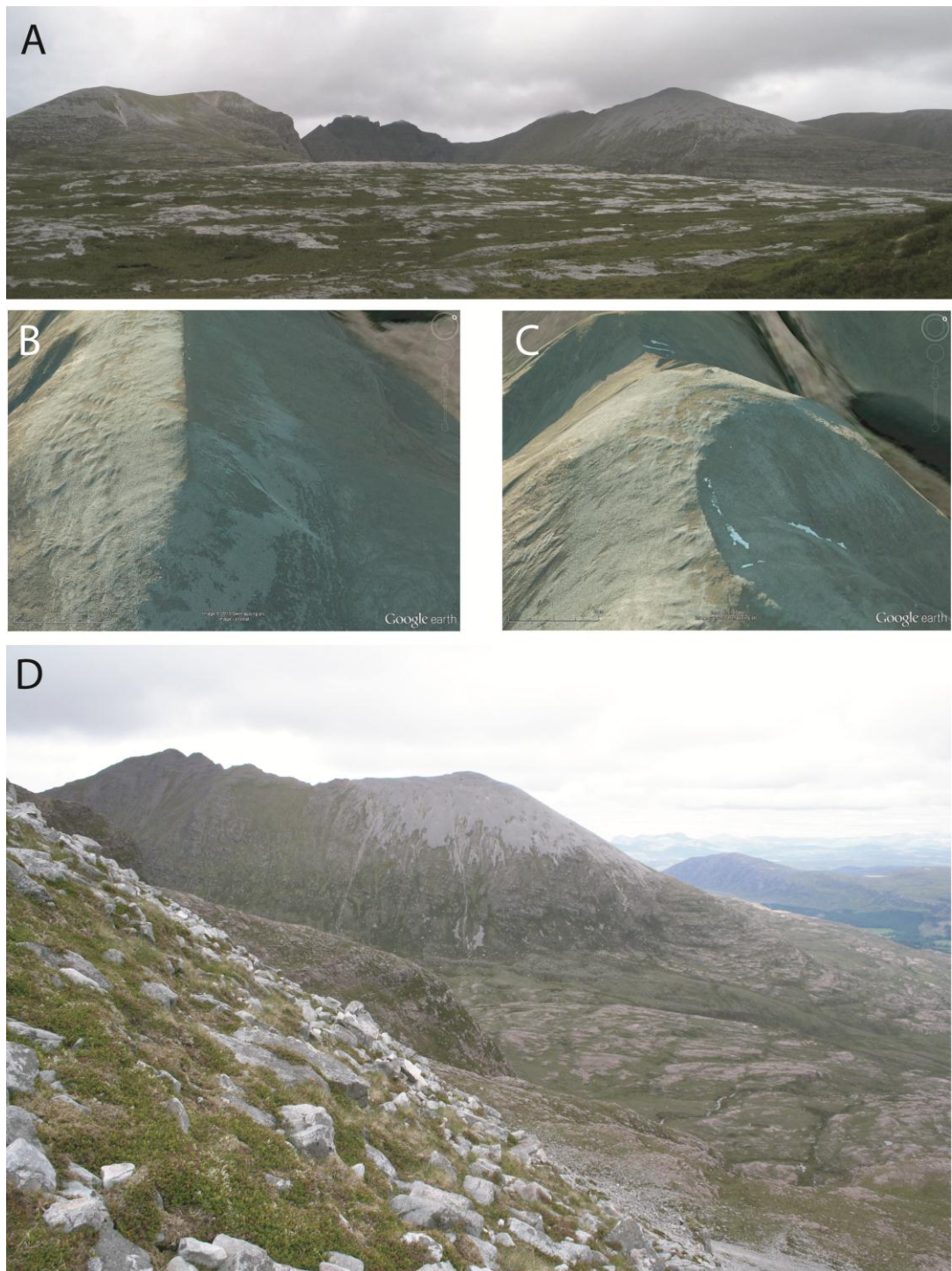


Figure 3.43: Sail Liath, An Teallach, Wester Ross. A - An Teallach looking NW, SL at left. Quartzite regolith above Torridon slopes. B - Solifluction, SL slopes. Image: Google Earth. C - Periglacial sediment sorting on summit. Image: Google Earth. D - Contrast in morphology and weathering seen in quartzite (foreground) and Torridon sandstone behind.



Figure 3.44: Close context Sail Liath. A - Regolith covered SE slope. Large Torridon erratics distinguishable by purple-red colour. B - SAIL01, Torridon cobble (circled) amongst quartzite regolith on summit. C - Torridon erratic illustrating boulder ploughing. D - SAIL04 Torridon erratic embedded in slope deposits. E - SAIL05 quartzite erratic seen amongst mixed lithologies comprising the surface lag. Photos: TB.

3.6.3. Little Loch Broom

In August 2007, two samples (BGSD1 and BGSD2) were retrieved by divers from a moraine ridge located on the seabed in Little Loch Broom (c. -30 m OD). The large moraine is part of a recessional series of seabed moraines stepping back from the maximum ice extent, towards a terrestrial margin (Figure 3.41). Currently in a marine setting (Figure 3.45, Figure 3.45 B), it is important to establish whether these seabed moraines have been sub-aerially exposed during their postglacial history to understand the effect of sea level change on the W margin of the last BllS. No exposure age could be generated for these samples as they contained no detectable concentration of ^{10}Be (Table 3.14 and Table 3.15). This indicates they have never been sub-aerially exposed.

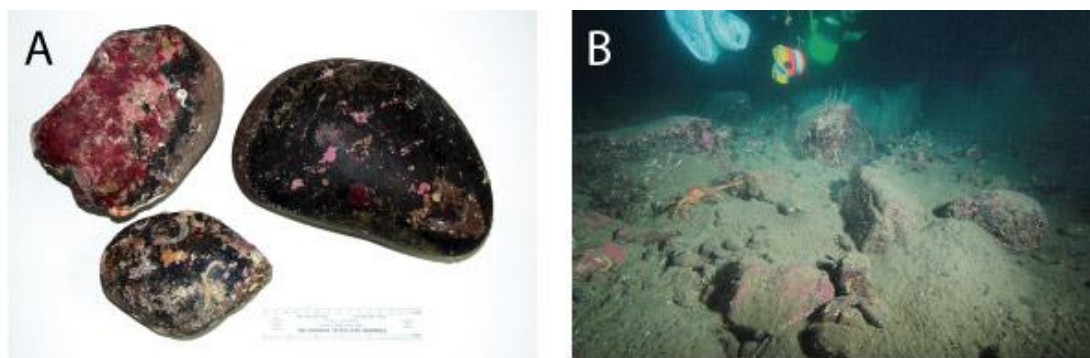


Figure 3.45: Samples acquired from submerged moraine, Little L. Broom. A- Three boulders retrieved from moraine. Note 'tideline' separating 'clean' sub-sediment surface from that encrusted with marine organisms. Photo: M. Stoker (BGS). B - Context of samples in seabed moraine surface beneath Little Loch Broom. Squat lobster body for scale c. 15 cm. Photo: (C) Richard Shucksmith, 2008.

Table 3.14: TCN sample locations and physical characteristics of samples from Little Loch Broom (dived) and Gruinard Bay, Wester Ross. See Table 3.1 for explanation of acronyms.

Location	Sample ID	Lat.	Long.	OS grid reference	Elev. (m)	Sample type	Sample dimensions a,b,c axes (m)	Litho.	Previous sediment cover	Post-depo. movement	Weathering indicators
Little Loch Broom	BGSD1	57.5365	-5.19880	NH: 208545, 854081	-30	Moraine	0.3,0.2,0.2	TS	P	P	MO
	BGSD2	57.5365	-5.19880	NH: 208545, 854081	-30	Moraine	0.2,0.15,0.15	TS	P	P	MO
Gruinard Bay	DD01	57.84951	-5.50613	NG: 192036, 889837	124	Moraine	0.5,0.5,0.2	BQ	P	U	None
	DD02	57.84998	-5.50614	NG: 192038, 889889	126	Moraine	2,1.5	LG	P	U	MT ~5cm

Table 3.15: TCN sampling data and surface exposure ages of samples from Little Loch Broom and Gruinard Bay, Wester Ross. For calculation details see footnote of Table 3.3.

Location	Sample ID	Lat.	Long.	Elev. (m)	Sample thickness (cm)	Topo shielding factor	[¹⁰ Be] (x10 ⁶ atom g ⁻¹)	Apparent exposure age (¹⁰ Be) kyr*
Little Loch Broom	BGSD1	57.5365	-5.19880	-30	4	1.0000	no detectable ¹⁰ Be	
	BGSD2	57.5365	-5.19880	-30	5	1.0000	no detectable ¹⁰ Be	
Gruinard Bay	DD01	57.84951	-5.50613	124	4	1.0000	7.38 ± 0.35	14.6 ± 1.0 (0.7)
	DD02	57.84998	-5.50614	126	2	1.0000	6.46 ± 0.55	12.5 ± 1.2 (1.1)

3.6.4. Gruinard Bay

Two samples were collected from a boulder spread representing the E end of the Aultbea moraine (part of the Wester Ross Readvance moraine originally mapped by Robinson and Ballantyne (1979) on a low plateau c. 120 m a.s.l. above Gruinard Bay Figure 3.46, Folio 1). Both boulders are glacially transported erratics with DD01 a Basal Quartzite and DD02 an orthogneiss (the country rock being the Applecross Formation of the Torridon Sandstone). The boulders were sampled to examine the timing of abandonment of this margin - probably an early terrestrial limit of the retreating Devensian ice. The apparent exposure ages for these samples are 14.6 ± 1.0 ka BP (DD01) and 12.5 ± 1.2 ka BP (DD02). Full TCN details in Table 3.14 and Table 3.15.

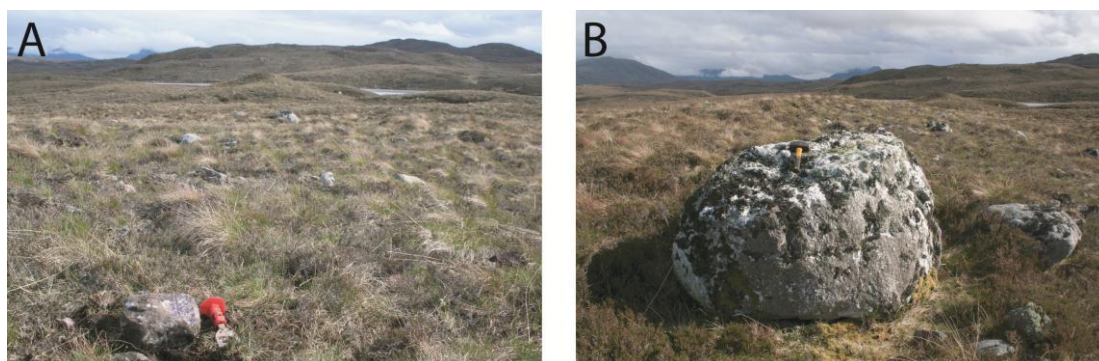


Figure 3.46: Setting of DD TCN samples, Druim Dubh plateau above Sand, Gruinard Bay. A - Sample DD01 (dug out) in foreground with moundy boulder scattered sediment of ice limit in middle ground. Looking SE over Loch Mòine Sheilg towards the Fisherfield hills. B - DD02 looking east. Photos: TB.

3.7. Newly identified geomorphic features

3.7.1. 'Rip-off zones'

Geomorphic investigations in NW Scotland revealed a feature not previously identified in the British Isles. Here termed 'rip-off zones', these erosional features bear strong similarities to the transverse lee-side scarps of Clarhall & Kleman (1999) identified in Northern Sweden. These features have been used to identify transition from frozen to thawed bed conditions under ice sheet cover. In NW Scotland five rip-off zones have so far been identified (this study).

The features bear several consistent characteristics. They show a strong lithological control, being expressed in quartzite only and bounded by a geological boundary, whether lithological or structural. Geomorphically, the features consist of an erosional depression on the lee-side of a major topographic obstacle. Material (largely bedrock) appears to have been removed in a structural sheet (Figure 3.47 C). Rip-offs are distinguished by their characteristic smooth, cleared bedrock patches amidst adjacent or surrounding regolith cover. In fact the features are most easily recognised from the absence of regolith which is otherwise ubiquitous on upland quartzite slopes in this region. These cleared areas often terminate upslope in a curvilinear scarp or sharp boundary but may show linear margins on one or more sides associated with rock structure. Several of the rip-offs display stepped faces in the cleared area (Figure 3.47 A & B). Erosional feature expression is transverse or oblique to local ice flow.

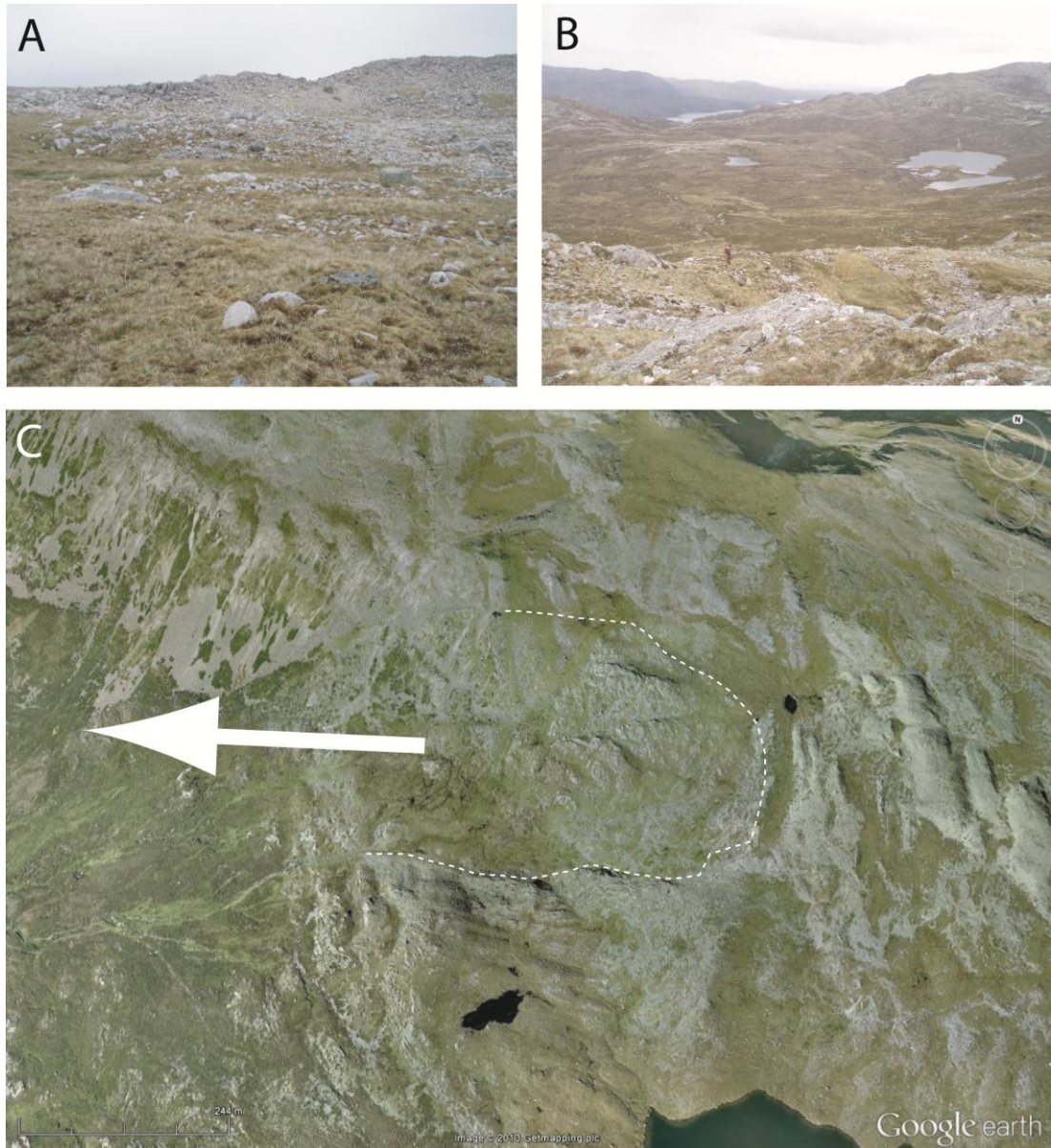


Figure 3.47: Beinn Uidhe rip-off, Assynt Mountains. A - Boulder blanket including orthogneiss erratics deposited at the head of the Allt Tarsuin below Mullach an Leathaid Riabach plateau looking east upslope. B - Rugged steps in the face of the rip-off surface, looking down slope (west) towards Loch Assynt in background. C - Vertical aerial image of rip-off feature showing contrast of cleared rock surface with plateau regolith cover above and sediment cover below. Arrow indicates direction of sediment evacuation. Image: Google Earth. See also Chapter 5 (Figure 5.13).

Beneath Conival a trace of smoothed sediment can be clearly seen to emanate from the rip off zone (Figure 3.48 A). Additional evidence that these features may act as major sources of erratics and glacially transported material is their correlation with the initiation of boulder trains (Figure 3.49).

The Beinn Uidhe rip-off shows a strong connection with significant surface loss, as demonstrated by nearby TCN data (Figure 3.31). The isolated ‘fresh’ rip-off appears to be the latest component of an erosional zone which reduces both the elevation and the regolith cover of the area between Beinn an Fhurain and Beinn Uidhe.

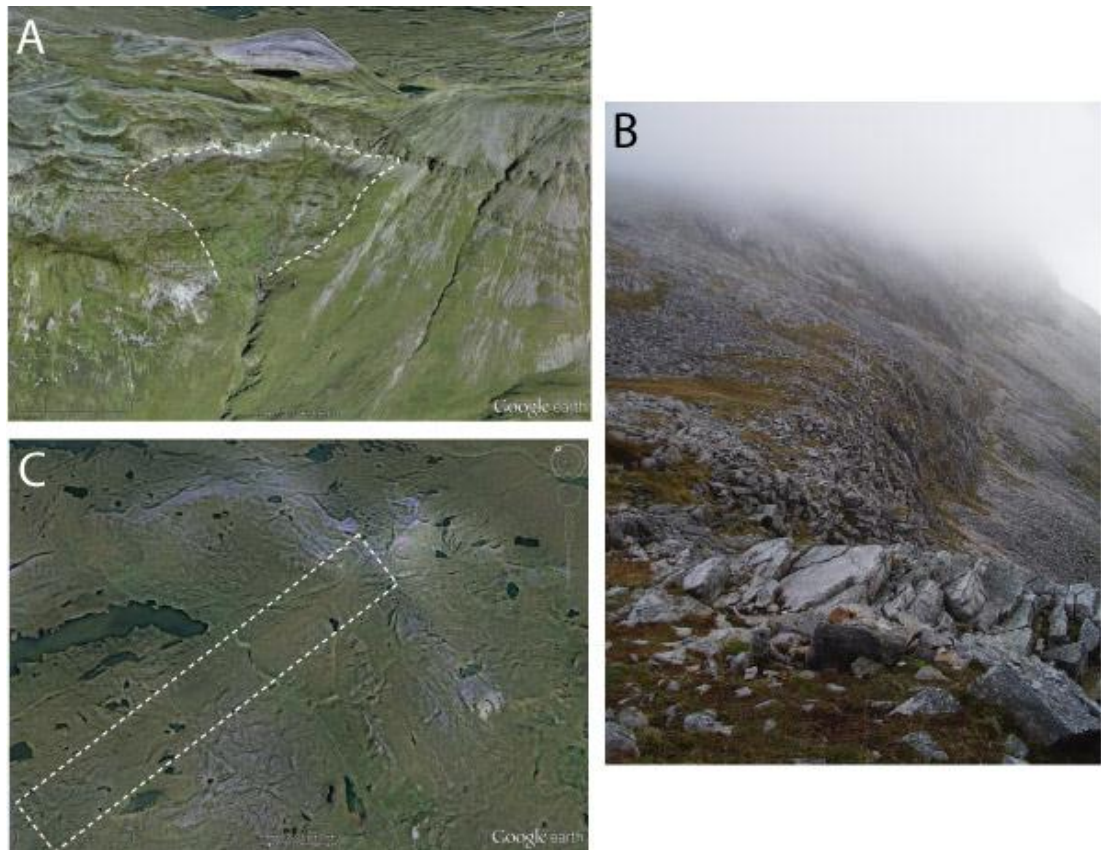


Figure 3.48: Conival rip-off, Assynt Mountains. A - Oblique view of scarp and stripped bedrock below Conival. B - Back scarp feature with small fresh talus cones below and uncleared regolith above. C - Sediment train (boxed) traceable SW from rip-off source area. Aerial images: Google Earth.

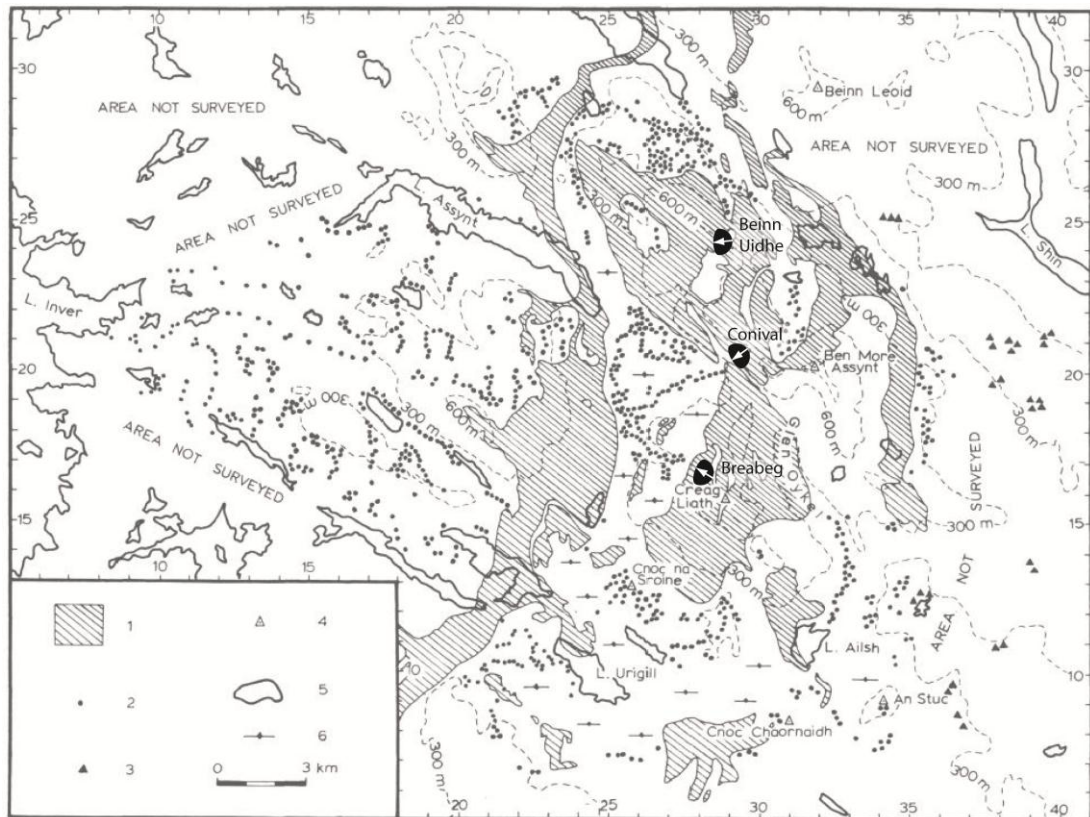


Figure 3.49: Relation of glacially transported boulders (GTBs) to sites of rip-off, Assynt Mountains. Adapted from Lawson, 1990. Sources (hatched) and deposits (dots) of glacially transported quartzite boulders, Assynt. Ice flow direction right to left (east to west). Rip offs indicated by black areas with white arrows indicating transport direction of entrained material. In Lawson's legend: 1. Outcrops of Cambrian quartzite. 2. Occurrences of quartzite erratics noted by Lawson. 3. Occurrences of quartzite erratics noted by the Geological Survey. 4. Areas examined where quartzite erratics are absent. 5. Selected lochs. 6. Areas of thick peat. Contours at 300 m intervals.

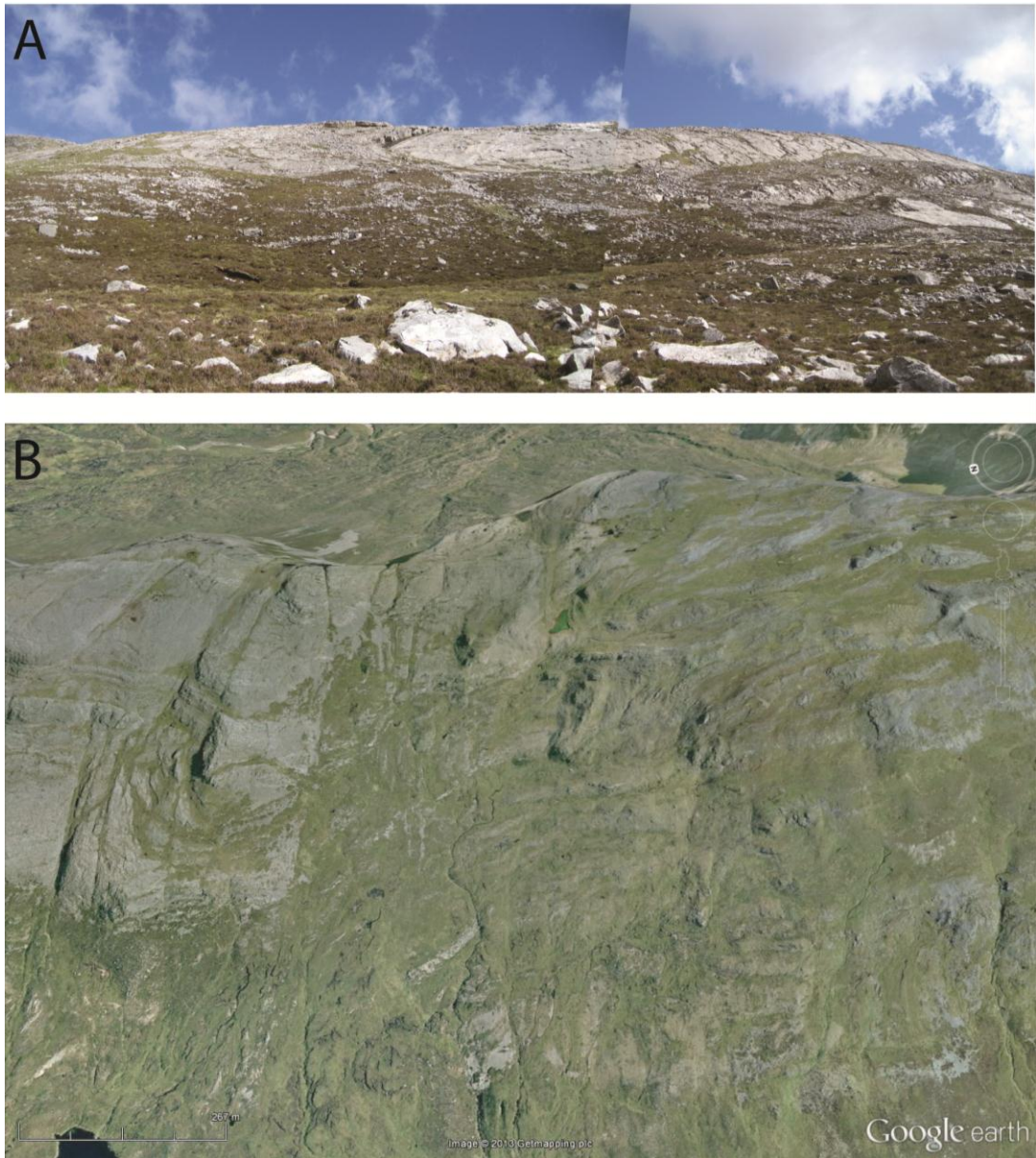


Figure 3.50: Breabeg rip-off, Assynt Mountains. A - Fuarain Ghlasa rip-off seen from below. B - Oblique aerial image (looking east) of young rip-off in the crags of Fuarain Ghlasa, Breabeg. Image: Google Earth.

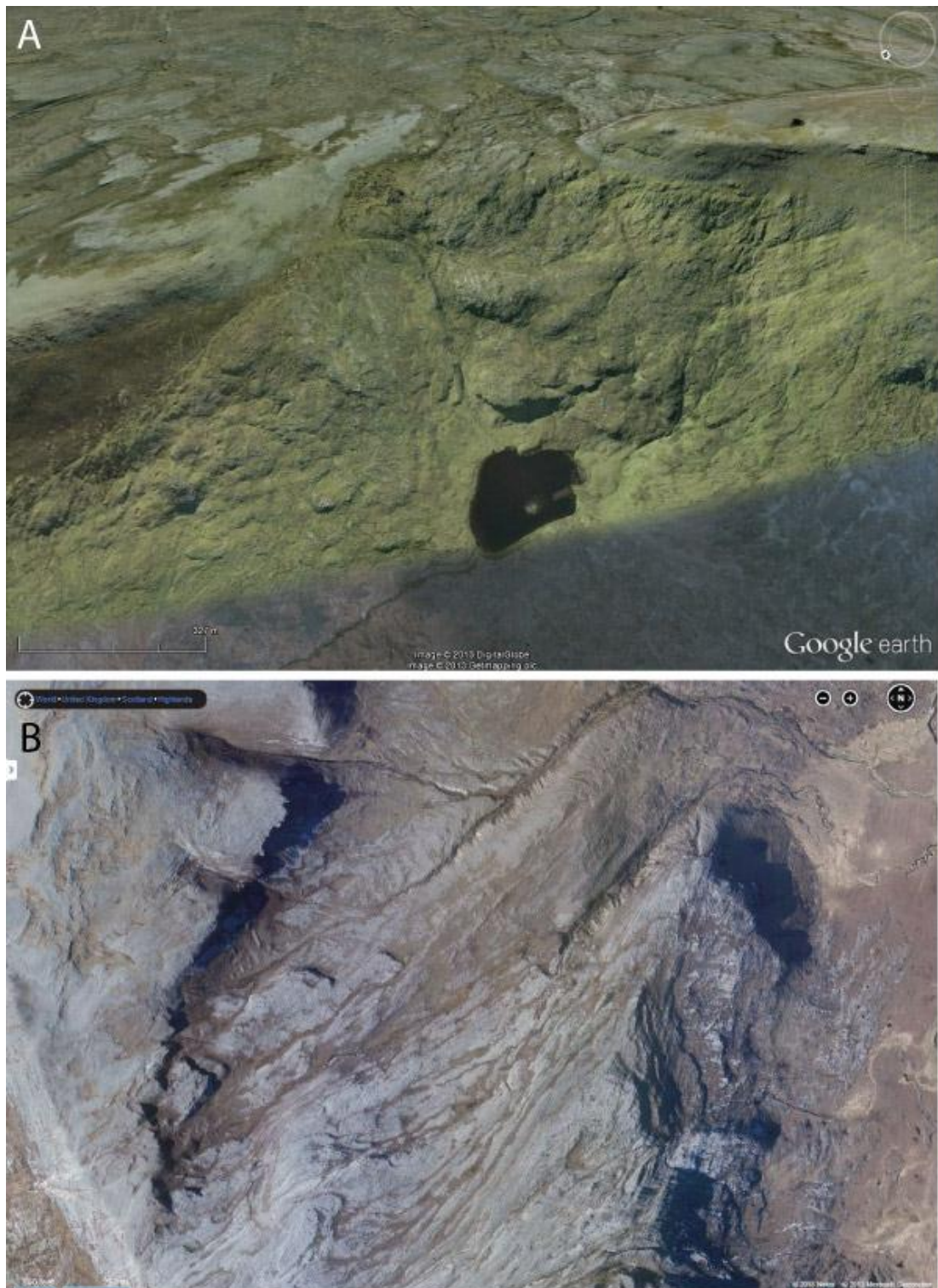


Figure 3.51: Rip-off features, Cranstackie range, Sutherland. A - Meall nan Cra rip-off oblique view from S. Dionard. Image: Google Earth. B - Coire na Cùile rip-off with NE facing steps. Sub-parallel meltwater channels, top right, initiate at lower edge of feature. Image: Bing maps.

3.7.2. *Till Tails*

The occurrence of large streamlined lee-side features abutting the inselbergs of NW Scotland (Figure 3.52) was noted by Bradwell during field mapping for the BGS NW Highlands project (2004-2008). Further field investigation (this study) has revealed the location of at least ten features: remnant in the back of Meall nan Cra (Strath Dionard), Foinaven-Arkle, Quinag, Stac Pollaidh (Figure 3.53), Ben Mor Coigach, An Teallach, Ben Ghoblaich (Figure 3.54), Cul Mor, Cul Beag, Ben Hope. All are identified by the following morphological criteria:

- lee-side position relative to isolated mountain;
- elongate streamlined form;
- smooth surface texture;
- ice-sheet flow-aligned orientation.

The forms are roughly semi-cylindrical or cone-like in appearance with a smoother surface than surrounding ground suggesting a thicker, till-rich sediment cover in contrast to the prevailing bedrock landscape around. The till tails show some association to large scour or channel forms, as at Ben Mor Coigach, but it is unclear whether this is a contemporaneous relationship with their formation or post-deposition modification. Initial sedimentological investigations on the northern shore of Loch Lurgainn (Stac Pollaidh/Ben Mor Coigach till tail) suggest that till tails comprise at least a carapace, if not thicker, component of glacial diamict (Figure 3.55). It is currently unclear whether till tails comprise a sediment carapace over a bedrock core or are composed entirely of sediment.

The results of field and remote sensing investigation have been presented here with only the minimal interpretation to aid their full depiction and assimilation into a regional description. This data is synthesised into an ice sheet sector scale discussion in the following two chapters.

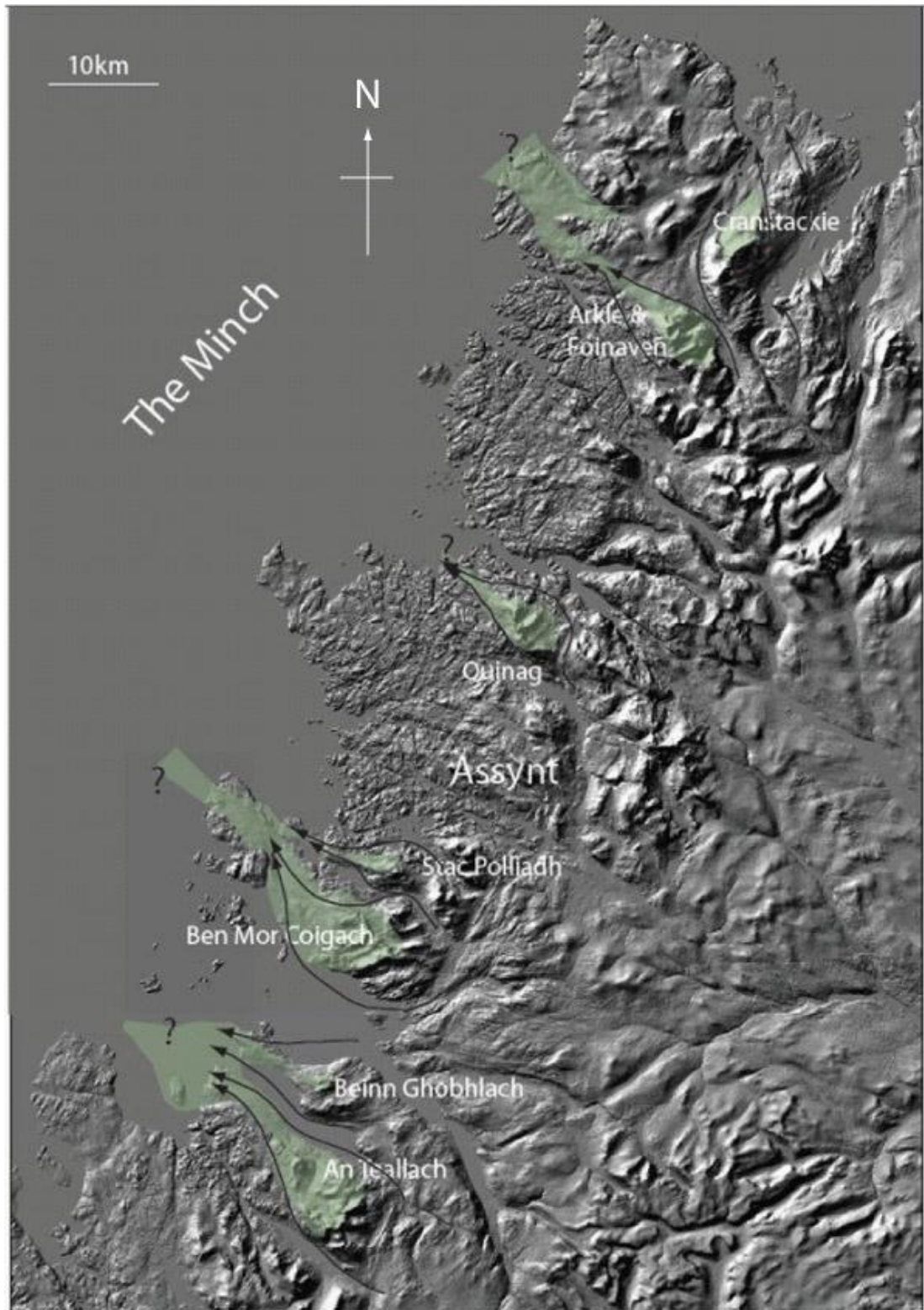


Figure 3.52: Schematic representation of the 'till tails' of NW Scotland overlain on NEXTMap hillshaded digital terrain model with NW illumination. Offshore extent is postulated in some areas where swath bathymetry reveals sediment trace continuity.



Figure 3.53: Stac Pollaidh - Ben Mor Coigach till tail. A - Ben Mor Coigach branch of the till tail, looking north. B - Combined Stac Pollaidh-Ben Mor Coigach till tail, Stac Pollaidh in background.

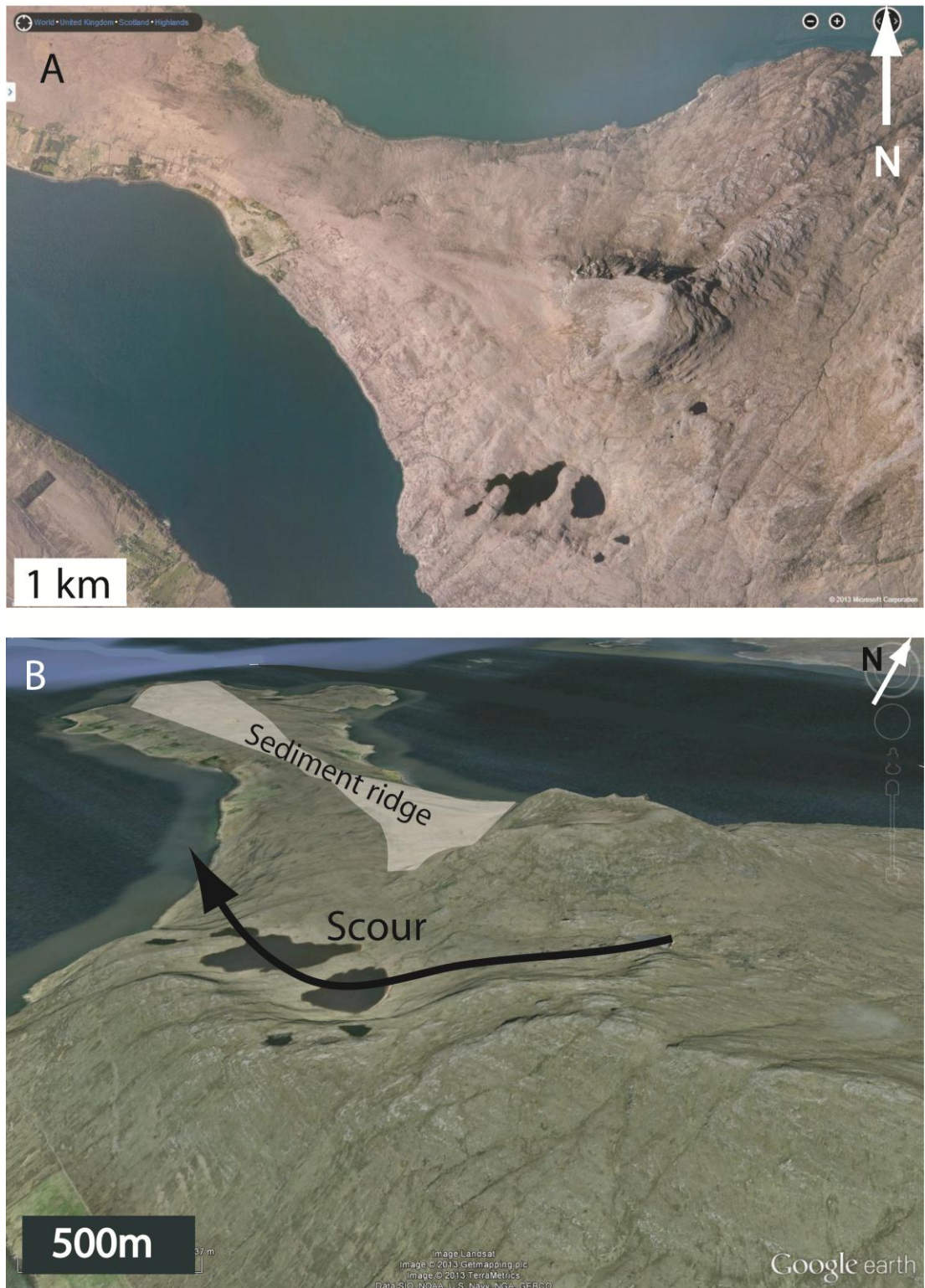


Figure 3.54: Till tail geomorphology: Beinn Ghobhlach example, Wester Ross. A - Aerial view showing scour in SW with lochan-filled bedrock basins and WNW trending (ice flow-aligned) sediment ridge. Image: Bing maps. B - Oblique image of Beinn Ghobhlach showing the association of hill, scour and till tail.

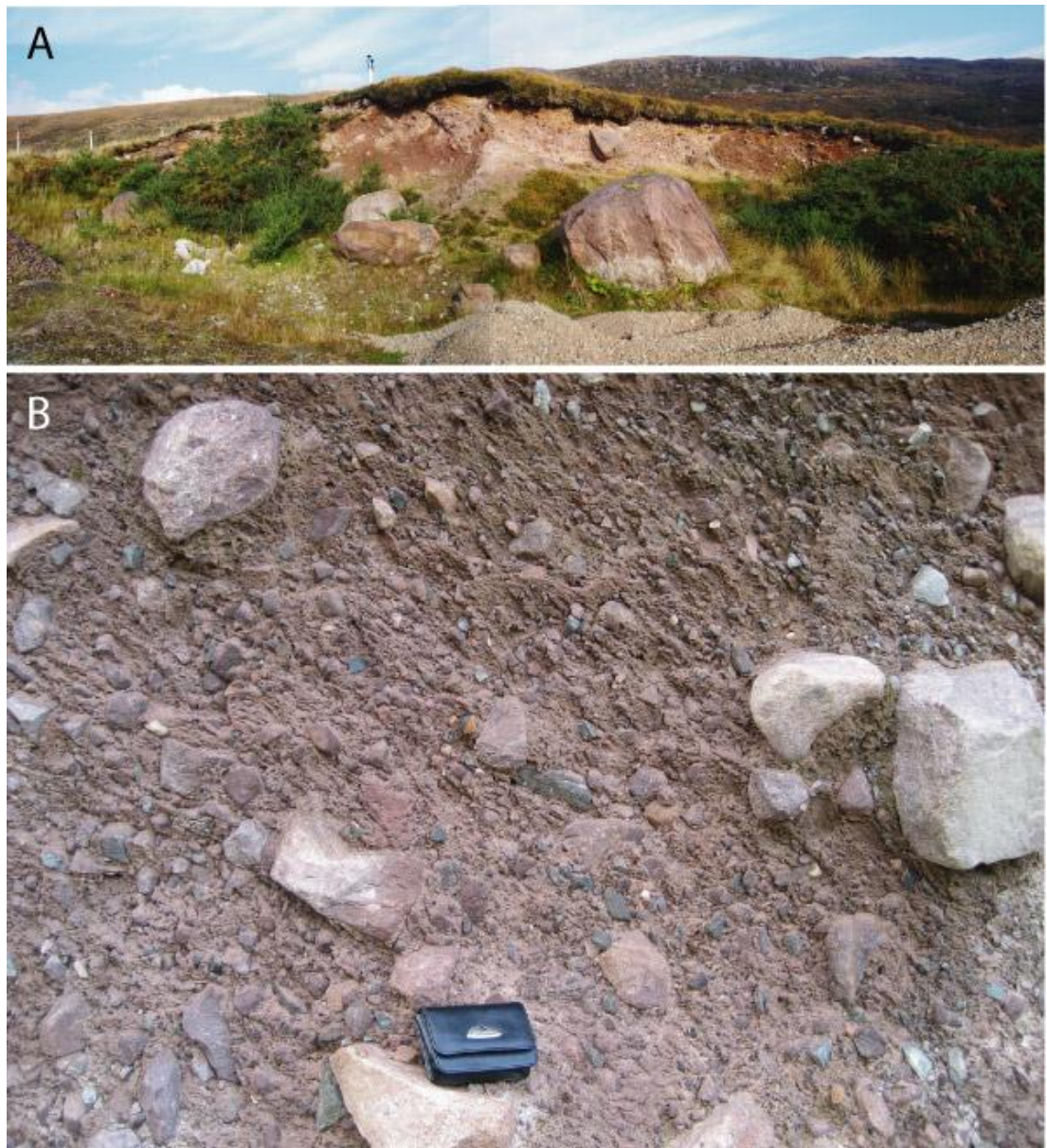


Figure 3.55: Till tail sediments, Stac Pollaidh. A - Context of sediment section exposed in a small quarry on the north bank of Loch Lurgainn. Behind (to the NE) the lower crags of Cul Beag. B - Heavily compacted matrix-supported diamict. Sandy Torridon matrix with cobble and boulder-sized quartzite and Torridon clasts. Camera case (10 cm) for scale.

CHAPTER 4: DISCUSSION: HORIZONTAL & VERTICAL ICE MARGIN RETREAT CHRONOLOGY

4.1. Introduction

This chapter combines elements of the geomorphic and TCN dataset to address the third research aim stated in the introduction, namely to: Chronologically and spatially constrain the retreat history of the NW sector of the last BISS. Specifically the data is discussed in relation to two main strands - the retreat chronology of lateral margins, and the evidence for ice sheet thinning. The long-debated question of ice persistence through the Lateglacial Interstadial is also briefly addressed, though the dataset was not designed specifically with this question in mind. These topics are then synthesised in relation to the operation of the Minch Palaeo-Ice Stream and wider glaciological organisation of the ice sheet as a whole.

4.2. Lateral ice margins

4.2.1. North Sutherland coast

With the majority of land lying below 400 m a.s.l., the far NW corner of Sutherland would have had a limited local area available for ice accumulation during glaciation. The highest ground, and natural snow and ice accumulation areas, lie to the south and east, namely Foinaven, Cranstackie and Ben Hope. During operation of the Minch palaeo-ice stream (Figure 4.1) to the west, ice would have flowed across the area from the high elevation source area to the SE (Figure 4.1 B). Following decay of the Minch ice stream ice would have been sourced more locally, with cessation of ice piracy from across the watershed to the SE (Figure 4.1 C).

Geomorphic evidence supports three main route-ways for ice feeding into the Eriboll-Hope area (Folios 1 & 3): the Bealach a' Chonnaidh (263 m), the watershed (192 m a.s.l.) at Loch Dubh and the pass of Glac an Tioraidh (130 m a.s.l.). Bealach a' Chonnaidh above Srath Coille na Feàrna would

have fed upper Srath Beag with ice overflowing from the Dionard glacier. The watershed at Loch Dubh, as not fully breached, would have controlled flow from the most likely regional ice accumulation centre, Druim nam Bad, via Glen Golly into Srath Coille na Feàrna. The pass of Glac an Tioraidh, on the interfluvium between Loch Eriboll and Loch Hope, would have controlled ice-flow into the Eriboll Glacier from the east.

The floor of the Hope valley, extending south as Strathmore, remains below 40 m a.s.l. up-valley to the foot of Druim nam Bad (~300 m a.s.l.), the probable local ice centre. Consequently the Hope valley would have experienced a more direct and persistent connection with the main ice accumulation area than the Eriboll valley, which was separated from direct ice flow by obstacles at 263 m, 192 m and 130 m elevation.

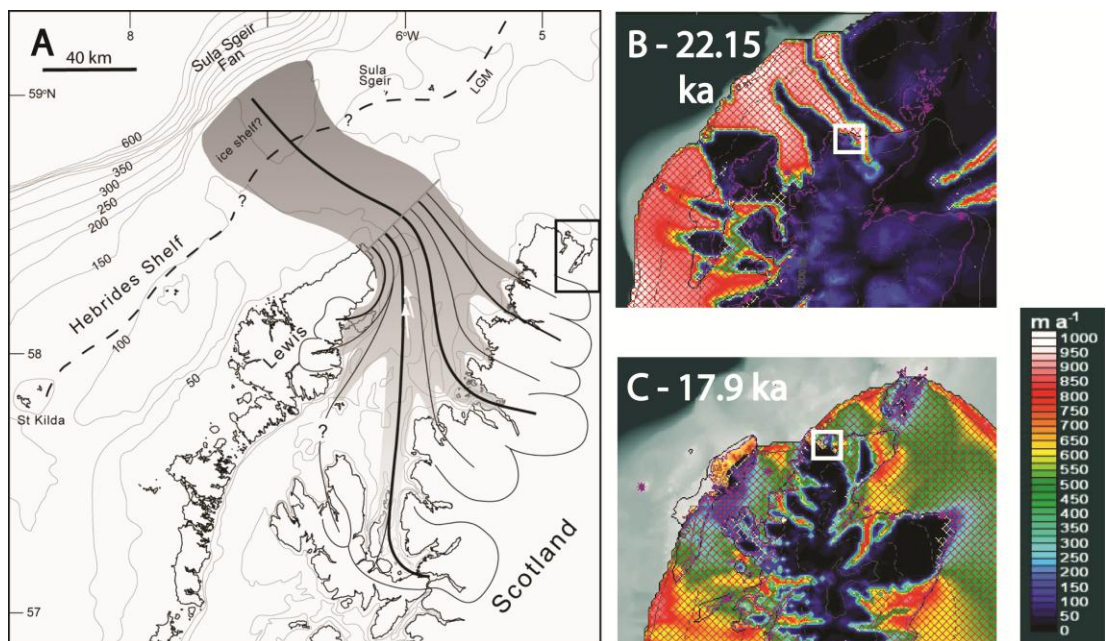


Figure 4.1: Relation of MPIS operation to ice flow in the Eriboll-Hope area. A - The Minch palaeo-ice stream (Bradwell et al. 2007) black box shows location of Loch Eriboll area. B & C - Time slices from Hubbard et al (2009) model of the last BIIS. White boxes show the location of the Eriboll-Hope area. In A the drag of ice to the NW, possibly due to ice stream operation, is clear. In B, during deglaciation, shutdown of the coastal ice streams and the spread of basal freezing enhance topographic control of ice flow.

The initiation of ice margin retreat across the Hebrides shelf is constrained by dating of glacially transported boulders on North Rona (c. 70 km offshore of Cape Wrath) at 28.46 ± 1.11 ka BP (using LLS LPR)(Everest et al., 2012). Seabed mapping from OLEX AS bathymetry data (Bradwell et al., 2008c) indicates a single large ice sheet moraine inside of the North Rona limit which may represent a final coherent ice stream margin prior to deglaciation (Figure 4.2). Landward of this feature, nested moraines indicate eastward margin retreat. Overprinting of this eastward retreat pattern is seen in the form of curvilinear fjord-sourced outlet lobes which truncate the earlier features along the northern coast, from Tongue Bay in the east to Cape Wrath.

Exposure ages (mean 17.6 ka BP) from the north coast (this study) at Rispond, towards the centre of the arced moraines, provide a minimum age for a major ice sheet reorganizational phase - from ice-stream dominated to lobate locally-sourced outlet situation as occurring c. 17.6 ka BP.

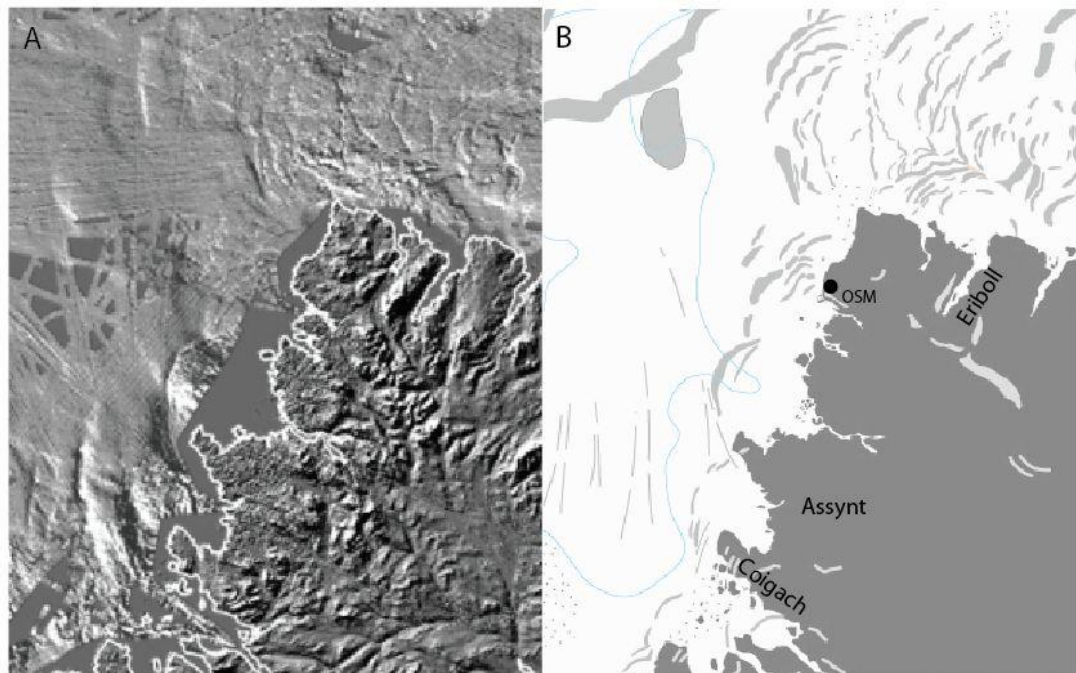


Figure 4.2: Glacial landforms on the continental shelf, NW Scotland. A - Merged on- and offshore topography/bathymetry surface model from NEXTMap digital surface model and OLEX AS bathymetry (modified from Bradwell et al., (2008c). B - Seabed landforms digitised from the OLEX dataset (Bradwell and Stoker, 2014). Location of key areas labelled, Oldshoremore (OSM) with a dot.

Consequently a significant phase of readvance or stabilisation is anticipated prior to this and following upon collapse of the MPIS and retreat from the Hebridean Shelf in the time bracket <28.46->>17.6 ka BP. The Rispond ages also constrain ice-sheet deglaciation of Cape Wrath at <> 17.6 ka BP indicating that this area was ice-free early, when ice in other areas was still extensive in other parts of Scotland (Finlayson et al., 2014, Clark et al., 2012).

The dated Rispond margin represents the edge of a large ice mass confluent with the Hope glacier (Figure 4.3) and probably with a surface at ~200 m above present sea level as suggested by ice-marginal meltwater channels on the western slope above Loch Eriboll (Folio 3 and Figure 4.3). This is the largest coalescent glacier stage indicated within the Eriboll area. Inside of this limit, marginal features track deglaciation back to independent local sources. Controlled recession, from the dated Rispond margin, is shown by ice-marginal meltwater channel suites around Portnancon and Laid. South west of this, the landform arrangement becomes more chaotic suggesting a transition in deglaciation style and/or rate of retreat.

The next dated limit comprises data from the channel-incised sandur surface near Laid and from the morainic debris spreads at Portnancon and to the south of Laid. This data has been grouped because these sampled surfaces are interpreted as components of a single ice marginal assemblage. This limit is associated with a Hope valley-sourced piedmont lobe spilling into the Eriboll valley and terminating at the foot of the western dip slope. Here the limit is ~10-30 m a.s.l., demonstrating significant thinning (>170 m) of the ice from the previous margin stage. Exposure ages on this landform assemblage range 14.9-17.1 ka BP with a weighted mean of 16.5 ka BP. Samples in this grouping are from the following sampling locations: PORT, LAID and ERW. Omitting the two youngest samples - LAID02 and ERW01 (the latter of which is likely to have experienced sediment shielding) the group mean exposure ages becomes 17.0 ± 1.0 ka BP. With continued mass loss the ice sheet geometry splits to form an independent Srath Beag-fed glacier and a more substantial Hope lobe.

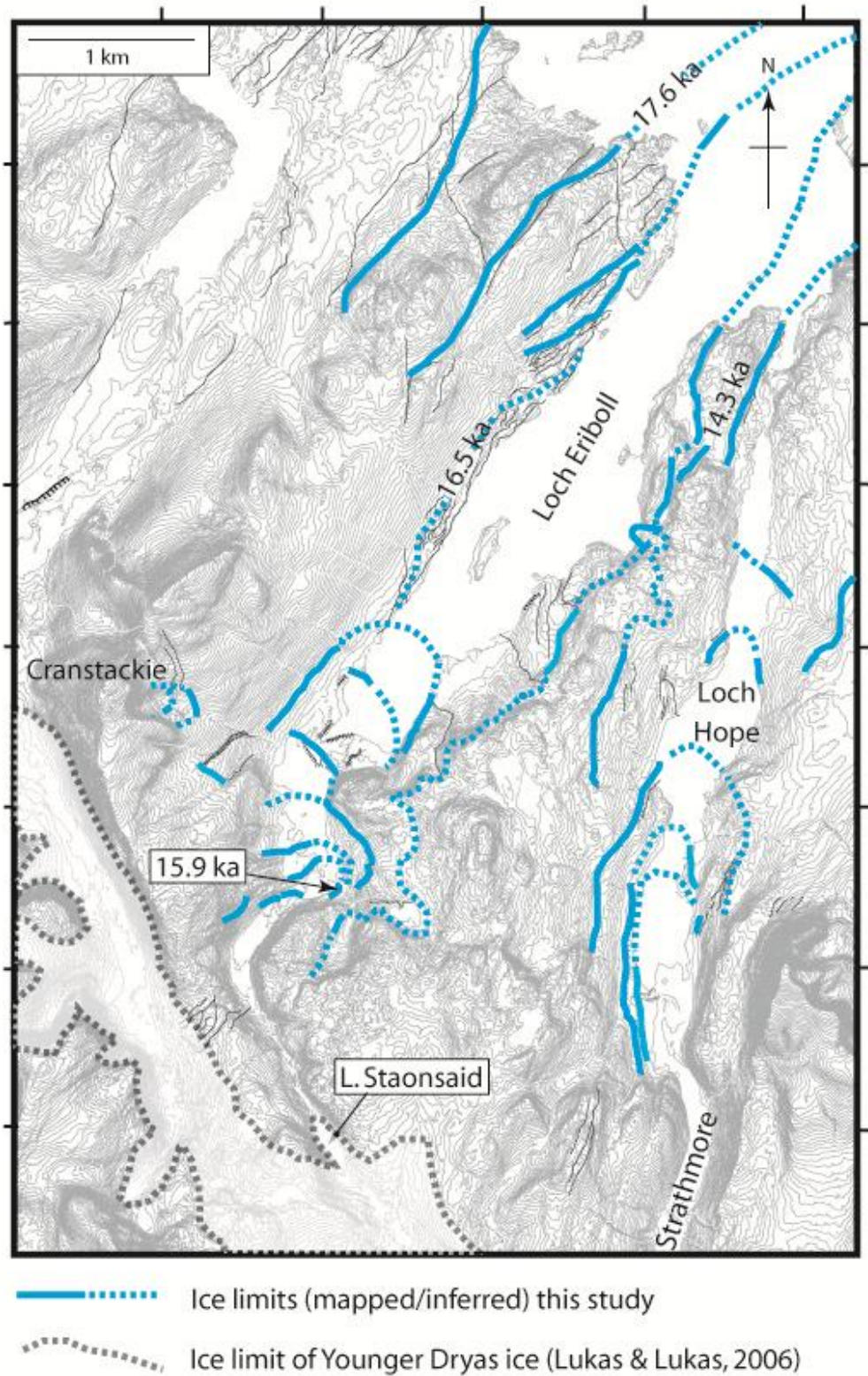


Figure 4.3: Mapped and inferred ice limits Eriboll-Hope area. Ages on limits from cosmogenic nuclide analysis (this study). Benn & Lukas (2006) Younger Dryas ice limit shown for comparison. For additional location details see Folio 3: Geomorphology and sediment cover of the Loch Eriboll area.

The consistent TCN exposure ages from the Srath Beag lateral margin (SBLM) samples on the eastern kame complex of Srath Beag indicate abandonment of this fluvioglacial suite c. 15.8 ka BP. The outwash terrace close to sea level at the head of Loch Eriboll, was laid down <15.8 ka BP as constrained by the Srath Beag kame terrace suite which sits c. 80-20 m above the outwash terrace. Fluvioglacial sediments would have been supplied from a glacier in Srath Beag glacier with likely contribution from ice on the east flank of An Léan-Chàrn. This steep margin is defined by the glacial sediment limit on Creag na Faolinn. Retreat of the Srath Beag branch, of the Eriboll Glacier, appears to have been complex: initially retreating towards a Cranstackie source, and later a Conamheall source. This is supported by the presence of a fan partially filling Loch Bad na h'Achlaise. Glacial sediment limits on the western wall of Srath Coille na Feàrna suggest that ice overflowing from the Dionard Glacier may have nourished a late stage Srath Beag glacier.

The final Late-glacial limit, at the junction of Srath Beag and Srath Coille na Feàrna, cannot be conclusively dated as there is a wide age discrepancy in sample ages from boulders on this limit with no overlap. SRAB01, a very large boulder (Figure 3.12), shows evidence of joint deepening suggesting the possibility of an old, previously exposed surface with some degree of nuclide inheritance. In contrast SRAB02, set in the surface of the feature has possibly experienced overturning and/or peat shielding because of its small size. A significant gap in glacial deposits (>4 km) occurs between this limit and the moraines assigned to Younger Dryas ice around Loch Staonsaid (Benn & Lukas, 2006). This may signify that there was not lateral continuity between the Glen Golly (Figure 4.3) source and a Srath Coille nan Feàrna-Srath Beag glacier. It is also possible that the intervening moraine record has been removed by erosion. The final ice remnant may therefore have been fed by local Conamheall-Cranstackie plateau ice.

Strong regional asynchrony of deglaciation from west to east is shown by survival of a large low-elevation Hope valley-sourced lobe near Heilam when Eriboll ice is already well in retreat. Dates on this margin are in the range 14.2-16.7 ka BP (n = 4) (Table 4.2). A small amount of nuclide

inheritance in bedrock is indicated by a separation of bedrock and erratic sample ages of c. 2.2 ka BP indicating limited glacial erosion in this area. Potential overturning of the small erratic cobbles sampled and the possibility of peat shielding suggest that these exposure ages are only minimum estimates of deglaciation.

Multiple ice limits (Figure 4.3) inside of the dated 14.3 ka BP limit at Heilam, but well outside mapped Younger Dryas ice masses, suggest that the Hope Glacier may have persisted into the Lateglacial Interstadial. Thick glacial sediments in kame terraces at the mouth of the River Hope and also towards the mouth of Loch Hope (Folio 3 and Figure 3.23) suggest two stable margin positions of the Hope Glacier. The elevation of terraces at 10-20 m a.s.l. along the Hope River combined with evidence for marine deposition (Figure 3.23) at the margins of the, now freshwater, Loch Hope indicate that a higher relative sea level (10-20 m above present) existed in this area during or following deglaciation i.e. before 14.3 ka BP.

South of the Heilam limit, the Hope Glacier retreated in a stepwise manner indicated by nested morainic sediment limits on the western flank of Loch Hope. Evidence for thinning is only found when retreat is well-advanced towards the head of the glen when the elevation of the lateral sediment limits drops. This suggests that the Mudale-Druim nam Bad ice source (Folio 1) remained important late into the deglacial period.

Proglacial channels flowing ~NW down the eastern flank of the Eriboll valley suggest that plateau ice may well have persisted on An Lean Chàrn following deglaciation of the main Eriboll valley. This small remnant ice cap may have been largely cold-based, buttressed in the east by overflowing Hope valley ice. The persistence of cold-based plateau-ice during glaciation is glaciologically-validated by Hubbard et al.'s (2009) ice sheet modelling which predicts widespread cold-based conditions for upland areas throughout much of deglaciation.

Evidence of cirque glaciation is evident around the margins of the Loch Eriboll area. The boulder limit below Creag a' Chàirn Chaoruinn (Folio 3) and the series of morainic ridges below Coire an Uinnseinn have not been dated. The frontal margins of these features sit at c. 260 and 150

m a.s.l. respectively. The former, higher glacier limit may relate to a small Younger Dryas glacier or snow patch as the regional firn line for this area (projected as ~400 m a.s.l. by Ballantyne (1984)) would sit feasibly above the limit at the foot of Coire Uinnseinn in the NE flank of Cranstackie suggesting cirque and plateau-fed ice. However, the low limit below Creag a' Chàirn Chaoruinn, with its small local accumulation area seems incompatible with a Younger Dryas designation. Consequently this small glacial bodies may have existed following regional main stage retreat and re-growth (i.e. <14.3 ka BP) during a cold period, such as the Older Dryas (GI-1d c. 14 ka BP) or Inter-Allerød Cold Period (GI-1b c. 13.3 ka BP) with ice-feeding from the plateau (~ 350 m a.s.l.).

4.2.2. *Sheigra - Oldshoremore*

The regionally unusual spread of boulders observed in the vicinity of Oldshoremore is difficult to interpret both in terms of geomorphology and in relation to the wide spread of cosmogenic exposure ages (17.0 - 13.7 ka BP). These are derived from 6 boulders and suggest multiple exposure events. For a morainic deposit a spread of ages would be expected from the unique exposure histories for each boulder in relation to lithology, transport path through the ice and erosion history (Figure 2.3). However, there is a possibility that changes in sediment cover may contribute to the exposure age range of dated boulders. Moraine erosion or sediment removal across the area since deglaciation is possible. Wind-blown deposits (Figure 3.28) and inland exposure of winnowed till suggests a significant degree of surface sediment may have been lost. The presence of dry stone walls in this crofting area also suggests that boulder cover in some areas will have been modified by modern humans with potential overturning of boulders and removal of older surface boulders. However, if deposition of materials was multi-stage or involved reworking of earlier deposits, designating a feature age, without strong geomorphic control, becomes speculative. Consequently the boulder spread and associated exposure ages will be interpreted cautiously and in the context of local and regional geomorphology.

The geomorphology of the region around Oldshoremore is defined by bedrock ribs of alternating Torridon sandstone and Lewisian orthogneiss which strike NE-SW (Figure 3.28). These bedrock knolls rise steeply from the coast to heights of above 80 m a.s.l., with a maximum regional height of 153 m a.s.l. (Cnoc Poll a' Mhurain). This high ground terminates abruptly against a NW-SE trending fault with lower peaty ground to the east. This regional morphology could have strongly controlled the ice sheet geometry in the latter stages when regional thinning forced the ice sheet to come under increasing topographic control.

With the main accumulation area to the SE and the nearest high ground c. 13 km away (Foinaven massif) glaciation of this area may have been dependent on extensive ice sheet conditions with NW ice flow. Situated at the boundary of two depressions, with the Loch Laxford - Loch Inchard trough to the south and Strath Shinary valley to the NE flow, the relatively high ground of the Oldshoremore coastal cnocs may have represented both a lateral pinning point and a local ice junction under different ice sheet configurations. The strong, but not topographically-governed, association of the Oldshoremore boulder spread with the coastal bedrock knolls suggests a boundary or transition, whether lateral or englacial.

The unusual concentration of boulders in a belt, in contrast to the surrounding scatter of GTBs, may therefore represent a gathering of boulders from a previously broader sparser spread. Different scenarios may be invoked to explain the location and distribution of the boulders and how they relate to ice-sheet configuration:

- Scenario 1: Oscillatory lobate behaviour of the deglaciating ice sheet;
- Scenario 2: Lateral thermal zonation during full and deglacial conditions;
- Scenario 3: Medial moraine composed of material supplied from Foinaven.

In Scenario 1 the boulder belt represents a latero-terminal moraine formed at the margin of an ice sheet lobe in the latter stages of deglaciation probably c. 17-15 ka BP (as supported by 5 of 7 exposure ages). Therefore the boulder belt may represent a remobilising and concentrating of boulders derived from the regional distribution of glacially transported boulders by the action of an oscillating margin in this area. The regionally unusual morphology and clast concentration of the boulder belt at Oldshoremore bears similarities to the boulder belts or ‘drop moraines’ described from South Victoria Land, Antarctica (Atkins, 2013). These clast-supported features are deposited passively from cold-based ice, cause minimal disruption of the underlying sediments and generally comprise supraglacial or reworked clasts.

Under Scenario 1, geomorphic evidence supports at least 5 ice margin configurations during deglaciation (Figure 4.4 and Figure 4.4). Early in the deglaciation timescale (Figure 4.4, Stages 1-4), ice is located to the west of the boulder spread with the bedrock knolls providing eastern pinning points for a lobe flowing through the Laxford-Inchard trough. At Stage 1, the curvilinear eastern end of the boulder spread delimits the SE section of the margin. Meltwater drained NNE under the margin and was gathered by major proglacial-submarginal channels which drained NW to the nicks in the coast near Rubha nan Cùl Gheodhachan and Rubh’ an Fhir Lèithe. The ice margin retreats in a SW direction (Stage 3) diverting drainage through Chlais Domhain and then perhaps out to the coast at Sheigra and Bàgh Sheigra. Later (Stage 4) a constrained local incursion is made into Am Meallan, the bay below Oldshoremore, potentially with meltwater draining SE. Occupation of the boulder limit occurs again (Figure 4.4: Stage 5), this time by a readvance of local ice as a diffluent of the Strath Dionard tongue, sourcing ice from the far south east. Coastal knolls form a western boundary preventing the ice from thinning seaward into the Laxford-Inchard trough. This ice margin configuration, as a thin late stage outlet glacier would probably have been cold-based and largely non-erosive. The gathering of a boulder belt at the proposed limit of this ice body and the limitation of meltwater channels to predominantly proglacial or lateral,

supports a cold-based interpretation with similarities to landform assemblages at modern cold-based glaciers in Antarctica (Atkins, 2013).

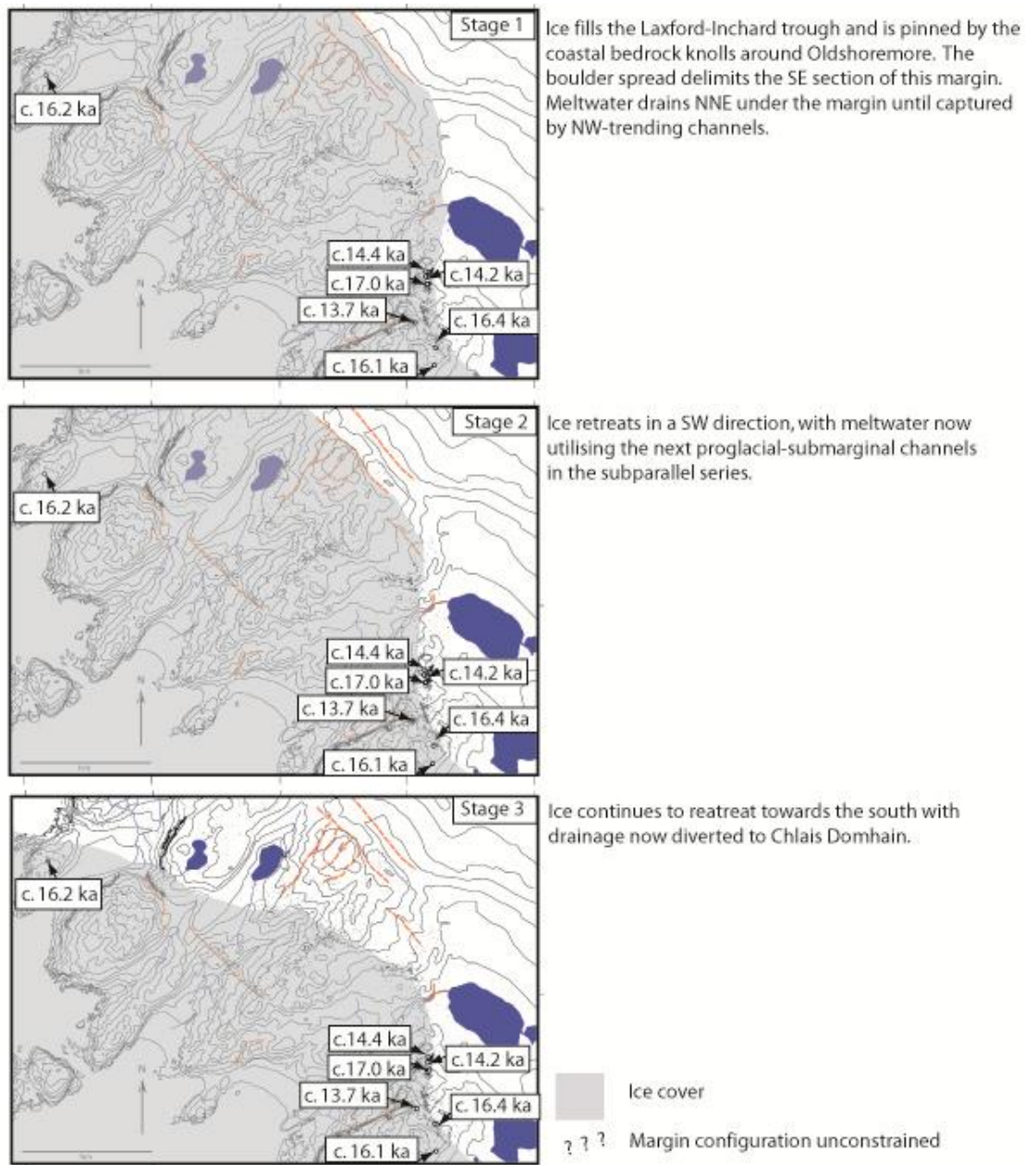


Figure 4.4: Proposed late stage ice margin configuration, Oldshoremore.

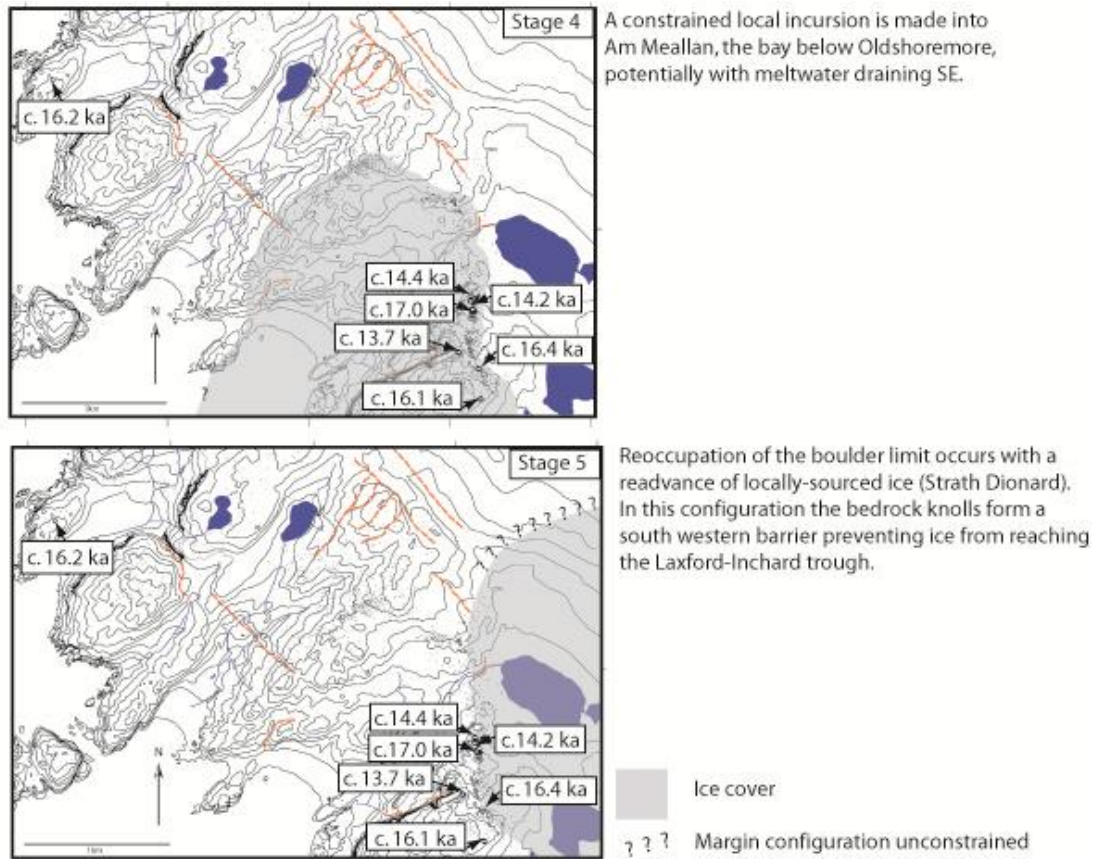


Figure 4.4: Proposed late stage ice margin configuration, Oldshoremore.

Hubbard et al.'s (2009) thermo-mechanical ice sheet simulations resolve 5 lobate advances over the Oldshoremore area between 16.95-15.20 ka BP in support of the glaciological validity of this geomorphic interpretation. Time slices are at 500 year intervals and therefore cannot resolve more short-lived fluctuations. These lobate readvances reach only to the modern coast or just beyond. Mapping of glacial landforms on the continental shelf off NW Scotland (Figure 4.2) has revealed arcuate moraines indicative of glacial lobes extending ~5-20 km beyond the modern coastline. Morainic features are noticeably absent around western Cape Wrath, with a cluster of arcuate ridges seen offshore at Oldshoremore. The ice margin configurations observed here strengthen the argument for an offshore lobe pushing eastward onshore at Oldshoremore and also support a land-based lobe extending offshore with a NW vector.

In scenario 2 the OSM boulder spread represents the location of an englacial thermal boundary - an area where the ice-bed interface

undergoes a transition from frozen to thawed. The major topographic low of the Loch Laxford-Loch Incharid corridor lies to the south of Oldshoremore (Folio 1). The Laxford trough (and upstream Loch Stack trough) once hosted the Laxford palaeo-ice-stream tributary as inferred and reconstructed by Bradwell (2013). Bradwell’s categorisation of glacial bedforms suggest that this area experienced fast ice-stream tributary flow with enhanced ice-bed coupling and softer ice rheology leading to high levels of bedrock abrasion. Bradwell’s mapping extends north to the head of Loch Incharid where tributary onset flow is designated; and to the east along the south western flank of Foinaven, a possible shear margin is suggested by the transition to less abrasive bedforms (Figure 4.5).

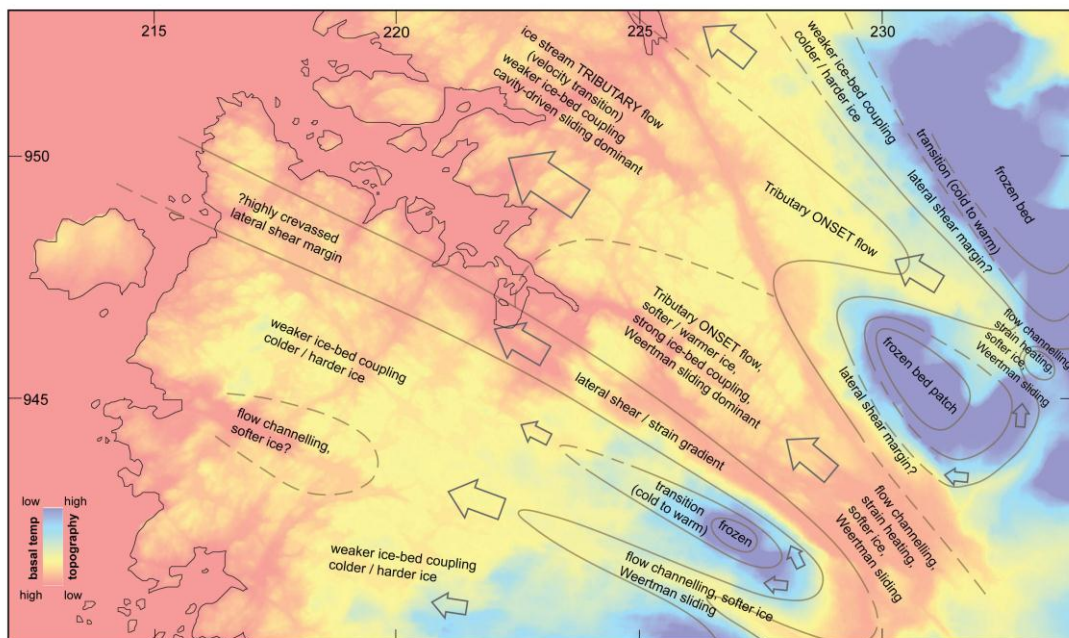


Figure 4.5: Laxford ice stream tributary palaeo-ice sheet dynamics (Bradwell; 2013 submitted). Colour ramp indicates elevation and is a proxy for ice sheet basal temperature. Oldshoremore field area (this study) occurs ~1km to the north of this area.

Observations from the Oldshoremore area (this study), bear some resemblance to the frozen bed patch model of Kleman and Borgström (1994), which illustrates how entrained material may become deposited at a thermal boundary (Figure 4.6). These observations support the designation of a lateral englacial shear margin in this location during the last glacial cycle while demonstrating strong bed-coupling and consequent whaleback

formation during an earlier glacial cycle where flow did not have the strong trough focussing predicted by Bradwell (2013) (Figure 4.5) and by Hubbard *et al.*'s (2009) models.

North of Oldshoremore, the Cape Wrath headland bears few glacial erosional landforms save the very large scale features which probably evolved over multiple glacial cycles under maximum ice-sheet conditions (Figure 3.25). Large meltwater channels near the Cape itself are likely to represent a significant marginal position during retreat. It is therefore logical to suggest that the Cape Wrath headland has not experienced the same degree of glacial modification as the Laxford-Inchard corridor.

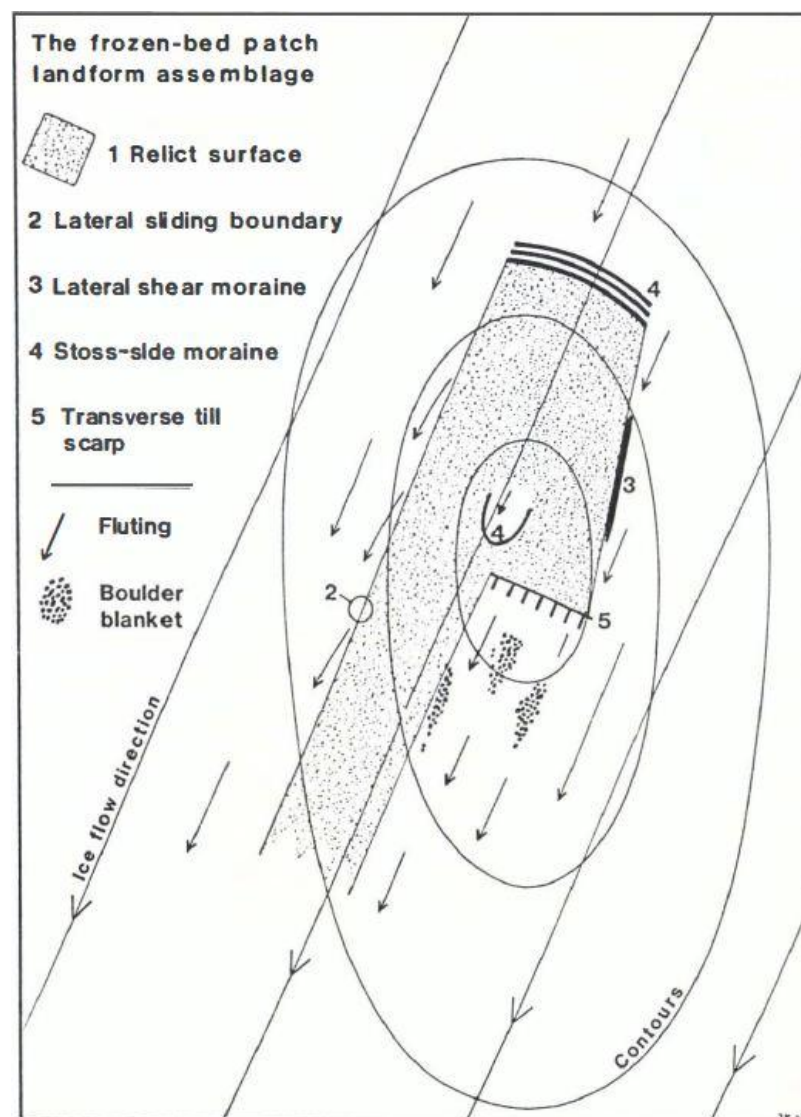


Figure 4.6: Landforms of the frozen-bed patch environment (Kleman & Borgström, 1994). The boulder belt at Oldshoremore potentially represents a former lateral shear moraine (3) where sediment gathers and is deposited against the margin of a frozen bed patch by warm-based ice flowing obliquely against the thermal boundary.

Nuclide inheritance in a bedrock surface (62.4 m a.s.l) at Sheigra excludes the possibility of highly erosive ice cover at this coastal site. This is regionally unusual, as ‘low’ elevation bedrock at Rispond (31 m a.s.l), below Quinag at 294 m a.s.l (D. Fabel pers. comm.) and near Heilam (60 m a.s.l) provide deglaciation ages indicating zero nuclide inheritance following fully warm-based erosive conditions in the last glacial cycle. Interestingly the degree of glacial modification which would have been assigned to the Sheigra region, on the grounds of geomorphic features alone, i.e. glacial shaping, would be in the same category as at Rispond (the thermal conditions in this area are discussed in more depth in Chapter 5: 5.2.2). The abrupt juxtaposition of scoured ground to the south west with limited bed modification and a discrete sediment deposit at Oldshoremore signals an unusually well-preserved transition possibly conforming to a subglacial thermal boundary.

Modelled time slices from Hubbard et al.’s (2009) ice sheet model (Figure 4.7) illustrate the sharp transition in basal thermal regime which existed in the vicinity of Oldshoremore throughout main stage and deglacial phases. It is known that sediment deposition occurs at thermal boundaries, which act as barriers to sediment transport, most notably, in the form of stoss side and lateral shear moraines. In the Oldshoremore situation a lateral shear margin moraine can be envisaged where mobilised boulders are gathered and deposited against the edge of the frozen-bed patch shielding the whole of Cape Wrath. Finally, the possibility that the Oldshoremore boulder spread represents a medial moraine between coalescent ice of the Dionard and Inchard sources cannot be excluded.

4.2.3. *Summer Isles - Glen Achall*

Bradwell et al. (2008) mapped the regional sequence of moraine ridges charting recession onshore from the Minch, crossing the WRR limit towards the Younger Dryas limit at Beinn Dearg (proposed by Finlayson, 2011). This mapping indicated an ice sheet margin position across the eastern edge of Tanera Mor (Figure 3.41), extrapolated between seabed ridges and the major onshore moraine. This moraine yielded a Lateglacial Interstadial exposure age c. 13.6 ka BP (CRONUS standard ^{10}Be production

rate) based on boulders sampled on a moraine near Achiltibuie on the Coigach peninsula. Recalculation of this exposure age using the Scotland site specific production rate (Fabel, 2012) increases the exposure age of the Achiltibuie moraine to 15.3 ka BP (Table 4.1 : Exposure ages (from ^{10}Be) for three samples from the Achiltibuie (ACH) moraine. Exposure ages are calculated using the standard global CRONUS production rate (as published in Bradwell et al. 2008) and the local production rate (LL LPR) utilised in this study.). Using the same production rate for all samples in the Coigach-Summer Isles-Little Loch Broom area allows direct inter-comparison and a revised attempt at a regional chronology.

Table 4.1 : Exposure ages (from ^{10}Be) for three samples from the Achiltibuie (ACH) moraine. Exposure ages are calculated using the standard global CRONUS production rate (as published in Bradwell et al. 2008) and the local production rate (LL LPR) utilised in this study.

Sample	CRONUS standard production rate		Local production rate (LL LPR)	
	Apparent exposure age (^{10}Be kyr)	Uncertainty	Apparent exposure age (^{10}Be kyr)	Uncertainty
ACH1	13.9	1.4	15.5	1.1
ACH2	13.8	1.4	15.4	1.1
ACH3	13.4	1.4	15.0	1.2
Mean age	13.7		15.3	

Interestingly, Hubbard et al.'s 2009 model generates a 'stable' margin position pinned amongst the Summer Isles from c. 17.55-14.65 ka BP. A relatively long period of ice-margin stability in Lateglacial terms with Loch Broom seen to operate as a major outlet glacier or fast flow zone from 15.3-14.75 ka BP (Figure 4.7 E & F).

With overlap in two of the three erratic samples from Tanera Mor, a mean age of ice sheet margin of c.16.8 ka BP has been inferred (this study). However, the quartzite erratic (TANM03 - 17.3 ka BP) potentially provides the most reliable deglaciation age, as this lithology shows very

little post-glacial sub-aerial weathering and therefore provides the most likely zero-erosion age. With this as the bounding age, the Achiltibuie moraine (re-dated c. 15.2 ka BP) may represent a retreat stage from this earlier margin or reorganisation of the lobe's lateral margin. The revised mean age of 14.8 ka BP from the Little Loch Broom lateral moraine sits comfortably within this succession at the onset of the Lateglacial Interstadial.

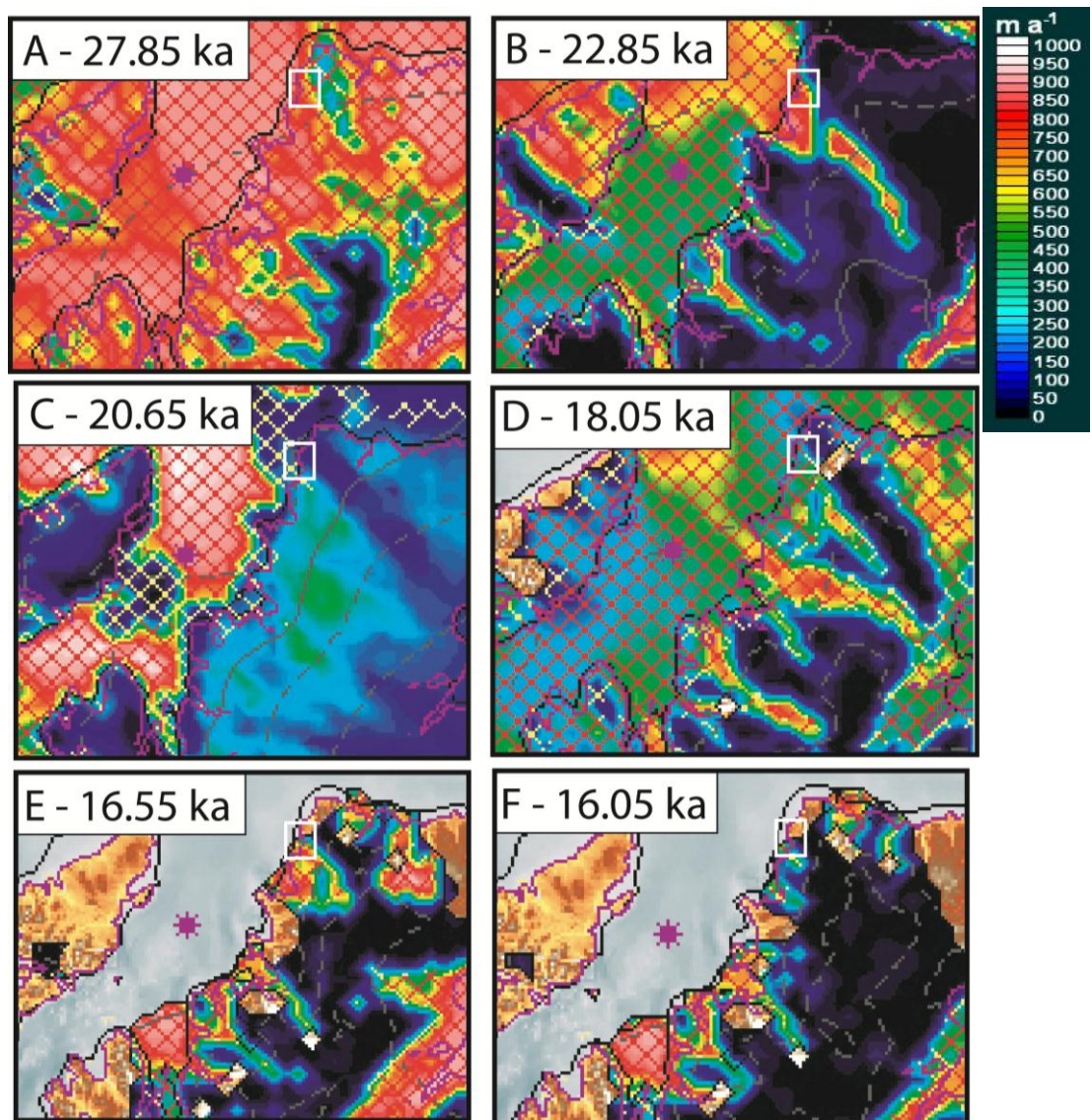


Figure 4.7: Time slices from BIIS thermo-mechanical model (after Hubbard et al., 2009). White box indicates location of Oldshoremore. Colour ramp indicates basal ice velocity.

4.2.4. *Glen Achall*

All TCN samples are derived from large Moine schistose boulders sitting on ridge crests or moraine mound peaks. GAC01 and GAC03 are statistically indistinguishable with a mean of 10.1 ± 1.2 ka BP, however GAC02 returns an older surface exposure age of 14.8 ± 1 ka BP. Here the younger ages seem unlikely as Younger Dryas ice extent is constrained further up the flow line by the Loch Droma ice free conditions before 12.9 ka BP (Kirk and Godwin, 1963). Consequently it is suggested that occupation of this limit is more likely to have been c. 14.8 ka and that the younger ages represent surfaces affected by moraine degradation through loss of loose sediment.

4.2.5. *Little Loch Broom*

LLB samples show that the moraines on the seafloor of Little Loch Broom have at no time been sub-aerially exposed; therefore moraines were probably laid down in a marine or deep glaciolacustrine setting. Relative sea level in this part of NW Scotland was around ~ -5 m below present sea level prior to 15 ka BP with a minimum of -10 m O.D. at the start of the Younger Dryas (Shennan & Horton 2002). Consequently even the shallowest parts of the Little Loch Broom marine basin would have remained underwater since deglaciation. This cosmogenic data therefore supports Shennan and co-workers predictions for RSL in the Loch Broom-Coigach area in that there is no ice-free subaerial signal from surfaces currently at -30 m OD demonstrating that the seafloor fjord has not been above sea level during or following deglaciation.

4.2.6. *Gruinard Bay*

The new local production-rate corrected (LLS LPR Fabel pers. comm.) age for the Achiltibuie moraine stage is 15.2 ka BP possibly indicating persistence of relatively low level ice (c.125 m a.s.l.) sheet limit in the Summer Isles region at this time. The two samples from Sand in Gruinard Bay (this study) statistically overlap yielding a mean of c. 13.6 ka BP. Like all ages in this study, these ages are minimum ages. DDO1,

partially excavated for sampling from peat, may have previously experienced shielding by sediment (peat or morainic material). DD02 also presents a ‘young’ age and may have lost surface material through post-glacial erosion as suggested by the varied micro-relief of its surface and by regional examples of surface loss on Lewisian gneiss lithologies. Consequently both ages probably underestimate the ‘true’ abandonment age of this ice-sheet limit. Interestingly, however, ice sheet modelling simulations (Hubbard et al., 2009) do maintain a substantial ice body, fed from the Torridon mountains, with a northern limit extending to the coast at Gruinard Bay, until c. 13.2 ka (model years).

4.3. Ice Sheet Thinning

Nine high level erratic boulders yield exposure ages relating to high level deglaciation conforming to a regional pattern. All nine ages are post-LGM (<26 ka BP) and fall in an age bracket of 16.5 - 14 ka BP. Seven erratic samples (from Ben Mor Coigach, Cul Beag and Beinn Uidhe) are excluded due to inheritance, burial or geological contributions which have not been quantified at this time. For five of these erratics (on Ben Mor Coigach and Cul Beag), due to the presence of blown sediment and grüs produced from the postglacial breakdown of Torridon Sandstone, the possibility of uncovering from significant post-glacial sediment burial had been noted at the time of sampling. As the samples in these situations yielded significantly younger ages than those sampled in more favourable and stable bedrock situations on Beinn Uidhe and Cranstackie, these younger ages were taken to as the product of complex exposure histories including an element of sediment shielding. They were therefore taken as unrepresentatively young for high elevation deglaciation ages. For the orthogneiss erratics from Beinn Uidhe, the lithology of the samples was less preferable to the other erratic sampled - a quartzite. There is evidence of chemical weathering of orthogneiss clasts in terms of discolouration, brittleness through conversion of parent minerals to clays. At low elevation there is some constraint on the post-glacial weathering of orthogneiss in

terms of surface loss, but this is through casual observation only. Consequently, as a zero post-glacial erosion history can be stated with more confidence for the quartzite erratic, the apparent exposure ages of the orthogneiss erratics are discarded, as deglaciation ages, because their erosion history is not sufficiently constrained.

Fabel et al.'s (2012) above-trimline erratic-deposition ages from Torridon mountains (when calculated with the same LLS LPR) have a mean of 16.12 ± 1.02 ka BP for samples in the elevation range 883-989 m. All the previously mentioned high level erratics from this study (elevation range 528 -840 m a.s.l.) overlap (within uncertainties) with the Torridon mean indicating they could be classed as the same deglacial stage or population. This may suggest that far northern areas experienced more extensive thinning during the period ~16.5-14.0 ka BP. The considerably lower accumulation area of high ground in the far north in comparison to that of Torridon; and the reliance upon cross-regional ice input from the east may explain this difference at the latter stages of GS-2.

The difference in elevation between summit height and highest dated erratic (Table 4.2) gives a minimum constraint on ice sheet thinning. This small dataset suggests some interesting patterns, the verification of which would require a larger scale erratic sampling strategy. The greatest ice thinning is observed in the north where lateral margin constraints also indicate rapid retreat of lateral ice margins following cessation of the MPIS. Sail Liath in the south, at the margin of the postulated Fannichs 'unzipping zone' (Finlayson et al., 2011), also demonstrates significant ice thinning.

Table 4.2: Minimum ice sheet thinning between maximum ice thickness and erratic deposition during the Lateglacial.

Mountain	Summit elevation (m a.s.l.)	Highest erratic (m a.s.l.)	Min Thinning* (m ice thickness)	Erratic exposure age (ka BP)
Sail Liath	954	840	114	15.1 (mean)
Cul Beag	769	760	9	14.2
Beinn Uidhe	740	714	26	16.5
Cranstackie	801	528	273	15.2

* Calculated from the elevation of the highest erratic. Initial ice thickness assumed to be at least the summit height of each mountain.

Fabel et al. (2012) indicate the possibility that some high level deglaciation ages may represent melting of ice fields which had earlier disconnected from the main lower elevation ice body, probably now less than c. 500 m a.s.l. Some erratic exposure ages from this study also leave open the possibility of plateau ice persistence during the Lateglacial Interstadial (GI-1) i.e. the ‘young’ ages from Ben Mor Coigach and Beinn Uidhe. The proposition of small cold-based plateau ice fields in NW Scotland is consistent with the findings of Lukas & Bradwell (2010b) who emphasise the important contribution of these high level (>700 m a.s.l.), but difficult to reconstruct, Younger Dryas glacier source areas. When recalculated with the LLS LPR, a glacially polished bedrock surface (CS0602) at 727 m on the western flank of Conival yields an exposure age of 13.8 ± 0.9 ka BP which may indicate persistence of a small localised ice (or snow) body well into the Lateglacial Interstadial. The possibility of sediment shielding cannot, however, be excluded as a possibility for explaining this young age (as at other anomalous sites).

Ice-free conditions in central Assynt (Allt nan Uamh caves - Folio 1) indicated by deposition of the gravel deposit in the Reindeer Cave (c. 330-340m a.s.l.) before 22 ka BP (Kirk and Godwin, 1963), support very early

ice retreat (i.e. ~ 5 kyrs earlier than suggested by the Hubbard model). Dates on the north coast (this study) suggest that the ice sheet retreated and thinned very quickly and permanently after 19 ka BP while remaining extensive further east and south.

4.4. Ice sheet stability

Early recession of the northern margin of the BIIS is indicated at North Rona, with ice-free conditions c. 25 ka (Everest et al., 2012). Earliest mainland deglaciation (this study) is seen at Rispond, on the north coast with ice-free conditions by 17.6 ka. Between these two sites is a distance of c. 90 km (straight line) or equivalent to c. 80 km flowline-parallel retreat to the northwest coast. The seabed landform record off the north coast indicates multiple ice margin positions between North Rona and the northern coast (Figure 4.8).

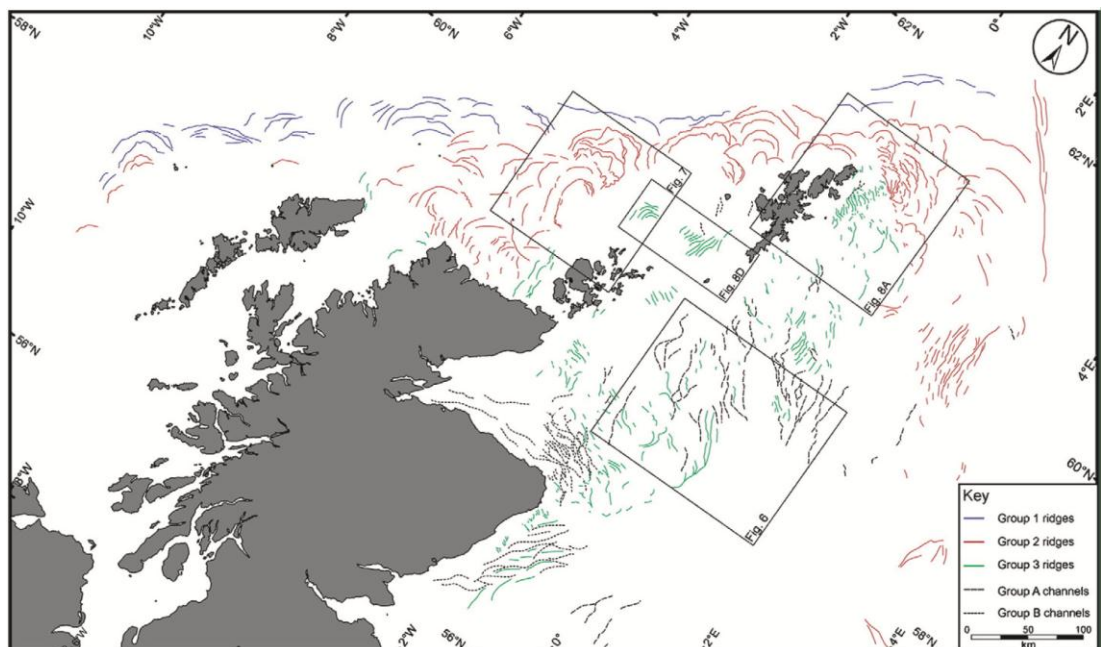


Figure 4.8: Seabed landforms on the northern UK continental shelf mapped from the Olex dataset. Solid line - positive features (ridges); dashed lines - negative features (channels). After Bradwell et al. 2008.

Between North Rona and Rispond the geometries of the ice margin alter rapidly from shelf-edge parallel to predominantly concave to the east - bounding eastern-sourced ice. This demonstrates important properties of the northwest sector of the lateglacial BIIS. Firstly, the Cape Wrath area and shelf beyond acted as an unzipping zone with early loss of ice, potentially around a calving bay, should sea levels have been high enough. Secondly the ice sheet underwent significant reorganisation during the period 25-17.6 ka as demonstrated by the ninety degree direction change in retreat pattern. This suggests that the Cape Wrath corner of the ice sheet had completely collapsed before 17.6 ka losing extension on to the shelf. In turn, this has implications for the MPIS, as its operation would have been needed to draw ice across Cape Wrath from sources to the south east. So, it may be proposed, that the MPIS weakened substantially within this period, potentially losing up to 200 km of extension, i.e. from St Kilda back towards Oldshoremore.

Consequently, it may be suggested that the MPIS became fed solely southern-sourced relatively ice early in deglaciation, with the far north coast and headland of Cape Wrath potentially ice-free, while The Minch still contained streaming ice. In support of this, offshore moraines appear to overprint with progression southward down the west coast which suggests that ice was latterly more extensive and persistent towards the south (Figure Figure 4.2).

The pattern of deglacial ages from the far northwest suggests that thinning and ice margin retreat occurred more rapidly in areas towards the north coast of Sutherland, and the southern part of Wester Ross. Around the loch Brooms, and central Assynt, the thinning appears less dramatic and there is evidence for persistence of low level ice further into the Lateglacial. It can be seen that most deglacial ages cluster (within uncertainties) between 18 and 15 ka. Comparing the deglaciation ages from NW Scotland (this study) and the $\delta^{18}\text{O}$ record from the NGRIP ice core (Figure 4.9) allows relationships to be drawn out between North Atlantic environmental forcings and BIIS volume and extent.

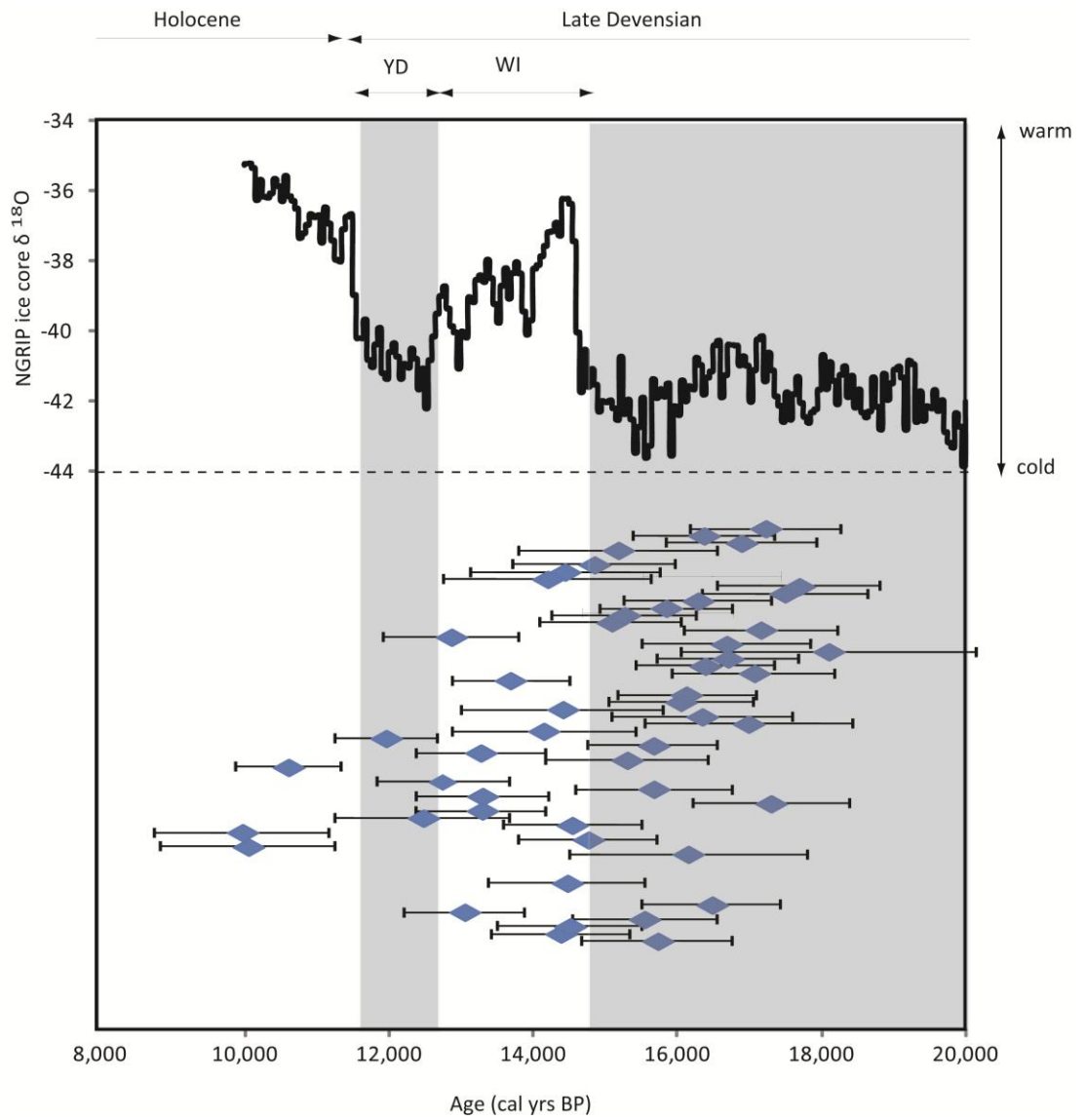


Figure 4.9: ^{10}Be exposure ages plotted against a portion of the $\delta^{18}O$ curve from the NGRIP ice core (North Greenland Ice Core Project Members, 2004). Vertical positioning of exposure age data points is arbitrary. Exposure ages are shown with full systematic uncertainties. YD = Younger Dryas, WI = Windermere Interstadial. Pre-LGM and Holocene (post-10 ka BP) exposure ages are omitted.

The early deglaciation of the far north may have been initiated by sensitivity to increases in air temperature, such as the pronounced peaks occurring during Greenland Interstadials 3 and 4 (c. 27-25 ka). However, rapid response to marine forcings appears to provide a well-correlated solution for early margin retreat and MPIS collapse. The IRD record from cores on the western continental shelf indicate a strong response of the BIIS to the Heinrich 2 Event (c. 25-24 ka) with significant tailing off of IRD delivery to Rosemary Bank between 25 and 20 ka (Scourse *et al.*, 2009). This suggests a purge of ice mass through calving early in deglaciation followed by ice exhaustion and retreat well-back to the continental shelf and neatly explains collapse of the Cape Wrath corner of the BIIS.

Knutz *et al.*'s (2001) data from the Barra Fan indicates that the latest readvance of ice on to the Hebrides Shelf was 17-16 ka. This suggests that the MPIS was still active at its south western quarter, as its presence would be needed to push a calving ice front out as far as the Hebridean shelf. Mega-scale glacial lineations preserved at the sea bed in The Minch and attributed glacial activity prior to c. 15 ka cal. B.P. (.12 785 ¹⁴C years B.P.; Graham *et al.* 1990), also support late stage active ice streaming in the inner Minch (Stoker & Bradwell, 2005).

An ice sheet which was extremely sensitive and response to marine forcings is therefore envisaged. The BIIS appears to have demonstrated the tendency to overstretch its margins due to the activity of major ice streams, including the MPIS. But, during deglaciation, these ice streams acted as conduits amplifying and transferring external forcings inwards towards the centre of the ice sheet and effecting large-scale glaciological reorganisation.

4.5. Ice sheet sector pattern of deglaciation: Major findings regarding chronology of retreat and glaciological organisation

- A period of widespread, broadly coeval thinning and margin retreat is proposed in the time period c. 16-15 ka BP.
- Thinning of ~300 m is seen in some areas prior to 14 ka BP.
- Rapid reduction of ice extent and volume following shutdown of the Minch palaeo-ice stream.
- The Minch palaeo-ice stream break up before ~ 17.6 ka BP led to a major reorganisation of the northern sector of the BIIS with resurgence of northern margins and subsequent stabilisation > 17.6 ka BP.
- Ice margin chronology suggests that most ice had retreated dramatically back to local accumulation areas by 15.8 ka BP.
- Correlation of low-level ice margin ages with erratic deposition ages c. 15 - 16 ka BP suggest large scale ice sheet reorganisation and down-wasting possibly resulting in separation and starvation of low-level valley glaciers from cold-based plateau remnants. This would precondition the remaining low level ice masses to rapid retreat due to increased surface area to volume ratios. This type of reorganisation which leads to the starvation of the lower level remnants has been observed in Northern Norway (Gellatly *et al.*, 1988 and 1989, Evans *et al.*, 2002) and is also suggested as a Lateglacial scenario for glaciers of the Monadhliath Mountains in the central Highlands of Scotland (Gheorghiu *et al.*, 2012).

5. DISCUSSION: THERMAL STRUCTURE AND FLOW REGIME OF THE LAST BIIS IN NW SCOTLAND

5.1. Introduction

The importance of constraining the evolution of ice sheet basal thermal regime through space and time has gained increasing recognition in ice sheet reconstruction research over the last c. 50 years (Sugden, 1968, Sugden and Watts, 1977, Hall *et al.*, 2012, Goodfellow, 2007, Briner *et al.*, 2006, André, 2002, Ballantyne, 1998, Gellatly *et al.*, 1988, Kleman and Glasser, 2007, Stroeven *et al.*, 2002, Kleman *et al.*, 1999a, Hattestrand *et al.*, 1999, Kleman *et al.*, 1999b, Clarhall and Kleman, 1999, Kleman, 1992, Fabel and Harbor, 1999). Identification of areas persistently covered by cold-based ice has significant implications for 1) concepts of landscape evolution over a multi-millennial timescale; and 2) glaciology and the thermal structure of ice sheets. This chapter discusses how the new geomorphic observations and exposure data, presented in this thesis from NW Scotland, can be used to reconstruct the basal thermal regime (BTR) and flow organisation of a large sector of the last BIIS.

5.2. Relict surfaces & glacial modification

Detailed studies in Fennoscandia and Arctic Canada (Blake, 1999, Jansson and Kleman, 1999, Briner *et al.*, 2003, De Angelis and Kleman, 2005, Kleman and Glasser, 2007, Angelis and Kleman, 2008, Kleman and Borgstrom, 1990, Kleman, 1992, Borgström, 1999, Clarhall and Kleman, 1999, Stroeven *et al.*, 2002, André, 2002, Ebert and Hättestrand, 2010, Hall *et al.*, 2012) have indicated the significance of the persistence, both spatially and temporally, of cold-based ice. Cold-based ice is frozen to its bed and has a higher viscosity than warmer ice. When ice is frozen to its bed basal sliding is inhibited, strain is predominantly taken up in shearing of the layers of the ice near the bed (Benn and Evans, 2010). When ice is frozen to the bed and inhibiting basal flow, the flux of ice which can be moved through an area is greatly reduced, leading to thickening of ice over and around these frozen-bed patches, often synonymous with ‘sticky

spots'. Consequently ice sheet thickness and flow organisation are highly dependent on the distribution of cold-based ice (Kleman and Glasser, 2007).

Identification of the transition from cold-based to thawed basal ice has proved particularly illuminating in terms of recognition of boundary conditions in ice sheet flow. Early work by Sugden (1968) building on initial observations by Linton (1949), recognised the sharp transition between relict surfaces and effective glacial erosion surfaces. Sugden suggested that these land surface changes represented discrete changes in ice properties; boundaries dictated by palaeo-ice flow configuration, underlying topography and ice sheet context. Subsequent studies in Scandinavia used landform classification, governed by former subglacial thermal conditions, to characterise 'modes of glaciation' (Figure 5.1) and to reconstruct ice sheet configurations and deglacial regimes over several glacial cycles (Kleman, 1992). More recently Angelis & Kleman (2008) and Bradwell (2013) have recognised the potential for partially frozen beds to indicate the location of ice stream onset zones - a glacial system transition rarely preserved in the hard-bed landform record. The application of TCN analysis to the paradox of juxtaposed erratic and relict surfaces (Stroeven *et al.*, 2002), provided strong empirical evidence of former cold-based ice cover.

In NW Scotland mapping of relict land surfaces and surface exposure dating have identified areas of cold-based ice at high, and perhaps more surprisingly, at lower elevation, which define persistent frozen bed conditions through at least one glacial cycle (Folio 4). Transitions to thawed bed conditions are also identified both laterally and vertically, sometimes with quantitative control on glacial erosion (Chapter 4: 4.2.2). Combined, these observations build towards a three dimensional picture of basal thermal regime and flow organisation during the last glacial cycle, and inform on long-term landscape evolution.

In Assynt, Coigach and Sutherland constraint of ice surface elevation and basal thermal regime is particularly important as it may inform ice stream dynamics. As much of the area is thought to have represented onset zones for the Minch palaeo-ice stream (Figure 5.2), understanding of the distribution of thawed and frozen bed conditions may offer insights into the

5: Discussion: Thermal structure & flow regime
 response of ice sheets, via marine-terminating ice streams, to major
 changes in atmospheric and/or ocean conditions.

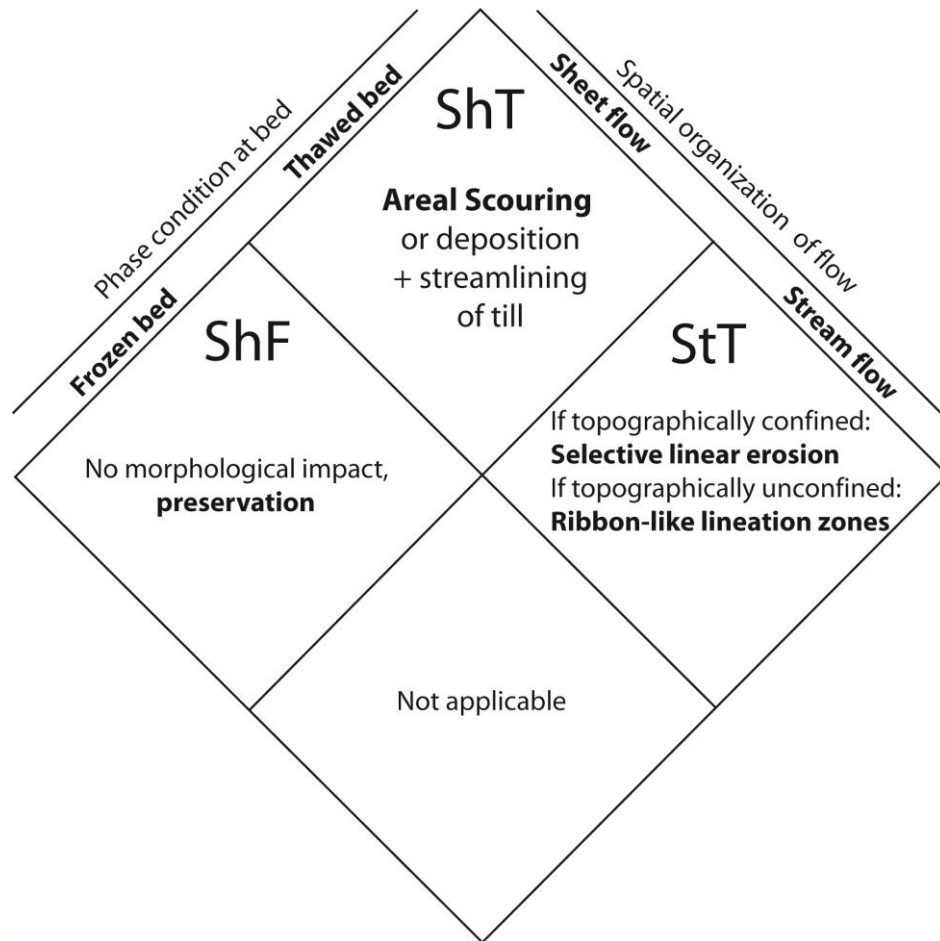


Figure 5.1: Inversion key for translating geomorphology into glacial basal thermal regime after Kleman et al. (1997) .

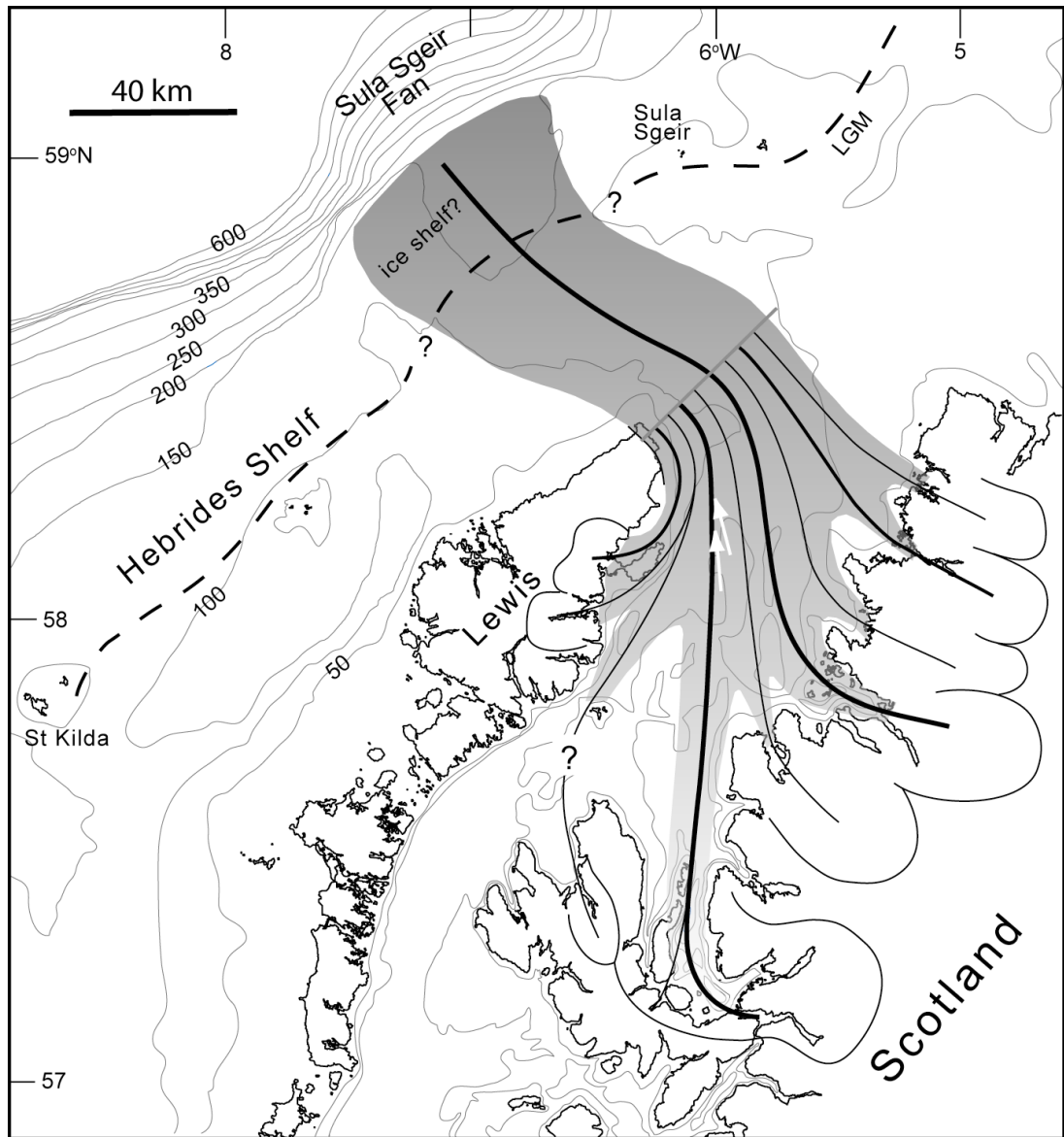


Figure 5.2: Proposed location of the Minch palaeo-ice stream and onset zone catchments, NW Scotland. After Bradwell et al. (2007)

5.2.1. High and intermediate level surfaces: Tors, Blockfields & Rip-offs

The existence of cold-based ice over large areas of high ground beneath the last BIIS has been widely suggested by field evidence (Sugden, 1968, Phillips *et al.*, 2008, Hall and Phillips, 2006, Glasser, 1995) and replicated by ice sheet models (Boulton and Hagdorn, 2006, Hubbard *et al.*, 2009). In NW Scotland, (Fabel *et al.*, 2012) have recently emphasised the important contribution of cold-based ice over the high ground of Torridon in extending both the thickness and the lifespan of the GS-2 ice sheet. Previous research in the Wester Ross - Sutherland area has shown the potential of high level cold-based ice cover to explain unresolved geomorphic questions on An Teallach (Stone *et al.*, 1998) and the Assynt Mountains in particular (McCarroll *et al.*, 1995b). In terms of long-term landscape evolution, invoking the occurrence of cold-based ice over the summits of the mountains of NW Scotland, may help to explain the distinctive geomorphology of the region which bears strong resemblance to the model proposed by Stroeven *et al.* (2013). Comparison of the Assynt inselbergs and Stroeven *et al.*'s (2013) model is shown in (Figure 5.3).

Previous ice thickness predictions for the last BIIS in NW Scotland, based on periglacial 'trimline' elevations have been recently re-evaluated (Ballantyne, 2010a) with evidence from Torridon supporting reinterpretation of trimlines as englacial thermal transitions (Fabel *et al.*, 2012). Here the exposure ages of erratics found above the trimline are found to be largely 'young' (post-LGM). This discovery requires that thick ice transported material to high elevation to elevations previously thought to have been ice-free nunataks due to their absence of glacial abrasional features. The lack of such erosional evidence in turn necessitates that the ice above the 'trimline' must have been below pressure melting point. Consequently trimlines may represent englacial thermal boundaries with the absence of glacial abrasional features relating to the properties, rather than the absence, of ice.

Tors are bedrock landforms sensitive to the severity of glacial erosion. The occurrence and location of tors within an area, can therefore serve as

a constraint on both ice thickness and basal thermal regime (Figure 5.4). A review of data from multiple studies (Hall and Phillips, 2006) indicated that tors probably have a Quaternary origin and persist, as surface or near-surface features, for periods of 200-845 kyr. That tors have persisted through multiple glacial cycles, despite ice-overriding, has been used to prove the existence of cold-based non-erosive ice conditions under the Laurentide, Fennoscandian and British-Irish ice sheets (Glasser, 1995, Hall and Sugden, 1987, Sugden and Watts, 1977, Ballantyne, 1994, Stroeven *et al.*, 2002, Phillips *et al.*, 2008, Hall and Phillips, 2006, Briner *et al.*, 2003).

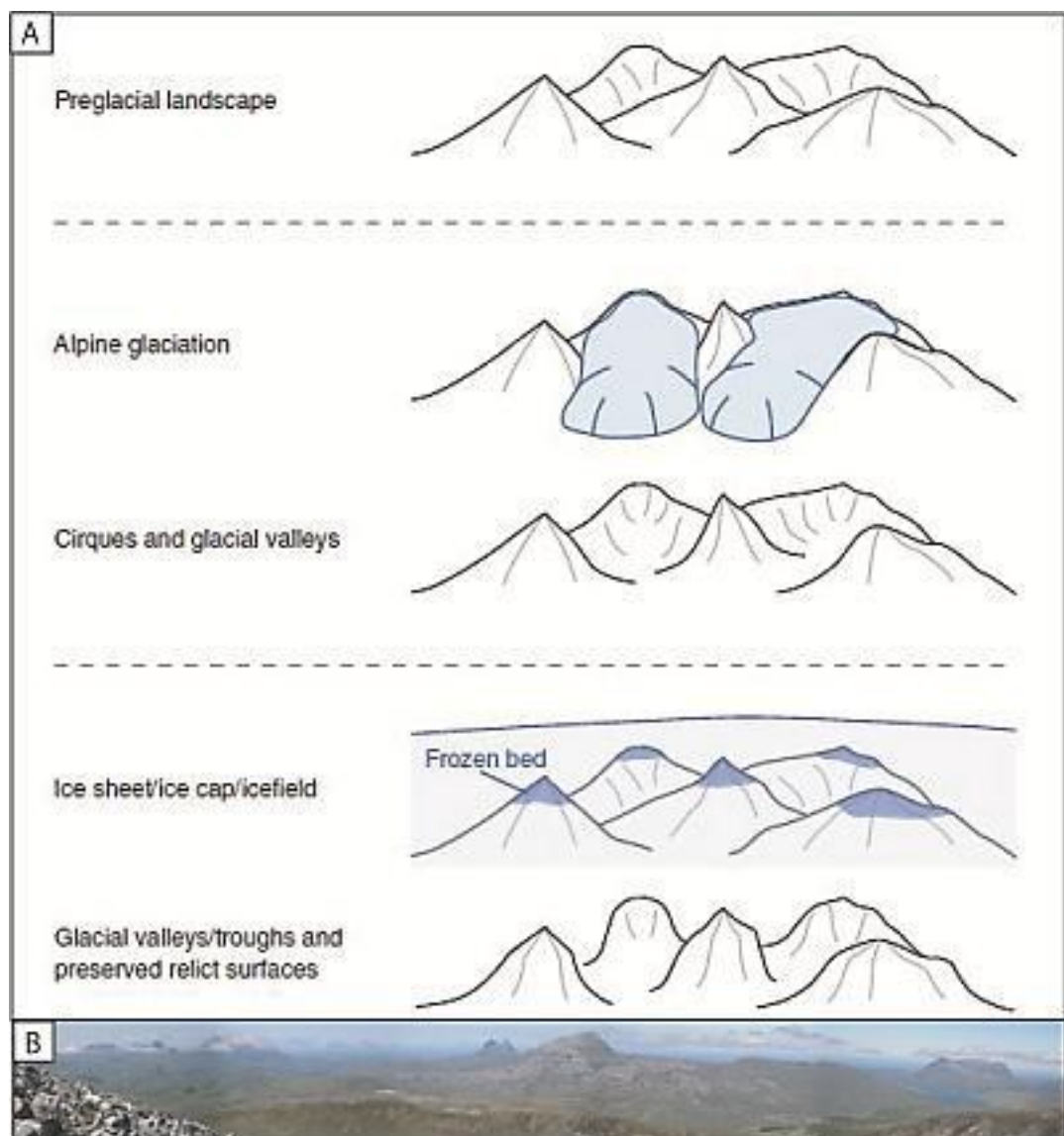


Figure 5.3: A - Landscape development with alpine and ice sheet/cap/field style glaciation after Stroeven *et al.* (2013) B - Assynt panorama showing inselberg hills with rectilinear forms.

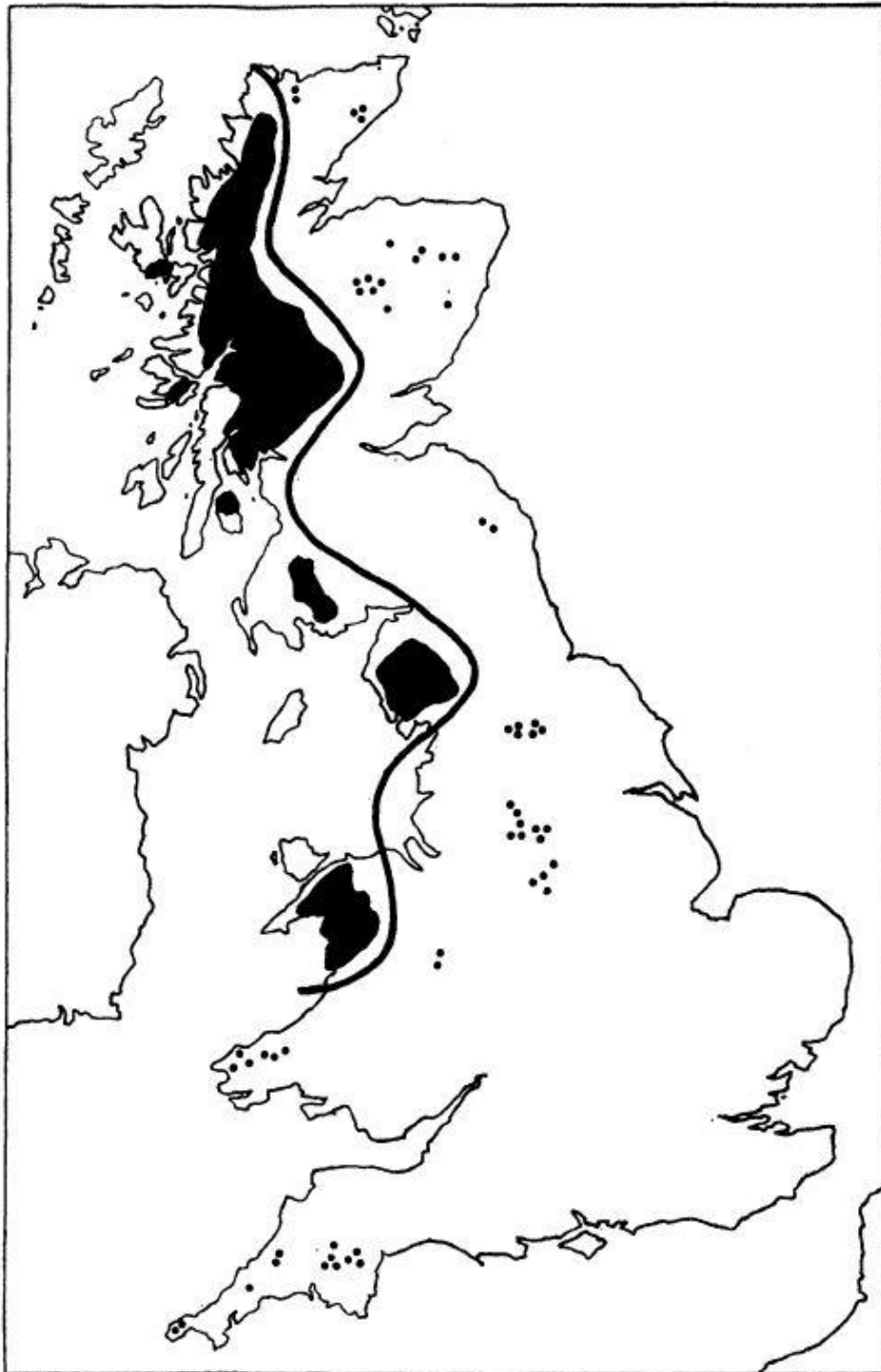


Figure 5.4: Distribution of main tor groups and areas which experienced intense glacial erosion after Linton (1955). Dots represent the main tor groups and shaded patches the main 'centres of intense local glaciation'. Linton divides these with a solid line suggesting discernible zonation.

Research on the large tors of the Cairngorm Mountains and low level tors of Buchan have made significant contributions to our understanding of ice sheet dynamics throughout the Quaternary. Phillips *et al.*'s (2006) work in the Cairngorms indicated that dry/cold-based ice can significantly modify tors through shunting and entrainment of blocks while not abrading bedrock surfaces (Figure 5.5). In Southern Caithness and Eastern Sutherland, erratic boulders (undated) sit on slopes above tors. Ballantyne & Hall (2008) sampled tor surfaces at c. 500 m a.s.l. which yielded pre-LGM TCN exposure ages >140 ka BP (CRONUS standard production rate) indicative of long potentially complex exposure histories. In an area known to have been overridden by ice, this evidence supported preservation of pre-glacial land surface remnants under cold-based ice and stimulated reinvestigation of the significance of postulated trimline elevations throughout NW Scotland.



Figure 5.5: Glacial modification of Tor at An Cnoidh, Cairngorms. Phillips et al. (2006). Ice has moved the tor block to the right exposing the 'fresh' surface the person is standing on. ^{10}Be ages from the pitted upper tor block surface and the lower bedrock surface are respectively c. 189.5 ka BP and c. 21.4 ka BP.

Widely cited as a classic landscape of areal scouring (Figure 5.4), and despite its fine examples of summit blockfield and periglacial forms, the far NW Highlands of Scotland have been largely overlooked in terms of tor

research. However, it may be argued, that this is an area of exceptional tor preservation in the British Isles. Though the individual tors in this region are modest in scale (<10 m relief), as a population they may be viewed as highly unusual and unique on at least two counts.

Firstly, in this region, tors occur in four different lithologies (quartzite, sandstone, psammite and syenite). Secondly the tors are found over a wide elevation range (420-758 m a.s.l.) (Table 5.1). That tors are preserved at all suggests that abrasional regimes, capable of planing off rock protrusions (>1 m relief) have not been ubiquitous across the region during the last glacial cycle. The occurrence of these tors over a wide elevation range throughout the region, suggests that the basal thermal regime of the last ice sheet included significant local vertical and horizontal perturbations. Consequently the setting and modification of tors and surrounding blockfield provides information on the thermal regime of the last glacial cycle and landscape evolution on a Quaternary timescale.

All tors show significant open joints within the rock along pseudo-bedding suggesting long-term sub-aerial weathering. Abrasional glacial regimes capable of removing >10 cm of intact rock are difficult to evoke as small scale weathering features, such as the weathering pits and tafoni observed on Cranstackie (Figures 3.16 & 3.18), would not have survived. Glacial modification is apparent to varying degrees on all the tors observed in NW Scotland (Table 5.1) in the form of perched blocks, block toppling or removal. Attempts have been made to distinguish and quantify progressive stages of, largely granite, tor modification by glacial over-riding by Hall & Phillips (2006). However, it is not possible to utilise the Hall & Phillips stage system in this study due to the distinctly different lithological characters of the tors examined both from Hall & Phillips' dataset and those within this study. Because the majority of the glacial modification involves evidence of enhanced basal ice deformation - block dislocation and toppling (Table 5.1, Figure 3.18) - ice thick enough to internally deform must be invoked. Consequently minimum ice columns 70 m thick (A. Hubbard pers. comm.) are suggested above tor locations (specifically at Cranstackie, Ben Mor Coigach and Ben Loyal) in order to account for this

5: Discussion: Thermal structure & flow regime modification. This provides criteria for reconstructing the ice sheet surface morphology.

Table 5.1: Comparison of tor features, NW Scotland

	Cranstackie	Stac Pollaidh	Cromalt Hills^a	Ben Mor Coigach	Ben Loyal^b
Mountain summit	801 m	612 m	427 m	743 m	765 m
Lithology	Quartzite	Torridon S/stone	Moine Psammite	Torridon S/stone	Syenite
Context	Summit slope	Summit ridge	Hillside	Summit ridge	Summit
Tor elevation	733 m	>550 m	410 m	565/580 m	c. 760-670 m
Tor relief	6 m		2 m	<1.5 m	c. 15 m?
Pinnacles or Super-structure	No	Pinnacles	?	Super-structure	No
Displaced blocks/ Boulder train	Yes	Yes	?	Possibly	Yes
Perched blocks	Yes	Yes	?	Yes	No
Striation/ Moulding	No	Yes	?	Weathering issues	Yes
Nearest glacial abrasion (elevation)	565 m	c. 560 m	Mega-grooves at same elevation	535-550 m?	549 m

^a *Cromalt Hills data from field observations and BGS mapping of Maarten Krabbendam (pers. comm.)* ^b *Ben Loyal observational data from Linton (1955).*

Some significant differences observed in the degree of tor modification across the region are important in relation to ice sheet basal thermal regime. Higher tors (Cranstackie and Ben Loyal) appear 'better preserved' i.e. they are larger, however these results are complicated by the lithological control on erosion, which also reduces the softer rocks (Moine psammite and Torridon sandstone) to lower elevations, while the higher tors occur in quartzite and syenite, which are more resistant to sub-aerial and subglacial erosion. Glacial bedforms and/or abrasion features occur in closer proximity to the lower tors i.e. horizontally adjacent to the Cromalt tor (megagrooves), 168 m lower on Cranstackie, 208 m lower on BMC, 211 m lower on Ben Loyal. This suggests that large tors can only be maintained where stable persistent non-abrasional regimes are encountered i.e. in the very cold upper zones of ice sheets or protruding above the ice as nunataks. In the situation of Ben Loyal, any weathering products in the vicinity of the tors appear to have been largely cleared by ice, with evidence of block transport towards the north. On Cranstackie, post-glacial weathering products are not seen, and there is evidence of glacial modification and mobilisation of soliflucted and deeply weathered material as discussed previously.

It is still surprising to note that a small tor persists in the Cromalt Hills, despite its proximity to megagrooves - features associated with thawed bed conditions and highly abrasive fast-flowing basal ice (Folio 4 and Figure 5.6). Bradwell's (2005) original explanation of megagroove formation, relating to bed permeability, may also explain the persistence of a tor in this vicinity i.e. that the bed-draining influence of the (highly permeable) Durness Limestone may couple the ice sheet to the bed in this location (Figure 5.7) leading to freeze-on. Glacial erosion would therefore be lower over the permeable rocks where subglacial water can be directed away from the ice-bed interface. Sugden modelled this situation down-ice of a zone of 'maximum erosion' within the Laurentide ice sheet (Figure 5.8). In Assynt an ice-sheet bed high, like the Cromalt Hills, probably promoted a cold based patch surrounded by warm-melting erosive conditions necessary for the formation of megagrooves.

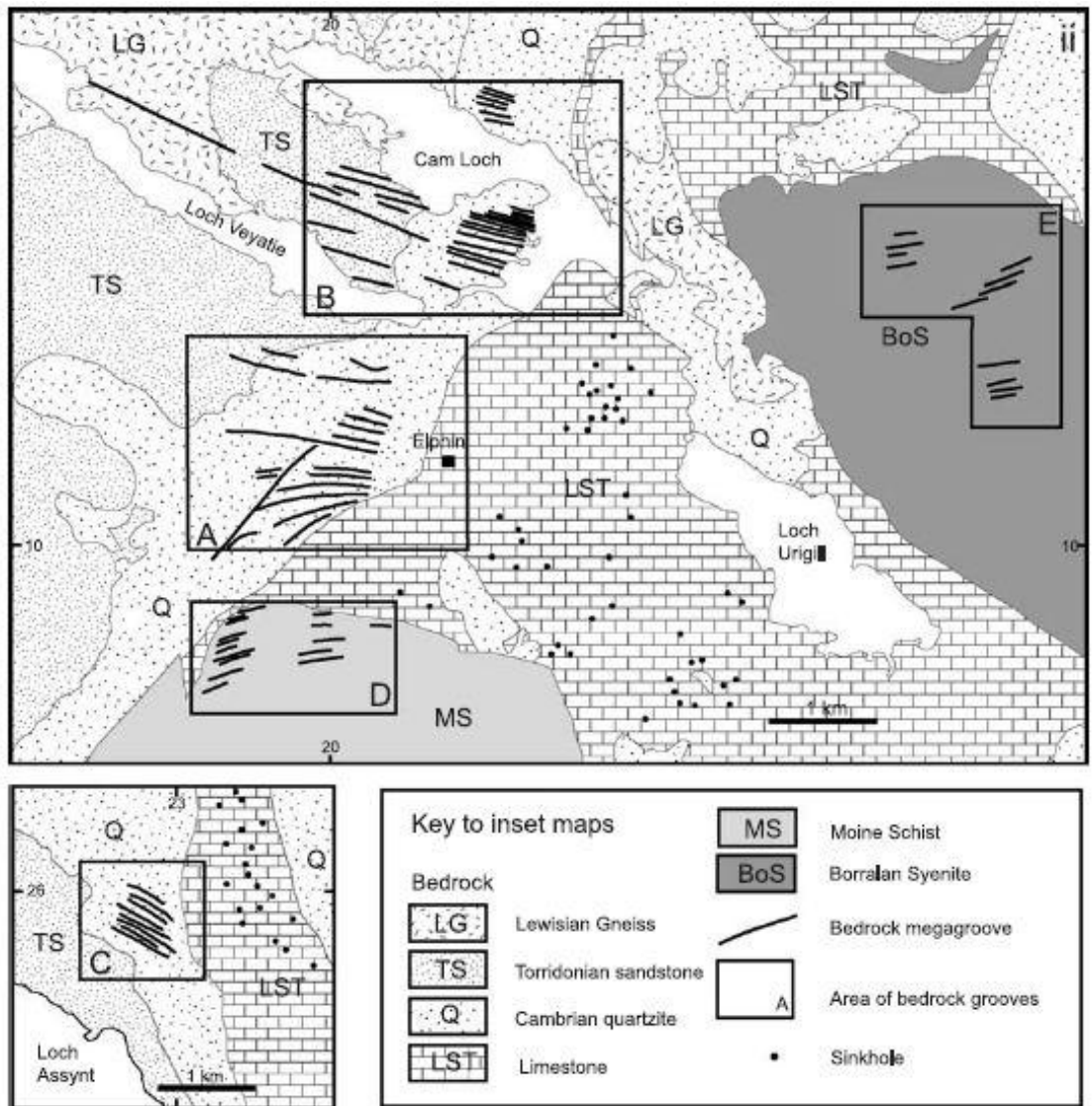


Figure 5.6: Megagrooves in Assynt (Bradwell, 2005). Box D shows location and geology of megagrooves situ on the edge of the Cromalt hills. Interestingly there is a hiatus in the channels where the knoll of Meall Odhar occurs from c. 350 - 427 m a.s.l. This is where the Cromalt tor (c.400 m a.s.l.) is situated.

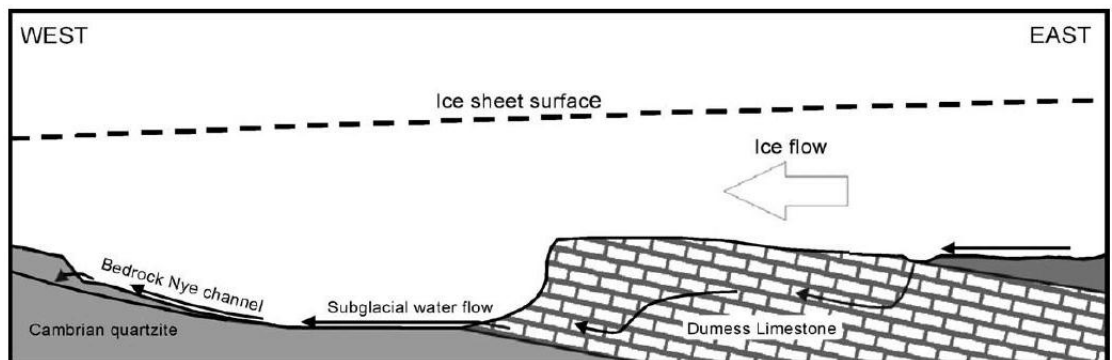


Figure 5.7: Theory of erosional-subglacial hydrology relations in relation to megagroove formation, Elphin in Assynt from Bradwell (2005).

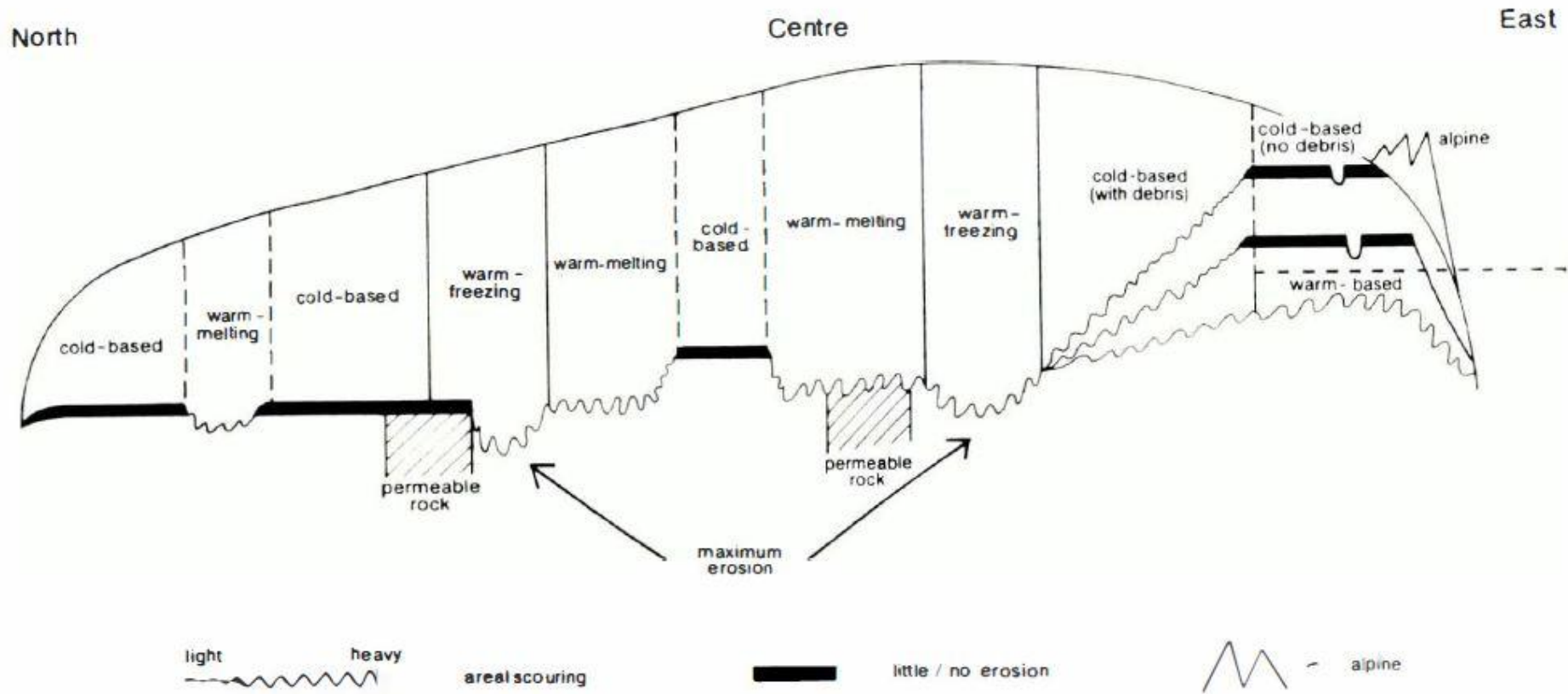


Figure 5.8: A model of the possible relationship between erosional landscapes and main variables affecting glacial erosion: basal thermal regime, topography and bedrock geology (Sugden, 1978).

A similarly fine line between a highly abrasional subglacial regime and a cold-based protective one may be drawn around Stac Pollaidh. Though its summit structures would not be traditionally described as tors, they are none the less delicate, sub-aerially weathered stacks of rock, which could not have withstood abrasive warm/wet-based ice cover. That evidence of glacial modification exists on the summit saddle and on ridge blocks themselves (Figure 3.36) attests to cover by deforming glacial ice at c. 550 m a.s.l. As an isolated inselberg in a lowland landscape, this evidence of active glacial processes has important repercussions for the debate on ice sheet thickness, and is discussed fully in section 5.3 (Ballantyne, 2003, Bradwell and Krabbendam, 2003). Transport of tor slabs beyond the immediate summit plateau, identified at Cranstackie and Ben Loyal, also requires entrainment of material. The old, probably complex, exposure history of the main summit tor on Cranstackie (c. 129 kyrs), combined with the preservation of long-term sub-aerial weathering features, indicates that glacial abrasion has been minimal with no polishing of surfaces detected. It is likely that no surface slabs were lost during the last glacial stage, but the planar nature of the tor top, as defined by pseudo-bedding suggests that overlying slabs may have been removed by previous glacial events (Ballantyne, 1998, Hall, 2007, Hall and Phillips, 2006) From the abundance of large slabs around the summit (Figure 5.9) it is possible to infer that previous glacial modification has mobilised surface layers from tor summits.

The volume of summit debris, and the scale and edge rounding of individual slabs (Figure 3.16) suggests mobilisation and generation of material from an exposed, elevated bedrock source i.e. a previously much larger tor field. Similar observations on Breabeg, where western near summit slopes bear a surface-armour of large quartzite slabs, are suggestive of remobilisation of summit materials whether glacially or periglacially. The distribution of summit-sourced materials along former glacial flow lines suggest that Quaternary glaciations, possibly including the LGM, remobilised sub-aerially weathered materials from summit plateaux probably through enhanced basal deformation and entrainment as blocks that show little indication of glacial rounding or fracture.

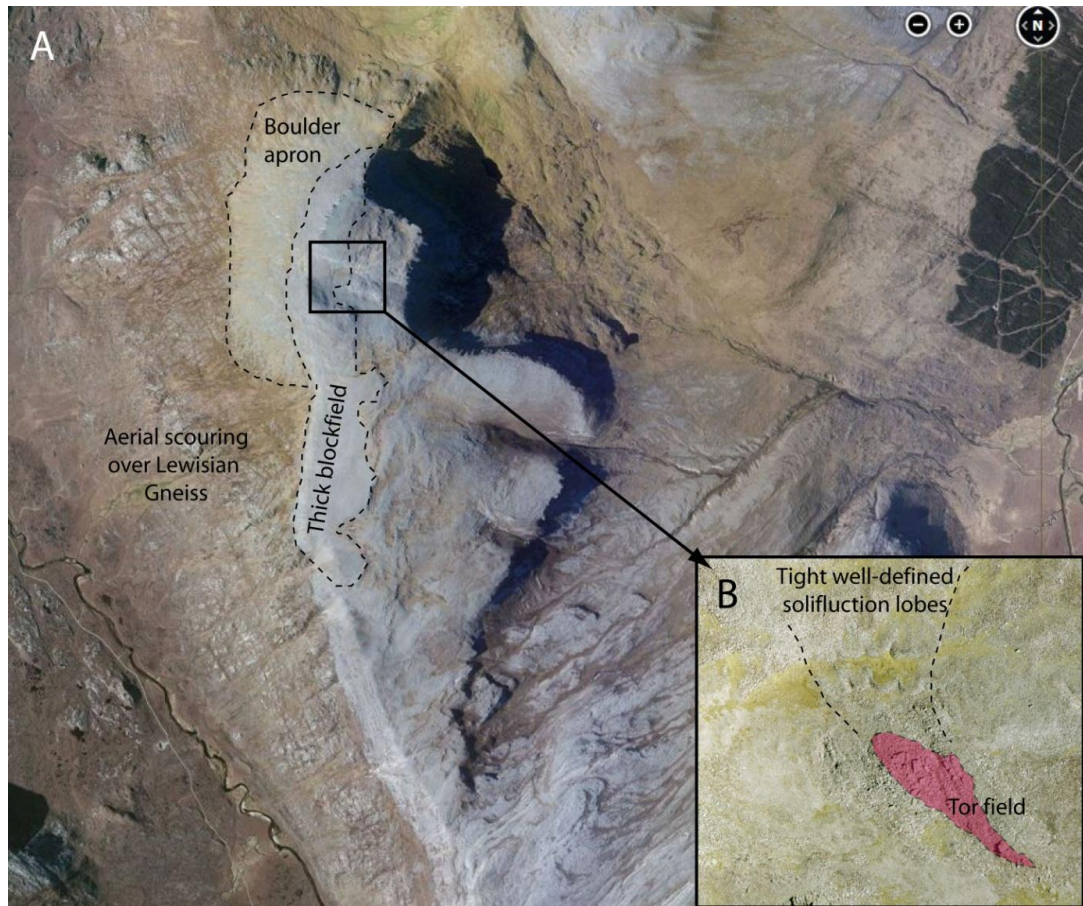


Figure 5.9: Glacial modification of pre-glacial surfaces, Cranstackie. A - Remobilisation of regolith on Cranstackie: apron of boulders glacially transported west onto Lewisian bedrock at lower elevation. Box indicates location of zoom-in (B). B - Detail of regolith features around Cranstackie tor. Tor field (shaded) with thicker blockfield with well-defined solifluction lobes in pressure shadow formed under NNW flow. Aerial images: Bing maps.

Widespread slab mobilisation from summit plateaux suggest not all glacial modification is attributed to the LGM, but possibly also to a previous more extensive glacial stages under which enhanced basal deformation may have been more active at high elevation. Suppositions from the Cairngorms are similar (Hall *et al.*, 2012). Recent thinking proposes that tors and blockfield evolve via a two stage process (Ballantyne, 2010b). Initial deep weathering processes require long-term subaerial exposure, followed by later stripping of saprolite to reveal residual monoliths, corestones and bedrock pavement - the original weathering front (Figure 5.10). This later stage requires a dominant erosion process. These prerequisite conditions enforce certain boundary controls on tor formation, therefore providing

important constraint on landscape and environmental history where tors are found.

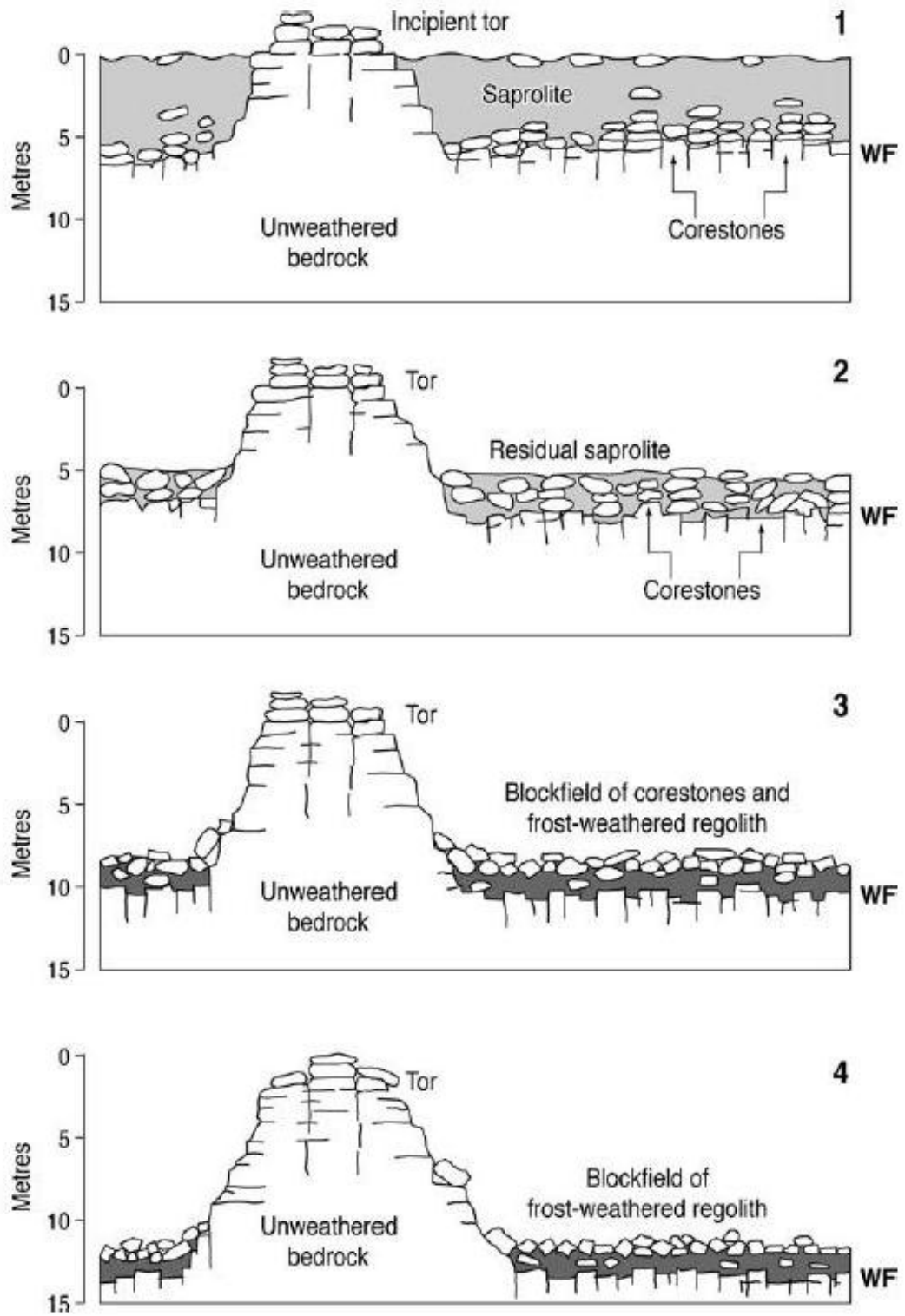


Figure 5.10: Model of tor emergence and autochthonous blockfield evolution, after Ballantyne (2010). WF = Weathering front.

In NW Scotland the lithological variation on mountain summits leads to a dichotomy in characteristics, with enhanced granular disaggregation noticeable in Torridon Sandstone and frost-shattering more prevalent in Quartzite lithologies. Consequently post-glacial and Holocene sediments and weathering products (regolith) may obscure the effects of glacial erosion and/or preservation - for example the aeolian deposits of An Teallach (Ballantyne and Whittington, 1987) and Ben Mor Coigach. More detailed fieldwork would be required to provide sufficient information for a full blockfield comparison and assessment.

Most summit plateaux in NW Scotland display evidence of four evolutionary stages similar to those suggested by Ballantyne (2010) (Figure 5.10). Some remnants of Neogene deep weathering remain, manifest in corestones and residual saprolite which occur in combination with Pleistocene products of frost-shattering in variable quantities dependent on lithological susceptibility. The Stage 4 scenario is particularly prevalent in the frost-susceptible close-jointed Basal Quartzite capped summits of the Assynt plateaux (e.g. Glas Bheinn and Beinn Uidhe). However, a more common occurrence, especially where lithological texture is granular rather than crystalline (i.e. Piperock Member Quartzite and Applecross Member Torridon Sandstone) is an extensive zone of predominantly corestones and bedrock pavement with regolith stripped back to the weathering front.

This situation is observed on the flanks of Speceinn Còinnich (Figure 3.38), portions of Breabeg's summit (Figure 3.33) and on sub-summit slopes of Cranstackie (Figure 3.16) conditions enforce certain boundary controls on tor formation therefore providing constraint on landscape and environmental history where tors are found.

When observed on quartzite, the exposed bedrock pavement preserves distinct features of deep weathering manifest as small-scale erosional overhangs, deep joint weathering and surface runnels (Figure 5.11). In these locations, it appears that glacial, and possibly post-glacial, erosion has been extremely effective in stripping loose saprolite; but periglacial processes have not generated significant regolith since. Limited evidence of periglacial activity is seen in this region with vegetated

nivation flushes occurring between patches of exposed bedrock, however there is little evidence of frost-shattered material.



Figure 5.11: Evidence of deep subaerial weathering of quartzite, Cranstackie. Land surface displaying evidence of deep weathering (corestone exposure indicated by white arrows), subsequent saprolite clearance (exposed bedrock pavement) and deposition of erratics (Basal Quartzite block circled in background). Figure at right for scale.

Fieldwork observations reveal that across the eastern Assynt plateaux (Glas Bheinn - Beinn. Uidhe - Beinn An Fhurain - Conival - Breabeg) the lower limit of subaerial weathering features occurs at c. 600 m a.s.l. The presence of patchy blockfield below this limit is however noted on the southern flank of Creag Liath (Breabeg) suggesting localised variation in subglacial thermal conditions. Krabbendam & Bradwell (pers. comm.) also note the presence of grüs (or clayey regolith) >0.5 m thick, with striae and ice-scoured bedrock on the summits of Conival (>900 m a.s.l.) and Creag Liath (~800 m a.s.l.). The summit of Creag Liath also bears erratic boulders. Further NW, McCarroll et al (1995) recorded the ‘problematic’ occurrence of gibbsite on Ghlas Bheinn at 710 m a.s.l, within the local

'trimline' range (700-730 m a.s.l) and at summit level (521 m a.s.l) on Farmheall, north of Foinaven (above 'trimline' elevation of 470-480 m a.s.l).

These occurrences highlight the incomplete removal of pre-glacial weathering products, indicating limited glacial erosion of sediments at plateau level. This suggests that the presence of subglacial water was extremely limited and perhaps dispersed, amid blockfield so that fluvio-glacial erosion of soft sediments was not possible. Across most of the Assynt plateaux, the mapped subaerial weathering limit is located about 200 m lower than the 'trimline' elevation proposed by McCarroll *et al.* (1995). This suggests the likely existence of a zone (c. 600-800 m a.s.l.) in which glacial erosion has been limited but variable and highly dependent on local topography and subglacial hydrology.

TCN analyses on bedrock from the Beinn Uidhe plateau suggest that glacial erosion has been more effective over regolith than over exposed bedrock. By comparing the relative concentrations of ^{10}Be nuclides in bedrock surfaces with the same deglaciation history it is possible to examine the comparative erosion history from evidence of nuclide inheritance. With the highest TCN concentrations, apparent minimum ages from Breabeg (mean ca. 103 ka BP) reflect the lowest level of glacial erosion on the Assynt plateaux, and provide an erosional baseline. Apparent exposure ages between this baseline of ca. 103 ka BP and the plateaux deglaciation age of ca. 16 ka BP provide a relative measure of erosional efficacy; the younger the age (lower TCN concentration), the greater the depth of erosion during GS-2.

Variation in TCN concentration is seen across the Beinn Uidhe plateau where a lower TCN concentration was obtained from bedrock sampled amongst regolith at BU03 (ca. 54.7 ka BP), compared to that of the marginally higher glacially abraded surface of BU04 (ca. 86.4 ka BP). Assuming that Breabeg represents a surface with zero postglacial erosion, the lower TCN concentration detected in bedrock on Beinn Uidhe indicates a greater depth of rock removal by glacial erosion over these surfaces.

Following Lal (1991), differences in bedrock TCN concentrations can be used to estimate the depth of rock removed (glacial erosion) across the plateaux:

$$N_z = N_0 e^{-z\rho/\Lambda}, \quad (2)$$

Where N_z is the TCN concentration at depth z , N_0 is the TCN concentration at the surface, ρ is the density of the overlying material, taken to be 2.7 g cm^{-3} for quartzite, and Λ is a cosmic ray attenuation length of 160 g cm^{-2} . Consequently, varying TCN concentrations may indicate that the present bedrock surfaces are derived from different depths in the pre-glacial surface; in short, that glacial erosion varied across that surface. The additional rock removal (Equation 2) in relation to the Breabeg baseline equates to ca. 16 cm at BU04 (exposed bedrock) and ca. 41 cm at BU03 (blockfield) during the last glacial stage. This evidence suggests that blockfield has been more susceptible to glacial erosion than exposed bedrock, with removal of blocks achieved through enhanced basal deformation or plucking. This is in accordance with recent thinking on blockfield evolution (Ballantyne, 2010b). The forces transmitted by overriding cold ice would be more easily taken up by dislocation of a frozen-on block, than by plucking or abrasion of in-situ bedrock.

The transition of ice from warm- to cold-based regimes across the plateau might be anticipated to incorporate basal material by regelation as suggested by Sugden (1978) (Figure 5.12) or enhanced basal deformation forced by the roughness of the blockfield surface.

The fact that tors and blockfields have been glacially modified at high elevation across NW Scotland, supplemented by the occurrence of high level erratics with post-LGM exposure ages, allows minimum constraints for palaeo-ice sheet surface elevations. Where this evidence exists, ice thicknesses $> 70 \text{ m}$ can be postulated - the minimum required for enhanced basal deformation. Where glacial abrasion occurs at summit level, such as Beinn Uidhe, thicker ice is indicated in order to generate basal melting.

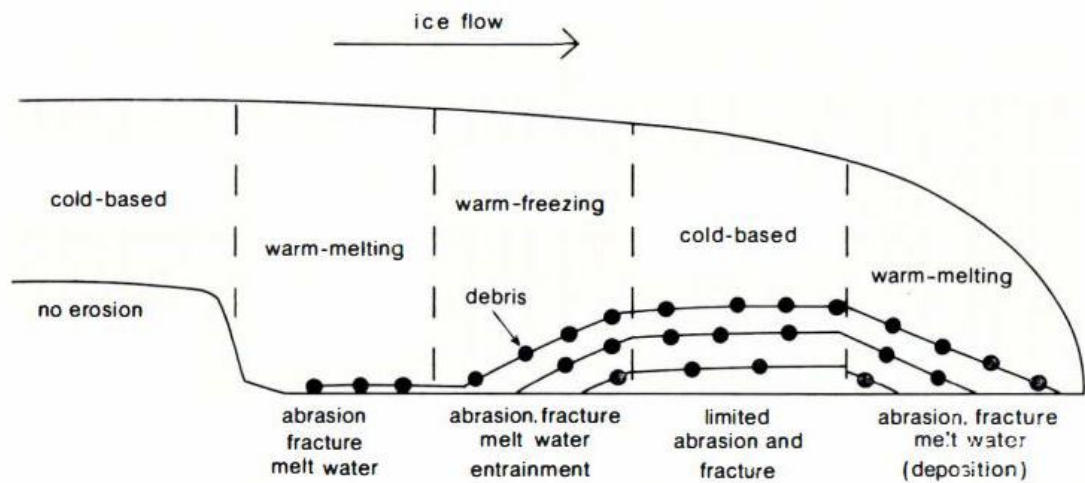


Figure 5.12: Debris entrainment in relation to subglacial basal thermal regime changes (Sugden; 1978).

As there is potential to measure, at least relatively, the removal of unconsolidated surface material by ice movement over blockfields, it may be that, where no TCN data exists, the nature of the blockfields can inform on style and magnitude of glacial erosion. This could be done by comparing the degree to which saprolite and associated regolith has been stripped and replaced by periglacial regolith (Figure 5.10). Regolith lowering over the duration of Quaternary has been estimated as c. 10-35 m (Hall and Phillips, 2006). A loss of 10 m depth of regolith would easily account for tor emergence on Cranstackie and for the thinning and mobilisation of summit blockfield required to expose the weathering front.

The discovery of quantitative evidence of erosional boundaries is supporting in the geomorphic record by identification of erosional scarps - rip-offs (Results: 3.7.1) and, in some locations by associated boulder deposits. The consistent characteristics of these features across the field area suggest that they may relate to genetically similar formation conditions and processes i.e. they represent thermal transitions and, in some cases, shear margins positions (Figure 5.13). Shear margins are locations where abrupt boundaries were present between ice with distinctly different properties, a contrast seen between faster-flowing, warm-based ice and sluggish col-based ice (Benn and Evans, 2010).

It appears that rip-offs often, but not exclusively, exploit geological weaknesses or contrasts. For example, the rip-off on the western flank of

Breabeg is situated in quartzite up-ice of a geological transition to dolomite/limestone dominated area where hydrological conditions at the bed may have been different. All three of the Assynt rip-offs occur in areas of complex stacked, folded and intruded quartzites. It may be that plucking of the bedrock, which is anticipated to have been the dominant process of rock removal, may have been particularly effective here due to the jointing and brittle fracture characteristics of the Basal Quartzite.

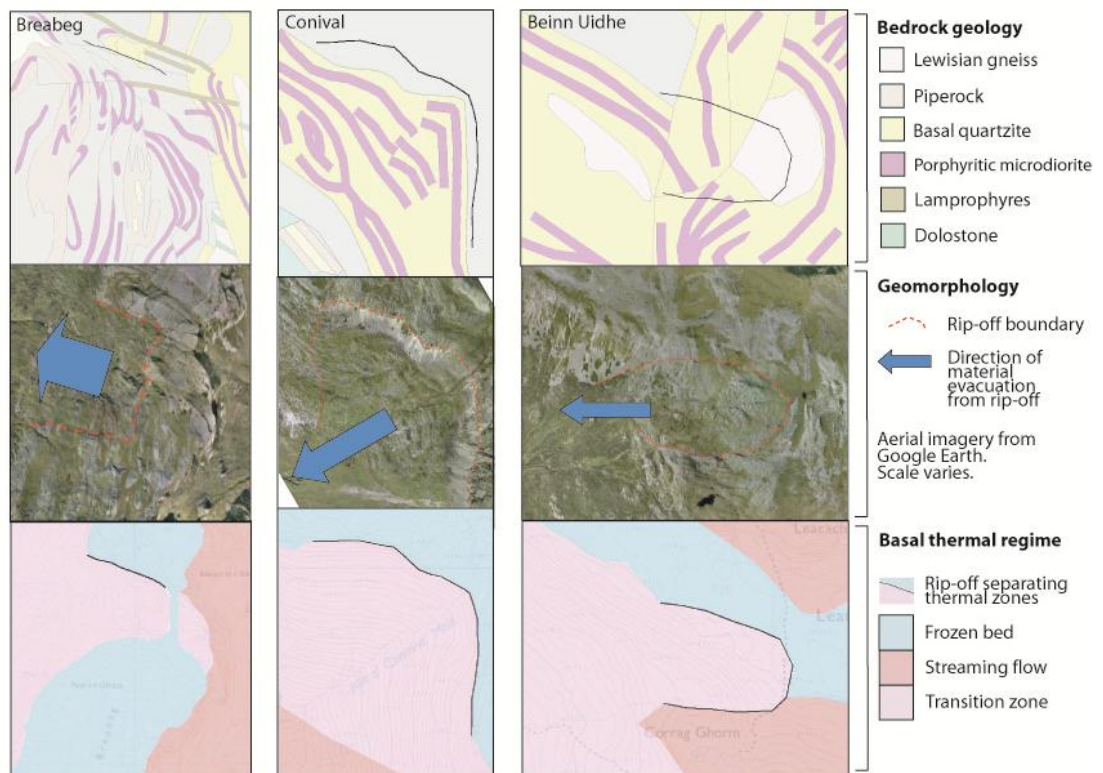


Figure 5.13: Rip-offs of the Assynt Mountains. Geological units, geomorphology and proposed relation to thermal transitions indicated.

The quartzite-topped ridge comprising the western flank of the Loch Eriboll trough displays clear geomorphic evidence of large-scale glacial erosion in the form of rip-off scars (Figure 5.14). The association of these features with the underlying geology provides a rare opportunity to constrain the depth of glacial erosion. There is currently no chronological constraint on the surface age of these features, and consequently whether they represent a cumulative erosional feature formed over successive glaciations is not known.

Table 5.2: Summary of blockfield features of selected mountains in NW Scotland

Mountain (elevation a.s.l.)	Litho. ^d	Fines at/nr surface	Clay minerals above weathering limit ^a	Core- stones	Rock pavement w. front exposed	Granular Disagg.	Periglacial blockfield	Blockfield description
Cranstackie (801 m)	CQ	X vegetated	Not available	X	X	X	X	Degraded solifluction lobes. Saprolite stripped
Beinn Uidhe (740 m)	CQ	X vegetated	Not available	X	X	X	X	Largely periglacial material
Breabeg (815 m)	CQ	X vegetated	Not available	X	X	X	X	Large 'tor slabs glacially transported West
Speceinn Còinnich (717 m)	TS	X vegetated	Not available	X	X	X	No too steep	Saprolite and corestones stripped
Sail Liath (956 m)	CQ	X vegetated	See An Teallach	X	X	X (below summit)	X	Periglacial products dominate summit
Beinn an Eòin (619 m)	TS	X vegetated	Not available	X	X	X Edge rounding	No	Saprolite stripped
Cul Mor (849 m)^b	TS	X	Q, K, I, G, L	X below summit	Not at summit	X	X	Possible remobilisation of tor blocks
Farmheall (521 m)^c	TS, CQ	X vegetated	Q,K,I	?	?	?	X	Not visited

Table 5.1 (continued): Summary of blockfield features of selected mountains in NW Scotland

Mountain (elevation a.s.l.)	Lithology ^d	Fines at/nr surface	Clay minerals above weathering limit ^a	Core- stones	Rock pavement/ weathering front exposed	Granular Disaggregation	Periglacial blockfield	Blockfield description
An Teallach (1062 m)	TS	X	Q, K, I, C, G	?	?	X	X	Patchy saprolite stripping
Beinn Spionnaidh (773 m)	CQ	?	Q,K,I,G	?	?	?	?	Not visited
Arkle (787 m)	CQ	?	Q,K,I,G	?	?	?	X	Not visited
Canisp (846 m)	CQ	?	Q,K,I,G	?	?	?	?	Not visited
Glas Bheinn (776 m)	CQ	No	Q,K,I,G	No	No	No	X	Periglacial blockfield dominates
Cul Beag (769 m)	TS	X	Not available	X	X	X	No	Widespread GD
Ben Mor Coigach (743 m)	TS	X	Not available	X Flags?	X occasionally	X c. 3 cm	No	Widespread GD

^a Clay mineral data from McCarroll et al. (1995). Some geomorphic data derived from widely available web-accessed remote sensing imagery and public image databases.).^d Lithological abbreviations: CQ - Cambrian Quartzite, LG - Lewisian Gneiss, PR - Piperock, TS - Torridon Sandstone. GD - Granular disaggregation.

On the Cranstackie-Beinn Spionnaidh ridge, the Cambrian Quartzite outcrops at the apex of the ridge and forms its eastern slope. The ridge (c. 9 km in length) descends gently to the north east, lowering from 801 m at the summit of Cranstackie, to 383 m at Beinn Ceannabeinne before dropping off sharply at the coast. Topographic breaches are notable in the saddles between Cranstackie and Beinn Spionnaidh, Meall Meadhonach and Beinn Ceannabeinne with several incisions of the watershed between (Figure 5.14). These locations correspond to sites of rip-off scarps, some, to the north, modified by later wet-based glacial erosion.

Rip-offs are here considered to be similar features to the transverse lee-side scarps described by Clärhall and Kleman (1999). The features initiate because of the presence of a thermal boundary at or beyond the lee of an obstacle in combination with lowered effective pressure in a lee-side declivity. Material is removed by brittle fracture or plucking with the thermally transitional nature of the site allowing the process of regelation to occur.

In the Cranstackie ridge situation, it may be proposed that the acceleration of ice into the Strath Dionard corridor and accentuated by the downdraw into the Minch from the nearby ice stream onset zone would exert a tensile stress on ice towards the crest of the ridge. Here, where ice thinned as it encountered the obstacle of high ground a thermal transition would be in place between colder higher tops and warming, thickening ice on the lee side of the ridge. This transition zone would act as a weakness where ice was reacting differentially to stresses and shearing internally to accommodate strain. The rip-off sites are proposed as areas, potentially of geological weakness, where strain was accommodated through failure of the rock structure beneath a thermal transition allowing material to be removed from the ridge crest.

It may be envisioned that as ice thickened in the area through the Devensian, the englacial thermal boundary separating thawed bed conditions below from frozen bed conditions at higher bed elevations moved upward as increased overburden increased the amount of ice above the pressure melting point. It is therefore possible that the suite of rip-off features may represent a time series working up the ridge from most

mature features towards the coast and youngest in the vicinity of Cranstackie.

The ridge sits unconformably on the Lewisian gneiss complex and stratigraphically below the Sole Thrust; consequently it has a simple planar succession with no repetition, thrusting or deformation of the sequence. In this area the Basal Quartzite outcrops with a maximum thickness of c. 100 m, and the overlying Piperock c. 50 m thickness. Anticipating that the whole eastern flank of the Eriboll basin was previously capped by this sequence it is possible to make tentative estimates of glacial erosion depth by observing the thickness of residual quartzite overlying the Lewisian orthogneiss basement.

Figure 5.15 illustrates how the quartzite cover has been punctuated by erosional 'windows' up to 200 m deep such as the topographic basin of the Coire na Cùile, directly below (to the east of) Cranstackie's summit (Folio 3). Comparison with the location of 'rip-off' features indicates that areas of deeper glacial erosion are associated with thermal transitions, evidenced by the prevalence of large scale plucking features (Results: 3.7.1). The linear watershed ridge, topped by Piperock, has been breached in several locations. Erosion is deepest where orthogneiss appears at the surface as the two overlying quartzite members have been removed. In some areas this appears to be equivalent to c. 150 m of rock erosion.

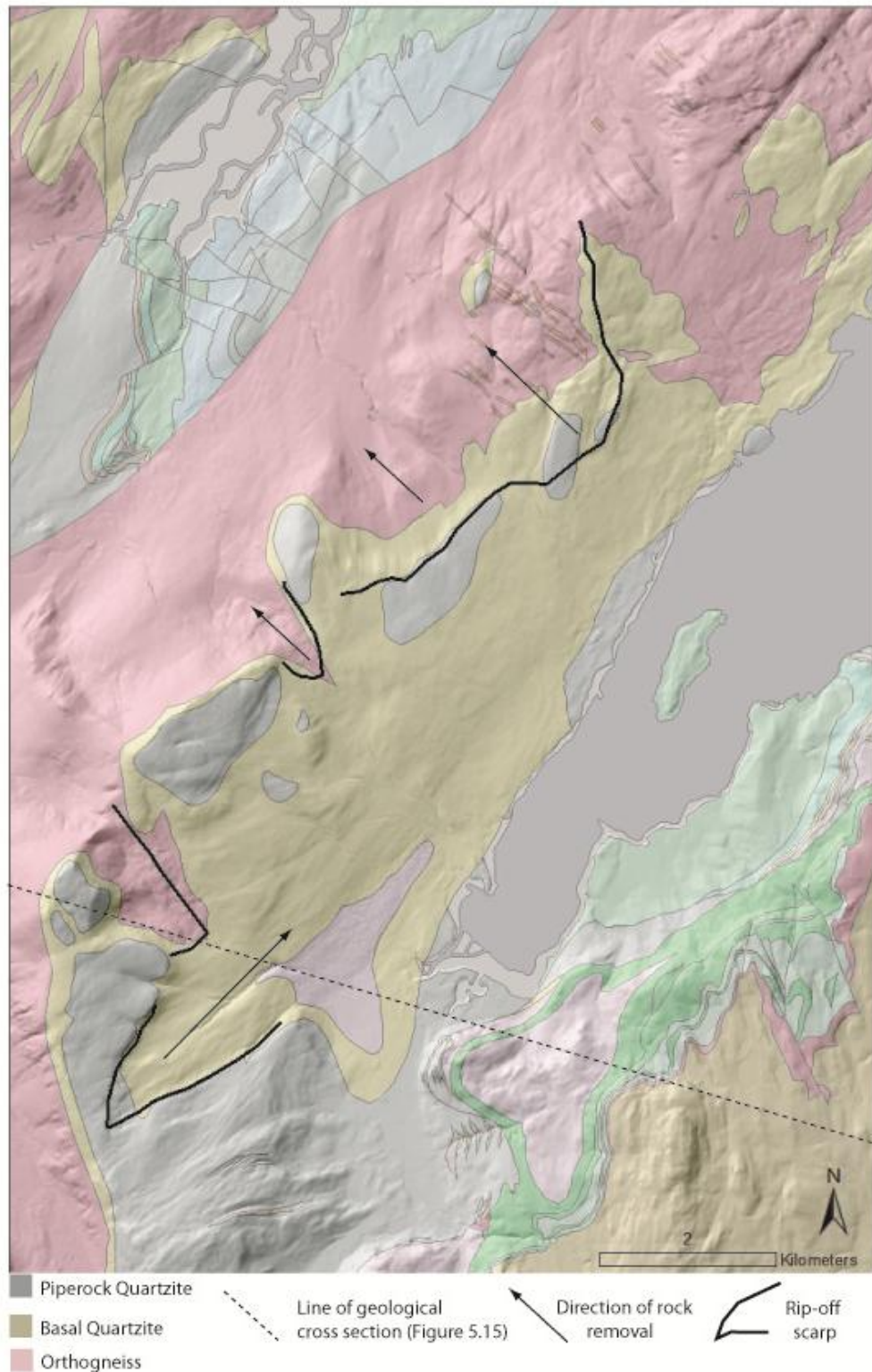


Figure 5.14: Association of cold- to warm-based thermal transitions manifest in 'rip-offs' with deeper glacial erosion, W. Loch Eriboll area. The regular watershed ridge (topped by Piperock) has been breached in several locations. Erosion is deepest where orthogneiss appears at the surface as the two quartzite members have been removed above it. In some areas this is equivalent to c. 150 m of rock removed.

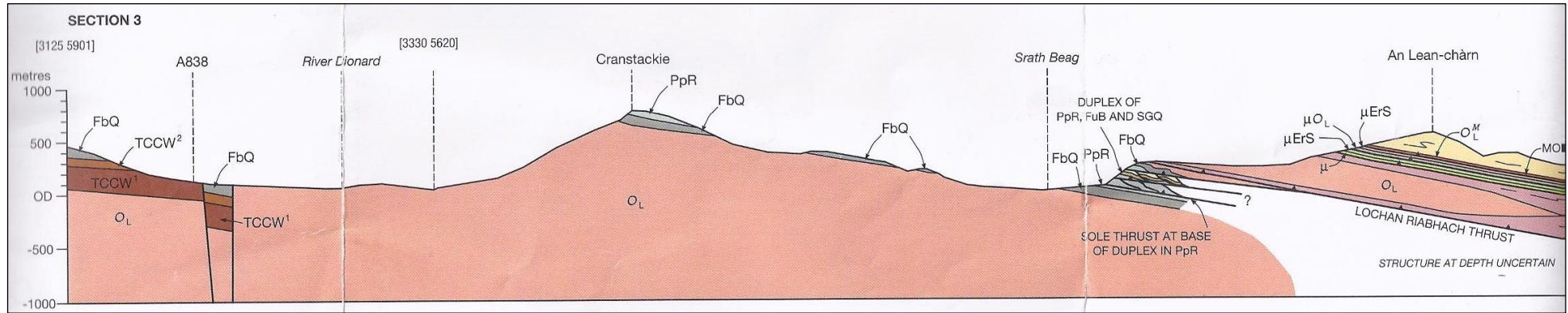


Figure 5.15: Geological cross section illustrating depth of glacial erosion, western flank of Loch Eriboll. Modified from Section line 3 (shown on Figure 5.13), British Geological Survey, 2002 © BGS/NERC. Loch Eriboll.

5.2.2. Low level surfaces

Recognition of ice stream onset conditions in well-defined corridors (Figure 1.7) and the Ullapool area (Bradwell *et al.*, 2008b)) has indicated the presence of lateral zonation into zones of differing erosional intensity. Vertical thermal zonation under ice sheets has been recorded in many areas where cold-based deglaciation preserved evidence of thermal zonation during main stage conditions (Angelis and Kleman, 2008, Kleman and Glasser, 2007, Briner *et al.*, 2003, Hall and Glasser, 2003, Kleman *et al.*, 1999b, Gellatly *et al.*, 1988). However, lateral thermal zonation has been more rarely preserved at low elevation sites due to the often high levels of subglacial erosion experienced during deglaciation with widespread warming of the ice-bed interface (Bradwell, 2013).

Interestingly, preservation of weathering fronts appears to occur in some low elevation locations in NW Scotland. The former presence of a lateral shear margin in the Oldshoremore-Sheigra area with cold-based ice sheet conditions to its north east side, has been suggested earlier (Discussion - Margins: 4.2.2) from the unusual boulder concentration and from nuclide inheritance in bedrock surfaces at Sheigra. In this context, selective and only limited (small scale) glacial modification on a small scale of largely inherited bedrock forms seems plausible. Unlike other low level areas such as Rispond and at Druim na h-Uamha Móire c. 290 m a.s.l. beneath Quinag (D. Fabel pers. comm.) where >3 m of subglacial erosion can be demonstrated, the smaller number of p-forms at Sheigra and the smaller scale relief of bedforms supports the ideas of less glacial modification.

The idea that glacial erosion is dominated by plucking at Sheigra and Oldshoremore is supported by the relatively high density of meltwater channels, and by the dominance of stoss-lee forms at least in the S of the area. Just ~5 km NW of Bradwell's (2013) rectangular study area, the Sheigra outcrops show some similarities to his Zone 3 landform classification, where subglacial cavities and hence plucking may have been more common. Nuclide inheritance detected in a sub-horizontal bedrock surface at Sheigra may support the idea that glacial plucking (block

removal) rather than abrasion has been the main form of glacial modification of bedrock surfaces at Sheigra. Evidence, for example, from S. Victoria Land, Antarctica suggests that some surface abrasion markings may be formed by the passage of clasts held in cold-based ice, and therefore need not represent significant basal melting and subglacial abrasion (Atkins, 2013).

It has been suggested that frozen bed conditions were much more widespread, even at low level, than previously anticipated. Working in eastern Scotland several authors (Hall and Mellor, 1988, Hall and Sugden, 1987), noted that deep weathering profiles were sometimes preserved at low level sites despite a known ice-cover. In these locations, palaeo-surface preservation could be attributed to cold-based ice or protection from erosive or streaming ice. It is possible, that the seaboard of NW Scotland used to have a thick saprolite cover, some of which remains on high ground as blockfield, grös or kaolinite in which clay minerals can be detected (McCarroll *et al.* 1995). On ground below c. 500 m this material has been removed, to leave a largely bedrock landscape, which in many locations may represent a surface almost equivalent to the weathering front.

The origin of the mammilated forms (Mather and Ritchie, 1977) of the low elevation Lewisian gneissose rocks of NW Scotland's western seaboard, widely described as knock-and-lochan or 'areal scoured' (Linton, 1963, Sugden and John, 1976, Haynes, 1977, Gordon, 1981, Rea and Evans, 1996), may be questioned in the context of long-term landscape evolution. It has been suggested that caution be employed when examining mammilated bedrock forms, as the assumption of high level of subglacial erosion may be too casually applied. Patterson, working in Minnesota, suggested that the undulating bedrock terrain observed did not require deep subglacial erosion to explain the geomorphology of closed depressions, bedrock knolls and well-rounded boulders. Instead they suggest that these forms on Precambrian crystalline bedrock forms result from deep chemical weathering (average depth of 30 m) with an irregular weathering front. Therefore the possibility arises that the relief of the knock and lochan landscape of the western seaboard is largely composed of a pre-glacial

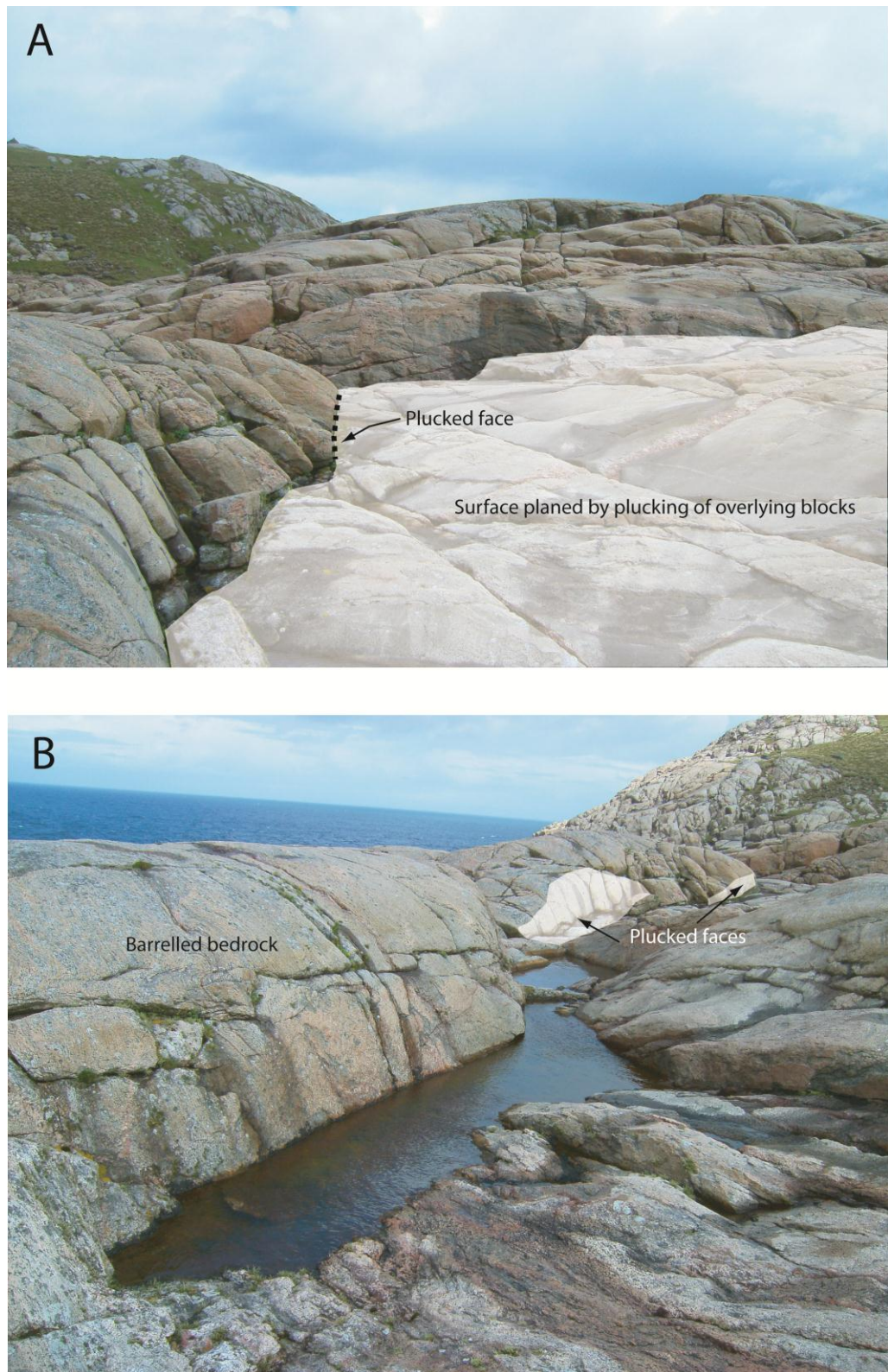


Figure 5.16: Gneiss bedrock morphology, Sheigra. A - Contrast between glacially 'cleared' surface and weathering front morphology. Ice flow right to left. B - Plucked faces modify the macro-geomorphology of the sub-aerially weathered topography. Ice flow towards the sea.

weathering front only slightly modified by glacial erosion. Bedrock forms at Sheigra (Figure 5.16) provide a good example of this and are contextualised by TCN data.

Within the knock and lochan landscape, variation in the density of rock basins is revealing in terms of glacial erosion and modification. Sugden (1978) found employment of this technique extremely useful in land-system and erosional zone designation on Somerset Island, Arctic Canada. Sugden's findings support the proposition that even some relatively low-lying areas can escape significant glacial erosion - as suggested here for Cape Wrath and the Sheigra-Oldshoremore areas in NW Scotland. Examples of contrasting lochan density on the western seaboard of NW Scotland (Figure 5.17) serve to demonstrate potential stripping of regolith and hence possibly glacial erosion efficacy.



Figure 5.17: Comparison of land surface characteristics - lochan density in NW. A - Cape Wrath. B - Laxford area. High density of bedrock basins many of which are structurally-controlled. Contrast seen to the NW where Bradwell indicates a thermal transition zone to frozen bed conditions (see also Folio 4 and Figure 4.5). Aerial images: Bing maps.

5.3. Thermal transitions & flow organisation

During the phase of maximum extent of the last ice sheet (GS-2) c. 20 ka BP (Hubbard *et al.*, 2009) the ice centre lay east of the modern watershed, perhaps as far east as the Cairngorms in NE Scotland. This positioning, combined with the influence of the Minch palaeo-ice stream, forced ice to be drawn across the NW from sources to the east (Lawson, 1990). Under this scenario, the high ground of Assynt, Sutherland and Wester Ross sat transverse, and obstructive, to ice-sheet flow. The pattern of geomorphic feature zones observed on the mountains in NW Scotland is very likely to be the product of vertical thermal zonation disrupted by local flow effects around topographic highs (Benn and Evans, 2010, Rea *et al.*, 2000). Geomorphic evidence of local thermal boundary disruptions, pressure shadow effects and variation in erratic transport, give information about the interaction of fast flowing ice with these topographic obstacles.

5.3.1. Vertical thermal zonation

Mountains across the study area provides 'dipstick' localities at which to observe the vertical thermal zonation present within the last ice sheet. This picture is cumulative rather than being a deglacial time slice, as in many places cold-based conditions during deglaciation have preserved the boundaries between thermal zones. Figure 5.18 summarises the geomorphic and exposure history evidence supporting assignment of vertical zonation of thermo-mechanical properties within the ice sheet. The exact elevation of the thermal boundaries can be seen to vary between different regions and in some areas some zones are completely absent. It is suggested that these variations are a product of two main factors: 1) lithology and 2) location in relation to the ice divide and main ice stream onset zones. Four zones are recognised each with different erosional and depositional characteristics.

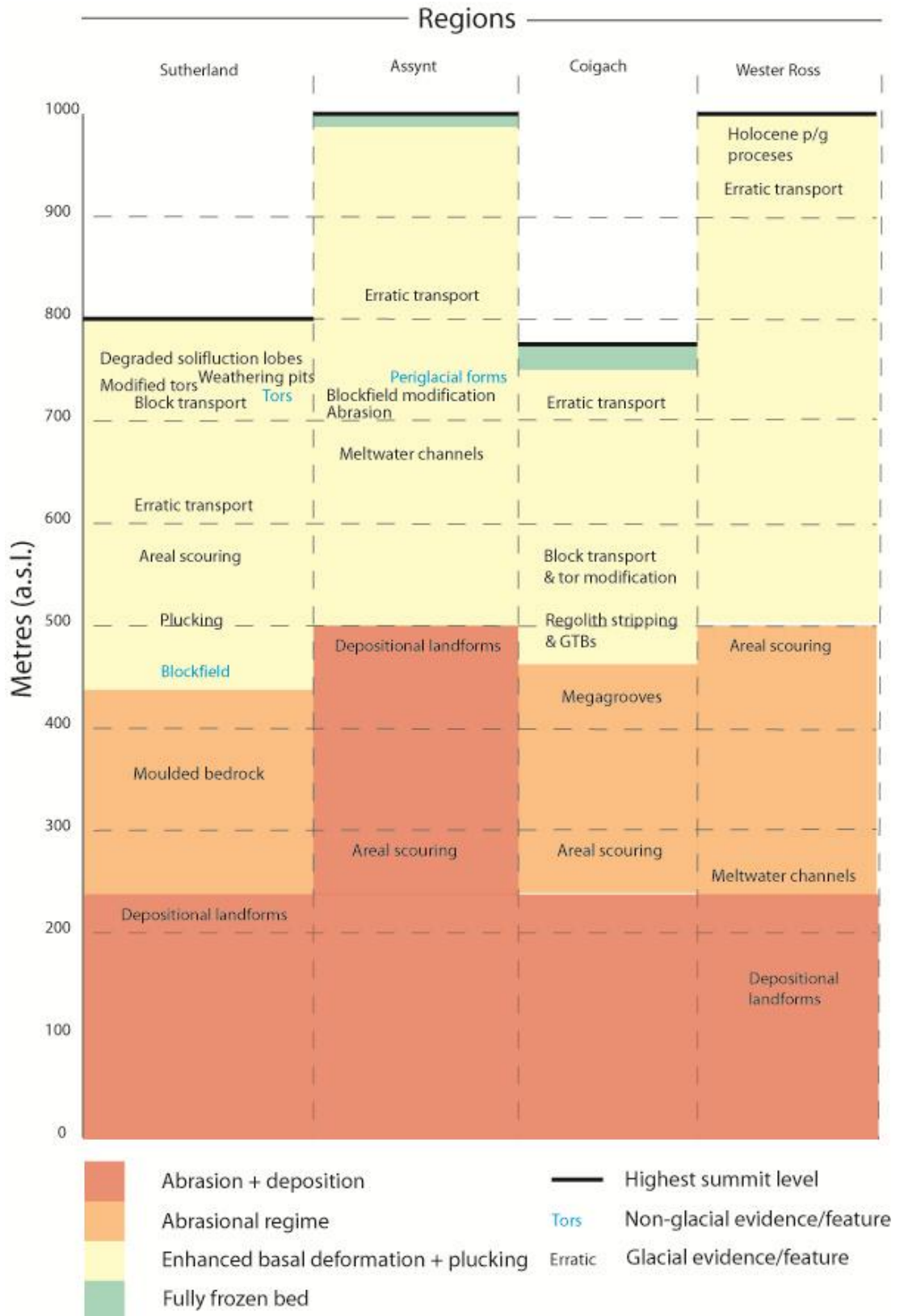


Figure 5.18: Comparison of regional thermal zones and supporting geomorphic evidence.

The boundary between the zones may be gradational, or more often, as in the case of the Zone 1-2 boundary, marked by a patchy archipelago type boundary (Figure 5.19) or sharp linear boundary in the form of a ‘rip-off’ scarp (Figure).

Table 5.3: Summary of vertical thermal zonation in NW Scotland (from evidence in Figure 5.18)

Zone	Elevation range (m a.s.l.)	Basal thermal regime	Glacial erosion	Glacial deposition
1	>730	Predominantly cold-based	Very limited	Erratics
2	c. 730-600	Cold-warm thawing transition	<ul style="list-style-type: none"> - Blockfield and tor modification - Enhanced basal deformation 	Erratics
3	c. 400-600	Patchy cold- and warm-based	<ul style="list-style-type: none"> - Tor and bedrock modification - Plucking dominated - Clearance of pre-glacial cover 	<ul style="list-style-type: none"> - Till and fluvioglacial sediment - Erratics
4	<400	Largely warm-based	<ul style="list-style-type: none"> - Abrasion dominated - Moulding and cavity-related bedforms 	<ul style="list-style-type: none"> - Deglacial landforms - Till preservation in protected locations including till tails

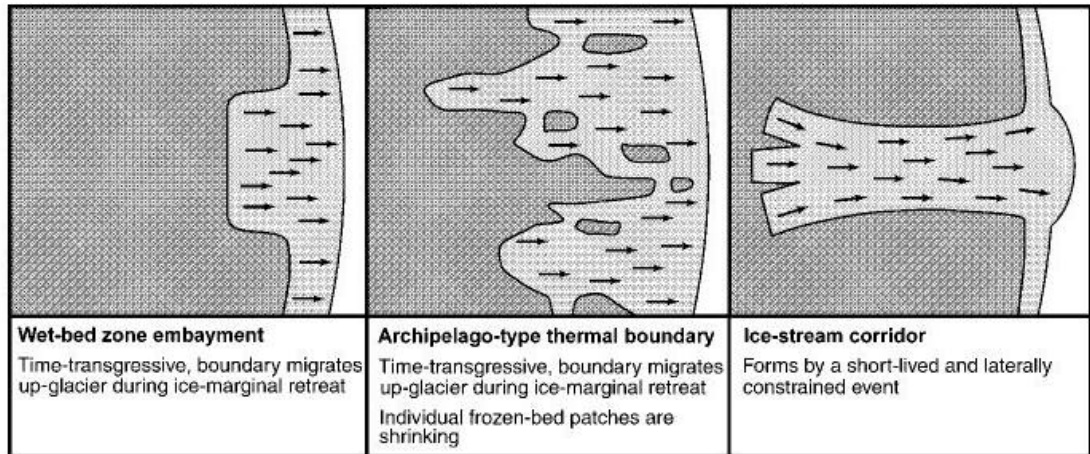


Figure 5.19: Frozen/thawed boundary types (Kleman *et al.*, 1999b). Dark grey shows frozen bed areas and light grey shows wet-bed areas.

The clarity of this thermal zonation is greatest in the vicinity of the Assynt Mountains where TCN data further constrains erosional discontinuities related to thermal regime. Figure 5.20 shows the strong topographic deflection of the vertical zonation exerted by a mountain massif. The zonation is similar to that predicted by Bradwell (2013) (Figure 5.21) in the Laxford onset zone. The trimline elevations for NW Scotland (McCarroll *et al.*, 1995b) fit reasonably comfortably with the location of the Zone 1-2 boundary reinforcing the now popular reinterpretation of weathering limits as englacial thermal boundaries (Ballantyne, 2010a, Fabel *et al.*, 2012). On An Teallach, the identification (Ballantyne, 1999) of a 'trimline' at c. 700 m a.s.l accords well with the previously mentioned thermal transition.

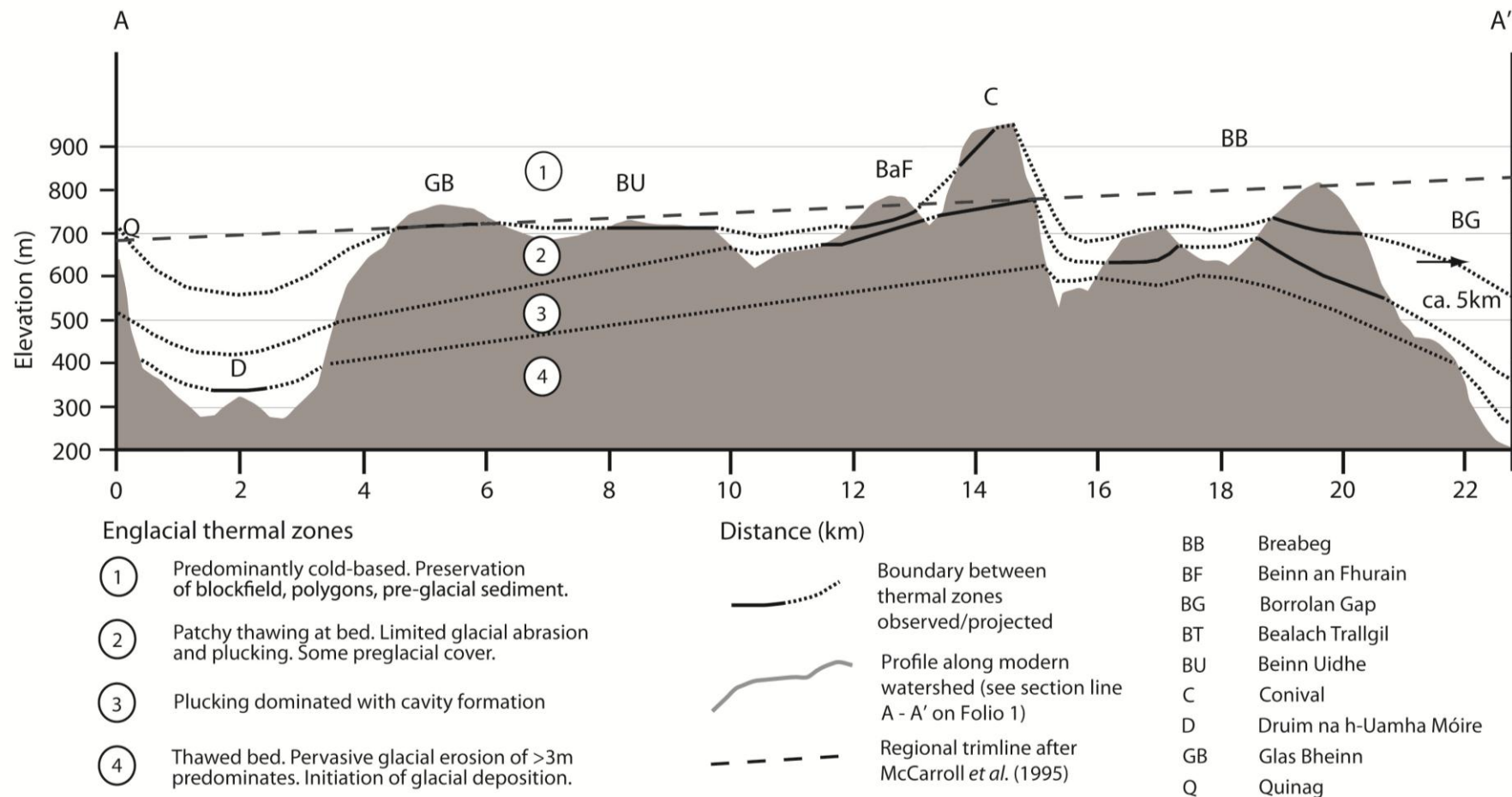


Figure 5.20: Thermal zonation in the vicinity of the eastern Assynt Mountains.

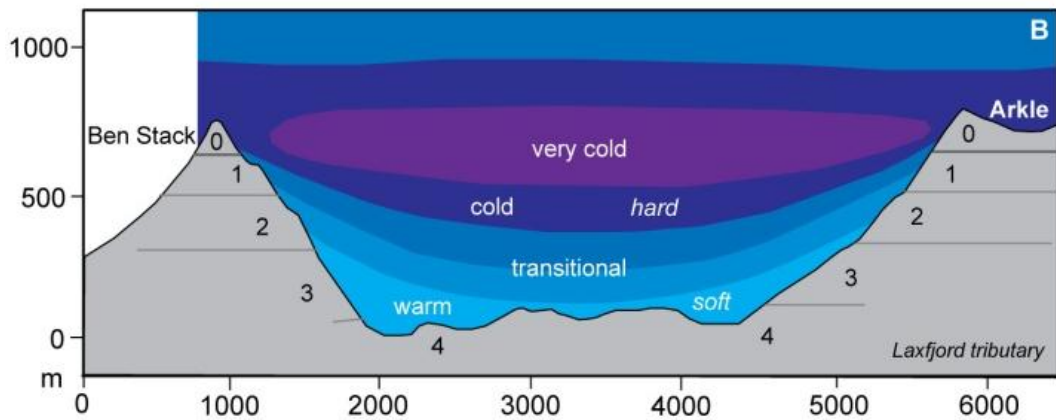


Figure 5.21: Thermal zones within Laxford ice-stream tributary. Bradwell (2013).

5.3.2. Flow disruption & organisation

Standing parallel or oblique to ice-sheet flow, the inselbergs of western Assynt and Inverpolly display geomorphic evidence of local excursions from the regional thermal zonation (Folio 4). In some locations steeper thermal boundaries manifest as substantial preservation zones can be associated with pressure shadow effects. This is in contrast to McCarroll *et al.*'s (1995) observations of 'trimlines', where the authors suggest that there is a regular decline in mapped weathering limits from east to west, which they interpret as proving the absence of pressure shadow effects. On Stac Pollaidh, Bradwell and Krabbendam (2003) recognised a weathering contrast at 480-520 m a.s.l sloping westward. This steeper slope (about 5 m/100 m) is in contrast to the ice surface projected by McCarroll *et al.* (1995) (about 1 m/100 m).

Asymmetry in Stac Pollaidh's N-S profile is also informative regarding differential glacial erosion of the mountain's flanks. The southern flank of the hill shows a smooth concave profile while the N side exhibits irregular convexities. Dominance of an abrasional subglacial regime against the south flank is proposed to result from frictional heating due to flow focussing through the Loch Lurgainn trough. Similar effects have been noted from Ice Stream C, West Antarctica, where the highest readings of basal friction occur where ice diverges around a large (400 km²) bedrock 'island' (Price *et al.*, 2001). Scouring around the base of Stac Pollaidh's S flank supports this,

while to the north, divergence of flow away from the trough may have favoured formation of cavities and consequently plucking in a lower pressure subglacial environment.

Further evidence of local thermal and flow irregularities are seen around the large mountain massif of Ben Mor Coigach (BMC). Here a lateral thermal boundary, possibly a sliding boundary, can be observed on the southern flank of BMC above Achiltibuie (Figure 5.22). It is suggested that a change in present day fluvial valley morphology related to a thermal transition boundary, occurs where the boundary crosses the mouth of Coire Rèidh. Above and below this boundary the rivers return to a fluvial 'v'-shaped form suggesting that Coire Rèidh, down-ice of the main BMC ridge, displays preserved pre-glacial features due to the existence of cold-based ice in this pressure shadow.

A contrast in basal ice properties is also suggested by the occurrence of high level erratics on the south east corner of Ben Mor Coigach (Figure 5.22) with the apparent absence on the western flank (recorded by early BGS survey). Interestingly, a north-south contrast in thermal boundaries is suggested by early BGS observations (Peach & Horne, 1892) noting the lack of glacial erosional or depositional features above 1500 ft. (457 m a.s.l). In contrast, glacial modification of a tor at c. 610 m a.s.l on the eastern plateau edge indicates a sharp transition to warm-based conditions at the plateau break similar to a boundary expected in a landscape of selective linear erosion (Hall & Glasser, 2003).

From this regional pattern, it may be suggested that Stone *et al.*'s (1998) study of An Teallach erratics, ~20 km to the S, can also provide information on the occurrence of cold-based ice sheet conditions in the pressure shadows of large topographic obstacles. Located down-ice and topographically lower (c. 600-870 m a.s.l.) than the main ridge (c. 800-1062 m a.s.l.) it may be anticipated that the highest ground would have experienced a pressure shadow effect. Four above-trimline samples display pre-LGM exposure ages and reduced $^{26}\text{Al}/^{10}\text{Be}$ ratios indicative of complex exposure histories with periods of burial. A further 'younger' erratic ($>22.6 \pm 2.4$ ka BP, standard CRONUS production rate) sampled 120-170 m above the other samples at 930 m a.s.l may represent a true deglaciation age

unbiased by pressure-shadow effects. It is proposed that lateral sliding boundaries and frozen bed patches are common across the wider field area (Folio 4), part of a thermal transition patchwork of landscape elements. It is suggested that this association of landscape elements is the product of ice sheet pressure and flow disruption effects related to topographic obstacles.

In Antarctica, 'sticky spots', as represented by frozen bed areas, are inferred to have existed in the transitional ice-sheet flow zone between crystalline bedrock and unconsolidated sediments, where flow acceleration leads to landform attenuation beneath West Antarctic palaeo-ice streams (Wellner *et al.*, 2001, Ó Cofaigh *et al.*, 2002, Ó Cofaigh *et al.*, 2005). In Scotland, with increasing evidence of the whole western sea board formerly hosting a number of ice stream onset zones (Bradwell *et al.*, 2008b, Bradwell *et al.*, 2007, Graham, 1990, Stoker *et al.*, 2006, Stoker and Bradwell, 2005) it may be that this transitional assemblage marks the initiation of ice-stream tributary flow.

Some of the most striking features of these assemblages observed are here termed 'till tails', though with a slightly different manifestation than those mapped by Dyke and Morris (1988) in Canada. Dyke and Morris' till tails relate to attenuation of sediment in a drumlin field at the onset of ice streaming, here the term is used to describe glacially-elongated sediment bodies in the lee of mountains. Ebert & Hattestrand's (2010) work on Swedish inselbergs recognised erosive features on the proximal and lateral parts of the hills, in combination with a bedrock-cored till tail as the signature of strong glacial erosion.

The till tail features bear similarities to flutes and to horned crag and tails with their pressure-shadow lee-side deposition and attenuation with glacial flow. The main distinguishing features of till tails were highlighted in Chapter 3. Feature on Ben Mor Coigach illustrate the (Figure 5.22) association of till tails with a lateral sliding boundary or shear margin. A linear ridge trends north west from the west end of BMC ridge interpreted here as sediment deposition at a lateral sliding boundary at a transition between cold-based ice in the pressure shadow of the mountain and faster flowing warm-based ice to the SW. A curvilinear scour is observed wrapping

round the SW corner of the mountain. An analogue for 'till tail' - scour pair formation may be given by the typical fluvial obstacle marks created in a laboratory flume (Figure 5.23) (Euler and Herget, 2012).

The proposed association of till tails with frozen bed spots, particularly around bedrock highs, draws strong associations with Jansson & Kleman's (1999) horned crag and tails. The form, geomorphic and glaciological context of the NW Scotland till tails, allows similar assumptions to be made about bedform deposition. Jansson & Kleman evoke a three stage process of horned crag and tail formation which is compared to till tail characteristics below (Table 5.2).

From comparison with Jansson and Kleman's (1999) work on horned crag and tails, till tails of NW Scotland may be a transitional form between horned crag and tails and regular crag and tails, thereby providing useful BTR information. A similar thermal history may be postulated for the regions where till tails occur, though the sediment infilling between horns perhaps suggests a longer duration of, or more extensive coverage by, warm-based ice conditions.

Further to examining their genesis, geomorphic analogues support ice-sheet basal thermal regime and ice flow inferences from the location, morphology and variation of till tails. Benn and Evans (2010) describe how close spacing of obstacles leads to concentration and acceleration of flow. This situation is encountered in the Inverpolly-Coigach area where multiple inselbergs occur in the path of a tributary feeder to the MPIS. Enhanced scour observed as broad erosional depressions around B. Ghoblaich and Stac Pollaidh, and as incision in the high density of loch basins, suggests flow is being focussed here. Spacing of obstacles also has implications for depositional regime and spatial distribution. In South Victoria Land, Antarctica, Atkins (2013) observed how material mobilised from a bedrock high by dry shear or brecciation, was plastered as a till patch on the stoss side of an obstacle in close vicinity.

Following Benn's (Benn, 1994) principles of flute formation, the elongation of the till tail features, i.e. great lateral continuity, suggests that the till had a lower strain rate and was deforming more readily than

the ice above it allowing the cavity (Figure 5.24) and sediment infill to propagate down-ice. Benn also reports that longer flutings record fast flow events with their elongation ratios potentially indicating duration of flow.

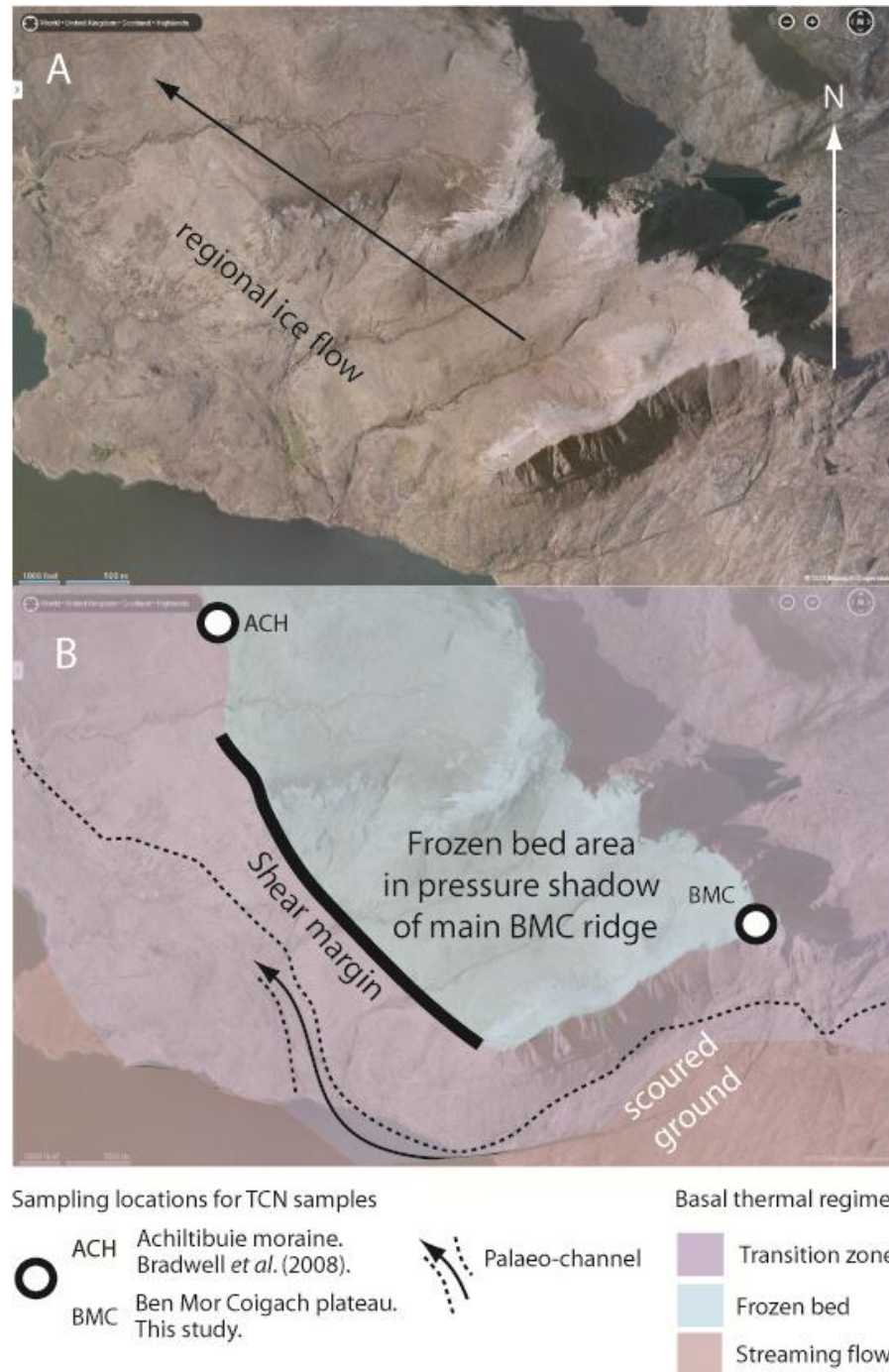


Figure 5.22: Geomorphic evidence for a shear margin on the south east flank of Ben Mor Coigach (BMC). A - Ben Mor Coigach with NW regional ice flow. B - Interpretation of geomorphology utilising the same basal thermal regime descriptions as on Folio 4.

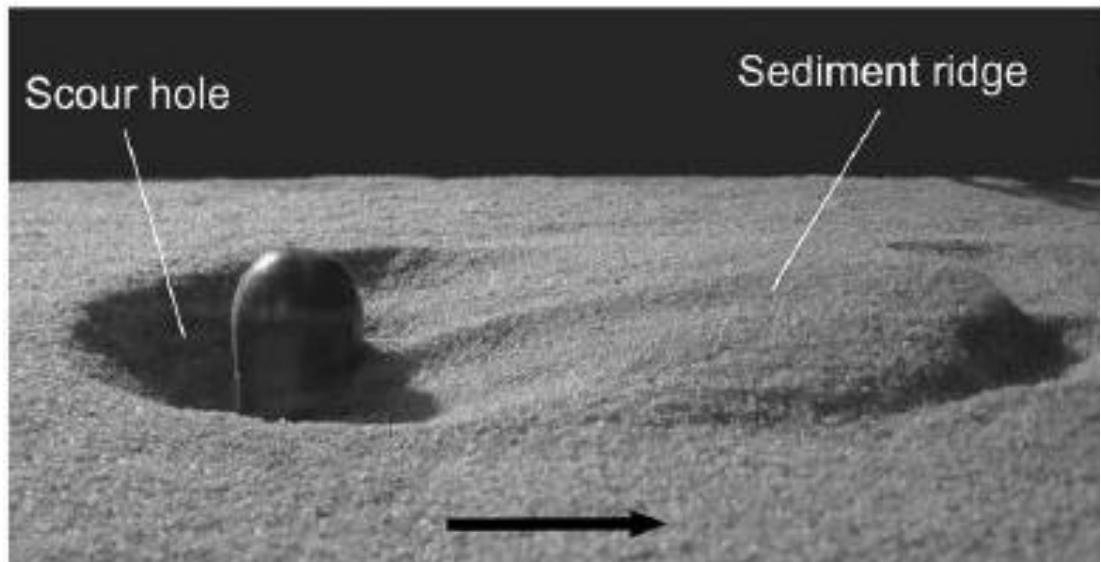


Figure 5.23: Experimental model analogue for 'till tail' and scour forms formation. (Euler and Herget, 2012). Typical fluvial obstacle mark (scour plus ridge), experimentally simulated in a laboratory flume using a cylinder with hemisphere as obstacle (diameter: 3cm). Arrow indicates flow direction.

Table 5.2: Comparison of horned crag and tail features and formation (after Jansson & Kleman, 1999) with till tails in NW Scotland (this study).

Stage	Thermal Regime	Horned Crag & Tail	NW Scotland Till Tails
1	COLD-BASED	Lee-side accumulation prevented	Central groove in lee-side position
2	THERMAL STRATIFICATION	Transport of material along wet-based shoulders	Sediment train nucleating at outer edges of obstacle
3	COLD-BASED	Preservation of twin tails	Preservation despite ice-stream location

In crag-and-tails, the length of tail is again thought to relate directly to the length of the pressure shadow in the lee of the obstacle (Benn & Evans, 2010). The pressure shadow is attenuated with velocity such that the longer the form, the higher the sliding velocity. Therefore comparison of individual till tail forms can potentially inform on ice-sheet flow velocities near the bed and ice-bed interaction.

Wider till tails appear to occur where ice moved over softer rock, and more plentiful, weaker till, i.e. the Ben Hope till tail over the Moine, and the Cranstackie and An Teallach till tails over Sandstone. Narrower forms are seen where ice moved only over Lewisian gneiss, e.g. in the lee of Stac Pollaidh and Quinag. However the form of the till tails is also influenced by their proximity to fast flow zones (Folio 3). Therefore the vertically tapering till tails observed in the lee of Suilven and Quinag may indicate higher strain rates in the ice with the ice deforming faster than the sediment and consequently closing the cavities. It is suggested that this situation is more likely to occur under sheet flow conditions. Consequently variation in till tail form may help reconstruct boundaries between ice streaming and sheet flow zones.

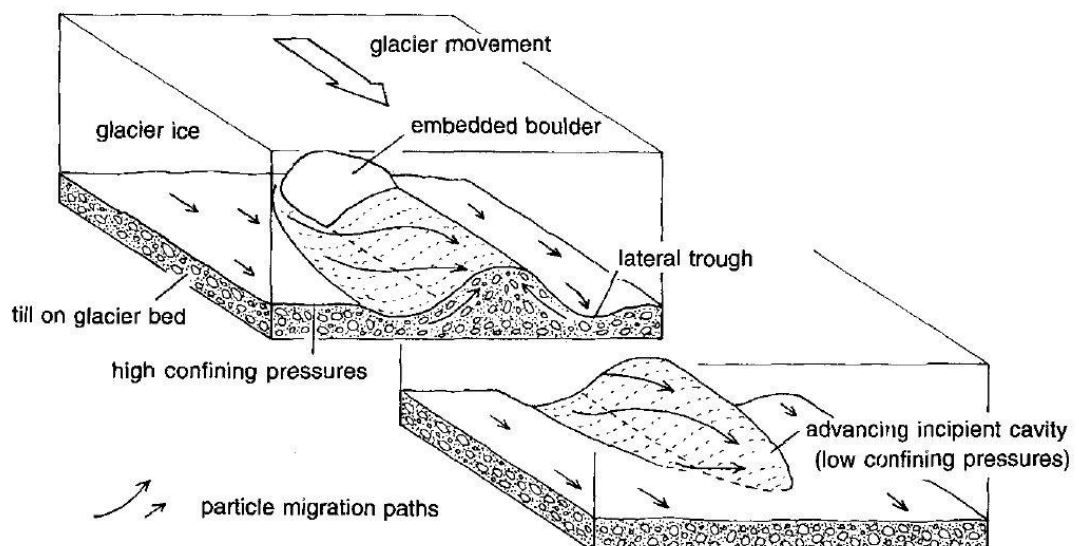


Figure 5.24: A model of flute formation by the sub-sole deformation of sediment into an advancing incipient cavity (Benn, 1994). This model provides a small-scale analogy for till tail formation, illustrating the importance of lee-side cavities and pressure gradients in the direction and concentration of material in these localities.

The preservation of till tails in NW Scotland, particularly as subglacial sediments are typically rare across the region, is unusual and significant, especially considering that ice stream conditions are thought to have dominated the area.

As explained in relation to the crag and tail analogy, cold-based deglaciation conditions provide a simple explanation for preservation throughout Inverpolly, Coigach and Wester Ross. The initiation of this switch from streaming to frozen-bed will be discussed later (5.4.2). With such distinctive forms and surface texture in contrast to the surrounding exposed bedrock, it is easy to pick out evidence of till tail modification across the region. In the north, an incomplete till tail is identified by a lee-side fill, now truncated by later erosion through the Strath Dionard corridor. This, along with the high level glacial lineations noted earlier (Results: 3.2.1) provide evidence for a switch in flow directions from NW, non-topographically constrained, to northward, valley-confined, flow at a later stage.

Another switch in thermal regime and flow style is recorded by transition from till tail formation to boulder train deposition. The Torridon boulder trains of the Assynt region have been described and mapped by Lawson (1995) and now warrant further examination in light of flow vectors ice-sheet thermo-mechanics associated with till tails. Till tails and the Assynt boulder trains share two features: a WNW flow-aligned elongation and initiation in the lee of high ground (Figure 5.25). These similarities indicate that material was probably transported under an equivalent flow vector (i.e. with the same general glaciological organisation), and that pressure shadows were translated down-ice of the obstacles leading to the sharp definition of feature margins. However, there the physical and glaciological similarities end. The sedimentological and volumetric difference between the two features is large. Till tails are large, $10^2 - 10^3$ m features (Figure 3.53) composed of diamicton (Figure 3.55) while boulder trains are widespread but mappable dispersal trails of blocks. This contrast could result from a different sediment transport route as well as assignment to a different timeframe in the last glacial stage. The form and composition of till tails suggests they have a sub/englacial origin with

possible later subglacial modification. Support for a subglacial origin for till tail forms is provided by parallels with features of the McClintock channel ice stream in Arctic Canada. Here, ridges, distinct from megalineations, up to 23km long with widths 500-800m, displaying some sinuosity and disregard for topography are classified as ice stream marginal moraines thought to form in the shear zone between an ice stream and adjacent sheet ice.

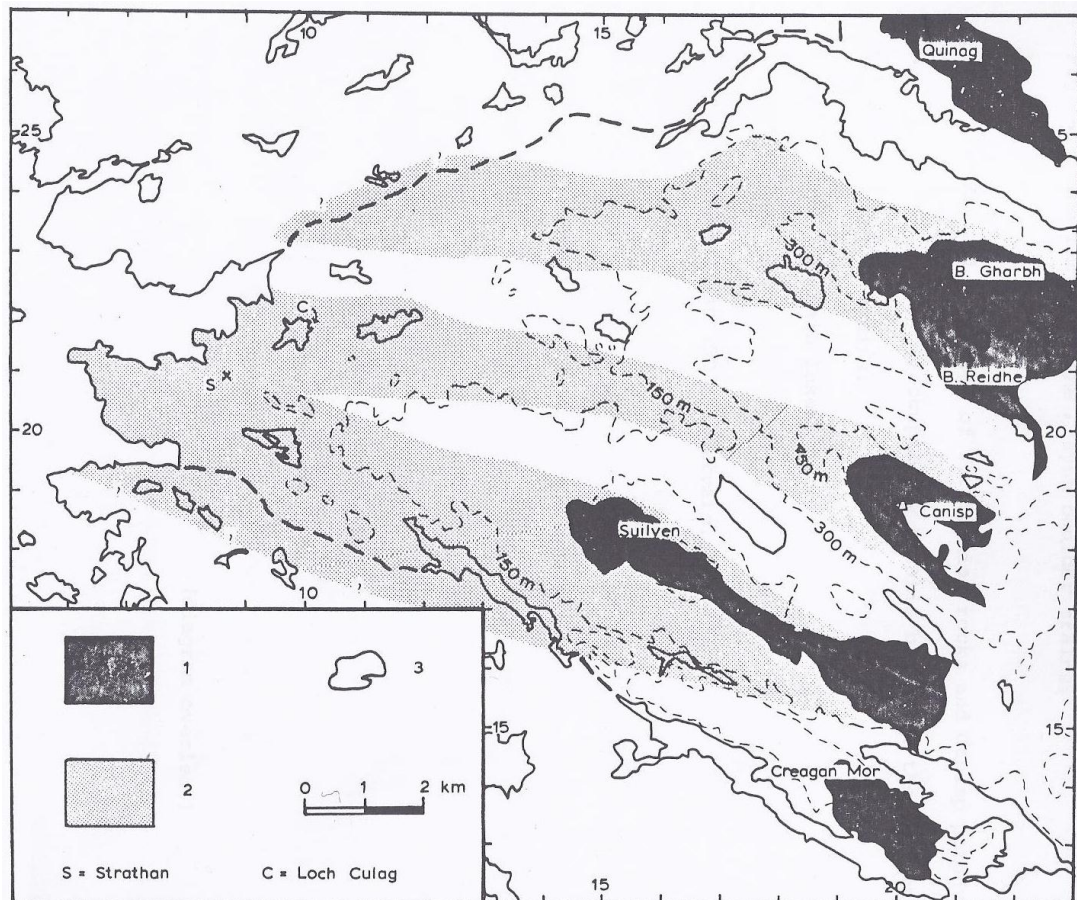


Figure 5.25: Torridon boulder trains, Assynt. After Lawson, 1995. 1 - Outcrops of Torridon rocks and Canisp porphyry. 2 - Areas occupied by erratic blocks of the boulder trains. 3 - Main lakes. Contours at 150 m intervals.

The matrix-less blocky boulder trains suggest minimal post-depositional modification and a plucking-related sediment production mechanism. Atkins (2013) observed boulder trains 10s -100s metres long in the lee of glaciotectonised bedrock obstacles in a formerly cold-based subglacial environment in Antarctica. It was suggested that the quarried

material accumulates in a lee side pressure shadow elongated parallel to the ice-flow direction. A supra-glacial source for much of the material may also be suggested, perhaps as mountains are revealed during ice-sheet thinning.

The occurrence of till tails and boulder trains in different areas may be a product of surveying omissions (Lawson only mapped between Suilven and Quinag in central Assynt) or may represent a true contrast in glaciological processes. That the boulder trains that occur over lower relief ground may indicate that a saddle, or lower ice-sheet surface, existed in this region and consequently the top of mountains were exposed supplying supra-glacial material, while westward flow was still active. Comparison of the distribution and elevation of glacially transported boulders (including erratics) is made in the following section.

5.3.3. Vertical transportation of erratics

High level, > 500 m a.s.l., erratics occur on the majority of mountain peaks across NW Scotland providing a conservative minimum constraint on regional ice thickness. More precisely, the erratic boulder positions provide a minimum estimate of the height of deforming ice. Erratics found at summit elevation in nearby Torridon (Fabel *et al.*, 2012) are some of the highest glacially transported material in the NW Highlands, with Fabel *et al.*'s dated samples selected from sites ranging from 883-989 m a.s.l. Comparison with geological source outcrops for these samples indicates that some of the erratics may have been transported vertically almost 300 m. The pattern of vertical transportation of erratics, hereafter "erratic uplift", within the field area stimulates discussion of glaciological and flow organisation in relation to thermal structure and ice sheet evolution. The occurrence, at 618 m a.s.l., of a Salterella Grit erratic on the SW flank of Cranstackie provides insight into regarding glaciological processes operating during full glacial conditions.

Local outcrops of Salterella Grit are extremely limited in spatial extent occurring as slivers (<600 m x 200 m exposures) in an isolated thrust bound slice between the Sole and Lochan Riabach Thrusts. The nearest Salterella Grit outcrops occur at 750 m a.s.l. on Foinaven (6.8 km to the

south) and in Srath Beag. The Srath Beag outcrops occur on both flanks c. 315 m a.s.l. on the eastern flank of Conamheall and at c. 150 m a.s.l. in the Allt na Craoibhe-caoruinn valley below An Lèan-Chàrn. The Foinaven outcrop is higher than the erratic location, requiring descending northward ice flow, with a ~130 m elevation drop evoked. Transporting erratics from Srath Beag requires reverse flow up the eastern flank of Cranstackie with emplacement of erratics c. 300-470 m above source outcrop. Both scenarios require full glacial conditions in order to have ice coverage at ≥ 750 m a.s.l (Foinaven source) or ≥ 618 m a.s.l (Srath Beag source). The Srath Beag source is suggested as more realistic because ice flow NW occurred during full glacial conditions whereas N and NE ice flow probably only occurred during reduced ice volume conditions when topographic control became important.

The uplift of erratics, >100 m elevation difference from outcrop to deposition site, is also observed throughout Assynt and Wester Ross (Figure 5.26). In Assynt the occurrence of Lewisian group erratics on the quartzite ridge of the eastern mountains indicates erratic uplift, under a westerly ice flow, of 100-200 m. Lawson, who mapped erratic distribution throughout Assynt (1990), particularly remarks the surprising occurrence of Lewisian erratics above 600 m a.s.l along the spine of the eastern Assynt Mountains; their source outcrop lying below on the flank of the mountains and in Glen Oykel (as low as c. 500 m below the plateau). In eastern Assynt, Moine schist erratics have been uplifted >300 m over a horizontal transport distance of <6 km (Lawson, 1990). Lawson's observations that Lewisian erratics occur largely above 600 m a.s.l on the Assynt ridge (Breabeg, Beinn an Fhurain, Beinn Uidhe) in the N of the area, whereas in the SE of the area they are also found below 600 m a.s.l suggest a difference in erratic transport and potentially thermal structure.

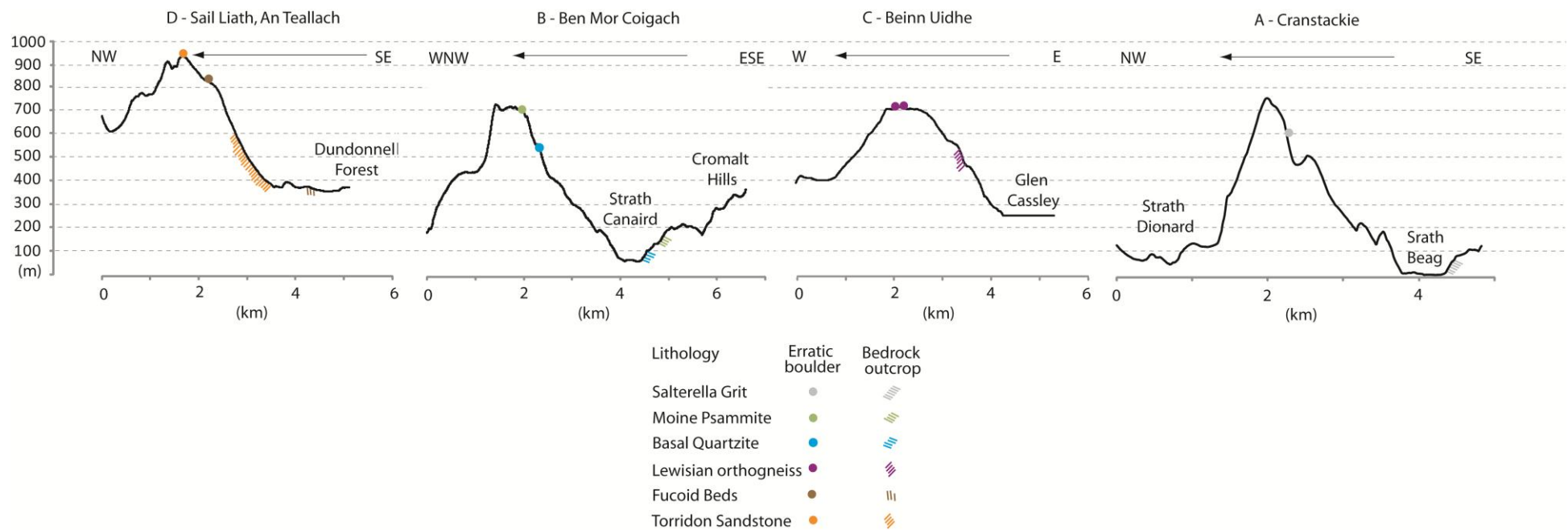


Figure 5.26: Erratic transport along four profiles (see Folio 1). Note varying horizontal distance scale on X axis. Elevation lines at 100 m intervals. Dots indicate location of erratic boulders. Shading indicates location of bedrock outcrops of lithologies found as erratics at high level sites. Hatching not indicative of dip or structure. Ice flow right to left in all figures with orientation of profile indicated.

To the west, in Coigach, uplift is greater with erratics c. 500-600 m above their presumed source outcrop in the bottom of the valley around Strath Canaird. A dramatic increase is seen therefore in upward mobility of erratics with movement westward. This observation may relate to scaling of lateral and vertical shearing with ice velocity and is discussed in the following sections.

5.3.3.1. *Glaciological significance of erratic uplift*

The significant uplift of erratics by glaciation throughout NW Scotland may be reflective of the unusual topography-ice flow interaction predicted here. This phenomenon is expected to be particularly pronounced where isolated peaks and high ground occur oblique or sometimes transverse to regional ice flow representing significant obstacles to ice movement. Ben Mor Coigach (with erratics emplaced at >700 m a.s.l) and the Cromalt hills sit in a corridor with glacially carved bedforms indicating fast flowing ice (megagrooves) at Elphin (to the north) (Bradwell, 2005) and the Rhidorroch Forrest area to the south. Foinaven (with its western boulder apron) is situated between Laxford Bridge strongly scoured ground (Bradwell, 2013) and major flow conduit of Strath Dionard. Cranstackie lies between the major troughs of Strath Dionard and the Eriboll-Hope glacier. The Assynt Mountains occur between the Loch Glencoul trough and Borrolan Gap. From these interesting geomorphic juxtapositions it is possible to suggest a possible causal relationship for erratic uplift and subsequently offer mechanisms to justify it.

Historically it has been difficult to explain the occurrence of high level erratics in NW Scotland, particularly when source outcrops for the material sit at lower elevations than their depositional sites. The problem is also complicated by the predicted occurrence of cold-based ice at high elevation, restricting basal sliding. Sugden & Watt's (1978) model of debris entrainment (Figure 5.8) provides a viable mechanism for erratic uplift relating to the likely of the thermal transitions anticipated in the vicinity of the inselbergs. To overcome the difficulty of moving material up and over steep faces, Lawson (1983) proposes a glaciological situation whereby

active ice shearing over a stagnant stoss-side ice mass, transports erratics from source outcrop to high elevation (Figure 5.27).

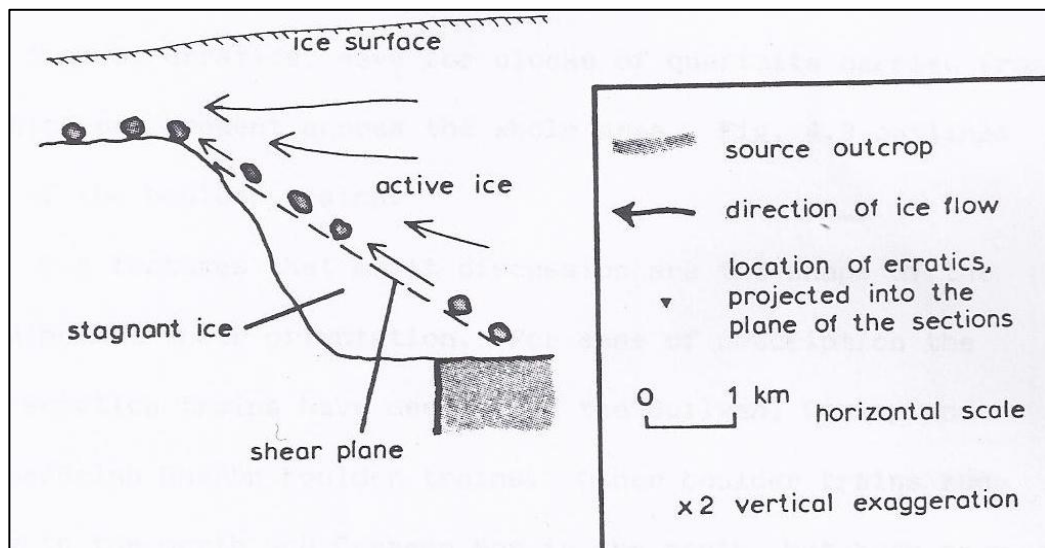


Figure 5.27: Suggested explanation of erratic uplift, involving movement along high-angled shear planes in the ice. After Lawson (1983).

The physical control on such a mechanism can be anticipated to relate directly to a transition in BTR as demonstrated by Sugden's (1978) warm to cold transition related to bed topography. The alignment of rip-off scarps with trains of glacial erratic boulders (Figure 5.28) again suggests the strong association of erratic sourcing with thermal transitions. Detailed studies in the Eastern Pyrenees, an area with relict plateaux land surfaces indicative of cold-based ice cover (Delmas *et al.* 2009), have indicated high rock wall recession rates over the Pleistocene in comparison to modest depths of glacial scour.

Increases in bed relief, such as the inselberg hills of NW Scotland, are known to cause perturbations in ice sheet flow and subglacial hydrology due to increased frictional stresses and changes in ice rheology and deformation (Nye, 1957; Hindmarsh, 2001). Radar profiles beneath Dome A, of the East Antarctic ice sheet, indicate that bed relief significantly disturbs an ice sheet's internal flow layering and surface elevation profile (Figure 5.29). Bell *et al.* attribute these deflections to the freeze-on of substantial masses of basal ice causing rheological disruption. In addition, research at the Siple Dome at the head of the Ross Ice Shelf suggest that where frozen

bed conditions, thin till or inter-ice stream ridges exist, ice doming may occur (Gades *et al.* 2000). This data and interpretations provide possible explanations for three unusual glacial phenomena observed in the field area. Firstly, it offers a mechanism by which material can be incorporated into basal ice in the vicinity of a cold-based system. This concurs with field evidence which excludes the possibility of significant basal sliding at high elevation. Secondly it illustrates how stoss- (erratics) and lee-side (till tail) sediment packages may be deposited in unusual settings due to flow disruption. Potentially, erratic uplift height may have been a function of increasing stoss side slope angle and with ice flow velocity, such that highest erratic uplift should occur where free faces abut streaming flow i.e. Ben Mor Coigach, Beinn Uidhe. Erratic deposition elevation could also be a product of overlying ice thickness. For example, if the ice dwarfs the topography, as in Antarctica, erratics may be largely excluded from deposition on the summit by the frozen bed mass and instead be deflected round it, whereas if ice is thinner, and the thermal boundary sits below the level of the summit, erratics may 'pool' around the boundary, in a stoss side setting (Clarhall and Kleman, 1999), and be deposited during deglaciation.

Thirdly, the observed entrainment of ice rip-up clasts in Antarctic ice streams, sourced at the junction between sheet flow and stream flow (Whillans *et al.*, 1987; Shabtaie *et al.*, 1987 and Bindschadler *et al.*, 1987) adds weight to the proposal that 'rip-offs' mark this glaciological transition. Clarke (1987) observed that this incorporation would necessitate a ragged transition between the two flow types with entrainment of large blocks of inland ice; where high bed relief occurred in the vicinity of this transition it might be proposed that plucked and entrainment of frozen-on bedrock, i.e. rip-off formation might also result.

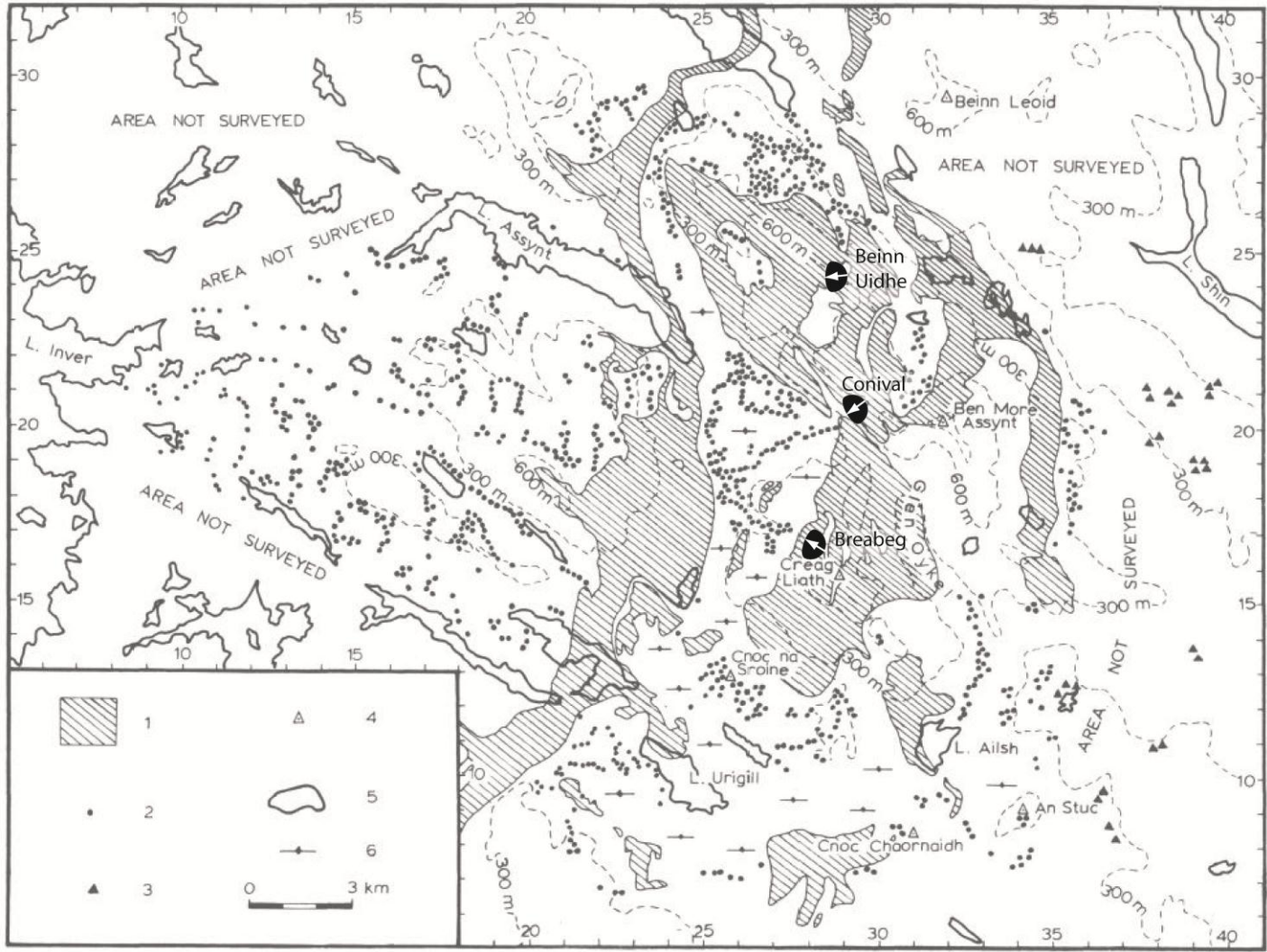


Figure 5.28: Relation of quartzite erratics to location of 'rip-offs', Assynt Mountains. Adapted from Lawson, 1990.

- 1 - Outcrops of Cambrian Quartzite.
 - 2 - Occurrences of quartzite erratics (noted by Lawson).
 - 3 - Occurrences of quartzite erratics (noted by Geological Survey cf. Read et al. 1926).
 - 4 - Areas examined where quartzite erratics re absent.
 - 5. Selected lochs.
 - 6. Areas of thick peat.
- Contours at 300 m intervals.
-  Rip off site (named - this study).
 - Arrow indicates direction of rock evacuation.

It is difficult to resolve some of the erratic transport routes with Lawson's model as, in some situations (Sail Liath and Beinn Uidhe), erratic sources are potentially located beneath his stagnant block, on the stoss side of the mountain. At these sites, a rotational mechanism, similar to the Bell model is required to quarry and then transport the erratic material to high elevation. Neither of the two models discussed provides a completely satisfactory mechanism to explain the distribution of uplifted erratics in NW Scotland. In order to better constrain the glaciological organisation responsible for the erratic uplift, it would be necessary to supplement the current dataset in two ways. Firstly, trace flow pathways through detailed geochemical provenance tracing. Secondly, better understand palaeo-ice flow around the specific topography of NW Scotland through high resolution three dimensional numerical modelling.

5.3.3.2. *Timing of erratic deposition*

In the NW Scotland field area, 14 out of 15 high level erratics, or glacially transported boulders, yielded post-LGM ages indicating emplacement during GS-2 (28-16 ka BP). Therefore it could be suggested that the majority of mountains in NW Scotland were overtopped by ice during the last glacial stage. The deposition and exposure of high level erratics on the nearby mountains of Torridon has been attributed to Lateglacial ice thinning by Fabel *et al.* (2012) a theory which is echoed by the patterns in exposure history seen throughout the field area in this study.

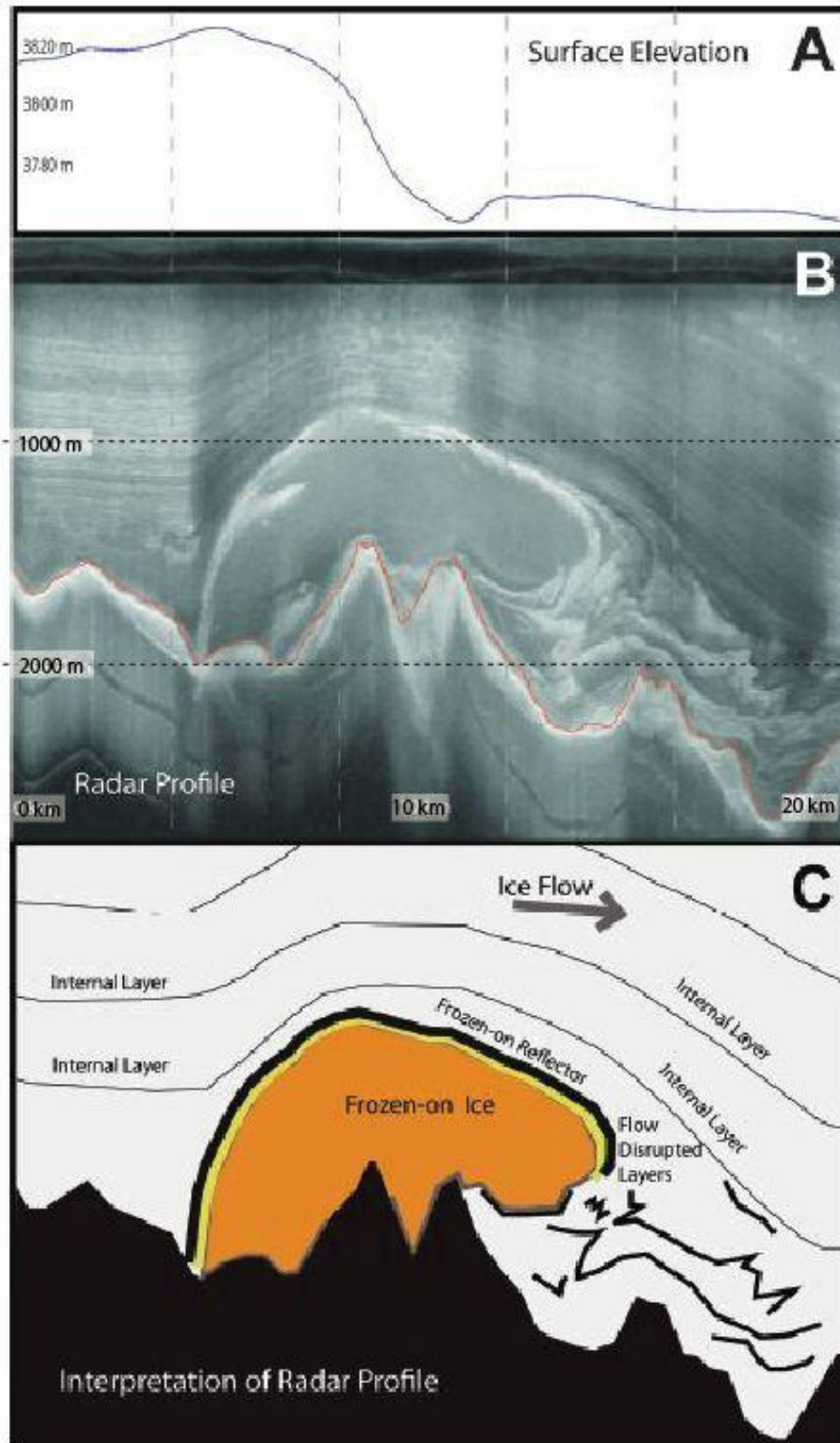


Figure 5.29: Large scale freeze on of basal ice, Antarctica. After Bell et al., 2011. A - Surface elevation of ice across line of radar survey. B - Radar image. C - Interpretation of radar profile showing frozen on ice above mountains and down-ice disruption of flow configuration.

5.4. Ice sheet thermal and land surface evolution

5.4.1. Towards an understanding of thermo-mechanical organisation of the last BISS in NW Scotland

NW Scotland is distinct in the British Isles as a bedrock landscape strongly influenced by the operation of a palaeo-ice stream. Like the Cairngorms and NE Scotland, NW Scotland shows evidence of relict land surfaces, but unusually these are within the context of an ice stream catchment. Parallels may also be drawn with N Sweden where a patchwork of warm- and cold-based geomorphic assemblages is observed (André, 2002, Clarhall and Kleman, 1999, Ebert and Hättestrand, 2010, Ebert *et al.*, 2012, Kleman, 1992, Stroeven *et al.*, 2002).

In order to compose a basal thermal regime map (Folio 4) it is necessary first to create a landscape classification system, by which detailed local field observations can be assimilated into a wider regional picture. In NW Scotland, the geomorphological record is a palimpsest; evidence of relict patches at high and low elevation, preservation of fine sediment lineations through deglaciation and evidence of truncation and modification of features indicate the potential to separate diachronous landscape evolution events. Geomorphic and TCN analyses have been used to define five land surface zones. These zones reflect *cumulative* glacial activity i.e. the designations relate to the predominant glaciological conditions in that area averaged over time. The categories are a combination of approaches used by Hall and Glasser (2008), cumulative thermo-erosional zonation, with principles of Kleman & Stroeven's (1997) geomorphic inversion key distinguishing between sheet flow, stream flow and frozen bed conditions.

Sheet flow designated areas are usually low elevation with bedrock at/near surface or a carapace of till. Where ribbon-like attenuation features (till tails) or streamlining of till are common, bedrock megagrooves and other streamlined bedrock features such as rock drumlins occur. *Transition zones*, most commonly relate to inselbergs and other isolated mountain massifs and show evidence of vertical zonation of erosion

(Figure 5.20). Where a *frozen bed* is designated, preservation of saprolite, a palaeo-weathering front, tors or other pre-glacial surfaces have been recognised. *Shear margins* occur as a clear lineation dividing one landscape type from another (most commonly delineating the boundary between frozen bed patches and transition zone surfaces). They may be marked by depositional features as at W edge of Ben Hope till tail and Oldshoremore boulder moraine, or may be represented by the initiation of erosion related to ice thickness or flow change such as in coastal and high level rip-offs.

Mapping of these landscape zones allows division of the region into sectors suggesting different modes of glacial operation. Along the north coast evidence of a late stage warm-based regime truncates and incises an earlier thermally zoned regime record. Evidence of fast flow is largely confined to the troughs and coastal margin where TCN data at Rispond highlight high (> 3 m) levels of subglacial erosion. The occurrence of till tails from Cranstackie and Ben Hope indicate significant pressure shadow effects affecting a broad area (truncated in the case of Cranstackie) suggesting earlier sheet flow accelerating towards (localised) streaming velocities.

The Cape Wrath promontory presents a large frozen 'island' situation-predominantly cold-based throughout the last glacial stage with a prominent shear margin at its south west margin marking the transition into the Laxford streaming onset zone (Bradwell, 2013). Warm-based activity of a Foinaven-sourced glacier overprints this pattern in the Sandwood Bay area.

Low ground between Loch Laxford and Eddrachillis Bay displays a dichotomous classification with the dominance of streaming apparent in the vicinity of the major troughs (Laxford, Inchard, Loch A Chairn Bhain) and intervening zones of slower sheet flow over northern Assynt and the knock and lochan ground between Scourie and Loch More. Streaming conditions may have initiated close to the modern coastline in response to flow acceleration as the ice sheet moves onto deformable sediments offshore.

The eastern Assynt Mountains (Glas Bheinn to Breabeg) are here classified as a transition zone. They exhibit thermal stratification (Figure 5.20) preserved particularly on their western sides due to their oblique orientation due to ice-sheet flow. The identification of rip-offs as shear margins suggests the head ward progression of warm-based conditions during ice sheet history. However, the preservation of erosion contrasts and relict plateaux surfaces indicate that cold-based ice cover persisted, or even expanded over this area during deglaciation. The pattern of erratic dispersal from this transition zone suggests a Boothia Type dispersal train (Figure 5.30) i.e. that erratic distribution has been focussed due to convergent flow.

In Assynt, a gradient of decreasing elevation of erratics uplift (from north to south) may be explained by regional localised topographic control of ice-sheet flow dynamics (Figure 5.20, Folios 1 & 4). In the north of Assynt, the dominant troughs and mountains run oblique to ice-sheet flow (E to W) preconditioning ice sheet thermo-mechanical disruption in this area. A steep thermal gradient and strong ice piracy effect may be anticipated in the source area around the head of Glen Oykel, with overflow ice quarrying from lower elevations to the east of the mountains and depositing material as erratics on the Assynt ridge in the west.

Where topography and ice flow were aligned, as in the south the 'uplifting' effects associated with cold-based ice would have been less significant with most ice volume channelled through the wide passes of the Borrolan Gap and Loch Sionascaig. Previous work, in the south of the region, has described the streaming-dominated landscape of the Rhidorroch-Loch Broom area (Bradwell, 2005, Bradwell *et al.*, 2008b) characterised by the prevalence of bedrock megagrooves. Mega-scale sediment lineations (till tails) conform to Kleman & Stroeven's (1997) ribbon-like lineation land system (Figure 5.1) suggesting stream flow without topographic control. The high density of shear margin 'transitions' throughout the region also reinforces the dominance of horizontal thermal zonation.

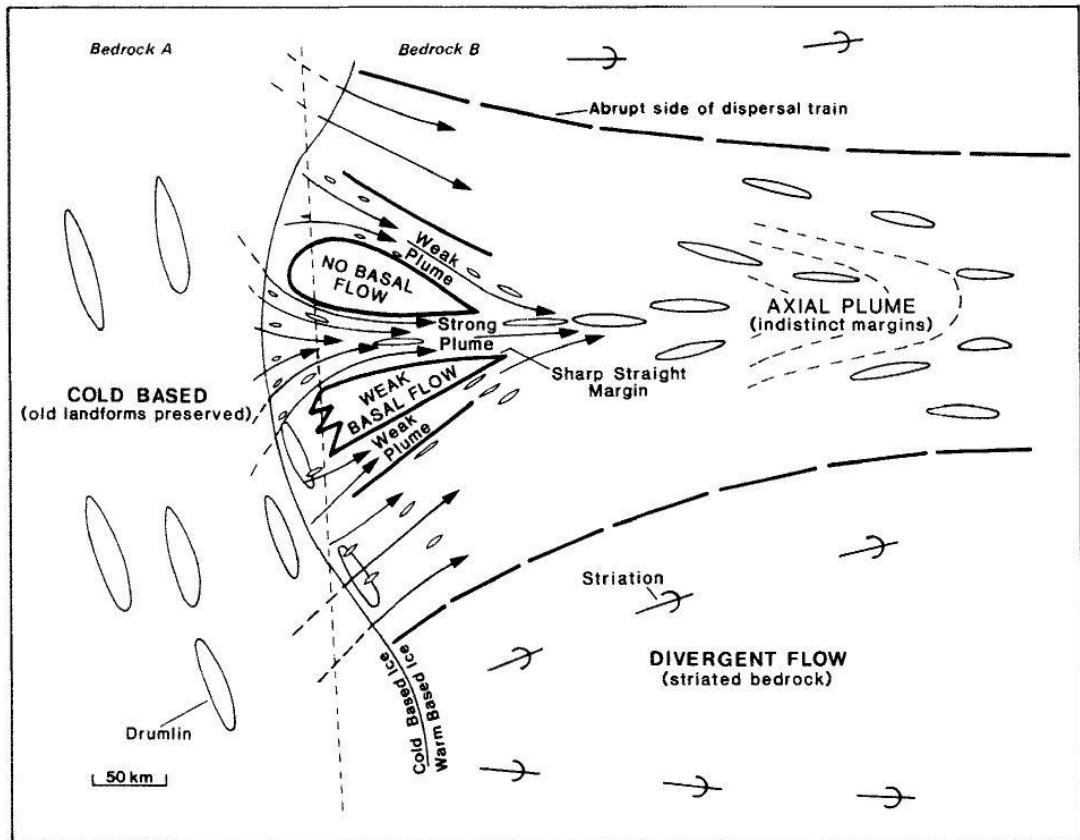


Figure 5.30: Details of landform assemblage associated with a Boothia-type dispersal train (Dyke & Morris, 1988).

The pattern of flow organisation indicated in NW Scotland conforms to observations of mesoscale (260 x 360 km) palaeo-ice stream-dominated systems (Kleman *et al.*, 1999b). Those authors noted that the pattern of relict surfaces is governed by inward-cutting ice stream erosion as seen around the troughs and within the onset of streaming ice-sheet flow west of the Assynt Mountains. They also note that the distribution of relict landsurfaces is not dictated by topography, but rather by flow divergence. This fits for Cape Wrath where flow is known to have diverged to the NE and SW despite only a modest relief increase from the surrounding ground.

5.4.2. Glaciological evolution of the BIIS in NW during GS-2

All indications, from the distribution and exposure age of high level erratics and evidence of plateaux modification, suggest that during GS-2 the BIIS overwhelmed even the highest summits of NW Scotland. During full glacial conditions, operation of the Minch palaeo-ice stream governed flow across the area in a NW-WNW direction and established vertical ice sheet thermal zonation and pressure shadow effects in the vicinity of high ground.

The results of this research project support the location of Bradwell *et al.*'s (2007) onset zones, which appear to correlate with regions dominated by a thermal regime signature of transition from cold-based to thawed bed conditions (Folio 4). The borders between onset zones also show reasonable alignment with the position of prominent till tails at An Teallach, Ben Mor Coigach and Foinaven. This promotes the idea that till tails sit at the site of previous inter-stream ridges. Additional support for streaming onset comes from the boulder trains of Western Assynt which, in combination with till tails, show strong similarities to Boothia type erratic dispersal trains (Figure 5.25, Figure 5.30). Evidence has also been provided for the location of lateral shear moraines such as at Ben Mor Coigach and Oldshoremore from geomorphic and also additionally in the latter case, surface exposure analysis. Together these features support an ice-stream onset landsystem in the northwest of Scotland.

This research suggests that the landscape of NW Scotland displays classic evidence of thermal transitions from predominantly frozen bed to warm-bed streaming conditions. The evolution of these transitions was probably diachronous, with vigour and longevity of streaming conditions varying by location. For example, in the Rhidorroch area, it is suggested that the acceleration of flow into the Loch Broom trough can be seen to have thermally excavated a wet-bed embayment (Figure 5.19) deep (>10 km) into the surrounding slower flow zone. The strong topographic depression of the Loch Broom trough is likely to have influenced even late stage flow and consequently this transition may be a long lived feature of the ice sheet.

Flow restriction and therefore concentration was associated with the formation of abrupt thermal boundaries at the margins of streaming/fast flow corridors. Evidence of head-ward spread of warm-based conditions is seen on high ground, expressed in rip-off scarps. Kleman and Glasser (2007) note that, wherever evidence of anastomosing ice-streams is preserved, frozen patches, ranging in size and shape, whether permanent (throughout one or more glacial cycle) or ephemeral, are intrinsic to these systems.

An 'archipelago-type' thermal boundary seen in Assynt and Coigach suggests incomplete thawing of the bed. In this area of limited topographic control, warm/wet-based ice streaming may have occurred only in narrow corridors with rapid switches of flow hierarchy between stream branches (Dowdeswell *et al.*, 2006, Vaughan *et al.*, 2008, Conway *et al.*, 2002). This association suggests that streaming in this area may have been in its infancy or unstable. Late stage freeze-on during ice-sheet thinning would explain the preservation of the 'frozen islands' configuration.

Along the north coast, evidence for short lived, late stage streaming exists around the major troughs with evidence of deep glacial erosion at the coast (5.2.2). Streaming flow here is in a topographically constrained ice-stream corridor configuration. Warm-based flow extending offshore is indicated by the suite of N-NE orientated flow traces and the occurrence of a rip-off scarp on the NE flank of Cranstackie (Figure 5.14). Offshore evidence (Figure 4.2) supports the existence of lobate, possibly surging or fast-flow lobes extending on to the shelf here.

Interestingly the evidence of streaming behaviour in NW Scotland is, in many locations, also, evidence of late-stage cold-based conditions. As previously described, the preservation of low elevation features such as till tails and the Cromalt tor, necessitate that extensive warm-based (highly erosive) conditions did not prevail everywhere across the area during deglaciation. Although the surprising scarcity of till and fluvio-glacial deposits in areas categorised as sheet flow zones may indicate that warm-based conditions persisted here during deglaciation, evacuating sediment to offshore depocentres. This dichotomous pattern may suggest that a glaciological reorganisation, possibly even described as a thermal inversion,

occurred in the latter stages of GS-2 such that fast flow corridors shutdown rapidly and froze onto their bed with flow subsequently diverted through the sheet flow zones.

Evidence of cold-based basal thermal regime to the east of the study area around Loch Shin has been identified in the form of Rogen Moraine (Finlayson and Bradwell, 2008). Formation of these landforms is attributed to the existence of a strong ice flow gradient forced by headward scavenging of the Moray Firth palaeo-ice stream. The Moray Firth ice-stream, draining the eastern portion of northern Scotland, is anticipated to have competed with the MPIS for ice catchment across the palaeo-ice shed throughout the late Devensian (Hubbard *et al.*, 2009). It can therefore be proposed that enhanced ice piracy by the Moray Firth ice stream, supported by formation of rogen moraine close to the LGM ice-shed, could have reduced westward ice flow over the Assynt Mountains. This could have provided a mechanism for significant ice sheet thinning, and consequently freeze-on, of the ice in Assynt and adjacent regions. Late stage freeze-on of outlet glaciers is also suggested by the lateral and deeply incised proglacial meltwater routing seen around the terminus positions of the Eriboll (Figure 4.3), Cape Wrath (Results: 3.2.1.10), Oldshoremore (Figure 3.28, Figure 4.4 & Figure 4.5) and possibly even Stoer Peninsular outlet lobes.

5.4.3. Evidence of active periglacial processes during the Holocene

The highest erratic sampled in this study, SAIL 01, Torridon Sandstone erratic found at 949 m a.s.l on the summit of Sail Liath, yielded an apparent exposure age of 8.4 ± 0.6 ka BP. The latest plausible age for Younger Dryas ice demise being 10.5 ka BP (Hubbard *et al.*, 2009), the exposure age of this sample is too young to represent even a Younger Dryas deglaciation age. The young age of this high elevation sample requires that the clast has experienced shielding of some kind for a period of time, with 8.4 ka BP representing an accumulation period, rather than surface

exposure age. With documented evidence of active periglacial processes occurring at this elevation on the An Teallach massif (Ballantyne, 1999) it is suggested therefore, that blockfield clasts, now at the summit surface have spent time in the subsurface being brought to less than 3 m of the surface during the Holocene, hence the young surface exposure age. Calculations using the age for SAIL02 (15.8 ± 1.0 ka BP) suggest that this nuclide concentration could be achieved by residence in the top 42 cm of sediment over this period, the active layer depth proposed by Ballantyne (Ballantyne, 1991). The simplest scenario to evoke is a periglacial overturning process, such as size-related clast sorting. The resulting conclusion is that periglacial processes have been active at this mountain top site during the Holocene. Evidence of active post-glacial or Holocene periglacial processes highlights the influence of post- and paraglacial processes in shaping the upland landscapes of NW Scotland.

5.5. Key findings regarding the thermal and landscape evolution history of NW Scotland

The key findings of this project in relation to the glacial basal thermal regime history are as follows:

- The glaciology of the region was dominated by the onset of ice streaming conditions. This potentially perpetuated cold-based ice cover at high, and selected low level elevations, through flow focussing in adjacent locations.
- Thermal stratification and sharp thermal contrasts developed in response to ice streaming. It is suggested that these are the main controls on bedrock erosion and terrestrial sediment deposition.
- The land surface record observed in NW Scotland is testament to the prevalence of cold-based ice over much of the field area at disparate times in ice sheet history.
- The region displays a long palimpsest landscape record due to the preserving cover of cold-based ice present during much of its Quaternary history. The unusual distribution and of landforms observed provides a valuable resource for landscape evolution studies.
- A thermal regime inversion may have been experienced during deglaciation which is responsible for the preservation of streaming features and for the evacuation of glacial sediments from the sheet flow areas. This research illustrates the value of bedrock sampling for constraining the erosional history of an area which can be consequently related to basal thermal regime over one or more glacial cycles.
- Description of 'till tails' for the first time in the British Isles has been instrumental in understanding the glaciological organisation and thermal evolution of NW Scotland.
- The emplacement of high level erratics was coeval with and potentially dependent upon the existence of cold based ice at high elevation. Recognition of this glaciological association may be useful in other field areas for constraining ice sheet thickness and basal thermal regime, and for understanding the influence of ice streaming.
- Recognition of rip-offs may be a key boundary condition indicator in ice-stream onset zones and may be identifiable in other previously glacially bedrock terrains.

1. CONCLUSIONS

This thesis has presented the products of a field and laboratory-based investigation into the palaeo-glaciology of NW Scotland. Using a landsystems approach, contextualised within the temporal framework provided by TCN analysis, it has been possible to gain insight into the operation of the last BISS and specifically, the role of the MPIS in the ice sheet's glaciological organisation.

The geomorphological map detailing major findings of this project (Folio 4), indicates that the dominant landsystem of NW Scotland is attributable to ice-stream onset conditions. Interestingly, despite the dominance of ice-streaming conditions, a long palimpsest landscape record is also preserved due to significant cold-based ice cover during the region's Quaternary history. Ice streaming may have perpetuated cold-based ice cover at high elevation, through ice surface drawdown, and at selected low elevations, through flow funnelling into adjacent troughs. Thermal stratification, and the existence of sharp thermo-mechanical contrasts, developed in response to ice streaming, are the main controls on bedrock erosion and terrestrial sediment deposition. New data supports the theory that trimlines in NW Scotland represent englacial thermo-mechanical boundaries through the identification of the diagnostic geomorphic expression of these boundaries - rip-offs, and by quantitatively demonstrating the increase in glacial erosion in the vicinity of these boundaries (≥ 25 cm depth of surface removed).

This landsystem comprises contrasting landform attributes associated with warm- and cold-based ice as exemplified by relict surfaces on inselberg summits juxtaposed with streamlined sediment ridges (till tails) and abraded bedrock. This landsystem is strongly dependent on the underlying geological structure and its varying susceptibility to sub-aerial weathering and glacial abrasion, but also on the thermo-mechanical organisation of the ice sheet itself.

Geomorphic and TCN evidence supports a conceptual model of thermal inversion following ice-stream cessation. The first description of 'till tails' in the UK has been instrumental in understanding the glaciological organisation and thermal evolution of NW Scotland. The preservation of these attenuated features in streaming zones suggests late stage freeze-down of thinning ice in Assynt and Coigach. In contrast, the truncation of till tails in western Sutherland by later locally sourced glacial advances (with associated till deposition) suggests late stage warm-based activity from thicker more dynamic ice further north. This thermal switch may also explain the surprising lack of sediment cover in northern Assynt and the evacuation of glacial sediments from the sheet flow areas. Full warm-based conditions did not occur for sufficient duration to leave a discernible sedimentary or erosional imprint. Persistence of these surfaces through glacial conditions, which are anticipated to have left no ice-free summits, suggests that thermal stratification existed in the vicinity of the mountain massifs with cold-based ice cover at summit elevations. The emplacement of high level erratics may have been coeval with, and potentially dependent upon, the existence of cold based ice at high elevation. Glacial modification of high level surfaces and features e.g. tor block rotation on Cranstackie and blockfield on Beinn Uidhe (16-41 cm rock removal) indicate that ice was deforming at this elevation but not sliding. This contrasts to Rispond where at least 3 m depth of erosion was achieved through the last glacial cycle (GS-2).

This project has contributed to our understanding of the last BISS, and glacial dynamics by providing empirical boundary constraints on basal thermal regime over the last glacial cycle. The occurrence of relict land surfaces at high elevation has demonstrated that sliding beneath ice sheet cover has been insufficient to obliterate the pre-glacial surface despite evidence of some glacial modification through enhanced basal deformation.

This research also aimed to chronologically and spatially improve the retreat history of the NW sector of the last BISS. This has been achieved by providing minimum constraints on ice thickness as geomorphic and TCN data indicate that mountain summits were covered by ice during maximal ice sheet conditions. Deglaciation ages from mountain top erratics indicate

they were uplifted and transported to high elevation during GS-2, before 16.5 ka BP. The full-glacial (GS-2) ages of high level erratics support dynamic thinning of the ice sheet leading to the stranding of cold-based plateau remnant ice-fields above the main mass of downwasting ice sheet. Thinning of ~300 m is estimated for some areas prior to 14 ka BP. Rapid thinning may have resulted in separation and starvation of low-level ice from cold-based plateau remnants with deglaciation ages from high level sites reflecting deglaciation of plateau icefields following earlier disconnection from the main ice sheet. A single Lateglacial age from the plateau of Beinn Uidhe (13.1 ka BP) allows the possibility of persistence of plateau ice-fields at high elevation through the Interstadial.

Importantly the project has focussed on bracketing cessation of the Minch palaeo-ice stream to examine how this affects ice sheet dynamics and deglaciation. The first dated terrestrial ice sheet limit following ice-stream collapse is found in this study area at Rispond. This is part of an ice sheet configuration with lobate northern and western margins. At Rispond a (mean) surface exposure age of 17.6 ka BP suggests initiation of retreat from locally-sourced ice extent and provides a minimum constraint on ice stream cessation. This indicates rapid loss of ice extent and volume following shutdown of the MPIS. Further surface exposure age data from the spreads of glacially transported boulders in the Oldshoremore area (13.7-17.0 ka BP) support early ice-free conditions at Cape Wrath following large scale glaciological reorganisation into northern and western lobate margins. Ice margin chronology from this study suggests that most ice had retreated back dramatically to local accumulation areas by 15.8 ka BP. Correlation of some low-level ice margin ages with erratic deposition ages c. 15 - 16 ka BP suggest large scale ice sheet reorganisation with significant ice sheet thinning and margin retreat prior to this time.

REFERENCES

- ANDRÉ, M.-F. 2002. Geomorphic evidence for recurrent cold-based ice conditions in Nordic uplands during the Quaternary glaciations (Aurivaara Plateau, North Sweden). *Norsk Geografisk Tidsskrift - Norwegian Journal of Geography*, 56, 74-79.
- ANGELIS, H. D. & KLEMAN, J. 2008. Palaeo-ice-stream onsets: examples from the north-eastern Laurentide Ice Sheet. *Earth Surface Processes and Landforms*, 33, 560-572.
- APPLEGATE, P. J. 2009. *Estimating the ages of glacial landforms from the statistical distributions of cosmogenic exposure dates*. Doctor of Philosophy, The Pennsylvania State University.
- ATKINS, C. B. 2013. Geomorphological evidence of cold-based glacier activity in South Victoria Land, Antarctica. *Geological Society, London, Special Publications*, 381, 299-318.
- BALCO, G., STONE, J. O., LIFTON, N. A. & DUNAI, T. J. 2008. A complete and easily accessible means of calculating surface exposure ages or erosion rates from ^{10}Be and ^{26}Al measurements. *Quaternary Geochronology*, 3, 174-195.
- BALLANTYNE, C. K. 1991. Holocene geomorphic activity in the Scottish Highlands. *Scottish Geographical Magazine*, 107, 84-98.
- BALLANTYNE, C. K. 1994. Gibbsitic soils on former nunataks: implications for ice sheet reconstruction. *Journal of Quaternary Science*, 9, 73-80.
- BALLANTYNE, C. K. 1997. Periglacial trimlines in the Scottish Highlands. *Quaternary International*, 38-39, 119-136.
- BALLANTYNE, C. K. 1998. Age and significance of mountain-top detritus. *Permafrost and Periglacial Processes*, 9, 327-345.
- BALLANTYNE, C. K. 1999. An Teallach: A late Devensian Nunatak in Wester Ross. *Scottish Geographical Journal*, 115, 249-259.
- BALLANTYNE, C. K. 2003. Stac Pollaidh - a late Devensian Nunatak? A comment on Bradwell and Krabbendam. *Quaternary Newsletter*, 101, 34-38.
- BALLANTYNE, C. K. 2010a. Extent and deglacial chronology of the last British-Irish Ice Sheet: implications of exposure dating using cosmogenic isotopes. *Journal of Quaternary Science*, 25, 515-534.
- BALLANTYNE, C. K. 2010b. A general model of autochthonous blockfield evolution. *Permafrost and Periglacial Processes*, 21, 289-300.
- BALLANTYNE, C. K. & MCCARROLL, D. 1995. The vertical dimensions of Late Devensian glaciation on the mountains of Harris and southeast Lewis, Outer Hebrides, Scotland. *Journal of Quaternary Science*, 10, 211-223.
- BALLANTYNE, C. K., MCCARROLL, D., NESJE, A. & DAHL, S. O. 1997. Periglacial trimlines, former nunataks and the altitude of the last ice sheet in Wester Ross, northwest Scotland. *Journal of Quaternary Science*, 12, 225-238.

- BALLANTYNE, C. K., MCCARROLL, D., NESJE, A., DAHL, S. O. & STONE, J. O. 1998. The last ice sheet in North-West Scotland: reconstruction and implications. *Quaternary Science Reviews*, 17, 1149-1184.
- BALLANTYNE, C. K. & STONE, J. O. 2012. Did large ice caps persist on low ground in north-west Scotland during the Lateglacial Interstade? *Journal of Quaternary Science*, 27, 297-306.
- BALLANTYNE, C. K. & SUTHERLAND, D. G. 1987. *Wester Ross: Field Guide*, Cambridge, Quaternary Research Association.
- BALLANTYNE, C. K. & WHITTINGTON, G. 1987. Niveo-aeolian sand deposits on An Teallach, Wester Ross, Scotland. *Earth and Environmental Science Transactions of the Royal Society of Edinburgh*, 78, 51-63.
- BENN, D. I. 1994. Fluted moraine formation and till genesis below a temperate valley glacier: Slettmarkbreen, Jotunheimen, southern Norway. *Sedimentology*, 41, 279-292.
- BENN, D. I. & EVANS, D. J. A. 2010. *Glaciers and Glaciation*, London, Hodder Education.
- BGS. 2002. *Loch Eriboll. Scotland Sheet 114W. Solid Geology*. Keyworth: British Geological Survey.
- BGS. 2007. *Scotland Special Sheet Assynt Bedrock*. Keyworth: British Geological Survey.
- BGS. 2008. *S101E - Ullapool*, 1:50,000. Keyworth: British Geological Survey.
- BGS. 2011. *Summer Isles*. Keyworth.
- BGS. 2012. *S102W - Oykel*, 1:50,000. Keyworth: British Geological Survey.
- BINDSCHADLER, R.A., STEPHENSON, S.N., MACAYEAL, D.R. & SHABTAIE, S. 1987. Ice dynamics at the mouth of ice stream B, Antarctica. *Journal of Geophysical Research*, 92 (B9), 8885-8894.
- BIRKS, H. H. 1984. Late-Quaternary pollen and plant macrofossil stratigraphy at Lochan an Druim, north-west Scotland. In: LUND, E. Y. H. A. J. W. G. (ed.) *Lake Sediments and Environmental History*. Leicester: Leicester University Press.
- BLAKE, W. 1999. Glaciated landscapes along Smith Sound, Ellesmere Island, Canada and Greenland. *Annals of Glaciology*, 28, 40-46.
- BORGSTRÖM, I. 1999. Basal ice temperatures during late Weichselian deglaciation: comparison of landform assemblages in west-central Sweden. *Annals of Glaciology*, 28, 9-15.
- BOULTON, G. & HAGDORN, M. 2006. Glaciology of the British Isles Ice Sheet during the last glacial cycle: form, flow, streams and lobes. *Quaternary Science Reviews*, 25, 3359-3390.
- BRADWELL, T. 2005. Bedrock megagrooves in Assynt, NW Scotland. *Geomorphology*, 65, 195-204.
- BRADWELL, T. 2006. The Loch Lomond Stadial glaciation in Assynt: A reappraisal. *Scottish Geographical Journal*, 122, 274-292.
- BRADWELL, T. 2013. Identifying palaeo-ice-stream tributaries on hard beds: mapping glacial bedforms and erosion zones in NW Scotland. *Geomorphology*, 201, 397-414.

- BRADWELL, T., FABEL, D., STOKER, M., MATHERS, H., MCHARGUE, L. & HOWE, J. 2008a. Ice caps existed throughout the Lateglacial Interstadial in northern Scotland. *Journal of Quaternary Science*, 23, 401-407.
- BRADWELL, T. & KRABBENDAM, M. 2003. Stac Pollaidh - a Late Devensian Nunatak? *Quaternary Newsletter* : 19-25.
- BRADWELL, T., STOKER, M. & KRABBENDAM, M. 2008b. Megagrooves and streamlined bedrock in NW Scotland: The role of ice streams in landscape evolution. *Geomorphology*, 97, 135-156.
- BRADWELL, T., STOKER, M. & LARTER, R. 2007. Geomorphological signature and flow dynamics of The Minch palaeo-ice stream, northwest Scotland. *Journal of Quaternary Science*, 22, 609-617.
- BRADWELL, T. & STOKER, M. S. 2014. Detailed ice sheet retreat pattern around Northern Scotland revealed by marine geophysical surveys. *Earth and Environmental Science Transactions of the Royal Society of Edinburgh*, 105.
- BRADWELL, T., STOKER, M. S., GOLLEDGE, N. R., WILSON, C. K., MERRITT, J. W., LONG, D., EVEREST, J. D., HESTVIK, O. B., STEVENSON, A. G., HUBBARD, A. L., FINLAYSON, A. G. & MATHERS, H. E. 2008c. The northern sector of the last British Ice Sheet: Maximum extent and demise. *Earth-Science Reviews*, 88, 207-226.
- BRINER, J. P., MILLER, G. H., DAVIS, P. T., BIERMAN, P. R. & CAFFEE, M. 2003. Last Glacial Maximum ice sheet dynamics in Arctic Canada inferred from young erratics perched on ancient tors. *Quaternary Science Reviews*, 22, 437-444.
- BRINER, J. P., MILLER, G. H., DAVIS, P. T. & FINKEL, R. C. 2006. Cosmogenic radionuclides from fiord landscapes support differential erosion by overriding ice sheets. *Geological Society of America Bulletin*, 118, 406-420.
- BROOK, M. S., KIRKBRIDE, M. P. & BROCK, B. W. 2004. Rock strength and development of glacial valley morphology in the Scottish Highlands and Northwest Iceland. *Geografiska Annaler: Series A, Physical Geography*, 86, 225-234.
- CHARLESWORTH, J. K. 1955. XIX.—The Late-glacial History of the Highlands and Islands of Scotland. *Earth and Environmental Science Transactions of the Royal Society of Edinburgh*, 62, 769-928.
- CLARHALL, A. & KLEMAN, J. 1999. Distribution and glaciological implications of relict surfaces on the Ultevis plateau, northwestern Sweden. *Annals of Glaciology*, 28, 202-208.
- CLARK, C. D., HUGHES, A. L. C., GREENWOOD, S. L., JORDAN, C. & SEJRUP, H. P. 2012. Pattern and timing of retreat of the last British-Irish Ice Sheet. *Quaternary Science Reviews*, 44, 112-146.
- CLARKE, G.K. 1987. fast Glacier Flow: Ice Streams, surging, and tidewater glaciers. *Journal of Geophysical Research*, 92 (B9), 8835-8841.
- CONWAY, H., CATANIA, G., RAYMOND, C. F., GADES, A. M., SCAMBOS, T. A. & ENGELHARDT, H. 2002. Switch of flow direction in an Antarctic ice stream. *Nature*, 419, 465-467.

- DE ANGELIS, H. & KLEMAN, J. 2005. Palaeo-ice streams in the northern Keewatin sector of the Laurentide ice sheet. *Annals of Glaciology*, 42, 135-144.
- DENTON, G. H. & HUGHES, T. J. 1981. *The Last Great Ice Sheets*, New York, Wiley Interscience.
- DOWDESWELL, J. A., OTTESEN, D. & RISE, L. 2006. Flow switching and large-scale deposition by ice streams draining former ice sheets. *Geology*, 34, 313-316.
- DOWDESWELL, J.A., O'COFAIGH, C., TAYLOR, J., KENYON, N.H., MIENERT, J., WILKEN, M., 2002. On the architecture of high-latitude continental margins: the influence of icesheet and sea-ice processes in the Polar North Atlantic. *Special Publications of the Geological Society of London*, 203, 33-54.
- DUNAI, T. J. 2010. *Cosmogenic Nuclides: Principles, Concepts, and Applications in the Earth Surface Sciences*, Cambridge, Cambridge University Press.
- DYKE, A. S. & MORRIS, T. F. 1988. Drumlin fields, dispersal trains, and ice streams in Arctic Canada. *Canadian Geographer / Le Géographe canadien*, 32, 86-90.
- EBERT, K. & HÄTTESTRAND, C. 2010. The impact of Quaternary glaciations on inselbergs in northern Sweden. *Geomorphology*, 115, 56-66.
- EBERT, K., WILLENBRING, J., NORTON, K. P., HALL, A. & HÄTTESTRAND, C. 2012. Meteoric ^{10}Be concentrations from saprolite and till in northern Sweden: Implications for glacial erosion and age. *Quaternary Geochronology*, 12, 11-22.
- EULER, T. & HERGET, J. 2012. Controls on local scour and deposition induced by obstacles in fluvial environments. *CATENA*, 91, 35-46.
- EVANS, D.J., REA, B.R., HANSOM, J.D. & WHALLEY, W.B. 2002. Geomorphology and style of plateau icefield deglaciation in fjord terrains: the example of Troms-Finmark, north Norway. *Journal of Quaternary Science*, 17(3), 221-239.
- EVEREST, J., BRADWELL, T. & GOLLEDGE, N. 2005. Scottish Landform Examples: Subglacial landforms of the Tweed palaeo-ice stream. *Scottish Geographical Journal*, 121, 163-173.
- EVEREST, J., BRADWELL, T., STOKER, M. S. & DEWEY, S. 2012. New age constraints for the maximum extent of the last British-Irish Ice Sheet (NW sector). *Journal of Quaternary Science*, 28(1), 2-7.
- EVEREST, J. D., BRADWELL, T., FOGWILL, C. J. & KUBIK, P. W. 2006. Cosmogenic ^{10}Be Age Constraints for The Wester Ross Readvance Moraine: Insights into British ice-sheet behaviour. *Geografiska Annaler: Series A, Physical Geography*, 88, 9-17.
- FABEL, D. 2012. Towards a ^{10}Be production rate for Scotland. *Quaternary International*, 279-280(0), 136.
- FABEL, D., BALLANTYNE, C. K. & XU, S. 2012. Trimlines, blockfields, mountain-top erratics and the vertical dimensions of the last British-Irish Ice Sheet in NW Scotland. *Quaternary Science Reviews*, 55, 91-102.

- FABEL, D. & HARBOR, J. 1999. The use of in-situ produced cosmogenic radionuclides in glaciology and glacial geomorphology. *Annals of Glaciology*, 28, 103-110.
- FENTON, C.R., HERMANN, R.L., BLIKRA, L.H., KUBIK, P.W., BRYANT, C., NIEDERMANN, S., MEIXNER, A. & GOETHALS, M.M. 2011. Regional ^{10}Be production rate calibration for the past 12 ka deduced from the radiocarbon-dated Grøtlandsura and Russenes rock avalanches at 69° N, Norway. *Quaternary Geochronology*, 6, 437-452.
- FINLAYSON, A. & BRADWELL, T. 2008. Morphological characteristics, formation and glaciological significance of Rogen moraine in northern Scotland. *Geomorphology*, 101, 607-617.
- FINLAYSON, A., FABEL, D., BRADWELL, T. & SUGDEN, D. 2014. Growth and decay of a marine terminating sector of the last British-Irish Ice Sheet: a geomorphological reconstruction. *Quaternary Science Reviews*, 83, 28-45.
- FINLAYSON, A., GOLLEDGE, N., BRADWELL, T. O. M. & FABEL, D. 2011. Evolution of a Lateglacial mountain icecap in northern Scotland. *Boreas*, 40, 536-554.
- GELLATLY, A.F., WHALLEY, W.B., GORDON, J.E., HANSOM, J. D. & TAVIGG, D. S. 1989. Recent glacial history and climatic change, Bergsfjord, Troms-Finnmark, Norway. *Norsk Geografisk Tidsskrift - Norwegian Journal of Geography*, 43:1, 19-30.
- GELLATLY, A. F., GORDON, J. E., WHALLEY, W. B. & HANSOM, J. D. 1988. Thermal regime and geomorphology of plateau ice caps in northern Norway: Observations and implications. *Geology*, 16, 983-986.
- GHEORGHIU, D.M., FABEL, D., HANSOM, J.D. & XU, S. 2012. Lateglacial surface exposure dating in the Monadhliath MOUNTAINS, Central Highlands, Scotland. *Quaternary Science Reviews*, 41, 132-146.
- GLASSER, N. F. 1995. Modelling the effect of topography on Ice Sheet Erosion, Scotland. *Geografiska Annaler: Series A, Physical Geography*, 77, 67-82.
- GODARD, A. 1965. *Recherches de Géomorphologie en Écosse du Nord-Ouest*. Publications de la Faculté des Lettres, Université de Strasbourg.
- GOEHRING, B.M., LOHNE, O.S., MANGERUD, J., SVENDSEN, J.I., GYLLENCREUTZ, R., SCHAFFER, J. & FINKEL, R. 2012. Late Glacial and Holocene ^{10}Be production rates for western Norway. *Journal of Quaternary Science*, 27(1), 89-96.
- GOLLEDGE, N. R. & STOKER, M. S. 2006. A palaeo-ice stream of the British Ice Sheet in eastern Scotland. *Boreas*, 35, 231-243.
- GOODFELLOW, B. W. 2007. Relict non-glacial surfaces in formerly glaciated landscapes. *Earth-Science Reviews*, 80, 47-73.
- GORDON, J. E. 1981. Ice-Scoured Topography and Its Relationships to Bedrock Structure and Ice Movement in Parts of Northern Scotland and West Greenland. *Geografiska Annaler. Series A, Physical Geography*, 63, 55-65.
- GOSSE, J. C. & PHILLIPS, F. M. 2001. Terrestrial in situ cosmogenic nuclides: theory and application. *Quaternary Science Reviews*, 20, 1475-1560.

- GRAHAM, D. K., HARLAND, R., GREGORY, D.M., LONG, D. & MORTON, A.C. 1990. The biostratigraphy and chronostratigraphy of BGS Borehole 78/4, North Minch. *Scottish Journal of Geology*, 26, 65-75.
- GREENWOOD, S. L., CLARK, C. D. & HUGHES, A. L. C. 2007. Formalising an inversion methodology for reconstructing ice-sheet retreat patterns from meltwater channels: application to the British Ice Sheet. *Journal of Quaternary Science*, 22, 637-645.
- HALL, A. 2007. The significance of tors in glaciated lands: a view from the British Isles. In: ANDRE, M. F. (ed.) *Du continent au bassin versant : theories et pratiques en g?ographie physique (Hommage au Professeur Alain Godard)*. Presses Universitaires Blaise-Pascal.
- HALL, A. M., EBERT, K. & HÄTTESTRAND, C. 2012. Pre-glacial landform inheritance in a glaciated shield landscape. *Geografiska Annaler: Series A, Physical Geography*, 95(1), 33-49.
- HALL, A. M. & GLASSER, N. F. 2003. Reconstructing the basal thermal regime of an ice stream in a landscape of selective linear erosion: Glen Avon, Cairngorm Mountains, Scotland. *Boreas*, 32, 191-207.
- HALL, A. M. & MELLOR, A. 1988. The characteristics and significance of deep weathering in the Gaick Area, Grampian Highlands, Scotland. *Geografiska Annaler: Series A, Physical Geography*, 70, 309-314.
- HALL, A. M., PEACOCK, J. D. & CONNELL, E. R. 2003. New data for the Last Glacial Maximum in Great Britain and Ireland: a Scottish perspective on the paper by Bowen et al. (2002). *Quaternary Science Reviews*, 22, 1551-1554.
- HALL, A. M. & PHILLIPS, W. M. 2006. Glacial modification of granite tors in the Cairngorms, Scotland. *Journal of Quaternary Science*, 21, 811-830.
- HALL, A. M. & SUGDEN, D. E. 1987. Limited modification of mid-latitude landscapes by ice sheets: The case of northeast Scotland. *Earth Surface Processes and Landforms*, 12, 531-542.
- HÄTTESTRAND, C., GOODWILLIE, D. & KLEMAN, J. 1999. Size distribution of two cross-cutting drumlin systems in northern Sweden: a measure of selective erosion and formation time length. *Annals of Glaciology*, 28, 146-152.
- HAYNES, V. M. 1977. The modification of valley patterns by ice-sheet activity. *Geografiska Annaler. Series A, Physical Geography*, 59, 195-207.
- HEISINGER, B., LAL, D., JULL, A. J. T., KUBIK, P., IVY-OCHS, S., NEUMAIER, S., KNIE, K., LAZAREV, V. & NOLTE, E. 2002. Production of selected cosmogenic radionuclides by muons: 1. Fast muons. *Earth and Planetary Science Letters*, 200, 345-355.
- HINDMARSH, R. C. A. 2001. Influence of channelling on heating in ice-sheet flows. *Geophysical Research Letters*, 28, 3681-3684.
- HUBBARD, A., BRADWELL, T., GOLLEDGE, N., HALL, A., PATTON, H., SUGDEN, D., COOPER, R. & STOKER, M. 2009. Dynamic cycles, ice streams and their impact on the extent, chronology and deglaciation of the British-Irish ice sheet. *Quaternary Science Reviews*, 28, 758-776.
- IPCC 2013. IPCC, 2013: Summary for Policymakers. In: STOCKER, T. F., QIN, D., PLATTNER, G.-K., TIGNOR, M., ALLEN, S. K., BOSCHUNG, J., NAUELS, A.,

- XIA, Y., BEX, V. & MIDGLEY, P. M. (eds.) *Climate Change 2013: The Physical Science Basis. Contribution of Working Group I to the Fifth Assessment Report of the Intergovernmental Panel on Climate Change*. Cambridge, UK & New York, NY, USA.: Cambridge University Press.
- JANSSON, K. N. & KLEMAN, J. 1999. The horned crag-and-tails of the Ungava Bay landform swarm, Quebec/Labrador, Canada. *Annals of Glaciology*, 28, 168-174.
- KING, A.M. & WHEELER, P.T. 1963. the raised beaches of the north coast of Sutherland, Scotland. *Geological Magazine*, 100 (4), 299-320.
- KING, E. L., HAFLIDASON, H., SEJRUP, H. P. & LOVLIE, R. 1998. Glacigenic debris flows on the North Sea Trough Mouth Fan during ice stream maxima. *Marine Geology*, 152, 217-246.
- KIRK, W. & GODWIN, H. 1963. A late glacial site at Loch Droma, Ross and Cromarty. *Transactions of the Royal Society of Edinburgh*, 65, 225-249.
- KIRK, W., RICE, R.J. & SYNGE, F.M. 1966. Deglaciation and vertical displacement of shorelines in Wester and Easter Ross.
- KITCHENER, A. C. & BONSALL, C. 1997. AMS radiocarbon dates on some extinct Scottish mammals. *Quaternary Newsletter*, 83, 1-11.
- KLEMAN, J. 1992. The palimpsest glacial landscape in Northwestern Sweden. Late Weichselian deglaciation landforms and traces of older west-centered ice sheets. *Geografiska Annaler. Series A, Physical Geography*, 74, 305-325.
- KLEMAN, J. & BORGSTROM, I. 1990. The boulder fields of Mt. Fulufjället, west-central Sweden - Late Weichselian boulder blankets and interstadial periglacial phenomena. *Geografiska Annaler. Series A, Physical Geography*, 72, 63-78.
- KLEMAN, J. & GLASSER, N. F. 2007. The subglacial thermal organisation (STO) of ice sheets. *Quaternary Science Reviews*, 26, 585-597.
- KLEMAN, J., HATTESTRAND, C., BORGSTROM, I. & STROEVEN, A. P. 1997. Fennoscandian paleoglaciology reconstructed using a glacial geological inversion model. *Journal of Glaciology*, 43, 283-299.
- KLEMAN, J., HOLMLUND, P. & JANSSON, P. 1999a. Preface. *Annals of Glaciology*, 28, v-vi.
- KLEMAN, J., HATTESTRAND, C., CLARKE, A. 1999b. Zooming in on frozen-bed patches: scale-dependent controls on Fennoscandian ice sheet basal thermal zonation. *Annals of Glaciology*, 28, 189-194.
- KNUTZ, P.C., AUSTIN, W.E.N., JONES, E.J.W. 2001. Millennial-scale depositional cycles related to British Ice Sheet variability and North Atlantic paleocirculation since 45 kyr B.P., Barra Fan, U.K. margin. *Paleocenography*, 16, 53-64.
- KRABBENDAM, M. & BRADWELL, T. 2011. Lateral plucking as a mechanism for elongate erosional glacial bedforms: explaining megagrooves in Britain and Canada. *Earth Surface Processes and Landforms*, 36, 1335-1349.

- KRABBENDAM, M. & GLASSER, N. F. 2011. Glacial erosion and bedrock properties in NW Scotland: Abrasion and plucking, hardness and joint spacing. *Geomorphology*, 130, 374-383.
- LAWSON, T. J. 1990. Former ice movement in Assynt, Sutherland, as shown by the distribution of glacial erratics. *Scottish Journal of Geology*, 26, 25-32.
- LAWSON, T. J. 1995. *The Quaternary of Assynt & Coigach: Field Guide*, Cambridge, Quaternary Research Association.
- LAWSON, T. J. 1996. Glacial striae and former ice movement: the evidence from Assynt, Sutherland. *Scottish Journal of Geology*, 32, 59-65.
- LAWSON, T. J. 2010. The Allt nan Uamh valley and its caves: Their significance for the chronology of glaciation and deglaciation of Northern Scotland. In: LUKAS, S. & BRADWELL, T. (eds.) *The Quaternary of Western Sutherland and adjacent areas: Field Guide*. London: Quaternary Research Association.
- LINTON, D. L. 1949. Watershed breaching by ice in Scotland. *Transactions and Papers (Institute of British Geographers)*, 1-16.
- LINTON, D. L. 1955. The Problem of Tors. *The Geographical Journal*, 121, 470-487.
- LINTON, D. L. 1963. The Forms of Glacial Erosion. *Transactions and Papers (Institute of British Geographers)*, 1-28.
- LOWE, J. J., RASMUSSEN, S. O., BJÖRCK, S., HOEK, W. Z., STEFFENSEN, J. P., WALKER, M. J. C. & YU, Z. C. 2008. Synchronisation of palaeoenvironmental events in the North Atlantic region during the Last Termination: a revised protocol recommended by the INTIMATE group. *Quaternary Science Reviews*, 27, 6-17.
- LUKAS, S. & BRADWELL, T. 2010a. *The Quaternary of Western Sutherland and Adjacent Areas: Field Guide*, London, Quaternary Research Association.
- LUKAS, S. & BRADWELL, T. 2010b. Reconstruction of a Lateglacial (Younger Dryas) mountain ice field in Sutherland, northwestern Scotland, and its palaeoclimatic implications. *Journal of Quaternary Science*, 25, 567-580.
- MACLEOD, A., PALMER, A., LOWE, J., ROSE, J., BRYANT, C. & MERRITT, J. 2011. Timing of glacier response to Younger Dryas climatic cooling in Scotland. *Global and Planetary Change*, 79, 264-274.
- MADEN, C., ANASTASI, P. A. F., DOUGANS, A., FREEMAN, S. P. H. T., KITCHEN, R., KLODY, G., SCHNABEL, C., SUNDQUIST, M., VANNER, K. & XU, S. 2007. SUERC AMS ion detection. *Nuclear Instruments and Methods in Physics Research Section B: Beam Interactions with Materials and Atoms*, 259, 131-139.
- MATHER, A. S. & RITCHIE, W. 1977. *The beaches of the Highlands and Islands of Scotland*, Perth, Countryside Commission for Scotland.
- MCCARROLL, D., BALLANTYNE, C. K., NESJE, A. & DAHL, S. O. 1995b. Nunataks of the last ice sheet in northwest Scotland. *Boreas*, 24, 305-323.
- MERRITT, J. W., AUTON, C. A. & FIRTH, C. R. 1995. Ice-proximal glaciomarine sedimentation and sea-level change in the Inverness area, Scotland: A review of the deglaciation of a major ice stream of the British Late Devensian ice sheet. *Quaternary Science Reviews*, 14, 289-329.

- NORTH GREENLAND ICE CORE PROJECT MEMBERS. 2004. High-resolution record of Northern Hemisphere climate extending into the last interglacial period. *Nature*, 431, 7005, 147-151.
- NYE, J. F. 1957. The distribution of stress and velocity in glaciers and ice-sheets. *Proceedings of the Royal Society of London. Series A. Mathematical and Physical Sciences*, 239, 113-133.
- Ó COFAIGH, C., DOWDESWELL, J. A., ALLEN, C. S., HIEMSTRA, J. F., PUDSEY, C. J., EVANS, J. & J.A. EVANS, D. 2005. Flow dynamics and till genesis associated with a marine-based Antarctic palaeo-ice stream. *Quaternary Science Reviews*, 24, 709-740.
- Ó COFAIGH, C., PUDSEY, C. J., DOWDESWELL, J. A. & MORRIS, P. 2002. Evolution of subglacial bedforms along a paleo-ice stream, Antarctic Peninsula continental shelf. *Geophysical Research Letters*, 29, 41-1-41-4.
- PATTERSON, C. J. & BOERBOOM, T. J. 1999. The significance of pre-existing, deeply weathered crystalline rock in interpreting the effects of glaciation in the Minnesota River valley, U.S.A. *Annals of Glaciology*, 28, 53-58.
- PAYNE, A. J., VIELI, A., SHEPHERD, A. P., WINGHAM, D. J. & RIGNOT, E. 2004. Recent dramatic thinning of largest West Antarctic ice stream triggered by oceans. *Geophysical Research Letters*, 31, L23401.
- PEACH, B. N. & HORNE, J. 1892. The ice shed in the NW Highlands during the maximum glaciation. *Reports of the British Association*, 720.
- PECK, V. L., HALL, I. R., ZAHN, R., ELDERFIELD, H., GROUSSET, F., HEMMING, S. R. & SCOURSE, J. D. 2006. High resolution evidence for linkages between NW European ice sheet instability and Atlantic Meridional Overturning Circulation. *Earth and Planetary Science Letters*, 243, 476-488.
- PENNINGTON, W. 1975. A chronostratigraphic comparison of Late-Weichselian and Late-Devensian subdivisions, illustrated by two radiocarbon-dated profiles from western Britain. *Boreas*, 4, 157-171.
- PENNINGTON, W. 1977a. Lake sediments and the Lateglacial environment in northern Scotland. In: LOWE, J. M. G. A. J. J. (ed.) *Studies in the Scottish Lateglacial Environment*, Oxford: Pergamon Press, 119-142.
- PENNINGTON, W. 1977b. The Late Devensian flora and vegetation of Britain. *Philosophical Transactions of the Royal Society*, 280B, 247-271.
- PENNINGTON, W., TUTIN, T. G., HAWORTH, E. Y., BONNY, A. P. & LISHMAN, J. P. 1972. Lake Sediments in Northern Scotland. *Philosophical Transactions of the Royal Society of London. B, Biological Sciences*, 264, 191-294.
- PHILLIPS, W. 2001. A review of cosmogenic nuclide surface exposure dating: ne challenges for Scottish geomorphology. *Scottish Geographical Journal*, 117:1, 1-15.
- PHILLIPS, W. M., HALL, A. M., BALLANTYNE, C. K., BINNIE, S., KUBIK, P. W. & FREEMAN, S. 2008. Extent of the last ice sheet in northern Scotland tested with cosmogenic ¹⁰Be exposure ages. *Journal of Quaternary Science*, 23, 101-107.
- PRICE, S. F., BINDSCHADLER, R. A., HULBE, C. L. & JOUGHIN, I. R. 2001. Post-stagnation behavior in the upstream regions of Ice Stream C, West Antarctica. *Journal of Glaciology*, 47, 283-294.

- PRITCHARD, H. D., ARTHERN, R. J., VAUGHAN, D. G. & EDWARDS, L. A. 2009. TI - Extensive dynamic thinning on the margins of the Greenland and Antarctic ice sheets. *Nature*, 461, 971 - 975.
- REA, B. R. & EVANS, D. J. 1996. Landscapes of areal scouring in NW Scotland. *The Scottish Geographical Magazine*, 112, 47-50.
- REA, B. R., EVANS, D. J. A., DIXON, T. S. & WHALLEY, W. B. 2000. Contemporaneous, localized, basal ice-flow variations: implications for bedrock erosion and the origin of p-forms. *Journal of Glaciology*, 46, 470-476.
- ROBINSON, M. & BALLANTYNE, C. K. 1979. Evidence for a glacial readvance pre-dating the Loch Lomond Advance in Wester Ross. *Scottish Journal of Geology*, 15, 271-277.
- SCHAEFER, J. M. & LIFTON, N. 2007. Cosmogenic nuclides dating/methods. In: ELIAS, S. A. (ed.) *Encyclopedia of Quaternary Science*. Amsterdam: Elsevier.
- SCOURSE, J. D., HAAPANIEMI, A. I., COLMENERO-HIDALGO, E., PECK, V. L., HALL, I. R., AUSTIN, W. E. N., KNUTZ, P. C. & ZAHN, R. 2009. Growth, dynamics and deglaciation of the last British-Irish ice sheet: the deep-sea ice-rafted detritus record. *Quaternary Science Reviews*, 28, 3066-3084.
- SHABTAIE, S. 1987. The morphology of ice streams A,B and C, west Antarctica, and their environs. *Journal of Geophysical Research*, 92 (B9), 8865-8883.
- SHENNAN, I., BRADLEY, S. MILNE, G., BROOKS, A., BASSETT, S. & HAMILTON, S. 2006. Relative sea-level changes, glacial isostatic modelling and ice-sheet reconstructions from the British Isles since the Last Glacial Maximum. *Journal of Quaternary Science*, 21, 585-599.
- SHENNAN, I., LAM, BECK, K. HORTON, B., INNES, J., LLOYD, J., MCARTHUR, J., PURCELL, T. & RUTHERFORD, M. 2000. Late Devensian and Holocene records of relative sea-level changes in northwest Scotland and their implications for glacio-hydro-isostatic modelling. *Quaternary Science Reviews*, 19, 1103-1135.
- STOKER, M., BRADWELL, T., WILSON, C., HARPER, C., SMITH, D. & BRETT, C. 2006. Pristine fjord landsystem revealed on the sea bed in the Summer Isles region, NW Scotland. *Scottish Journal of Geology*, 42, 89-99.
- STOKER, M. S. & BRADWELL, T. 2005. The Minch palaeo-ice stream, NW sector of the British-Irish Ice Sheet. *Journal of the Geological Society*, 162, 425-428.
- STOKER, M. S., HITCHEN, K. & GRAHAM, C. C. 1993. United Kingdom offshore regional report: the geology of the Hebrides and West Shetland shelves and adjacent deep-water areas. In: BRITISH & SURVEY, G. (eds.). London: British Geological Survey.
- STOKES, C. R. & CLARK, C. D. 1999. Geomorphological criteria for identifying Pleistocene ice streams. *Annals of Glaciology*, 28, 67-74.
- STONE, J. O. 2000. Air pressure and cosmogenic isotope production. *Journal of Geophysical Research: Solid Earth*, 105, 23753-23759.

- STONE, J. O. & BALLANTYNE, C. K. 2006. Dimensions and deglacial chronology of the Outer Hebrides Ice Cap, northwest Scotland: implications of cosmic ray exposure dating. *Journal of Quaternary Science*, 21, 75-84.
- STONE, J. O., BALLANTYNE, C. K. & FIFIELD, K. 1998. Exposure dating and validation of periglacial weathering limits, northwest Scotland. *Geology*, 26, 587-590.
- STROEVEN, A. P., FABEL, D., HARBOR, J., HÄTTESTRAND, C. & KLEMAN, J. 2002. Quantifying the erosional impact of the Fennoscandian ice sheet in the Torneträsk-Narvik corridor, northern Sweden, based on cosmogenic radionuclide data. *Geografiska Annaler: Series A, Physical Geography*, 84, 275-287.
- STROEVEN, A. P., HARBOR, J. & HEYMAN, J. 2013. Glacial Erosion - Process and form: Erosional landscapes. In: SHRODER, J. F., Giardino, J.R., Harbor, J.M. (eds.) *Treatise on Geomorphology, Volume 8: Glacial and periglacial geomorphology*, 100-112. San Diego: Academic Press.
- SUGDEN, D. E. 1968. The selectivity of glacial erosion in the Cairngorm Mountains, Scotland. *Transactions of the Institute of British Geographers*, 45, 79-92.
- SUGDEN, D. E. 1978. Glacial erosion by the Laurentide ice sheet. *Journal of Glaciology*, 83, 367-391.
- SUGDEN, D. E. & JOHN, B. S. 1976. *Glaciers and landscape: a geomorphological approach*, London, Edward Arnold.
- SUGDEN, D. E. & WATTS, S. H. 1977. Tors, felsenmeer, and glaciation in northern Cumberland Peninsula, Baffin Island. *Canadian Journal of Earth Sciences*, 14, 2817-2823.
- VAUGHAN, D. G., CORR, H. F. J., SMITH, A. M., PRITCHARD, H. D. & SHEPHERD, A. 2008. Flow-switching and water piracy between Rutford Ice Stream and Carlson Inlet, West Antarctica. *Journal of Glaciology*, 54, 41-48.
- WELLNER, J. S., LOWE, A. L., SHIPP, S. S. & ANDERSON, J. B. 2001. Distribution of glacial geomorphic features on the Antarctic continental shelf and correlation with substrate: implications for ice behavior. *Journal of Glaciology*, 47, 397-411.
- WHILLANS, I.M., BOLZAN, J. & SHABTAIE, S. 1987 Velocity of ice streams B and C, Antarctica. *Journal of Geophysical Research*, 92 (B9), 8895-8902.

APPENDIX 1:

University of Glasgow
Geographical and Earth Sciences

Mineral Separation
and
Quartz Cleaning

Mineral Separation and
Geochemistry Laboratories
4th Floor, Gregory Building

Procedures

Manual

Table of Contents

Table of Contents	2
Security	4
Manual Handling	4
Resource Use, Waste Minimisation and Recycling	4
General Laboratory Practice	5
Personal protective equipment (PPE) requirements	5
Safety Considerations	6
Sample handling and laboratory practice	7
Some general suggestions	7
Laboratory Cleanliness	8
Contamination	8
Washing up	8
Teflon	8
Glassware	9
Common Reagents	10
Parent acids	10
Working acids	10
Chemicals	12
Glass	12
Quartz Cleaning	13
Initial Quartz Cleaning	13
Summary	13
Sample crushing, milling, sieving and washing	15
PROCEDURE	15
HCl/HNO ₃ leaching to remove carbonates and metals	15
PROCEDURE	15
Floatation of feldspars and mica	15
PROCEDURE	16
Magnetic separation	16
PROCEDURE	16
Aluminosilicate dissolution in pyrophosphoric acid	17
PROCEDURE	17
HF leaching to remove feldspar and remove meteoric ¹⁰ Be	18
	2

GU quartz separation and purification for cosmogenic nuclide analysis

PROCEDURE _____	18
HF leaching _____	18
Sample recovery _____	19
Aluminium Determination from a Mineral Aliquot (MA) _____	20
PROCEDURE _____	20
Cosmogenic Al and Be Chemistry Induction Checklist _____	21

Security

The laboratory must be locked whenever unattended. If you leave the laboratory and there is no one else there, lock the door as you leave.

If you see anyone you don't know behaving suspiciously in the laboratory or the building, ask them what they are doing. Report any suspicious persons to the laboratory supervisor or Campus Security (ext. 4284).

Manual Handling

A manual handling risk assessment form must be completed before undertaking any task with a significant manual handling risk; this must be done in consultation with the laboratory supervisor and the Safety Officer.

Always consider the risk of manual handling before you lift or move large or heavy items; this applies to items in the field as well as in the laboratory. If possible, subdivide items into smaller lots before moving them (ie., boxes of rock samples). If you have any doubts about your ability to move an item, get someone else to assist you. Numerous trolleys are available throughout the Department for moving large or heavy items.

Resource Use, Waste Minimisation and Recycling

Always be aware of the environmental implications of your activities in the laboratory and in the field. Minimising the amount of consumables that you use conserves resources and greatly reduces waste. Before you commence a procedure, assess the method you are using and consider any alternatives that might require smaller amounts of chemicals to be used, less water or power, or materials to be reused or recycled. Be particularly careful to minimise 'intractable' waste, ie. substances such as heavy metals that remain detrimental to the environment.

GENERAL LABORATORY PRACTICE

PERSONAL PROTECTIVE EQUIPMENT (PPE) REQUIREMENTS

1. SUITABLE CLOTHING must be worn, long trousers are recommended for all staff and students.
2. PROTECTIVE CLOTHING must be worn for protection in case of fire or chemical spillage. It is usually a knee-length white coat, but for some operations more elaborate protection may be required.
3. SOUND FOOTWEAR must be worn. Thongs, sandals, and other open-style shoes are PROHIBITED.
4. SAFETY GLASSES are compulsory and must be worn at all times.
6. SAFETY GOGGLES or a full-face shield must be worn by persons wearing contact lenses.
7. The storage and/or consumption of FOOD and DRINK in the areas where chemicals are stored and/or used is PROHIBITED.
8. VISITORS to laboratories must wear SAFETY GLASSES at all times.
9. Laboratory coats and other protective clothing are not to be worn in eating and "tea" areas.
10. All accidents/incidents must be reported to the Technical Unit Manager (Yvonne Finlayson, ext. 2325) as soon as possible.

SAFETY CONSIDERATIONS

Hydrofluoric Acid (HF) is lethal, hot HF is worse. Quartz purification requires handling large amounts of concentrated HF. Lab coats and safety glasses are mandatory, and gloves must be worn when handling beakers and bottles. Be alert to drips when pouring HF, and droplets of condensation when opening lids or uncovering beakers. Absolutely no bare feet, or sandals in the lab. Wear long trousers and the apron for protection.

Make sure you read the MSDS and HF Hazard Alert in this folder.

Handle acids in fume hoods. Be sure you know what you're doing before mixing acids (or any reagents, in fact). Mixtures such as concentrated HCl + HNO₃ (aqua regia) evolve toxic chlorine (Cl₂) gas. Mixtures of HCl and oxidisers such as H₂O₂ or NaOCl (hypochlorite bleach) do likewise. Beware of exothermic reaction when diluting acids, especially H₂SO₄.

Always add dense acid to water, not water to acid.

SAMPLE HANDLING AND LABORATORY PRACTICE

Some general suggestions

- Keep reagent containers, wash bottles, etc. separate from sample containers.
- Try not to dispense from wash bottles directly into sample beakers. Splash-back onto the dispenser spout may go unnoticed and can contaminate future samples. Better to transfer reagents to an intermediate beaker and dispense with a clean disposable pipette.
- Always triple-rinse measuring cylinders with MilliQ water before you use them.
- Try not to work over the top of samples. Sit or stand back from work areas. Reach around, not over open beakers when moving them around.
- Handle beakers with gloves at all times.
- Write everything down. Always record sample and beaker numbers when samples are transferred. Keep records in a bound notebook and on the sample data sheets. Don't write on scraps of paper, intending to transcribe.
- Label beakers, centrifuge tubes, etc.
- Order your samples in the numbered beakers, bottles etc. in an easily remembered way. This may save you if you forget to note down a transfer, drop a rack of vials, etc.

LABORATORY CLEANLINESS

Contamination

Dust and soil contain large amounts of ^{10}Be compared to quartz samples. Always try to minimise dust coming into the clean lab (try to avoid trekking dust and soil in on shoes, sports clothes, etc.). Use a dedicated lab coat - not one you use during rock crushing. Cloth fibres also contribute to general lab dirt. Try to avoid wearing sweaters in the lab. Soil samples and rock powders should not be analysed in the clean lab.

Washing up

Wash up used lab ware as soon as you have moved your samples on to the next stage of the chemistry.

PROCEDURE

Teflon

Wearing gloves...

Rinse a couple of times with MilliQ water, to remove soluble sample residues (e.g. Al salts).

Take a kimwipe soaked in alcohol and scour the interior surface thoroughly to remove sticky organic deposits and fine-grained hydrophobic material (e.g. graphitic carbon, Fe, Ti - oxides). These will not be removed by hot acids. Always take care not to scratch Teflon surfaces. Rinse again with MilliQ water.

Put the items in a washing-up beaker containing 10 - 20 % HNO_3 . Cover with a watch glass and heat (just below boiling) overnight. Make sure acid contacts all interior surfaces of the vessels - i.e. none are upside down, trapping air.

Use tongs to remove items from the beaker. Rinse three times in MilliQ water, making sure all interior surfaces are contacted, draining thoroughly between re-fills. The final draining should be done especially carefully.

Dry in the drying oven, either individually or in the collander. Nitric acid dries slowly and any residues not rinsed away will be seen as tiny droplets on vessel surfaces, or as brown oxidation marks in kimwipes placed underneath the items. There should be no acid residue after rinsing.

GU quartz separation and purification for cosmogenic nuclide analysis

Glassware

Wash glassware using a scouring pad. For heavy soiling, soaking in 3 - 5% Decon works well.

COMMON REAGENTS

Parent acids

Name	Formula	Usual strength of concentrated acid	Molarity
Hydrochloric	HCl	36% w/w	11.6 M
Hydrofluoric	HF	40% w/w	29 M
Nitric	HNO ₃	70% w/w	15.8 M
Sulfuric	H ₂ SO ₄	95 - 100% w/w	18 M (= 36N)

Working acids

Label	Uses	Recipe
"2% HNO ₃ "	AAS analysis	20 ml HCl + 980 ml MilliQ water.
"1.2 M HCl"	Cation columns - conditioning, loading and Be elution. Anion columns - pre-cleaning and stripping.	100 ml HCl + 900 ml MilliQ water.
"4 M HCl"	Cation columns - pre-cleaning, Al elution, stripping.	68 ml HCl + 134 ml MilliQ water.
"6 M HCl"	Conversion of samples to chloride form. Anion columns - Al+Be elution for low Ti samples	104 ml HCl + 96 ml MilliQ water.
"0.5 M H ₂ SO ₄ "	Ti elution.	14 ml H ₂ SO ₄ + 486 ml MilliQ water.
"0.2 M H ₂ SO ₄ "	Dry-down and sulphate conversion.	6 ml HNO ₃ + 494 ml MilliQ water.
"1:1 HNO ₃ "	Mild dry-down oxidation's.	Equal parts conc. HNO ₃ + MilliQ water.
"1:1 HClO ₄ "	Severe dry-down oxidation's.	Equal parts conc. HClO ₄ + MilliQ water.

Always add dense acid to water, **not**
water to acid

Waste Disposal

Chemicals

No acid should be poured down the sink. Acids should be neutralised using sodium bicarbonate or sodium hydroxide. Check the pH prior to pouring the neutral solution down the sink. Use ample water.

Do not put HF wastes with other acid wastes. Neutralise HF waste using the designated container and sodium carbonate.

Empty acid containers (Winchesters and HF bottles) should be left to fume dry in the fume hood. When dry, rinse them three times with water and dispose of them in the skip at the back of the Gregory Building.

NOTE: Waste containers often generate heat and pressure...therefore, do not screw lids too tightly on waste containers, as they are liable to explode.

Glass

Waste glass that is free of chemical residues is to be placed in the glass bin under the sink.

QUARTZ CLEANING

*Note: Only persons who have gone through the induction process are allowed to work in the Rock Crushing Room and the Geochemistry Laboratory. Do **NOT** attempt the chemistry unless you have been trained to do so by a qualified person.*

INITIAL QUARTZ CLEANING

Summary

For preparing very pure quartz separates.

Most silicate minerals dissolve faster than quartz in dilute HF and can be etched away to leave a very pure quartz residue. Some quartz is lost - usually ~10% of coarse-grained fractions (500-850 μm) and up to 20-30% of fine-grained fractions (250-500 μm). It is difficult to get good yields from this procedure using grain sizes <250 μm .

The HF leach has the added advantage of dissolving the outermost shell of the quartz grains, as well as etching cracks, where any contamination by meteoric ^{10}Be would be concentrated.

Some minerals will not dissolve (e.g. garnet, zircon, rutile, ilmenite). Fortunately, except for garnet, these are trace constituents of most rocks. Muscovite is the only other common mineral that causes problems. It dissolves at about the same rate as quartz, so the procedure won't concentrate quartz relative to muscovite.

Several techniques are available to remove interfering minerals.

- Magnetic separation can be used to remove most magnetic minerals. Quartz and feldspar are not magnetic and can not be separated in this manner.

GU quartz separation and purification for cosmogenic nuclide analysis

- An initial heavy liquid separation will remove garnet and muscovite (as well as most other mafic silicates and oxide minerals), if present. Heavy liquid separation will not result in complete removal of feldspar from the sample.
- Froth floatation techniques may be more useful. Froth floatation is the most rapid method for removing feldspar and mica from the sample.
- Digestion in phosphoric acid will remove aluminosilicates very efficiently, however it is time consuming and expensive.

Not all rocks need to be processed beyond a HNO_3/HCl leach before HF treatment. Small amounts of zircon, ilmenite, etc. in the final sample do not cause problems in the subsequent Al-Be extraction chemistry.

Sample crushing, milling, sieving and washing

For cosmogenic nuclide dating we require pure quartz with a grainsize of 200 – 500 μm . Samples are usually in the form of rocks that consist of many minerals. The aim of the physical disintegration of the samples is to permit extraction of quartz from among the other minerals.

PROCEDURE

In the rock crushing lab (basement of the Gregory Building), and wearing a dust mask and safety glasses...

- (1) Turn on the dust extraction system.
- (2) Make sure the jaw crusher, grinding mill, and sieves are clean.
- (3) reduce the sample to <1 cm chunks with the jaw crusher
- (4) feed the crushed material into the grinding mill
- (5) separate the sample into 3 size classes: >500 μm , 250-500 μm and <250 μm using the designated stack of sieves. If there is not enough 250-500 μm material repeat step 2 with the >500 μm fraction.
- (6) Transfer the >500 μm and <250 μm size fractions into labelled plastic bags.
- (7) Place the 250-500 μm fraction into a cleaned aluminium dish and rinse out the very fine materials, taking care not to loose the coarser sample material. Continue rinsing until the rinse water remains clear.
- (8) EITHER place the aluminium dish into the drying oven, OR transfer about 100g of the wet sample into a 600ml glass beaker for further processing in the Geochemistry Lab.
- (9) Clean the jaw crusher and grinding mill.
- (10) Carefully clean the sieves, making sure no grains remain in them.

HCl/HNO₃ leaching to remove carbonates and metals

Pre-clean samples in hot 10% HNO₃. All carbonates must be removed before reacting the samples with HF.

PROCEDURE

For samples brought directly to the Geochem. Lab from the Rock Crushing Lab the first 2 steps can be omitted.

- (1) Pour about 100 grams of sample into a glass beaker.
- (2) Wash the sample with water to remove the remaining fines.
- (3) Under the fume hood and wearing gloves add enough 10% HCl/HNO₃ to cover the sample.
- (4) Place the beaker on a hotplate on **LOW** setting and cover it with a watch glass. **Do not heat the sample too vigorously.** Leave the sample overnight.
- (5) Cool the beaker and carefully pour the acid into the hazardous waste container without loosing sample.
- (6) Rinse the sample several times with water and discard the liquid into the hazardous waste container.
- (7) Once the rinse solution is clean dry the sample in the drying oven.

Floatation of feldspars and mica

Separate feldspar and mica from quartz using froth floatation.

GU quartz separation and purification for cosmogenic nuclide analysis

PROCEDURE

- (1) The frothing technique is done with a soda carbonator and a mixture of 1 ml/L acetic acid and 1 g/L lauryl amine in 1 L pure water. The lauryl amine dissolves better in the acetic acid and keeps the pH ~5. This solution is then mixed with 10 L water and then carbonated.
- (2) The quartz must be pre-treated for 1 hour with a 1% solution of hydrofluoric acid. This HF solution changes the surface chemistry of the feldspar/mica and quartz grains making the feldspar/mica hydrophobic and the quartz hydrophilic.
- (3) After 1hr, decant the 1% HF solution, *do not rinse and dry*, and pour the sample material into the large salad bowl.
- (4) Add a few drops of pure eucalyptus oil to the mineral mixture and then the carbonated solution. The eucalyptus oil will hold the bubbles together and it will form a head (like on top of a beer) where the feldspar/mica will be.
- (5) Wait a few seconds to let the solution of carbonated minerals settle down. Then, pour off the feldspar/mica and what is left will be quartz and other heavy minerals. Repeat if necessary.
- (6) Decant the quartz-rich and feldspar-rich fractions into separate labelled drying dishes and dry in the oven.
- (7) Biotite cannot be separated this way, you need to use a magnetic separator.

Magnetic separation

Separate magnetic minerals using the Frantz Magnetic Separator in the Mineral Separation Lab.

PROCEDURE

- (1) Turn on the magnetic separator
- (2) Set the magnetic field strength to 0.1A
- (3) Pour the sample into hopper. Turn on the hopper and chute.
- (4) Collect the magnetic and non-magnetic fractions.
- (5) Turn off the magnetic separator and clean it.
- (6) Turn the magnetic separator on again and set the magnetic field to 0.5A.
- (7) Repeat the magnetic separation using only the non-magnetic fraction derived from Step 4.
- (8) Turn off the magnetic separator and clean it.
- (9) Turn the magnetic separator on again and set the magnetic field strength maximum (1.2A).
- (10) Repeat the magnetic separation using only the non-magnetic fraction derived from Step 4.
- (11) Turn off the magnetic separator and clean it.
- (12) EITHER transfer the separated fractions into labelled plastic bags, OR pour the non-magnetic fraction into a labelled 500ml polyethylene (PE) bottle for treatment by HF leaching.

Aluminosilicate dissolution in pyrophosphoric acid

Pyrophosphoric acid rapidly dissolves aluminosilicates, but only minimally attacks quartz. The acid quite efficiently dissolves feldspars, but is less efficient at removing amphiboles, garnets, and oxides.

PROCEDURE

- (1) Pour ~40 g of sample into a 1000ml round flask with a flat bottom. Tie a kimwipe around the neck of the flask to stop drips from running down the outside into the heating mantle. Add 400ml 85% ortho-phosphoric acid. Insert the temperature probe connected to the controller into the flask. Make sure the temperature probe does not touch the bottom of the flask. I have it suspended by feeding the probe through a glass funnel and sitting the funnel on the flask like a lid. Set the controller to maintain a temperature of 240°C. Place the flask into a 600W mantle and switch on the controller. The ortho-phosphoric acid must be heated to between 220°C and 250°C to convert to pyrophosphoric acid and dissolve aluminosilicates.
- (2) The controller will heat the acid to ~240°C and keep the acid at that temperature. As the acid heats, the 15% water boils off vigorously. Using a heat glove pick up the flask and swirl it to re-suspend grains deposited on the walls of the flask by the boiling. The acid will continue to boil until it converts to pyrophosphoric acid at 220°C. At this point, boiling subsides and the acid becomes more viscous. Mineral dissolution proceeds rapidly.
- (3) After 30 - 60 minutes of pyrophosphoric acid digestion, turn the power off and remove the flask from the heat and set to cool.
- (4) After ~20 minutes, when the acid has cooled to ~150°C, carefully decant the acid into a beaker containing 500ml of cold tap water. Be careful not to pour out the sample. Dispose of the acid (+/- gel) into the acid hazardous waste container.
- (5) Rinse the flask with hot tap water (60-70°C) to dissolve remaining acid and silica, and decant the rinsate into the beaker and then into the acid hazardous waste container. Rinse repeatedly with water. There will be a film of gelatinized, supersaturated silica solution adhering to the flask and quartz grains, which must be dissolved with sodium hydroxide.
- (6) Add ~200 ml water and ~200 ml sodium hydroxide solution (50%), and boil for 10 minutes using the 600W mantle. **BE CAREFUL** this boiling can be very vigorous. Once the solution has boiled for 10 minutes turn off the power, let the solution cool and decant the solution into the acid waste container. Be careful not to pour out the sample. Rinse repeatedly in water.
- (7) Transfer the sample into a beaker and dry, or alternatively transfer the sample to HF/HCl leaching.
- (8) Clean up glassware and temperature probe with warm water.

HF leaching to remove feldspar and remove meteoric ¹⁰Be

Most silicate minerals dissolve faster than quartz in dilute HF and can be etched away to leave a very pure quartz residue. Some quartz is lost - usually ~10% of coarse-grained fractions (500-850 μm) and up to 20-30% of fine-grained fractions (250-500 μm). It is difficult to get good yields from this procedure using grain sizes <250 μm .

The HF leach has the added advantage of dissolving the outermost shell of the quartz grains, as well as etching cracks, where any contamination by meteoric ¹⁰Be would be concentrated.

PROCEDURE

BEFORE PROCEEDING - WARNING: Contact with hydrofluoric acid is extremely dangerous. Burns from small amounts of concentrated HF (48-50%) can be lethal. Read the safety literature. Wear heavy nitrile gloves, apron, and face shield throughout the following procedure. Wear sturdy clothes and shoes when working with HF and around the HF processing area. Know where the calcium gluconate is kept and how to use it to initiate treatment for any contact with HF. Know where the eyewash stands and emergency shower are located. Wipe up any drops (even suspect droplets) with multiple wet paper wipes and soak under running water for several minutes before discarding. Never dispose of HF-contaminated material in the trash. Neutralise waste solutions in the HF waste container.

HF leaching

- (1) Label a clean 500 ml polyethylene (PE) bottle with the sample name or number.
- (2) Transfer 30-60g of the sample to the bottle.
- (3) Add 450ml of MilliQ water to the bottle.
- (4) In the fume hood add 10ml of 40% HF and 10ml of concentrated HNO₃.
- (5) Gently squeeze the bottle before capping. This gives the contents room to expand when the bottle heats up. Also, loss of vacuum will alert you to the possibility that the bottle has leaked. Check that the bottle is tightly sealed and holding its slight vacuum.
- (6) In the fume hood, gently invert it 3-4 times to mix the contents.
- (7) Mark the bottle to indicate how many times it has been processed.
- (8) Place the bottle in the ultrasonic bath for 72 hours. Gently invert the bottles to mix the contents several times during sonication.

After the first 3-days, change the HF as follows.

- (9) Cool the bottles (if they are warm).
- (10) In the fume hood, uncap the bottle and discard the solution into the HF waste container. Be careful not to pour out the sample.

GU quartz separation and purification for cosmogenic nuclide analysis

- (11) Rinse the remaining grains thoroughly with 3 changes of MilliQ water, decanting off the rinse water into the waste acid container while any clay or fine, milky fluoride precipitate is still suspended, but after "fine sand"-sized grains have settled. Don't worry about losing some of the very fine grains, unless the sample is unusually small.
- (12) Add 2% HF and HNO₃ solution to the bottle just like in the first treatment and repeat the 3-day processing for a second time.

Sample recovery

Pure quartz samples have a uniform appearance and do not cake on the floor of the bottle. Impure samples usually appear speckled and may contain a cloudy fluoride precipitate.

If the sample does not appear pure, repeat the HF leaching for another 3-day period.

If the sample appears pure, recover the sample:

Cool the bottle.

- (1) In the fume hood, uncap the bottle and discard the solution into the HF waste container.
- (2) Rinse with at least 6-8 changes of MilliQ as above. Try to rinse away any trace of milky fluoride. The rinse water must be clear (and absolutely free of residual HF).
- (3) Dry in the oven.
- (4) Cool the samples and transfer them to a labelled ziplock bags.

Aluminium Determination from a Mineral Aliquot (MA)

To assess the purity of the quartz we determine the aluminium content of the cleaned separate. It is essential to obtain the lowest possible Al concentration. The higher the Al concentration, the lower the $^{26}\text{Al}/^{27}\text{Al}$ ratio for measurement, the fewer ^{26}Al nuclides counted and the worse the counting statistics. The Al concentration should preferably be in the range 10 - 100 ppm. A higher concentration generally (though not always) indicates the presence of an impurity such as feldspar, muscovite or an insoluble fluoride residue from the quartz clean-up (e.g. Na_3AlF_6). Note that ~0.5% feldspar gives ~1000 ppm Al.

PROCEDURE

Static charge should always be removed before weighing.

1. Label and weigh a 15 ml Teflon vial and lid on the 4-figure balance. Record the tare weight to 4 decimal places on the sample data sheet. Using a stainless steel spatula, transfer 0.3 - 0.6 g of the sample into the vial. Replace the lid and record the weight. The amount of sample is not too critical, but its weight must be recorded accurately. Be careful when replacing the lid, as static charge may cause small grains to jump up onto the lid or out of the vial. Clean the spatula with a kimwipe (\pm ethanol) before using it for the next sample.
2. When all the samples have been weighed into vials, open the vials in the scrubbed fume hood and add approximately 5 ml of conc. HF and 5 - 10 drops of 1:1 H_2SO_4 .
3. In the fume hood, place the open vials on the edge of the hotplate at low setting for 8 hours. Keep track of which lid belongs to which vial. The quartz will dissolve as the solution slowly evaporates. Increase the heat to fume off HF/ H_2SO_4 . Do not overheat the small flat-bottomed vials, as solutions will boil and damage the hotplate surface. Tilting the hotplate a few degrees by propping up the front will ensure that the solid fluorides crystallise as a small clump in one "corner" of the vial.
4. Once all the HF/ H_2SO_4 has evaporated, the residue should be a small dot of liquid or a dry, white/pale brown speck, containing a few hundred μg total of Al, Fe and Ti fluorides. If any quartz remains (usually only if the original sample was very coarse-grained), **cool the vials** and repeat the procedure with a further 2 - 3 ml of HF and 5 drops of 1:1 H_2SO_4 .
5. Cool the vials. Dissolve the dry residue in 5 ml of 3% HNO_3 (use the Eppendorf 1-5 ml adjustable pipettor and the attachment dedicated to dilute HNO_3). Cap the vials with their original caps and leave to stand (preferably overnight). The residue should dissolve totally to give a clear (or perhaps faintly green) solution.
6. Invert the capped vials a few times to homogenise the solutions, then weigh and record the vial+solution weights.
7. Decant the solutions into labelled centrifuge tubes for AAS or ICP analysis.

Clean the Teflon ware using the procedure outlined in General Lab Practice.

COSMOGENIC AL AND BE CHEMISTRY INDUCTION CHECKLIST

Name:	Date	Initial	Initial of supervisor
.....			
<i>I have read the:</i>			
Laboratory Safety and Procedure Manual			
Department of Geographical and Earth Sciences Safety Manual			
<i>I know the location of and how to use the:</i>			
First aid kit			
Spill kit			
Personal protective equipment (PPE)			
Fire extinguisher			
Danger 'out of service' tags			
MSDS sheets			
<i>I am familiar with the:</i>			
General laboratory rules as they apply to safety			
Protocol with regard to working out-of-hours			
Manual handling procedures			
PPE requirements in this laboratory			
Safe procedure in waste disposal			
Safe procedure in quartz cleaning			

Signed:	
Signed (Supervisor):	

APPENDIX 2:

Glasgow University

Cosmogenic Isotope Laboratory

(Room 8, Scottish Universities Environmental Research
Centre)

Terrestrial in situ cosmogenic
 ^{10}Be and ^{26}Al Chemistry

Procedures

Manual

Table of Contents

Table of Contents	24
Manual Handling	Error! Bookmark not defined.
Resource Use, Waste Minimisation and Recycling	25
General Laboratory Practice	26
Personal protective equipment (PPE) requirements	26
Safety Considerations	27
Sample handling and laboratory practice	28
Some general suggestions	28
Laboratory Cleanliness	29
Contamination	29
Washing up	29
Teflon	29
Ion exchange columns	30
Quartz crucibles, lids and pestles	30
Glassware	31
Bottles used for leaching	31
Cleaning Pt crucible:	31
Common Reagents	34
Parent acids	34
Working acids	34
Waste Disposal	35
Chemicals	35
Glass	35
Cosmogenic ^{10}Be and ^{26}Al Chemistry	36
Initial Quartz Cleaning	36
Summary	36
Sample pre-treatment and loading	37
QUARTZ CLEANING PROCEDURE	37
Aluminium Determination from a Mineral Aliquot (MA)	40
Carrier Addition and Sample Digestion	41
Sample weighing	41
Be carrier addition	41
Sample digestion	42
Splitting for Aluminium Determination	43

Parent Solution Dry Down and Chloride Conversion _____	44
Ion Exchange _____	45
Procedure for ANION EXCHANGE CHROMATOGRAPHY _____	45
BULK Al removal _____	47
To convert the residue to sulphate form _____	47
Procedure for CATION EXCHANGE CHROMATOGRAPHY _____	48
Precipitation as Hydroxides _____	50
Be fraction _____	50
Al fraction _____	50
SILVER CO-PRECIPIATION PROCEDURE _____	Error! Bookmark not defined.
Drying and Oxidation _____	51

Manual Handling

Always consider the risk of manual handling before you lift or move large or heavy items; this applies to items in the field as well as in the laboratory. If possible, subdivide items into smaller lots before moving them (ie., boxes of rock samples). If you have any doubts about your ability to move an item, get someone else to assist you. Trolleys are available for moving large or heavy items.

Resource Use, Waste Minimisation and Recycling

Always be aware of the environmental implications of your activities in the laboratory and in the field. Minimising the amount of consumables that you use conserves resources and greatly reduces waste. Before you commence a procedure, assess the method you are using and consider any alternatives that might require smaller amounts of chemicals to be used, less water or power, or materials to be reused or recycled. Be particularly careful to minimise 'intractable' waste, ie. substances such as heavy metals that remain detrimental to the environment.

General Laboratory Practice

Personal protective equipment (PPE) requirements

1. SUITABLE CLOTHING must be worn, long trousers are recommended for all staff and students.
2. PROTECTIVE CLOTHING must be worn for protection in case of fire or chemical spillage. It is usually a knee-length white coat, but for some operations more elaborate protection may be required (refer to specific COSHH forms for details).
3. SOUND FOOTWEAR must be worn. Thongs, sandals, and other open-style shoes are PROHIBITED.
4. SAFETY GLASSES are compulsory and must be worn at all times.
6. SAFETY GOGGLES or a full face shield must be worn by persons wearing contact lenses.
7. The storage and/or consumption of FOOD and DRINK in the areas where chemicals are stored and/or used is PROHIBITED.
8. VISITORS to laboratories must wear SAFETY GLASSES at all times.
9. Laboratory coats and other protective clothing are not to be worn in eating and "tea" areas.
10. All accidents/incidents must be reported to the laboratory manager as soon as possible.

Safety Considerations

Hydrofluoric Acid (HF) is lethal, hot HF is worse. ^{26}Al and ^{10}Be chemistry requires handling large amounts of concentrated HF. Lab coats and safety glasses are mandatory, and gloves must be worn when handling beakers and bottles. Be alert to drips when pouring HF, and droplets of condensation when opening lids or uncovering beakers. Absolutely no bare feet, or sandals in the lab. Wear long trousers and the apron for protection.

Make sure you read the COSHH forms before starting any work in the laboratory.

Beryllium is toxic and carcinogenic. Take care when handling even tiny amounts of Be in solution (always wear gloves). Never handle or attempt to weigh Be metal or Be salts - special precautions are required. Make it a habit to wash your hands after every session in the lab.

Perchloric (HClO_4) and nitric acids are strong oxidisers. Concentrated perchloric acid will explode if mixed with organic solvents. If allowed to soak into wood or paper and dry, the resulting products can detonate on contact weeks or months later. Many heavy metal perchlorates are also explosive. Mixtures of nitric acid and alcohols will fume and can boil explosively if heated. Both acids can set fire to dry paper. Therefore.....***Never mop up spills with dry paper towels - dampen them with water to dilute the acid as you pick it up*** (neither acid has much oxidising power once diluted). Avoid all contact between perchloric acid and wooden articles. Never evaporate perchloric acid in a standard fume hood; never evaporate organic solvents (or use them for cleaning) in the fume hood used for perchloric acid evaporation. Store wash bottles of acetone and alcohol outside the fume hoods. Don't store organic solvents in the same cupboard as perchloric and nitric acid.

Handle acids in fume hoods. Be sure you know what you're doing before mixing acids (or any reagents, in fact). Mixtures such as concentrated $\text{HCl} + \text{HNO}_3$ (aqua regia) evolve toxic chlorine (Cl_2) gas. Likewise, mixtures of HCl and oxidisers such as H_2O_2 or NaOCl (hypochlorite bleach). Beware of exothermic reaction when diluting acids, especially H_2SO_4 .

Always add dense acid to water, not water to acid.

SAMPLE HANDLING AND LABORATORY PRACTICE

Some general suggestions

- Keep reagent containers, wash bottles, etc. separate from sample containers.
- Try not to dispense from wash bottles directly into sample beakers. Splash-back onto the dispenser spout may go unnoticed and can contaminate future samples. Better to transfer reagents to an intermediate beaker and dispense with a clean disposable pipette.
- Always triple-rinse measuring cylinders with MilliQ water before you use them.
- Try not to work over the top of samples. Sit or stand back from work areas. Reach around, not over open beakers when moving them around.
- Handle beakers with gloves at all times.
- Write everything down. Always record sample and beaker numbers when samples are transferred. Keep records in a bound notebook and on the sample data sheets. Don't write on scraps of paper, intending to transcribe.
- Label beakers, centrifuge tubes, etc.
- Order your samples in the numbered beakers, bottles etc. in an easily remembered way. This may save you if you forget to note down a transfer, drop a rack of vials, etc.

LABORATORY CLEANLINESS

Contamination

Dust and soil contain large amounts of ^{10}Be compared to quartz samples. Always try to minimise dust coming into the clean lab (try to avoid trekking dust and soil in on shoes, sports clothes, etc.). Use a dedicated lab coat - not one you use during rock crushing- and overshoes at all times. Cloth fibres also contribute to general lab dirt. Try to avoid wearing sweaters in the lab. Soil samples and rock powders should not be analysed in the clean lab.

Washing up

Wash up used lab ware as soon as you have moved your samples on to the next stage of the chemistry.

PROCEDURE

Teflon

Wearing gloves...

Rinse a couple of times with MilliQ water, to remove soluble sample residues (e.g. Be salts).

Take a kimwipe soaked in alcohol and scour the interior surface thoroughly to remove sticky organic deposits and fine-grained hydrophobic material (e.g. graphitic carbon, Fe, Ti - oxides). These will not be removed by hot acids. Interior surfaces of bottles can be reached by manipulating a kimwipe inside the bottle with a round-ended quartz rod. Always take care not to scratch Teflon surfaces. Rinse again with MilliQ water.

Put the items in a washing-up beaker containing 10 - 20 % HNO_3 . Cover with a watch glass and heat (just below boiling) overnight (set hot plate to $\sim 130^\circ\text{C}$). Make sure acid contacts all interior surfaces of the vessels - i.e. none are upside down, trapping air. When cleaning Teflon bottles (particularly 500ml bottles) it is easier to fill them up with 10% HNO_3 (aq), cap them loosely and place them directly over the hot plate at 50°C - 70°C (set point 2 1/2)

Use tongs to remove items from the beaker. Rinse three times in MilliQ water, making sure all interior surfaces are contacted, draining thoroughly between re-fills. The final draining should be done especially carefully.

Dry in the clean drying oven (set at 70°C), either individually or in the collander. Nitric acid dries slowly and any residues not rinsed away will be seen as tiny droplets on vessel surfaces, or as brown oxidation marks in kimwipes placed underneath the items. There should be no acid residue after rinsing.

Ion exchange columns

As a precaution before removing resin from columns, strip it with MilliQ water. Try not to let used resin dry out in the columns.

Wash resin out of the columns. If it has dried, first wet it from above with MilliQ water. Remove it by forcing a gentle stream of MilliQ water through the tip. The resin should wash out as a plug.

Fill and rinse a couple of times with MilliQ water to clear out all traces of resin.. Place the columns upside down in a tall plastic container. Fill the container with 2% HNO₃ -as full as possible - making sure the solution soaks the frits (no air trapped in the top of the columns).

Cover and sonicate twice during 99' each time –without applying any heating- to remove fine resin particles from the frits.

Drain and rinse three times with MilliQ water.

Dry upright in the oven, allowing the final drops to drain out of the columns.

Quartz crucibles, lids and pestles

Place quartz crucibles, lids and pestles in a white Teflon beaker. In a beaker of 250 ml capacity will be OK to clean 50 items of each; 150 all together. Fill beaker with 50% HNO₃; cover with Teflon watch-glass and heat up to boiling or almost boiling point (hot plate to 200°C –setting 4_{1/2} to 5- will be OK - not need for boiling), for 3hours. After the required period let the beaker cool. Decant the solution into the dedicated acid waste container. Fill the beaker with MilliQ and swirl it a few times. Decant the solution into the dedicated acid waste container. Repeat the last step as many times as necessary until pH is neutral. Place the lids, pestles and crucibles into separate, clean containers for drying in the oven. When dry put into the dedicated plastic containers.

Cathodes

Place cathodes (max of 250) to be cleaned in a PTFE or Teflon beaker. Fill beaker with ELLIX water and ultra-sonicate for 10'. Empty water and fill beaker –just to cover the cathodes- with acetone and ultra-sonicate for 10'. Empty acetone in a beaker and leave to evaporate inside a fume hood. Dry cathodes in oven at 70°C. Once dry, place in a clearly labelled bag.

Glassware

No sample work should be done in glass! To wash glassware used for rinse solutions etc. wash with 3 - 4 changes of MilliQ water and dry in oven at 70°C. For heavy soiling, soaking in 3 - 5% Decon works well.

Bottles used for leaching

Rinse bottles with tap water vigorously three times to ensure that no grains are left in the bottle. Dry them in the oven at 70°C.

Funnels and no Teflon bottles (e.g. PP)

Put the items in a washing-up beaker containing 10 - 20 % HNO₃. Cover with a watch glass and heat (just below boiling) for a couple of hours (set hot plate to ~130°C). Make sure acid contacts all interior surfaces of the vessels - i.e. none are upside down, trapping air.

Use tongs to remove items from the beaker. Rinse three times in MilliQ water, making sure all interior surfaces are contacted, draining thoroughly between re-fills. The final draining should be done especially carefully.

Dry in the clean drying oven (set at 70°C), either individually or in the collander.

Cleaning Pt crucible:

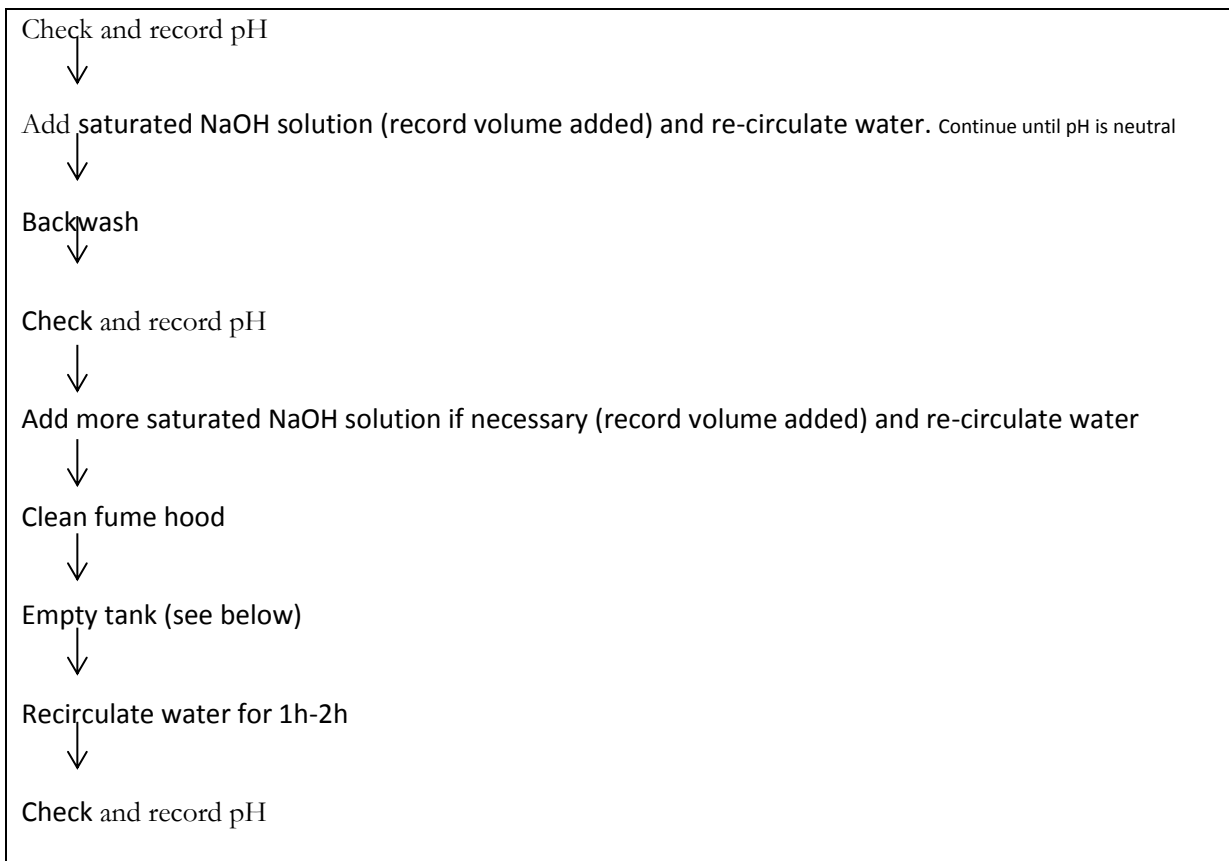
The most effective cleaning procedure for Pt crucibles is to heat the crucible overnight (~120-130°C) in 10% NaOH followed by washing in 10% HNO₃ at 200°C for a couple of hours.

Neutralisation of WATER TANKS located in fume cupboards with scrubber system and the ACID WASTE container

Prepare a saturated NaOH solution (~19.3M NaOH see 16/04/01 calculations DF note book) by adding ~210 ml of tap water to 162 g NaOH (Rectapur) (~44% NaOH) . Use a glass beaker to prepare solution, weigh Na OH in the beaker and add the required amount of water to the beaker **INSIDE** the fume hood as fumes will be generated during reaction. Be careful as solution is exothermic (handle beaker with heat resistant gloves).

- If neutralising water tanks add the ~210 ml of solution and circulate water during 10²-15'. Measure pH and add more 19.3 M NaOH solution if necessary.

The general procedure when neutralising the tanks is as follows (please record information on the wash-down reservoir check sheet provided) :



- If neutralising the acid waste container add the 19.3 M NaOH solution very slowly as the reaction can be violent. Try to stir solution in the container to help neutralisation reaction as acid layer is less dense than alkaline layer.

PROCEDURE TO EMPTY TANKS

PLEASE DO MAKE SURE BEFORE PROCEEDING THAT THE TANK HAS BEEN NEUTRALISED AND CLEANED AS INDICATED ON THE WASH-DOWN RESERVOIR CHECK SHEET!!!!

1. Hold float in a fixed position using the help of the hook provided (tape hook to the side of the fume hood to fixed its position)
2. Isolate tank by closing Valve A
3. *Isolate pump (optional)*
4. Empty tank by opening Valve B (connected to the hose) and the help of the bucket provided
5. Once the tank is empty close Valve B
6. Fill up the tank by releasing the hook
7. Open Valve A
8. *Open pump if you isolated it as indicated on step 3*

COMMON REAGENTS

Parent acids

Name	Formula	Usual strength of concentrated acid	Molarity
Hydrochloric	HCl	37% w/w	11.98 M
Hydrofluoric	HF	48% w/w	29 M
Nitric	HNO ₃	70% w/w	15.8 M
Perchloric	HClO ₄		
Sulfuric	H ₂ SO ₄	95 - 100% w/w (>98%)	18 M (= 36N) (>18.4M)

Working acids

Label	Uses	Recipe
"2% HNO ₃ "	ICP analysis, final uptake/storage of Be samples.	20 ml HNO ₃ + 980 ml MilliQ water.
"1.2 M HCl"	Cation columns - conditioning, loading and Be elution. Anion columns - pre-cleaning and stripping.	100 ml HCl + 900 ml MilliQ water.
"4 M HCl"	Cation columns - pre-cleaning, Al elution, stripping.	167 ml HCl + 333 ml MilliQ water.
"6 M HCl"	Conversion of samples to chloride form. Anion columns - Al+Be elution for low Ti samples	250.4 ml HCl + 249.6 ml MilliQ water.
"0.5 M H ₂ SO ₄ "	Ti elution and sulphate conversion	14 ml H ₂ SO ₄ + 486 ml MilliQ water.
"Trace of H ₂ SO ₄ "	Sulphate conversion.	2ml 1:1 H ₂ SO ₄ + 500ml MilliQ water (2*9.2M=500 X); X= 0.0368M
"0.2 M H ₂ SO ₄ "	Cation exchange	6 ml H ₂ SO ₄ + 494 ml MilliQ water. (Add 1ml H ₂ O ₂)
"1:1 HNO ₃ "= (7.9 M HNO ₃)	Mild dry-down oxidation's.	Equal parts conc. HNO ₃ + MilliQ water.

"1:1 HClO ₄ "	Severe dry-down oxidation's.	Equal parts conc. HClO ₄ + MilliQ water.
--------------------------	------------------------------	---

Always add dense acid to water, not water to acid

WASTE DISPOSAL

Chemicals

No acid should be poured down the sink. Any acid waste should be disposed in the designated acid waste container. There are two acid waste containers in the laboratory; one designed for acid waste not containing HF and a second one for acid waste containing HF. Be careful to dispose the acid waste in the correct container and do not fill them beyond the marked line. Once the acid waste reaches the marked line on any of the containers they need to be neutralised; use sodium Hydroxide (for no-HF acid waste) and sodium bicarbonate (for HF-containing acid waste). Check the pH prior to pouring the neutral solution down the sink. Use ample water.

Empty acid containers (Winchesters and HF bottles) should be left to fume dry in the fume hood. When dry, rinse them three times with water. Label the rinsed bottles as safe for disposal.

NOTE: Waste containers often generate heat and pressure...therefore, do not screw lids too tightly on waste containers, as they are liable to explode.

Glass

Waste glass that is free of chemical residues is to be placed in the glass bin provided in the laboratory.

COSMOGENIC ^{10}Be AND ^{26}Al CHEMISTRY

This method is used to separate Al and Be for AMS analysis from pure quartz samples. After adding Be carrier, quartz is dissolved in HF. The solution is sub-sampled for determination of total Al content, then dried to remove Si. Al and Be are separated from the remaining metals (typically Fe, Ti, alkalis, Mg and Ca) and purified in 3 stages. This method covers the first two: (i) Anion exchange in HCl (removes Fe(III)), (ii) Cation exchange in dilute H_2SO_4 and HCl (removes Ti and alkalis, separates Be from Al). The third stage, hydroxide precipitation (eliminates residual alkalis, Mg, Ca), is carried out prior to loading cathodes for AMS. The procedure described below will cope with up to ~10 mg of Fe and 3-5 mg of Ti, assuming the total amount of Al, Be and other metals is less than 3-5 mg. It can be modified to accommodate larger samples by increasing the size of vessels, ion exchange columns, etc.

Note: Only persons who have gone through the induction process are allowed to work in the clean laboratory. Do NOT attempt the chemistry unless you have been trained to do so by a qualified person.

INITIAL QUARTZ CLEANING

Summary

For preparing very pure quartz separates. Most silicate minerals dissolve faster than quartz in dilute HF and can be etched away to leave a very pure quartz residue. Some quartz is lost - usually ~10% of coarse-grained fractions (500-850 μm) and up to 20-30% of fine-grained fractions (250-500 μm). It is difficult to get good yields from this procedure using grain sizes <250 μm .

Some minerals will not dissolve (e.g. garnet, zircon, rutile, ilmenite). Fortunately, except for garnet, these are trace constituents of most rocks. Muscovite is the only other common mineral that causes problems. It dissolves at about the same rate as quartz, so the procedure won't concentrate quartz relative to muscovite.

An initial heavy liquid separation will remove garnet and muscovite (as well as most other mafic silicates and oxide minerals), if present. However, not all rocks need to be processed in heavy liquids before HF treatment. Small amounts of zircon, ilmenite, etc. in the final sample do not cause problems in the Al-Be extraction chemistry.

The HF leach has the added advantage of dissolving the outermost shell of the quartz grains, as well as etching cracks, where any contamination by meteoric ^{10}Be would be concentrated.

Sample pre-treatment and loading

- (1) Pre-clean samples in hot 2% HNO_3 . All carbonates must be removed before reacting the samples with HF. If necessary, separate the "quartz" fraction ($2.63 \text{ g/cc} < r < 2.67 \text{ g/cc}$) in heavy liquid.
- (2) Judge the amount of sample, aiming to finish up with 30-60 g of quartz after the full clean-up procedure. If you've done a density separation, use the entire "quartz" fraction. This procedure will remove composite grains and most minerals other the quartz likely to remain in the $2.63 \text{ g/cc} < r < 2.67 \text{ g/cc}$ density fraction.
- (3) Label a clean 500 ml polyethylene (PE) bottle with the sample name or number.
- (4) Transfer the sample to the bottle.

BEFORE PROCEEDING - WARNING: Contact with hydrofluoric acid is extremely dangerous. Burns from small amounts of concentrated HF (48-50%) can be lethal. Read the safety literature. Wear heavy nitrile gloves, apron, sleeve guards, and face shield throughout the following procedure. Wear sturdy clothes and shoes when working with HF and around the HF processing area. Know where the calcium gluconate is kept and how to use it to initiate treatment for any contact with HF. Know where the eyewash stands and emergency shower are located. Wipe up any drops (even suspect droplets) with multiple wet paper wipes and soak under running water for several minutes before discarding. Never dispose of HF-contaminated material in the trash. Neutralise waste solutions in the HF waste container.

QUARTZ CLEANING PROCEDURE

Note: The quartz cleaning procedures should only be performed in **Glasgow lab?**. Do not take dirty quartz into the clean lab.

Pre-treatment

- (8) Pour about 60 grams of sample into a 600 ml glass beaker.
- (9) Wash the sample with water to remove the remaining fines.
- (10) Under the fume hood and wearing gloves add enough aqua regia ($10\% \text{HCl} + 10\% \text{HNO}_3$) to cover the sample.
- (11) Place the beaker on a hotplate on **LOW** setting ($\sim 50^\circ\text{C}$) and cover it with a watch glass. Stir the sample; if gas evolves after stirring be very careful with heating applied to sample as gas may get trapped in sample's layers having an "explosive" effect. **Never heat the sample too vigorously.** Leave the sample overnight.
- (12) The next day stir the sample. If solution gets yellower and grains lighter go to step 6; if not heat the sample longer and at a slightly higher temperature. Bubbles will evolved (we are getting rid of Fe_2O_3)
- (13) Cool the beaker and carefully pour the acid into the hazardous waste container without loosing sample.

- (14) Rinse the sample several times with water and discard the liquid into the hazardous waste container. After thorough rinsing, solution should be clearer and pH~5.2.
- (15) Once the sample is clean dry it in the drying oven.
- (16) Once samples are dry bag them up

HF leaching

- (13) Using 500ml bottles designated for HF leaching transfer up to 60 g of sample per bottle. Weight the bottle before the transfer; tare the bottle's weight and weight again after samples' transfer -to monitor samples' mass loss-. It is expected a loss of 1 g per leach of pure quartz; greater losses indicates the presence of other minerals (e.g. feldspars). If processing more than 60 g of sample split it in as many bottles as necessary (usually a maximum of 120g/sample is sufficient).
- (14) Under the fume hood make up a ~2% HF +2%HNO₃ (nominal) solution in the 5 liter container (4800ml H₂O + 100ml HF+100ml HNO₃). All leaches except the last one are prepared with RO water, the last one with MQ water.
- (15) Fill the sample bottle with the 2% HF +2%HNO₃ solution to within 2 cm of the top.
- (16) Gently squeeze the bottle before capping. This gives the contents room to expand when the bottle heats up. Also, loss of vacuum will alert you to the possibility that the bottle has leaked. Check that the bottle is tightly sealed and holding its slight vacuum.
- (17) In the fume hood, gently invert it 3-4 times to mix the contents.
- (18) Mark the bottle to indicate how many times it has been processed.
- (19) Place the bottle in the ultrasonic bath for 72 hours applying heat and ultrasound 3 times per day for a period of 99' each time. Mix the contents of the bottle several times during sonication.

After the **first 3-days**, change the solution as follows:

- (20) Cool the bottles (if they are warm).
- (21) In the fume hood, uncup the bottle and discard the solution into the HF waste container. Be careful not to pour out the sample.
- (22) Rinse the remaining grains thoroughly with 2 changes of RO water; decanting off the rinse water into the waste acid container while any clay or fine, milky fluoride precipitate is still suspended, but after "fine sand"-sized grains have settled. Don't worry about losing some of the very fine grains, unless the sample is unusually small.
- (23) Add ~2% HF +2%HNO₃ in RO water solution to the bottle just like in the first treatment and repeat the 3-day processing for a second time. A minimum of 2 leaches with 2% HF +2%HNO₃ in RO water ARE NECESSARY.

After the **second 3-days**, check the appearance of the sample as follows:

Pure quartz samples have a uniform appearance and do not cake on the floor of the bottle. Impure samples usually appear speckled and may contain a cloudy fluoride precipitate.

If the sample does not appear pure, repeat the HF leaching for another 3-day period with 2% HF +2%HNO₃ in RO water. If the sample appears pure repeat the leach with 2% HF +2%HNO₃ in MQ water. Remember, LAST LEACHING SHOULD BE WITH 2% HF +2%HNO₃ in MQ water.

Sample recovery

After the last leach (in MQ water) has been carried out in a pure quartz sample cool the bottle.

- (5) In the fume hood, uncap the bottle and discard the solution into the HF waste container.
- (6) Rinse with at least 3 changes of MilliQ as above. Try to rinse away any trace of milky fluoride. The rinse water must be clear (and absolutely free of residual HF).
- (7) Dry in the oven at 70°C.
- (8) Cool the samples and transfer them –with the help of funnels- to a labelled ziplock bag. Weight the bag before and after sample's transfer and record the weight of sample and number of leaches carried out.

Chapter 1: ALUMINIUM DETERMINATION FROM A MINERAL ALIQUOT (MA)

To assess the purity of the quartz we determine the aluminium content of the cleaned separate. It is essential to obtain the lowest possible Al concentration. The higher the Al concentration, the lower the $^{26}\text{Al}/^{27}\text{Al}$ ratio for measurement, the fewer ^{26}Al nuclides counted and the worse the counting statistics. The Al concentration should preferably be in the range 10 - 100 ppm. A higher concentration generally (though not always) indicates the presence of an impurity such as feldspar, muscovite or an insoluble fluoride residue from the quartz clean-up (e.g. Na_3AlF_6). Note that ~0.5% feldspar gives ~1000 ppm Al.

PROCEDURE

Static charge should always be removed before weighing.

- Label and weigh a 15 ml Teflon vial and lid on the 4-figure balance. Record the tare weight to 4 decimal places on the sample data sheet. Using a stainless steel spatula, transfer 0.3 - 0.6 g of the sample into the vial. Replace the lid and record the weight. The amount of sample is not too critical, but its weight must be recorded accurately. Be careful when replacing the lid, as static charge may cause small grains to jump up onto the lid or out of the vial. Clean the spatula with a kimwipe (+ethanol) before using it for the next sample.
- When all the samples have been weighed into vials, open the vials in a fume hood and carefully add approximately 5-10 ml of conc. HF(c) (40% w/w) to each using the 500ml HF(c) safety dispensing bottle. The vials should be approximately half-full. (*Don't try to pour these quantities of HF and sulfuric acid from bottles. Better to transfer the amount needed for the batch into a clean Teflon beaker and dispense into individual vials with a clean plastic disposable pipette (one squeeze is roughly 2.5 ml). Rinse the inside of the teflon beaker several times with MilliQ water before drying the beaker. Triple rinse the pipette with water before throwing it into the bin.*)
- In the fume hood, leave the open vials to stand for 8 hours (overnight). Keep track of which lid belongs to which vial. The quartz will slowly dissolve. After total dissolution has been achieved, add 2 drops of 1:1 H_2SO_4 and place the vials on the hotplate to fume off HF (set 4). Due to its higher boiling point the H_2SO_4 will not evaporate. Do not overheat the small flat-bottomed vials, as solutions will boil and damage the hotplate surface. Tilting the hotplate a few degrees by propping up the front will ensure that the H_2SO_4 and insolubles will form a small drop in one "corner" of the vial.
- Once all the HF has evaporated, the residue should be a brown drop, containing H_2SO_4 and a few hundred μg total of Al, Fe and Ti fluorides. If any quartz remains (usually only if the original sample was very coarse-grained), **cool the vials** and repeat the procedure with a further 2 - 3 ml of HF and 1 drop of 1:1 H_2SO_4 .
- Cool the vials. If the sample will be analysed by AAS, dissolve the residue in 5 ml of 2% HNO_3 . If sample will be analysed by ICP-OES dissolve in 10 ml of 2% HNO_3 . Use the Eppendorf 1-5 ml adjustable pipettor and the attachment dedicated to dilute HNO_3 . Cap the vials with their original caps and leave to stand a few hours. The fluorides should dissolve totally to give a clear (or perhaps faintly green) solution.
- Invert the capped vials a few times to homogenise the solutions, then weigh and record the vial+solution weights. Decant the solutions into labelled centrifuge tubes and send them off for analysis.
- The expected concentration of Al in pure quartz is <100 ppm

Clean the Teflon ware using the procedure outlined in General Lab Practice.

Chapter 2: CARRIER ADDITION AND SAMPLE DIGESTION

Our aim is to extract Beryllium from the quartz sample and to measure the $^{10}\text{Be}/^9\text{Be}$ ratio using AMS. However, Be is a very rare element in quartz. Therefore it is necessary to spike the sample with a known quantity of ^9Be . The aim of spiking is that we can trace the movement of the Be through the processing and that the very low concentrations of naturally occurring Be will follow the same path as the added Be. Also need to end up with enough Be to generate an ion beam in the AMS. Obviously we do not want to introduce ^{10}Be to the sample since this is the nuclide we are trying to measure. For this reason we have Be carrier solutions with known concentrations of ^9Be . It is critical that a low-level carrier is used for samples with potentially low levels of ^9Be .

The amount of sample required for the AMS measurement of ^{26}Al is a minimum of 1 mg, but larger amounts are easier to run. For samples containing 50 ppm Al, at least 20 g of quartz should be dissolved, but note that processing more than 40 g becomes unwieldy; 20g should be enough unless sample is quite young (~25 g of sample should be processed in that case). In some samples the Al concentration is so low that it needs to be spiked with Al carrier. We aim to have a total of 1000-1500ug Al on each sample. If the sample has less Al, add carrier to reach this value but never spike with more than 1000ug of Al. For blanks, add 1ml of 1000ppm Al carrier solution. To add Al carrier solution to samples use the same procedure as for the Be carrier.

PROCEDURE

Sample weighing

1. Label, remove static (by wrapping bottle in foil paper or using the anti static cathode) and weigh a clean FEP Teflon bottle (bottle+lid). Make sure to use a bottle (250 or 500ml) large enough to contain the HF (~5ml per gram of sample). Record the tare weight on the sample data sheet. Transfer the sample to the bottle. This is best done with the help of a funnel (one per sample). It helps to reduce static if bottle is wrapped in foil paper when transferring the sample. Some grains will charge and cling to the bottle walls. No problem. Cap the bottle.
2. Remove static and re-weigh. Subtract the bottle tare to determine the sample weight.

Be carrier addition

(to add 250-300ug of Be to all samples including the blank 1ml of TCW Be carrier-)

1. Take the current Be carrier bottle, invert it a few times to homogenize the solution. Be sure drops of condensation around the lid are mixed in. Remove static (by wrapping bottle in foil paper or using the anti static cathode) and weigh it. Record the initial weight in the blank sample log sheet (and if possible, confirm that it equals the final weight from its last use).
2. Load the 1000 μl Eppendorf pipette with a clean tip and uptake 0.820ml of Be carrier (0.820g*299ug/g= \sim 246ug Be). Be sure the tip does not touch anything while handling the pipette. If

the tip does touch something, discard it and take another. **DON'T RISK CONTAMINATING THE CARRIER.**

3. Start the Be carrier addition with the blank sample of the batch. Open the sample bottle.
4. Tare the balance to zero. Remove the carrier, open it and pipette carrier into the sample bottle. Eject the carrier smoothly, being sure not to leave a drop in the tip. If this happens uptake MQ water and dispense over the sample to ensure ALL carrier is added. Don't allow the tip to touch the sample bottle. Recap the carrier bottle as quickly as possible, remove static and re-weigh it. The balance will read the weight removed. Record the weight and the Be concentration of the carrier. Calculate the Be added.
5. Repeat the process from point 3 until Be carrier is added to all samples.
6. At the end of each session tare the balance to zero and record the final weight of the carrier bottle in the blank log sheet for cross-checking. Check that the cap is screwed on firmly and seal it with parafilm.

Sample digestion

1. In fume hood, wearing gloves and goggles....Using the measuring cylinder marked for concentrated HF, add 5ml AR grade HF for each gram of quartz in the sample bottle. Add ~100ml HF (c) to the blank bottle.
2. Cap the bottle, tighten the lid down, then back it off ~1/4 turn. The bottle must not be gas-tight (check by squeezing it gently). **Beware if the sample is fine-grained** – the reaction may proceed fast and the bottle may get very hot. If it looks like starting to boil, be prepared to sit it in a beaker or basin of cold water to quench the reaction a bit. Don't swirl the bottle at first – the initial reaction doesn't need any encouragement. **Never shake the bottle!**
3. Once the reaction has subsided (usually 1-2 hours), the bottles can be placed around the edges of the hotplate set on a low temperature (set 2, ~50°C). They only need very gentle warming to ensure overnight dissolution. From this point on, they can also be swirled occasionally to mix HF down into the dense H_2SiF_6 forming around the quartz grains (**REMEMBER TO CLOSE THE LID TIGHTLY BEFORE** swirling sample). During the day the temperature can be increased slightly (SET 3, ~ 100 °C)
4. Once all the quartz has been dissolved turn off the hotplate and cool the bottles to room temperature. The time required for dissolution varies depending on sample. 30 g of pure quartz may take up to 3 days; 60 g may take 4 days. If solution seems to be saturated (dissolution goes very slowly) add more HF(c) to sample. (If brown-black grains are present in solution and do not dissolve after adding more HF; heating and swirling samples for a long period of time they are probably not quartz. Make a note of it and carry on with sample preparation as indicated in point 5).
5. Tighten the caps, being wary of any droplets of condensation inside the screw threads that might be squeezed out onto the surface of the bottle.

SPLITTING FOR ALUMINIUM DETERMINATION

Accelerator mass spectrometry does not provide absolute values of nuclide concentrations in the sample. Rather AMS provides a ratio between the cosmogenic nuclide and the stable nuclide occurring in the sample but not produced by cosmic ray interaction. For example, AMS gives us the $^{26}\text{Al}/^{27}\text{Al}$ ratio, where ^{26}Al is the cosmogenic nuclide and ^{27}Al the stable, native aluminium in the sample. Therefore, to determine the actual concentration of cosmogenic ^{26}Al in the sample we need to know the ^{27}Al concentration in the sample. Because cosmogenic ^{26}Al is so rare we can estimate the stable ^{27}Al concentration by measuring the total Al in the sample solution (parent solution). Total Al in an aliquot of the parent solution is measured by ICP.

PROCEDURE

1. Homogenize the solutions by swirling and inverting the bottles to mix in HF condensed around the top of the bottle. Total sample Al concentrations will be determined from splits (aliquots) of these solutions, so they must be thoroughly mixed.
2. Weigh the bottles. For all but the smallest samples it will be necessary to use the top-loading balance (accurate to 3 decimal places). Subtract the bottle tare weight and calculate the total solution weight.
3. For each sample calculate the expected Al concentration (ppm) of the parent solution and use this to calculate the amount of parent solution required to obtain a **10ml solution with 3ppm Al**
4. For each sample, take a Teflon vial. Label, remove static, weigh the vial and record the weight on the sample data sheet.
5. In the fume hood; open the vials; open the sample bottle. Using a pipette transfer the calculated amount of parent solution into each vial. Remember you are transferring HF.
6. Without rushing, but as quickly as possible, close the vials. Weigh them and record the weights. Calculate the weight of each split. **Take care not to splash any of the split solutions onto the lids of their vials when transferring them to the balance.**
7. After splitting each sample, the aliquots can be dried down to remove HF in preparation for ICP-OES analysis. Transfer aliquots back to the fume hood, taking care not to splash liquid into the lids of the vials. Add 1-2 drops of 1:1 H₂SO₄ to each and dry at setting 4 (~90°C-140°C) on the hotplate (OK to leave overnight at set 3 ½ - 4). A small dot of liquid or a precipitate of Fe-Al-Be-Ti alkali salts should appear in the base of each vial after evaporation.
8. Cool the vials. Dissolve the dry residue in 10 ml of 5% HNO₃ -**Primar Plus** grade-, always use this grade when preparing solutions for ICP-OES analysis. Use the Eppendorf 1-50 ml adjustable pipettor and the attachment dedicated to dilute HNO₃. Cap the vials with their original caps and leave to stand a few hours. The fluorides should dissolve totally to give a clear (or perhaps faintly green) solution.
9. Weigh and record the vial+solution weights.
10. Invert the capped vials a few times to homogenise the solutions, decant them into labelled (sample name-ICP-OES Al) centrifuge tubes and store in designated drawer. Prior to ICP-OES analysis a 5mls aliquot of this solution will be taken out and Y will be added as IS (concentration will be ~3ppm Al and ~3 ppm Y in 5% HNO₃ PRIMAR PLUS the final volume 5.16 if Y 100ppm is used as the working concentration. This solution will be analysed by ICP-OES to determine [Al].

Clean the Teflon ware using the procedure outlined in General Lab Practice.

PARENT SOLUTION DRY DOWN

AND CHLORIDE CONVERSION

Successive evaporation and re-dissolution eliminates fluoride (as HF) almost entirely. Fe, Ti, Al, Be, alkalis etc. should be left as chloride salts ready for anion exchange clean-up. The final solution will generally be coloured a deep yellow-green by FeCl₃. By the end of this procedure, however, some samples may have thrown a fine, powdery, white precipitate that will not re-dissolve. This is TiO₂. No Al or Be is co-precipitated with the Ti, which should be removed by centrifuging before moving on to the anion exchange columns.

PROCEDURE

1. Carefully transfer the parent solution to a clean and labelled Teflon beaker (250 or 500 ml).
2. Rinse the bottle with a few ml of MilliQ and add the rinsate to the beaker. Take care not to let any sample solution splash back onto the MQ wash bottle.
3. Using separate disposable transfer pipettes add 2-3 ml of 6M HCl and 1ml of 8M HNO₃ to each beaker.
4. **SWITCH THE WATER PUMP ON** to allow water to recirculate through the system. Place the beakers on the hotplate and dry at setting 4 (~90°C-140°C) overnight; during the day temperature can be increased up to set 5 **ONLY if PTFE Teflon is used!!** (130°C –180°C). For <100 ml, the beakers will dry down in 12 - 15 hours. Larger solution volumes may take a bit longer. When drying large volumes droplets will condense on the rim of beakers, do not worry they will dry off. When dry, there will be a thin covering of white to gray-green fluoride salts on the floor of the beaker. There may also be some residual tiny droplets on the beaker walls - don't worry about these.

To convert the residue to chloride form...

5. Take the beakers off the hotplate and cool them. Using a disposable pipette, add ~2 ml of 6N HCl (the amount is not critical; samples with a very large fluoride cake may require a little more). The cake should mostly re-dissolve instantaneously, and in most cases will go back into solution entirely after warming on the hotplate.
6. Return the beakers to the hotplate and dry again at setting 4 (~90°C-140°C).
7. Cool and repeat the 6N HCl addition.
8. Dry again, cool and re-dissolve a third time, then take down as close to dryness as possible. Try to avoid complete drying at the end of this step, to make it easy to get the sample back into solution for anion exchange. Don't worry if drying is unavoidable, however.
9. Add 2 ml of 6N HCl to each sample container. The precise volume is not critical and can be measured from the marks on a disposable pipette. Swirl the liquid to pick up and dissolve the

entire sample from the floor of the container. Leave standing overnight. Do not warm to promote dissolution - evaporation will change the acid strength.

10. After standing overnight (or at least a few hours) transfer each sample to a labelled centrifuge tube -using a clean disposable pipette for each sample-. Add a further ml of 6N HCl to each sample container and rinse. Swirl to pick up any remaining droplets of the original sample solution. Pick the rinse solution up and add to their appropriate centrifuge tube. If necessary -presence of TiO₂ (smoky white insoluble material) or other insoluble particulates -solutions will have to be centrifuged before running them through the columns. Spin the tubes at maximum speed (notionally 3500 RPM) for 10 minutes and keep centrifuge tube with residue material until results are obtained. The pipettes used for each sample should be reserved (in the original sample containers) for loading onto columns. If sample is fully dissolved centrifugation is not necessary. The samples can be stored indefinitely in centrifuge tubes.

CENTRIFUGE: *Make sure that the loads in the centrifuge are balanced. Use a massed dummy tube if there is a spare slot in the centrifuge.*

11. Samples are now ready for anion exchange chromatography.

ION EXCHANGE

Anion exchange columns are used to separate remaining impurities such as Fe and Ti from the sample. In strong HCl, Fe(III) forms a range of anionic Cl⁻ complexes (FeCl₄⁻, FeCl₅²⁻ and FeCl₆³⁻), which bind tightly to the anion exchange resin. These can be seen as a brown stain in the top few mm of the resin. Al and Be do not form strong Cl⁻ complexes and wash through the column as HCl is added. Titanium is a bit more problematic; Ti(IV) forms TiCl₆²⁻, which binds, but some Ti always seems to remain cationic, form neutral species or revert to Ti(III), which doesn't form strong Cl⁻ complexes. Ti is seldom 100% stripped from the Al + Be fraction. Al and Be are split and Ti is further removed using cation exchange columns.

TO NOTE:

Before addition of sample; conditioned resin (applicable to AX and CX) could be left unused overnight only if it is strictly necessary. To keep them moist store them in 1ml of conditioning solution (e.g. 6N HCl for AX and 0.2M H₂SO₄ for CX), wrap column holders with clean parafilm (bottom and top) and secure the film around the holder with tape. The next day allow solution to drain and add an extra 1ml of conditioning solution if resin is dry (*CAUTION: pale decolouration of resin at the bottom indicates presence of air in the resin*).

Procedure for ANION EXCHANGE CHROMATOGRAPHY

AX chromatography may take up to 4 hours. (6ml takes ~30' to be eluted)

- (1) Load a column stand with ion exchange columns. Place a plastic container underneath.
- (2) Squirt some alcohol (ethanol, isopropanol, whatever is on hand) into each to wet the frit (to eliminate trapped air).

- (3) Using AG-1 X8 200-400# anion resin from stock soaking in 1.2N HCl, pipette a very **loose slurry** into each column (use a disposable pipette). The aim is to block the column and back up a head of acid so that the resin bed can be built up from suspension. This prevents trapping of air bubbles.
- (4) Now continue slurrying resin into the columns to build 2 ml resin beds. If too much resin is added, a long pasteur pipette can be used to adjust the volume. If too thick a slurry is added and bubbles get trapped in the bed, the column must be emptied and re-packed. Bubbles will channel flow through the column and ruin the separation. Once the resin has compacted to the correct height, allow the supernatant to drain through.
- (5) Wash the resin with 10ml HCl –up to top of column holder- (1.2M ("10%") HCl is convenient, though more dilute HCl does a better job. Allow the wash solution to drain through the resin bed.
- (6) Condition the resin with 10ml 6N HCl. Add the first ml by running drops down the column walls - try to keep the top surface of the resin bed flat to ensure uniform flow through the column when the sample is added. The resin will darken and shrink as it adjusts to the higher acid strength (it may not be noticeable).
- (7) Take a batch of 20 ml Teflon vials and label them with sample ID (**Al and Be fraction**).
- (8) Once the 6M HCl conditioning solutions have drained, carefully remove the plastic container from beneath the columns and replace them with 20 ml Teflon vials. The HCl in the container should be disposed in the acid waste container.
- (9) Using separate disposable pipette for each sample (those centrifuged will already have one), load the sample solutions onto the columns. Drip the solution down the column wall, reaching as far as possible into the column with the pipette. Do NOT pour the sample into the column. Try to transfer the sample quantitatively. Try not to disrupt the top surface of the resin. Return each pipette to its sample container.
- (10) Allow the loading solution to drain fully into the resin.
- (11) Elute **Al + Be** from the columns by adding 6ml 6M HCl. The first ml should be added carefully from a disposable pipette so as not to disrupt the top of the resin bed. Allow to drain through before adding the remaining 5 ml.
- (12) Once Al + Be have been eluted, remove the vials and replace them with labelled 15ml disposable centrifuge tubes (*the long tubes with plug caps*) (**Fe and Ti fraction**).
- (13) If **BULK Al removal is REQUIRED** continue with steps 16 and 17 and proceed with the Al/Be fraction as indicated in the BULK Al REMOVAL section.
- (14) If **BULK Al removal is NOT REQUIRED**, Add 1 drop of 2% H₂O₂ to each Teflon vial. Change of colour to yellow-orange indicates the presence of Ti in the fraction. Note changes to monitor fractions during following sample prep steps.
- (15) If **BULK Al removal is NOT REQUIRED**, Add 1 ml of 0.5M H₂SO₄ with a trace of H₂O₂ (0.5 mmol) to each Teflon vial and dry on the hotplate overnight. Dry at setting 3 ¼ (70°C-90°C) to avoid boiling the sample. After dry down, proceed with the Al/Be fraction as indicated in the section

To convert the residue to sulphate form. (ignore the section in Bulk Al removal if samples do not required this step).

- (16) Wash **Fe + Ti** off the resin with 10ml MQ water. (Fe reverts to the cationic \pm FeCl₃⁰ form - HCl will drip yellow-green after a few ml). Rinse out and discard the sample and dispensing pipettes. Rinse out and wash the sample transfer containers.
- (17) Rinse out resin and clean the columns as described under Laboratory Cleanliness.

.....

BULK Al removal

- Once Al + Be have been eluted (step **12 from AX**) dry fraction on the hotplate overnight. Dry at setting $3 \frac{1}{4}$ (70°C-90°C) to avoid boiling the sample
 - When the sample is nearly dry remove beaker from hotplate
 - Add 10ml MQ water and 2ml HNO₃ (c)
 - Warm up if necessary -at very low temperature- to aid dissolution (with the lid on)
 - Transfer to 50ml centrifuge tube
 - Rinse beaker with 20ml 1M HNO₃ and add rinsate to sample
 - Add NH₄OH (c) to solution until pH 8 is reached. A total volume of 2ml of conc. ammonia may be needed but it needs to be added with caution (by adding volumes of 0.3 ml initially and drops when the pH is close). If pH goes above 8 add DROPS of HNO₃ (c) to adjust pH back to 8. The pH of a solution will not go higher than 10 if we use ammonia so in the first step of the Al BULK REMOVAL we use ammonia to reach pH 8. At this pH both Al and Be will precipitate.
 - Set in a bath of warm water for at least 2 hours.
 - Adjust to pH 11.5 using small amounts of 50% NaOH (~12.5 M NaOH) initially (in 0.2ml additions) and drops of 6M NaOH (~25% NaOH) when pH is closer to 11.5. If pH goes above 11.5 acidify solution but try not to go below pH 8, if this occurs; start the process as if the precipitation at pH 8 is happening for the first time. At pH 11.5 ONLY Al will re-dissolve, Be is still in a precipitate form.
 - Vortex samples.
 - Centrifuge at 3500rpm during 10'
 - Collect the supernatant (Al fraction) into 50ml centrifuge tubes. Add drops of HNO₃ (c) to acidify the solution (<pH 4) and store.
 - The precipitate (Be, and maybe Al, Ti..) needs to be washed by adding 20ml MQ water with 2 drops of concentrated ammonia (to keep solution alkaline).
 - Vortex samples
 - Centrifuge at 3500rpm during 10'
 - Transfer supernatant to 50ml centrifuge tubes and stored until results are obtained
 - Add 5ml 1.2 M HCl to the original 50 ml centrifuge tube containing the precipitate (Be and maybe Al, Ti..)
 - Vortex
 - Transfer solution to Teflon vial
 - Rinse centrifuge tube with 2ml 1.2 M HCl
 - Vortex and transfer to Teflon vial
 - Dry down solution in Teflon vial (Be, and maybe Al, Ti... fraction in a total 7ml of 1.2 M HCl) at setting $3 \frac{1}{4}$ overnight
 - Fraction (Be, and maybe Al, Ti...) is now ready for sulphate conversion.
-

To convert the residue to sulphate form

Once the samples have dried down they may turn an alarming dark-brown to black colour. This is due to chary reaction products formed from organics which bled from the anion resin. Don't worry, it will disappear gradually over the next few steps.

- (18) Cool the vials. Add 5-6 drops of ~2% H₂O₂. Add 2ml MilliQ containing a trace of 0.5M H₂SO₄ (Solution ~0.0368 M H₂SO₄ prepared by adding 2ml 1:1 H₂SO₄ to 500 ml MQ water) (~74 μmol). The cakes will begin to dissolve, taking on an amber/gold color (TiO[H₂O₂]²⁺) if Ti is present. Reheat the vials. The black charry material will disperse and disappear (do not worry if it does not happen straight away; the heat applied will help the dispersion).
- (19) Dry the samples down again (max at set 4 (90°C -150°C) if you are in the lab; set 3 if left overnight). The H₂O₂ oxidises the organics. It also indicates the presence of Ti in the sample by turning the solution yellow-orange. The darker the colour, the more Ti is present.
- (20) Cool the vials and repeat the H₂O₂/MilliQ water addition, and dry the samples a second time. At the end of this procedure, the samples should end up either as compact white cakes; small, syrupy droplets of involatile H₂SO₄ or orange/yellow syrupy cakes. If they remain charry or discolored, repeat the peroxide/water addition and dry them down as many times as necessary
- (21) Take the sample up (as a cake or 1-2 drops) in 2ml H₂O containing a trace of 0.5M H₂SO₄. Add 1 drop of ~2% H₂O₂. Leave overnight.
- If sample does not contain Ti (e.g. 2nd CX, take sample up in 2ml 1.2 M HCl. Transfer to centrifuge tube. Rinse beaker with 1ml 1.2 M HCl and add rinsate to appropriate centrifuge tube).***
- (22) If samples do not dissolve completely after leaving overnight warm them a little. Don't risk evaporating too much water – keeping the acid strength low for column loading gives a sharper elution and cleaner Ti-Be cut. The samples are now in ~0.398 M H₂SO₄ (500+ (4*74) μmol/2ml) as addition/dry down is carried out a total of 3 times on average.
- (23) Transfer sample to a labelled centrifuge tube. Add a further ml of 0.5M H₂SO₄ (500 μmol) (final concentration ~ 0.432M H₂SO₄) with a trace of H₂O₂ to the sample containers and rinse. Swirl to pick up any remaining droplets of the original sample solution. Pick the rinse solution up and add to their appropriate centrifuge tubes. If necessary (dissolution is not complete) centrifuge sample and keep centrifuge tube with residue material until results are obtained. If sample is fully dissolved centrifugation is not necessary. The samples can be stored indefinitely in centrifuge tubes.
- (24) Samples are now ready for cation exchange to remove Ti and to split Be and Al into separate fractions.

Procedure for CATION EXCHANGE CHROMATOGRAPHY

CX chromatography may take up to 7 hours. (10ml takes ~30' to be eluted)

- (1) Load a column stand with ion exchange columns. Place a plastic container underneath.
- (2) Squirt some alcohol (ethanol, isopropanol, whatever is on hand) into each to wet the frit.
- (3) Using AG 50W - X8 200-400# cation resin from stock soaking in dilute HCl (1.2 M HCl) , pipette a very loose slurry into each column (use a disposable pipette). The aim is to block the column and back up a head of acid so that the resin bed can be built up from suspension. This prevents trapping of air bubbles.
- (4) Now continue slurring resin into the columns to build 2 ml resin beds. If too much resin is added, a long pasteur pipette can be used to adjust the volume. If too thick a slurry is added and bubbles get trapped in the bed, the column must be emptied and re-packed. Bubbles will channel flow through the column and ruin the separation. Once the resin has compacted to the correct height, allow the supernatant to drain through.
- (5) Strip the columns with 10ml (up to top of column holder) 4M HCl followed by 10ml 1.2M HCl.
- (6) Condition the columns with 10ml 0.2M H₂SO₄ (with a trace of H₂O₂)

- (7) Once the 0.2M H₂SO₄ conditioning solutions have drained, carefully remove the plastic beaker from beneath the columns and replace them with labelled 15 ml disposable centrifuge tubes (*the long tubes with plug caps*) to collect the Ti fraction.
- (8) Using separate disposable pipettes for each, load the sample solutions onto the columns. Drip the solution down the column wall, reaching as far as possible into the column with the pipette. Do NOT pour the sample into the column. Try to transfer the sample quantitatively. Try not to disrupt the top surface of the resin. Return each pipette to its sample container. [column conditioning solution]<[sample]<[mobile phase] ~ (0.2M<0.432M<0.5M)
- (9) Allow the loading solution to drain fully into the resin. If present, Ti will have formed an orange band at the top of the column.
- (10) Add a total of 8ml 0.5M H₂SO₄ with a trace of H₂O₂ to the columns but **PIPETTING the first 2 ml** to avoid disturbing the resin. Allow to drain through before adding the remaining 6 ml (DO NOT TRANSFER DIRECTLY, PIPETTE THE FIRSTS mls) and watch the band of Ti move down the column.
- (11) If not all Ti has been eluted the elutant/tip are yellow and/or an orange band will be present in the resin. In all cases (all Ti has been eluted or not) add 2 further mls of 0.5 M H₂SO₄ with a trace of H₂O₂ Do not add more than 2ml as Be will start to be eluted then. If not all Ti is eluted after the further 2mls added make a note of the sample and Ti will be separated from fraction by precipitating it at pH 4 (*see Precipitation as Hydroxides*)
- (12) Replace the centrifuge tubes with labelled 20ml Teflon vials to collect the Be fraction.
- (13) Elute Be from the columns by adding 10ml 1.2 N HCl. The first few ml should be added carefully from a disposable pipette so as not to disrupt the top of the resin bed. (Yellow elutant indicates the presence of Ti)
- (14) Once the columns have drained replace the vials with labelled 15ml centrifuge tubes (use the tubes that will fit in the centrifuge) to collect Al.
- (15) Add 5 drops of 8M HNO₃ (to dry off Boron, more drops may cause static problems) to the Teflon vials. Dry them down overnight at setting 2 ³/₄ (~60C) to avoid total dryness if possible.
- (16) Elute Al from the columns by adding 6ml of 4M HCl. The first few ml should be added carefully from a disposable pipette so as not to disrupt the top of the resin bed. Once the columns have drained cap the tubes and store them until hydroxide precipitation.
- (17) Clean the columns as described under Laboratory Cleanliness.

If sample does not contain Ti proceed with step 1 to 5 as indicated. Load sample solution (~in 3ml 1.2M HCl) into the columns and then follow up from step 12 onwards.

PRECIPITATION AS HYDROXIDES

Be fraction

1. Once the Be solutions have dried down (near dryness as possible), cool the vials. There should only be a small white dot or small drop in the bottom of the vials.
2. Add **2ml 1% HNO₃** to the vials. The Be should dissolve readily. If it doesn't you can heat the vials to assist dissolution.
3. Transfer the solutions to labelled 15ml centrifuge tubes.
4. Add another **1ml 1% HNO₃** to the vials, swirl it around and transfer the rinse solution to the appropriate tube.
5. If Ti is present in sample use 10%-20% NH₄OH solutions to bring **pH up to 4**. Ti will precipitate as hydroxide whilst Be will remain in solution. Centrifuge the solutions at 3500rpm for 10 minutes. **Decant and collect supernatant (Be fraction) in ~15 ml centrifuge tubes.** Precipitate is Ti hydroxide.
6. Using 25%-50% NH₄OH solutions, bring Be solutions in the 15 ml centrifuge tubes to **pH 8 (8- 8.5)** (beyond pH 10 Be will re-dissolve) to precipitate Be as a hydroxide. Addition of ammonium hydroxide may have to be drop by drop with pH checks in-between. Leave the tubes standing for a few hours. (To speed up precipitation you can place the tubes into a warm water bath).
7. Centrifuge the solutions at 3500rpm for 10 minutes.
8. Decant and discard the supernatant into the acid waste tank.
9. Rinse the samples with 5 ml MilliQ water and 1 drop 25% NH₄OH added to the centrifuge tubes.
10. Disperse the samples by vortexing (until precipitate is re-dissolved)
11. Centrifuge again at 3500rpm for 10 minutes.
12. Decant and discard the supernatant into the acid waste tank.
13. Repeat the MilliQ + NH₄OH rinse three times (in total).

Al fraction

1. Using conc. - 50% NH₄OH solutions, bring Al fraction (in 6mls 4MHCl) in the 15 ml centrifuge tubes to **pH 8** (beyond pH 10 Al will re-dissolve) to precipitate Al hydroxide. **Always start with conc. NH₄OH** solution. Addition of ammonium hydroxide may have to be drop by drop with pH checks in-between. Leave the tubes standing for a few hours. (To speed up precipitation you can place the tubes into a warm water bath). Reaction is exothermic. (Al precipitation is initially not as easy to see as Be precipitation)
2. Centrifuge the solutions at 3500rpm for 10 minutes.
3. Decant and discard the supernatant into the acid waste tank.

4. Rinse the samples with 5 ml MilliQ water and 1 drop 25% NH_4OH added to the centrifuge tubes.
5. Disperse the samples by vortexing (until precipitate is re-dissolved)
6. Centrifuge again at 3500rpm for 10 minutes.
7. Decant and discard the supernatant into the acid waste tank
8. Repeat the MilliQ + NH_4OH rinse three times.

DO NOT store Al and Be as hydroxides in alkaline solutions (salts are formed under this condition). It is OK to store them as fractions collected after CX chromatography (acid solutions) or as dry hydroxides.

DRYING AND OXIDATION

1. Carefully open the 15 ml centrifuge tubes containing the Be and Al hydroxides and lie them on a kimwipe in the drying oven. It helps to put a folded kimwipe under the **open ends** to keep them slightly elevated. Keep track of which lid belongs to which tube. Cover the tubes with a kimwipe and dry overnight at 70°C.
2. When dry, cap the 15 ml centrifuge tubes with their respective lids and let them cool. (Tap them slightly to free the oxide).
3. Weigh a cleaned quartz crucible and lid to 4 decimal places (*for instructions on cleaning quartz crucibles see Laboratory Cleanlines*). Place the crucible into the perspex holder. On a piece of paper write down the relative positions of the quartz crucibles and the Sample ID of the sample which will be transferred into them.
4. **For Be hydroxides:** In the Be box, wearing a new pair of gloves, and a face mask pour the small pellet of dried Be hydroxide over a clean weighing paper and transfer it to the quartz crucible. Use the help of a spatula if the pellet does not come off the walls of the centrifuge tube easily. If you experience problems with static electricity; use the anti-static device or wrap tubes with foil paper. Pour the pellet over a clean weighing paper and transfer it to the quartz crucible. Cover the quartz crucible with its respective quartz lid. Place the crucibles in their position in the Perspex holder. **Avoid sample cross contamination.**
For Al Hydroxides: Same as for Be hydroxide but the transfer can be done on the open lab bench without the need of the face mask.
5. Transfer perplex holder to the furnace. Place crucibles (covered with lids) inside the furnace making sure that the relative positions of the crucibles is maintained.
6. Bake the crucibles at 800 °C for 2 hours. (*The furnace is programmed for this*)
7. Let the furnace and crucibles cool down (15 hours).
8. Remove the crucibles from the furnace, weigh them and subtract the tare weight to get the weight of the oxides. Transfer them to the perplex holder keeping their relative position.
9. Al oxides will be pressed in the AMS lab. Carefully transfer the perplex holder (with oxides) to a plastic box and take to the AMS lab. Be oxides will be pressed in the CIF-CfG lab (Room 8 at SUERC)

All materials in direct or potential contact with Be should be disposed of in the Be hazardous waste container.

MIXING AND PRESSING

Mixing Be oxide standard material or machine blank material

Before starting to mix prepare your working area:

- Wipe the surface of the acrylic box with MQ water or alcohol.
- Cover the surface of your working area with foil paper.
- Wrap the acrylic glass stand with foil paper and place on the working area.
- Place antistatic cathode inside the acrylic box.
- Select devices needed for mixing (for standards or blanks depending on the material you are mixing): agate mortar and pestle, spatula and wipe them with alcohol.
- Place eppendorf vial containing Nb powder and Nb spatula beside balance. Wipe spatula with alcohol.

To mix your material:

Wear required safety equipment as indicated in the relevant COSHH form.

1. Wrap the vial containing BeO in foil paper and pass through the antistatic cathode.
2. Place the vial (still wrapped in foil paper) inside the small plastic box provided and very carefully transfer to the balance (be very cautious- the balance is outside of the acrylic box). Record the weight (*before BeO removal*).
3. Transfer the small plastic box containing the BeO vial back to the acrylic box, unwrap the vial carefully (do keep the foil paper for step 5) and transfer the desired amount of BeO material to the agate mortar.
4. Handle the BeO material very gently with the agate pestle to avoid any spills, especially if the material is brittle. First, knock only gently on the solid without grinding. Start grinding only after it is obvious that this will not cause any spilling.
5. Wrap the vial containing the BeO in the foil paper used on step 1; place vial on the small plastic box (as on step 2) and very carefully transfer to the balance to weigh (be very cautious- the balance is outside of the acrylic box). Record the weight (*after BeO removal*). Calculate the transferred BeO mass.
6. Calculate the mass of Nb powder needed to mix with the transferred BeO material (six times the BeO mass).
7. After grinding the beryllium oxide to fine powder, add the calculated, weighed mass of niobium (Nb) powder and homogenize gently in the mortar.
8. Once the mixture is homogenised transfer to a weighing paper and from there to a labelled eppendorf vial. Use the help of a spatula to remove the mixture from the mortar as completely as possible.
9. Clean all devices used thoroughly with alcohol (wipe 2 to 3 times). The Kimwipes used for cleaning can be discarded after being sealed in disposable gloves (however, the first wipe of the mortar should go to the Be waste). All devices used during mixing will be stored in the cabinet inside the acrylic glass box.
10. The vial containing beryllium oxide/niobium mixture is placed in a sealed bag along with a sheet of paper where you should record your name, date, BeO compound name, total weight of mixture and how many cathodes are expected to be pressed

(approx.) from the mixture. Store in the appropriate drawer in the cabinet inside the acrylic glass box.

11. Record mixing details (your name, date, BeO compound name, total mixture amount) in the laboratory mixing and pressing book.

Mixing Al oxide standard material or machine blank material

The same procedure used for Be applies when mixing Al standard material or Al machine blank material; the only differences are that you should mix with Ag powder (Al_2O_3 ; Ag 1:2) rather than Nb powder and the mixing is carried out in an open bench. No mask is needed during Al mixing.

Pressing BeO standard material or machine blank material

Before starting pressing:

- Wipe the surface of the acrylic box with MQ water or alcohol.
- Cover the surface of your working area with foil paper.
- Wrap one of the acrylic glass stands with foil paper and place on the working area.
- Place antistatic cathode inside the acrylic box.
- Place a weighing paper on top of the acrylic glass stand. This will allow you to recover any spilt material and will keep the working area clean. Change the weighing paper when necessary.
- Select pressing devices needed. Depending on the expected $^{10}\text{Be}/^9\text{Be}$ isotope ratio, blank or standard devices (press parts and spatula) are used. Blank devices are used for ratios less than $1\text{E}-12$ and standard devices are used for ratios above $1\text{E}-12$. There is also a separate spatula for relatively hot samples ($^{10}\text{Be}/^9\text{Be}$ ratio between $5\text{E}-13$ and $1\text{E}-12$). Wipe with alcohol once and set up.
- Place anvil assembly on the acrylic stand on top of a weighing paper to facilitate its movement.
- Ensure that you have enough clean cathodes, wipes and alcohol.
- Record an entry on the mixing & pressing lab book detailing your name, date, material to be pressed and parts used.
- Label eppendorf vials (each one may contain up to 6 cathodes).

To press:

Wear required safety equipment as indicated in the relevant COSHH form.

1. Select material to press and pass it through the antistatic cathode.
2. Wrap in foil paper and place inside a sealed bag. Weigh in the balance outside of the box. Tare the balance to 0. Bring vial back to the box and unwrap. Keep foil paper and bag for step 3.
3. Place a clean cathode inside the anvil assembly. Transfer $\sim 5.5\text{-}6\text{mg}$ of BeO-Nb mixture directly into the cathode using a spatula. To ensure that you are transferring the necessary amount of mixture weigh the vial again (wrapped in the original foil paper and inside the same bag). The minus figure shown in the balance is the amount transferred to the cathode. Once the required amount is transferred record it in the lab book.
4. Tap the anvil assembly gently to allow the mixture to funnel through to the cathode.
5. Transfer the anvil assembly to the press. It is vital to support the assembly – holding all parts together- when transferring it for pressing; otherwise the sample may be lost.
6. Bring the needle down and apply $\sim 125\text{-}150\text{psi}$ Pressure once the needle is inside the cathode, turn anvil assembly 180 degrees and repeat. **DO NOT** apply excessive pressure as the cathode

may be damaged as a consequence, making its removal from the assembly very difficult. Release needle holding the anvil assembly down.

7. Bring the anvil assembly down to acrylic stand, open the assembly and remove the cathode with the help of the spanner.
8. Place cathode in the appropriate labelled eppendorf vial.
9. Before you start pressing a different material wipe all devices used with alcohol a couple of times, the first wipe should go into the BeO waste bag.
10. Repeat the process. Once all cathodes are pressed place them in a labelled bag and store them inside the cabinet until they are submitted to the AMS for analysis

Pressing Al oxide standard material or machine blank material

The same procedure used for Be applies when pressing Al samples; the only differences are that the total mixture amount transferred should be ~0.0075-0.009g and the pressing is carried out in an open bench. No mask is needed during Al pressing.

Mixing and pressing unknown BeO samples

Before starting mixing and pressing unknown BeO samples:

- Wipe the surface of the acrylic box with MQ water or alcohol.
- Cover the surface of your working area with foil paper.
- Wrap one of the acrylic glass stands with foil paper and place on the working area.
- Place a weighing paper on top of the acrylic glass stand. This will allow you to recover any spilt material and keep the working area clean. Change the weighing paper between samples' mixing and pressing if necessary.
- Place antistatic cathode inside the acrylic box.
- Place stand holding BeO samples (in crucibles with lids) on the working area inside the acrylic box.
- Select devices needed for mixing and pressing your targets (unless known otherwise we assume that for unknowns Be¹⁰/Be⁹ isotope ratio <1 E-12 therefore blank devices should be used): Blank pressing device, Blank pressing needle and tweezers. Wipe with alcohol once and set up.
- Place anvil assembly on the acrylic stand on top of a weighing paper to facilitate its movement.
- Ensure that you have enough clean cathodes, clean quartz pestles, wipes and alcohol.
- Place eppendorf tube containing Nb powder and Nb spatula beside balance. Wipe spatula with alcohol.
- Prepare a table with the following columns: samples name, BeO amount (g), Nb powder required (g) and comments. Refer to previous tables if necessary.
- Label one eppendorf vial per sample (write name of sample clearly on the side and top of vial-remember to add the prefix G to all sample names) and place in the appropriate order in a stand so they will be ready to be filled with the target.
- Cut small square pieces of foil paper (one per sample) to make a "skirt" for each one of the quartz pestles that you will be using (one per sample).

To mix and press the samples:

Wear required safety equipment as indicated in the relevant COSHH form.

1. Place a clean cathode inside the anvil assembly.
2. Weigh the required amount of Nb powder needed for the sample. Half of a weighing paper can be used for this purpose and can be re-used to weigh Nb for the following samples until it becomes difficult to remove the Nb from it.
3. Record the weight in a piece of paper.
4. Remove the sample (crucible and lid) from stand using the tweezers. Pass it through the antistatic cathode and place on top of the weighing paper.
5. Take the weighing paper containing the Nb to the box and place on a secure place.
6. Take a quartz pestle and make a “skirt” using the square pieces of foil paper. Leave carefully beside the acrylic stand and remember to avoid cross-contamination.
7. Remove the quartz lid and set aside.
8. Add the Nb powder to the BeO sample.
9. Grind and try to homogenise the mixture, in the middle of this process you can put the lid on and pass through the anti-static device again.
10. Once the mixture looks homogenised transfer directly to the cathode (placed inside the anvil assembly) with the help of the tweezers.
11. Tap the anvil assembly gently to allow the mixture to funnel through to the cathode.
12. Transfer the anvil assembly to the press. It is vital to support the assembly – holding all parts together- when transferring it for pressing; otherwise the sample may be lost.
13. Bring the needle down and apply ~125-150psi Pressure once the needle is inside the cathode, turn anvil assembly 180 degrees and repeat. DO NOT apply excessive pressure as the cathode can be damaged as a consequence; making its removal from the assembly very difficult. Release needle holding the anvil assembly down.
14. Bring the anvil assembly down to acrylic stand, open the assembly and remove the cathode with the help of the spanner.
15. Place cathode in the appropriate labelled eppendorf vial.
16. If there are no traces of BeO in the quartz lid it can be clean and re-use again but only keep the lid if you are absolutely sure that there are no traces of BeO; if in doubt throw it away in the BeO waste bag.
17. The quartz crucible should be disposed of in the BeO waste bag. Wipe all devices used with alcohol a couple of times, the first wipe should go into the BeO waste bag.
18. Weigh the paper used for weighing the Nb and calculate how much Nb was added to the sample and record this weight in the table.
19. Repeat the process for the following sample. Once all samples are pressed place them in a labelled bag and store them inside the cabinet until they are submitted to the AMS for analysis.

Mixing and pressing unknown Al oxide samples

The same procedure applies when mixing and pressing Al samples; the only differences are that you should mix with Ag powder (Al_2O_3 : Ag 1:2) rather than Nb powder and the mixing is carried out in an open bench. No mask is needed during Al mixing and pressing.